Chapter 8
Hydrogen Energy

Abstract Hydrogen may be considered as a secondary energy source, since it is not available as a pure hydrogen gas. Pure hydrogen must be produced from its compound using another energy source prior to its use. For example, the electricity that is produced from a primary energy source can be used to produce hydrogen from water by electrolysis. The supply of hydrogen on demand also requires a storage system. Hydrogen production, storage, and distribution methods are discussed in this chapter.

8.1 Introduction

Hydrogen is abundant on the earth's surface, however, it is mainly bound with other chemical compounds, such as water (H_2O) and organic compounds. Hydrogen is an energy carrier; it can store and deliver usable energy. Hydrogen must be first dissociated from bound chemical compounds using a primary energy source. Hydrogen is an environmentally attractive fuel as it produces only water during its combustion and use as a fuel.

Various physical and chemical properties of hydrogen are given in Table 8.1. Before using hydrogen as a fuel, its combustion properties should be known and compared with other common fuels such as methane and gasoline to determine its effectiveness. Combustion related properties of hydrogen are compared with that of methane and gasoline in Table 8.2.

Hydrogen can be used in any application in which fossil fuels are being used today, except where carbon is specifically needed [1–4]. Hydrogen can be used as a fuel in furnaces, internal combustion engines, turbines and jet engines, more efficiently than fossil fuels, i.e., coal, petroleum and natural gas. Automobiles, buses, trains, ships, submarines, airplanes and rockets can run on hydrogen. Hydrogen can also be converted directly to electricity by using fuel cells, which can be fed directly to the grid or to operate automobiles. Combustion of hydrogen with oxygen results in pure steam, which has applications in industrial processes and space heating.

T.K. Ghosh and M.A. Prelas, *Energy Resources and Systems: Volume 2: Renewable Resources*, DOI 10.1007/978-94-007-1402-1_8,

Table 8.1 Various physical and chemical properties of hydrogen

Properties	Values
Atomic hydrogen	
Atomic number	1
Atomic weight	1.0080
Ionization potential	13.595 eV
Electron affinity	0.7542 eV
Nuclear spin	1/2
Nuclear magnetic moment (nuclear magnetons)	2.7927
Nuclear quadrupole moment	0
Electronegativity (Pauling)	2.1
Molecular hydrogen	
Bond distance	0.7416
Dissociation energy (25°C)	104.19 kcal/mol
Ionization potential	15.427 eV
Density of solid	0.08671 g/cm^3
Melting point	−259.20°C
Heat of fusion	28 cal/mol
Density of liquid	0.07099 at −252.78°C
Boiling point	−252.77°C
Heat of vaporization	216 cal/mol
Critical temperature	−240.0°C
Critical pressure	13.0 atm
Critical density	0.0310 g/cm^3
Heat of combustion to water (g)	−57.796 kcal/mol

Table 8.2 A comparison of fuel properties of hydrogen with that of methane and gasoline

Properties	Hydrogen	Methane	Gasoline
Lower heating value, kW h/kg	33.33	13.9	12.4
Self ignition temperature, °C	585	540	228–501
Flame temperature, °C	2,045	1,875	2,200
Ignition limits in air, vol%	4–75	5.3–15	1.0–7.6
Minimum ignition energy, mWs	0.02	0.29	0.24
Flame propagation in air, m/s	2.65	0.4	0.4
Detonation limits, vol%	13–65	6.3–13.5	1.1–3.3
Detonation velocity, km/s	1.48–2.15	1.39–1.64	1.4–1.7
Explosion energy, kg TNT/m^3	2.02	7.03	44.22
Diffusion coefficient in air, cm^2/s	0.61	0.16	0.05

Moreover, hydrogen is an important industrial gas and raw material for numerous industries, such as the computer, metallurgical, chemical, pharmaceutical, fertilizer and food industries. The major use of hydrogen is listed below.

- Ammonia (NH_3) production for use in fertilizer
- Oil industry
- Semi conductor production

- Glass industry (shielding gas)
- Hydrogenation of fats and oils
- Methanol production
- Production of HCl
- Plastics recycling
- Rocket fuel
- Welding and cutting

8.2 Hydrogen Economy

A hydrogen economy is envisioned as an economy in which hydrogen will be the main energy source [5–13]. The current global economy is called the carbon economy since most of the primary energy resources are derived from carbon or fossil fuels: Coal, Petroleum, and Natural gas. Hydrogen energy based economy is attractive as hydrogen can be produced from water; a resource that every country on the earth has. The regional dominance of an energy source can be eliminated leading to a better political environment. Various components of the hydrogen economy are discussed in Volume 4 of this book series.

8.3 Hydrogen Demand

Total hydrogen production worldwide is about 550 billion Nm^3/year. Approximately 50% of it is used for ammonia based fertilizer production. The consumption of hydrogen in refineries per year is around 200 billion Nm^3. Other major uses of hydrogen include methanol production (8%) and the use as fuel in space programs (1%). Ninety-five percent of hydrogen production is captive, i.e., produced at the site where it is used. Other 5% is called merchant produced, which is sold for industrial and chemical uses.

Hydrogen demand in the United States in 2006 was 11 million tons/year and accounted for 5% of the natural gas consumed in the US for its production. Centrally produced merchant hydrogen, which is sold for industrial and chemical uses, amounts to 1.5 million tons. Hydrogen use in the USA in 2006 is shown in Fig. 8.1. The usage is expected to double by 2010. However, this represents only a small increase in the production capacity in the USA from 2003 and 2008 (see Table 8.3). The production capacity must be increased to meet the future demand. The supply of hydrogen could be a significant issue, if hydrogen fuel cell cars are introduced in the market in large numbers.

The main objective of a hydrogen economy is to use hydrogen as a fuel source. Its major use as fuel will be in fuel-cell cars. The working principle of fuel cells is discussed in Volume 3 of this book series. It is assumed that fuel cell cars will go

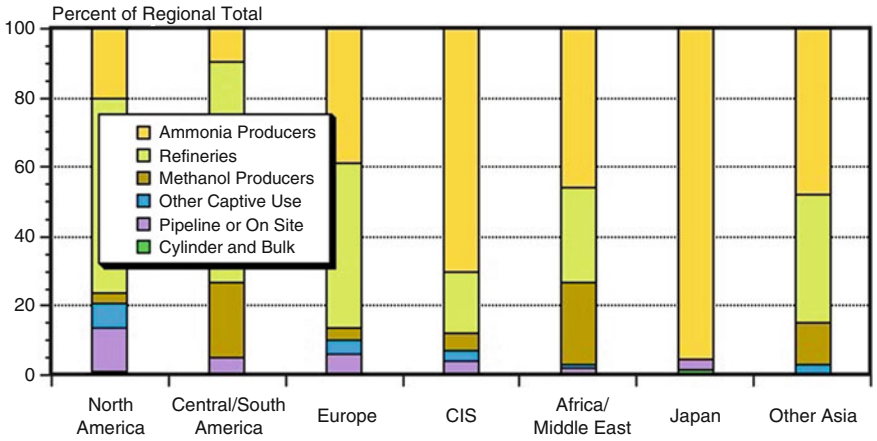

Fig. 8.1 Hydrogen use by end users in 2006 (Courtesy of Suresh et al. [14])

Table 8.3 Hydrogen production capacity in the US in 2003 and 2008

	Production capacity (thousands metric tons per year)	
Capacity type	2003	2008
On-purpose capacity[a]		
Oil refinery	2,870	2,723
Ammonia	2,592	2,271
Methanol	393	189
Other	18	19
On-purpose merchant[a]		
Off-site refinery	976	1,264
Non-refinery compressed gas (cylinders and bulk)	2	2
Compressed gas (pipeline)	201	313
Liquid hydrogen	43	56
Small reformers and electrolyzers	<1	<1
Total on-purpose	7,095	6,839
Byproduct		
Catalytic reforming at oil refineries	2,977	2,977
Other off-gas recovery[b]	462	478
Chloro-alkali production	–	389
Total byproducts	3,439	3,844
Total hydrogen production capacity	10,534	10,683

Source: Energy Information Administration (EIA) [15]

[a]On-purpose are those units where hydrogen is the main product as opposed to byproduct units where hydrogen is produced as a result of processes dedicated to producing other products

[b]From membrane, cryogenic and pressure swing adsorption (PSA) units at refineries and other process plants

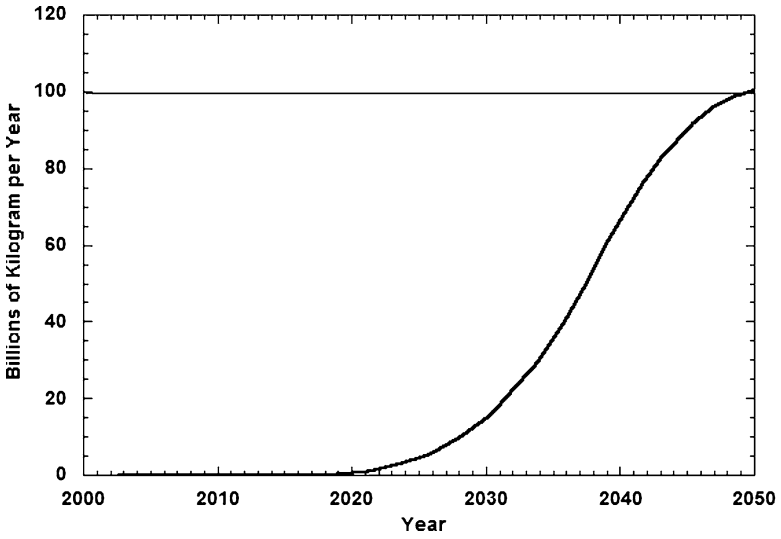

Fig. 8.2 U.S. Hydrogen demand assuming commercialization of the fuel cell vehicles in 2015 (Courtesy of An "optimally plausible" solution based on NRC report.3 3 [16])

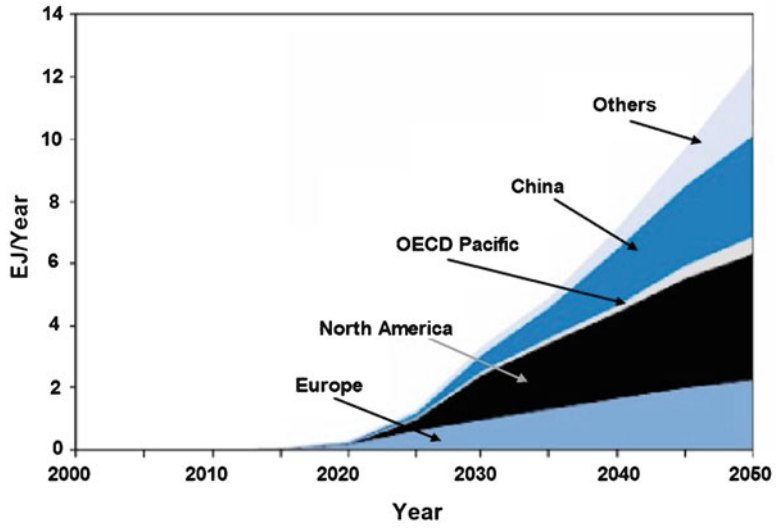

Fig. 8.3 Projected hydrogen demand in various regions of the world (Source: Argonne National Laboratory [17])

into mass scale commercial production in the US around 2015, and consequently the demand for hydrogen will also increase. The increase in demand for hydrogen in the US is shown in Fig. 8.2.

It is anticipated that by 2040, the use of hydrogen in fuel cell powered cars and light trucks could replace consumption of petroleum by about 18.3 million barrels per day. If it is assumed that hydrogen powered vehicles will have 2.5 times the energy efficiency of improved gasoline vehicles, this reduction in petroleum use would require the annual production of approximately 150 million tons of hydrogen by 2040. The use of hydrogen is yet to take off, but the anticipation is that its use by most of the countries will start around 2020. An exponential growth following the initial period of slow growth is expected as shown in Fig. 8.3.

8.4 Hydrogen Internal Combustion Engine

The use of hydrogen as a fuel for internal combustion engines (ICE) has been explored in the last several decades [18–23]. Hydrogen use in ICE has several advantages including wide range of flammability, low ignition energy, small quenching distance, high autoignition temperature, high flame speed at stoichiometric ratios, high diffusivity, and very low density. The ability for H_2-ICEs to burn cleanly and operate efficiently is due to the unique combustion characteristics of hydrogen that allow ultra-lean combustion with significantly reduced NO_x production and efficient low-engine load operation. Some of these properties are given in Table 8.4.

Most of the cars use an Otto cycle engine. The theoretical thermodynamic efficiency of an Otto cycle engine is based on the compression ratio of the engine and the specific-heat ratio of the fuel as shown in Eq. 8.1.

$$\eta_{th} = 1 - \frac{1}{\left(\frac{V_1}{V_2}\right)^{\gamma-1}} \tag{8.1}$$

where,

$V_1/V_2 =$ the compression ratio
$\gamma =$ ratio of specific heats
$\eta_{th} =$ theoretical thermodynamic efficiency

Table 8.4 Fuel properties at 298 K and 1 atm pressure relevant to internal combustion engines

Property	Hydrogen	CNG	Gasoline
Density (kg/m^3)	0.0824	0.72	730[a]
Flammability limits (φ)	0.1–7.1	0.4–1.6	≈0.7–4
Quenching distance (mm)[b]	0.64	2.1[c]	≈2
Stoichiometric fuel/air mass ratio	0.029	0.069	0.068
Stoichiometric volume fraction %	29.53	9.48	≈2[d]
Heat of combustion (MJ/kg$_{air}$)[b]	3.37	2.9	2.83

Source: White et al. [24]
[a]Liquid at 0°C
[b]At stoichiometry
[c]Methane
[d]Vapor

Equation 8.1 suggests that higher is the compression ratio and/or the specific-heat ratio, the higher is the thermodynamic efficiency of the engine. The compression ratio limit of an engine is based on the fuel's resistance to knock. A lean hydrogen mixture is less susceptible to knock than conventional gasoline, and, therefore, can tolerate higher compression ratios. The high RON (Research Octane Number) and low lean-flammability limit of hydrogen provide the necessary combination to attain high thermal efficiencies in an ICE. The stoichiometric air/fuel (A/F) ratio for the complete combustion of hydrogen in air is about 34:1 by mass. This is much higher than the 14.7:1 A/F ratio required for gasoline. However, because of hydrogen's wide range of flammability, hydrogen engines can run on A/F ratios of anywhere from 34:1 (stoichiometric) to 180: 1. The specific heat ratio is related to the fuel's molecular structure. The less complex is the molecular structure, the higher is the specific-heat ratio. Hydrogen ($\gamma = 1.4$) has a much simpler molecular structure than gasoline, and, therefore, its specific-heat ratio is higher than that of conventional gasoline ($\gamma = 1.1$). Hydrogen fueled ICEs have demonstrated efficiencies in excess of 20% compared to conventional gasoline-fueled ICEs.

Auto mobile companies including BMW [25] and Ford [26] are investing significant amount of their resources to develop hydrogen fueled ICEs. Berckmüller et al. [25] supercharged a single-cylinder engine up to 1.8 bar and reported 30% increase in specific power output compared to a naturally aspirated gasoline engine. Natkin et al. [27] also reported increase in specific power while investigating a supercharged 4-cylinder 2.0-l Ford Zetec engine and a 4-cylinder 2.3-l Ford Duratec engine that was used in conventional and hybrid vehicles [26]. Musashi Institute of Technology showed a 35% increase in power for two Nissan hybrid engines when using hydrogen fuel. NO_x emissions were 10 ppm, same as other gasoline engines [28].

8.5 Hydrogen Production Methods

There are three aspects of hydrogen production and these are:

1. Identification of a source (chemical compound) for hydrogen.
2. Identification of a primary energy source.
3. A method for using primary energy source to extract hydrogen from its sources.

Hydrogen can be produced from a number of sources such as water, natural gas, coal, various hydrocarbons, and biomass. Processes for extraction of hydrogen from these sources are source specific [29–36]. For example, biomass may have to be converted to methane or an alcohol, such as ethanol, before hydrogen can be produced. Hydrocarbons must be reformed to produce hydrogen, which is a very energy intensive process. This could result in a higher price than the direct use of gasoline. Hydrogen produced from natural gas may cost twice as much compared to the use of gasoline directly in automobiles.

A primary energy source is necessary to extract hydrogen from its compounds (see Fig. 8.4). Although all kinds of energy sources can be used, the cost would vary

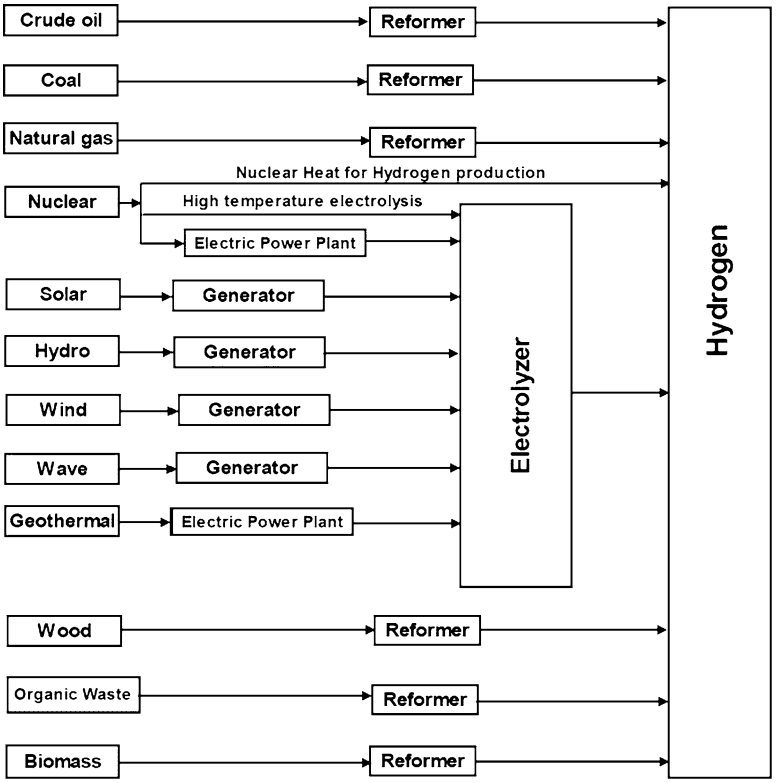

Fig. 8.4 The use of various energy sources and pathways for hydrogen production (Source: Yacobucci and Curtright [36])

significantly depending on the methods selected for hydrogen extraction from its compounds. For example, to generate hydrogen from water, the process may need the heat from a primary energy source, electricity from a power plant, or sunlight to split water into hydrogen and oxygen. Methods for production of hydrogen can be divided into several categories and are given in Table 8.5.

One of the most common processes for hydrogen generation is called the thermal process. In thermal processes, feed stocks are natural gas, petroleum based liquid fuels (propane or higher hydrocarbons), biomass, coal (hydrogen present in coal), and water (direct thermal decomposition). The heat from a primary source is used directly to dissociate hydrogen containing compounds into hydrogen and other constituents. The specific chemical processes used in the thermal process are given below:

- Reforming of natural gas
- Gasification of coal
- Gasification of biomass

Table 8.5 Processes for hydrogen production

Primary method	Process	Feedstock	Energy
Thermal	Steam reformation	Natural gas	High temperature steam
	Thermochemical water splitting	Water	High temperature heat from advanced gas-cooled nuclear reactors
	Gasification	Coal, Biomass	Steam and oxygen at high temperature and pressure
	Pyrolysis	Biomass	Moderately high temperature steam
Electrochemical	Electrolysis	Water	Electricity from wind, solar, hydro, nuclear, coal or natural gas
	Photoelectrochemical	Water	Direct sunlight
Biological	Photobiological	Water and algae strains	Direct sunlight
	Anaerobic digestion	Biomass	High temperature heat
	Fermentative microorganisms	Biomass	High temperature heat

Source: National Hydrogen Association [37]

- Reforming of renewable liquid fuels
- Nuclear energy
- Solar energy

8.5.1 Reforming of Natural Gas

About 95% of hydrogen produced in 2008 in the USA was generated via steam methane reforming. Worldwide about 50% of the total hydrogen is produced by this method. In this process, methane (CH_4) is reacted with either steam (called steam reforming reaction), oxygen (called partial oxidation), or both in sequence (called autothermal reforming). A steam-methane reforming process [38–58] consists of essentially four steps: Feed purification, Steam reforming reactions, Water gas shift reaction, and Product purification (CO_2 and trace impurities removal). The process flow diagram is shown in Fig. 8.5.

The source for methane is natural gas, which contains a variety of impurities that must be removed prior to feeding it to the catalytic reactor. Natural gas purification involves removal of sulfur (S) and chlorine (Cl), which act as poisons for the catalyst, to increase the life of the downstream steam reforming and other catalysts. Organic sulfur compounds are first hydrogenated converting sulfur to H_2S, which next reacts with zinc oxide in a column to form zinc sulfide. It is a solid and is removed from the bed as a waste. For high or variable sulfur loadings, more

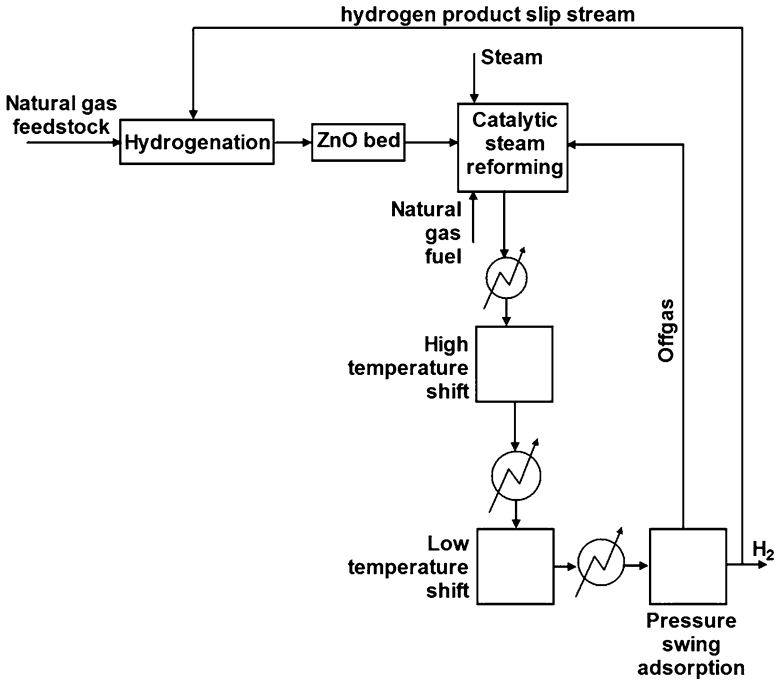

Fig. 8.5 Main components of a hydrogen production plant using natural gas (Source: Spath and Mann [58])

complicated systems using separate reactors for conversion and adsorption are necessary. Often several conversion and adsorption vessels are used in series.

Steam methane reforming reactions producing hydrogen consist of two reactions. The first reaction involves methane reacting with steam at 750–800°C (1, 380–1, 470°F) under 3–25 bar pressure in the presence of a catalyst to produce hydrogen, carbon monoxide, and a relatively small amount of carbon dioxide. The steam reforming reaction can be written as:

$$CH_4 + H_2O \xrightarrow{Catalyst} CO + 3H_2, \quad \Delta H^0_{298} = 206\,\text{kJ/mol} \tag{8.2}$$

The gas mixture of CO and H_2 (three-part H_2 and one-part CO) is called the synthetic gas (or syngas). The positive ΔH suggests that it is an endothermic reaction.

Carbon monoxide (CO) further reacts with steam, which is known as "water-gas shift reaction," over a catalyst to produce carbon dioxide and more hydrogen. This process occurs in two stages, consisting of a high temperature shift (HTS) at 350°C (662°F) and a low temperature shift (LTS) at 190–210°C (374–410°F). The overall reaction can be written as:

$$CO + H_2O \xrightarrow{Catalyst} CO_2 + H_2, \quad \Delta H^0_{298} = -41\,\text{kJ/mol} \tag{8.3}$$

This is an exothermic reaction, but the heat released in the reaction is much smaller compared to the amount consumed by first reaction (Eq. 8.2).

A number of other hydrocarbons can be used as a feedstock for hydrogen production using the same steam reforming reaction:

Propane: $$C_3H_8 + 3H_2O \xrightarrow{Heat} 3CO + 7H_2 \tag{8.4}$$

Ethanol: $$C_2H_5OH + H_2O \xrightarrow{Heat} 2CO + 4H_2 \tag{8.5}$$

Gasoline (using iso-octane and toluene as example compounds from the hundred or more compounds present in gasoline):

$$C_8H_{18} + 8H_2O \xrightarrow{Heat} 8CO + 17H_2$$
$$C_7H_8 + 7H_2O \xrightarrow{Heat} 7CO + 11H_2 \tag{8.6}$$

One of the problems of using higher hydrocarbon is the formation of carbon via following reactions. Also, if higher hydrocarbons are present with methane, carbon may also form, which will deposit on the catalyst reducing its activity, and the product yield. The methane decomposition reaction is given below:

$$CH_4 \rightarrow C(s) + 2H_2, \Delta H = 75\,\text{kJ/mol} \tag{8.7}$$

A similar reaction (Eq. 8.7) is more favorable for higher hydrocarbons. Carbon deposition can also occur via the Boudouard reaction given below:

$$2CO \rightarrow C(s) + CO_2, \Delta H = -172\,\text{kJ/mol} \tag{8.8}$$

In the product purification unit, CO_2 and other impurities are removed from the gas stream by the pressure-swing adsorption (PSA) process leaving essentially pure hydrogen. Prior to feeding the gas stream to a PSA unit, entrained liquids (water and condensed hydrocarbons) are removed in a condenser. The PSA unit that contains carbon and zeolite based adsorbents removes unreacted CH_4, CO, CO_2, and unrecovered hydrogen from the gas stream. The PSA off-gas (regenerated stream from the adsorption bed) is used to fuel the reformer; 80–90% of the required heat can be supplied by burning this stream. The remaining heat is provided by supplemental natural gas. As shown in Fig. 8.6, the process, when using other non-methane feed, is not significantly different from the process shown in Fig. 8.5 for the natural gas feed.

8.5.1.1 Steam Methane Reforming Catalyst

Catalysts are required for both the steam methane reforming and the water gas shift reactions. The key component of the reformer system is the catalyst. A variety

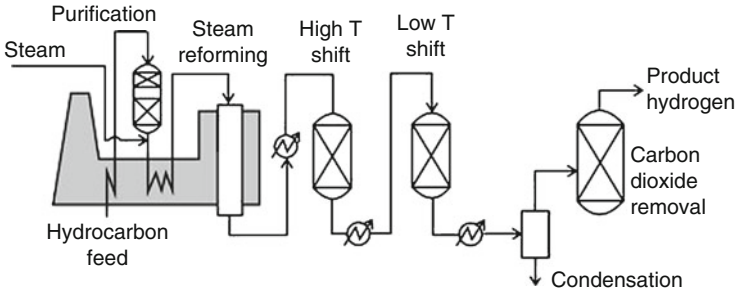

Fig. 8.6 Process for producing hydrogen from hydrocarbon feed (Source: Elder [59])

of catalysts have been explored for the reforming reaction [60–101]. However, the main steam reformer catalyst is supplied as a 10–33 wt% NiO supported on alumina, cement, or magnesia substrate. During startup, the catalyst is first heated in a stream of inert gas and then by steam. Once the catalyst attends the operating temperature, hydrogen or a light hydrocarbon is introduced to the stream to reduce NiO to metallic Ni. Although Ni-catalysts are widely used in the industry, its deactivation, poisoning by sulfur and other impurities, and carbon deposition are of great concerns. A number of other active metals that include iron, cobalt, rhodium, ruthenium, platinum, and palladium, have been tried for replacement of Ni-catalysts. However, all of them were found unacceptable by the industry: Iron based catalysts oxidize rapidly, cobalt cannot withstand steam pressure, and others are too expensive.

For the high temperature water shift (HTS; 300–450°C) reaction, an iron oxide-chromium oxide (Fe_3O_4−Cr_2O_3) based catalyst is used, whereas the major component of the low temperature shift catalyst (LTS; 180–270°C) is copper oxide, usually in a mixture with zinc oxide (Häussinger, 2000). The LTS catalyst is sensitive to changes in operating conditions. Typical lifetime for both HTS and LTS catalysts is 3–5 years. The HTS catalyst is supplied in the form of ferric oxide (F_2O_3) and chromium oxide (CrO_3), which is reduced by hydrogen and carbon monoxide in the feed gas as part of the start-up procedure to obtain the desired form of the catalyst. The LTS catalyst is supplied as CuO on a ZnO support. The copper is reduced by heating it in a stream of inert gas containing hydrogen.

The coke formation, when using heavy feedstock, may be reduced by using promoters, such as potassium, lanthanum, ruthenium, and cerium during the reforming reaction. Promoters can increase the steam gasification of solid carbons reducing the coke formation. Nickel-free catalysts containing mostly strontium, aluminum and calcium oxides have been successfully tested on feedstocks heavier than naphtha, however, the product gas contains high concentrations of methane which requires a secondary reformer for its conversion to H_2.

LTS catalysts are highly sensitive to sulfur, but HTS catalysts can tolerate sulfur concentrations up to several hundred parts per million, although their catalytic activity declines. Several researchers are trying to develop sulfur tolerant catalysts, but

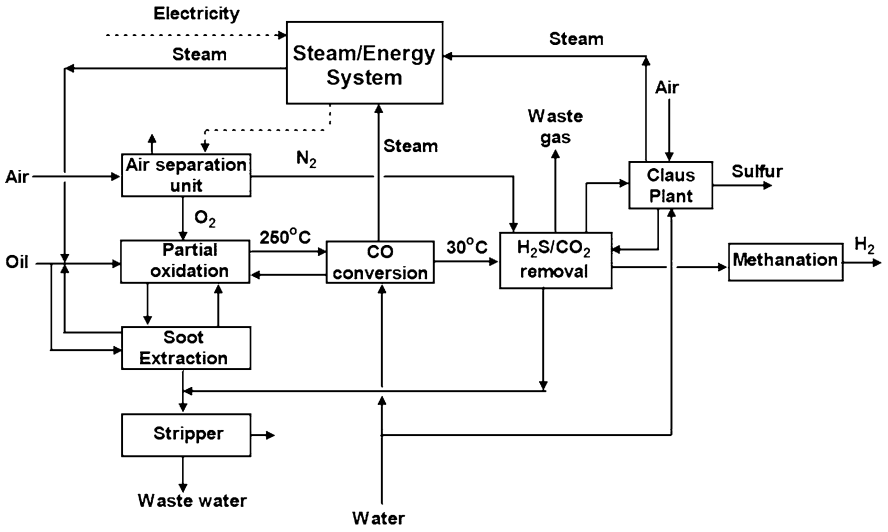

Fig. 8.7 A flow diagram of partial oxidation system for hydrogen production (Printed with permission from Kothari et al. [115])

with a limited success. ICI Katalco, USA, makes sulfur tolerant catalysts consisting of cobalt and molybdenum oxides, which operate at temperatures between 230°C and 500°C. The ratio of steam to sulfur in the feed gas and the catalyst temperature are the controlling factors.

8.5.1.2 Partial Oxidation

In this method, methane is reacted with less than a stoichiometric amount of oxygen (typically, from air) to partially oxidize certain amount of methane [102–115]. Reaction products contain primarily hydrogen and carbon monoxide. However, nitrogen from the air and a relatively small amount of carbon dioxide remain in the product gas stream. Higher hydrocarbons react in a similar manner; only the oxygen content will vary depending on the molecular weight of the hydrocarbon. The reaction is followed by the water-gas shift reaction, where the carbon monoxide reacts with water to form carbon dioxide and more hydrogen. A schematic of the process is shown in Fig. 8.7.

The partial oxidation process has several advantages. It is an exothermic process and also a much faster process than steam reforming and requires a smaller reactor vessel. The main drawback of this approach is that it initially produces less hydrogen per unit of input fuel than is obtained by steam reforming of the same fuel. Partial oxidation reactions of various hydrocarbons are given below.

Methane: $$CH_4 + 1/2\ O_2 \rightarrow CO + 2H_2 + Heat \tag{8.9}$$

Propane: $$C_3H_8 + 1\ 1/2O_2 \rightarrow 3CO + 4H_2 + Heat \quad (8.10)$$

Ethanol: $$C_2H_5OH + 1/2O_2 \rightarrow 2CO + 3H_2 + Heat \quad (8.11)$$

Gasoline (using iso-octane and toluene as example compounds from the hundred or more compounds present in gasoline):

$$C_8H_{18} + 4O_2 \rightarrow 8CO + 9H_2 + Heat \quad (8.12)$$

$$C_7H_8 + 3\ 1/2O_2 \rightarrow 7CO + 4H_2 + Heat \quad (8.13)$$

8.5.1.3 Autothermal Reforming for Hydrogen Production

Autothermal reforming combines steam reforming and partial oxidation into a one-step process [116–130]. Methane or a hydrocarbon is reacted with both steam and oxygen from air to produce the syngas. A reaction temperature of 950–1,100°C and a pressure up to about 10 MPa are maintained in the reactor. Both the steam reforming and partial oxidation reactions occur concurrently. The process can be optimized to supply all the heat from the partial oxidation reaction. An efficiency of 80–90% is possible. The syngas is then subjected to the water gas shift reaction to produce more hydrogen. The process can be compact, since a number of heat exchangers can be eliminated. Additional heat is not required making the process more attractive than the steam reforming process.

8.5.2 Biomass Gasification

Biomass can be converted to the syngas mixture, which then can be subjected to the water-gas shift reaction for production of hydrogen. Biomass gasification processes have been discussed in Chap. 6.

8.5.3 Reforming of Biofuel

Another route of hydrogen production from biomass is to convert it to a liquid fuel such as ethanol, bio-oils, and biodiesel. This is discussed later in this chapter. The advantage of doing this is that liquid fuels can be transported at relatively low cost to a reforming facility to produce hydrogen. Reforming bioliquids to hydrogen is very similar to reforming natural gas. The liquid fuel is first reacted with the steam at high temperatures in the presence of a catalyst to produce the syngas, followed by the water-gas shift reaction. Finally, the hydrogen is separated out and purified. The steam reforming reaction of ethanol is given below.

$$C_2H_5OH + H_2O \xrightarrow{Heat} 2CO + 4H_2 \quad (8.14)$$

8.5.4 Hydrogen from Coal

Coal gasification is the oldest method for hydrogen production. This type of plant has long been operating in Europe, South Africa, and the U.S. There are large supplies of coal in the U.S., other North American countries, and the world. Coal is mainly carbon, which can be converted to syngas by reacting it with steam. Coal gasification processes have been discussed in Chap. 6 of Volume 1 of this book series.

8.5.5 High-Temperature Water Splitting

8.5.5.1 One Step Reaction

The direct decomposition of water into hydrogen and oxygen is a very challenging chemical process [131–134]. Complete decomposition of water (100% dissociation) requires a temperature of about 4027°C at a pressure of 1 bar. At a temperature of 2227°C and a pressure of 1 bar, only 9% water dissociates. A partial decomposition of 25% may be achieved at 2227°C if pressure is reduced to about 0.05 bar. The one step reaction occurs as follows:

$$H_2O = H_2 + 1/2\ O_2 \tag{8.15}$$

Reaction given in Eq. 8.15 is a reversible reaction, and the recombination of hydrogen and oxygen upon cooling must be prevented otherwise no net production would result. Solar energy may be used to generate such a temperature by using a solar concentrator. Quartz windows, using dish-type mirrors, focus the solar radiation into a cavity to achieve the high temperature that is necessary for the decomposition of water. However, materials of construction for such a cavity and large temperature swings (heating and cooling cycles) would make the process very expensive.

8.5.5.2 Two or Multiple Step Reactions

The reaction temperature can be reduced significantly by using two or more chemical steps. A Temperature in the range of 1427–2727°C would be sufficient to achieve an efficiency in the range of 40–50%. For multi-step thermochemical water splitting, two energy sources that can provide temperatures in this range are:

- Nuclear energy
- Solar energy

Processes that are proposed for production of hydrogen, using these energy sources are listed below. Although these processes are technically viable, these may not be economically suitable.

- High temperature electrolysis
- Metal/metal oxide based systems
- Sulfur iodine cycle
- Hybrid sulfur cycle
- Steam methane reforming cycle
- Direct methane cracking cycle

The current process configurations (without the use of solar or nuclear energy) for direct steam methane reforming and direct methane cracking cycles are most economical and provide excellent positive energy balance. In direct processes, a portion of methane is burned to provide all the heat making the process economical. The use of solar or nuclear energy will add additional instability and increase operating costs. Both solar and nuclear energy can be used for high temperature electrolysis, but solar energy is most suitable for metal/metal oxide based water decomposition process, whereas nuclear energy provides the best economics for sulfur iodine and hybrid sulfur cycles.

8.6 Nuclear Energy for Hydrogen Production

Nuclear energy is a prime candidate to supply heat for the large scale production of hydrogen [135–141]. Three options are available where nuclear energy can be used for commercial hydrogen production. These options are:

- The use of the electricity generated from nuclear power plants for conventional water electrolysis.
- The use of both high-temperature heat and electricity from the nuclear power plant for high-temperature steam electrolysis (HTSE) or the hybrid processes.
- The use of the heat from nuclear plant for thermochemical processes.

Although a high operating temperature is necessary for high efficiency and efficient operation of the plant, the advantages of using nuclear energy are: (1) no emission of greenhouse gases (GHG) and CO_2 during the operation of nuclear reactors, and (2) nuclear energy can contribute to large-scale hydrogen production. The demand for energy is growing in all sectors worldwide, particularly in the transportation sector. Large scale hydrogen production systems will be essential to address this issue, which cannot yet be sufficiently addressed by the renewable energy resources. One of the major disadvantages of solar energy or other renewable energy sources is their low power density and intermittency. Technologies available for hydrogen production using nuclear energy are shown in Fig. 8.8.

8.6.1 Water Electrolysis

The electrolysis of water at room temperature can lead to the decomposition of water into hydrogen and oxygen. Although electrolysis process is more than 85% efficient,

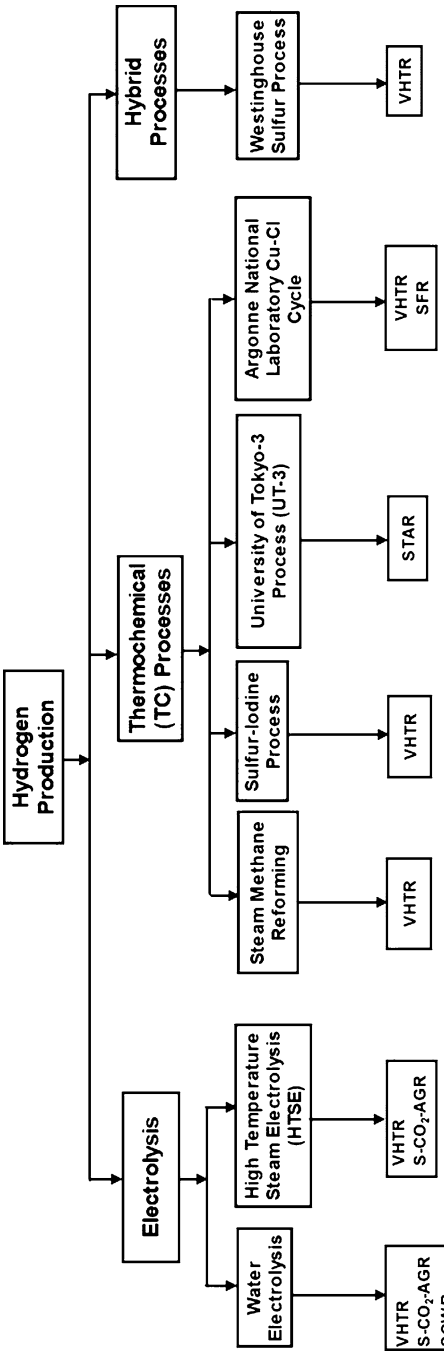

Fig. 8.8 Hydrogen production technologies for a specific nuclear reactor. *VHTR* Very High Temperature Reactor, *S-CO2-AGR* Supercritical-Carbon Dioxide Advanced Gas Reactor, *SCWR* SuperCritical Water Reactor, *ALWR* Advanced Light Water Reactor, *STAR* Secure Transportable Autonomous Reactor, *SFR* Sodium-cooled Fast Reactor (Source: Yildiz and Kazimi [160])

it requires high electrical energy consumption that makes the overall process not only inefficient, but also expensive. The current electricity generating processes (steam turbine based nuclear or coal power plants) have only 37–40% thermal efficiency. Therefore, combination of such a power plant and water electrolysis will make the process only 30–32% efficient. As a result, a high-temperature steam electrolysis process that is more energy efficient for hydrogen production is being developed.

8.6.2 High Temperature Electrolysis (HTE) of Steam

The decomposition of water is accomplished by using both thermal and electrical energies, which can be provided by nuclear energy [142–159]. Water is heated by an outer heat source, in the present case by the heat from a nuclear plant, before feeding it into an electrolysis cell as steam, which is supplied to the cathode of the electrolysis cell that decomposes water into hydrogen and oxygen according to Eq. 8.16.

$$H_2O + 2e^- \rightarrow H_2 + O^{2-} \tag{8.16}$$

Hydrogen is removed as the product. Oxygen ions move through the electrolyte that is conductive only to oxygen ions towards the anode, where they release electrons producing molecular oxygen. The reaction at the anode is given by:

$$O^{2-} \rightarrow \frac{1}{2}O_2 + 2e^- \tag{8.17}$$

This overall reaction can be described as:

$$H_2O \rightarrow H_2 + \frac{1}{2}O_2 \tag{8.18}$$

The process is shown schematically in Fig. 8.9.

A major component of the high temperature electrolysis system is the electrolyte, which is a solid oxide capable of oxygen-ion-conduction. Most common electrolyte is Yttria-Stabilized Zirconia (YSZ) with porous, electrically conducting electrodes deposited on either side of the electrolyte. The construction of the electrolysis cell using YSZ is shown in Fig. 8.10. A mixture of steam and hydrogen at 750–950°C is supplied to the cathode side of the electrolyte. The oxygen ions are drawn through the electrolyte by the applied electrochemical potential, liberating their electrons and recombining to form molecular O_2 on the anode side. The entering steam-hydrogen mixture may contain as much as 90% steam. Similarly, the exiting mixture may contain as much as 90% H_2. The product steam and hydrogen gas mixture is passed through a condenser or membrane separator to produce pure hydrogen. In a commercial unit, several electrolytic cells are combined to form a stack, separated by electronically conducting interconnects.

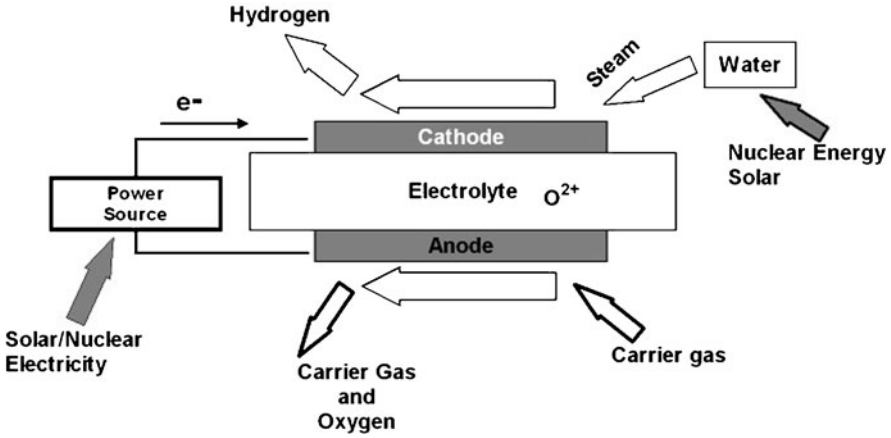

Fig. 8.9 A schematic representation of high temperature steam electrolysis

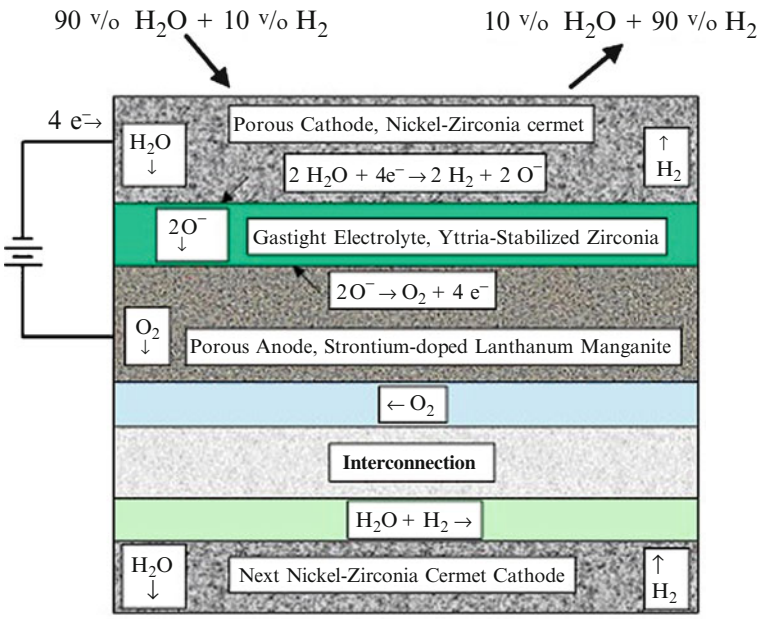

Fig. 8.10 Components of a high temperature electrolysis cell (Source: O'Brien et al. [161])

Although the construction of the electrolysis cell is similar to a fuel cell, operation of the cell in the electrolysis mode is fundamentally different than the operation in the fuel cell mode. In the fuel cell mode, hydrogen ions combine with oxygen ions releasing heat, whereas in the electrolysis mode, the steam reduction

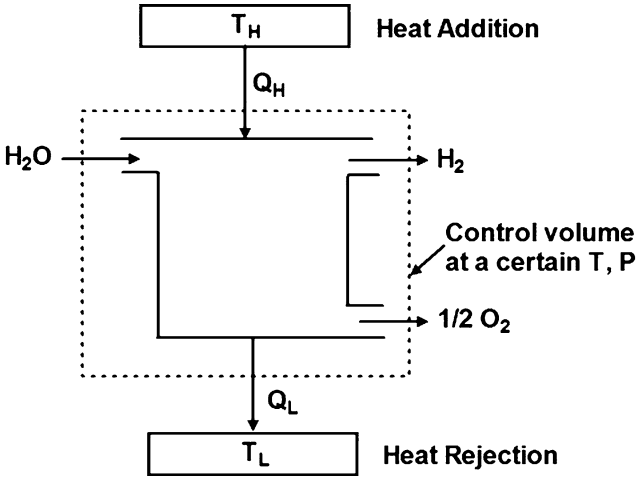

Fig. 8.11 Thermodynamic system

reaction is endothermic. Therefore, heat must be supplied continuously to maintain the high reaction rate. Depending on the current density, the net heat generation in the stack may be negative, zero, or positive.

The conceptual design of a plant that combines a nuclear reactor with a hydrogen production unit is described in Chap. 9 of Volume 1 of this book series. In this concept, a nuclear reactor generates both electrical power and supplies heat to the high temperature electrolysis unit for hydrogen production.

8.6.2.1 Efficiency of High Temperature Electrolysis Cycle

For dissociation of steam into hydrogen and oxygen by HTE, both thermal and electrical energies are required. The total energy input to the system may be described by Eq. 8.19.

$$\Delta H = \Delta G + T\Delta S \tag{8.19}$$

In this equation, ΔH is the enthalpy change which may be viewed as negative of the hydrogen combustion heat, ΔG is the Gibbs free energy change, ΔS is the entropy change in the reaction, and T is the reaction temperature in Kelvin. The term $T\Delta S$ represents the thermal energy input, and ΔG is the electrical energy input. The thermodynamic process may be represented by the simple Carnot system as shown in Fig. 8.11.

The overall thermal efficiency can be expressed in terms of the net enthalpy change of the working fluid divided by the heat input at high-temperature to the system:

$$\eta = \frac{\Delta H}{Q_H} \tag{8.20}$$

where ΔH can be written from the first law of thermodynamics as:

$$\Delta H = Q_H - Q_L \tag{8.21}$$

where Q_H is the heat input and Q_L is the heat rejected by the system. The second law provides:

$$\Delta S_R \geq \frac{Q_H}{T_H} - \frac{Q_L}{T_L} \tag{8.22}$$

Substitution of Eqs. 8.20 and 8.21 into Eq. 8.22 provides the following expression for efficiency:

$$\eta = \frac{1 - \frac{T_L}{T_H}}{1 - \frac{T_L \Delta S}{\Delta H}} \tag{8.23}$$

The entropy ΔS can be replaced by the Gibbs free energy of formation of water at a reference temperature by using Eq. 8.24.

$$\Delta S = \frac{\Delta H}{T_L} - \frac{\Delta G^0_{f,H_2O}}{T_L} \tag{8.24}$$

Substitution of Eq. 8.24 into Eq. 8.23 provides the following expression for efficiency:

$$\eta = \left(1 - \frac{T_L}{T_H}\right)\left(\frac{\Delta H}{-\Delta G^0_{f,\,H_2O}}\right) \tag{8.25}$$

Since, $\Delta G^0_{f,\,H_2O}$ for water is negative, the maximum theoretical efficiency may be calculated assuming that ΔH is equal to the high heating value. The efficiency as a function of temperature is shown in Fig. 8.12.

In this plot, the value of T_L is assumed to be 20°C. A maximum theoretically possible efficiency of around 87.5% is possible at 1,000°C. This is the Carnot efficiency. For a practical cycle, about 65% of the Carnot efficiency is achievable. A high temperature electrolysis system can attend an overall efficiency of around 60%.

8.6.3 Thermochemical Water Splitting

Thermochemical water-splitting refers to the decomposition of water into hydrogen and oxygen by a series of chemical reactions at high temperatures [162–177]. The same overall result is obtained, but using a much lower temperature compared to the direct thermal dissociation. Brown et al. [167] conducted an extensive review of about 115 thermochemical cycles. They identified 25 cycles that have good commercial potential and merit further study. These 25 cycles are listed in Table 8.6. Among these 25 cycles, three cycles: sulfur-iodine, Ca–Fe–Br, and Cu–Cl cycles were explored further. These three cycles are discussed below.

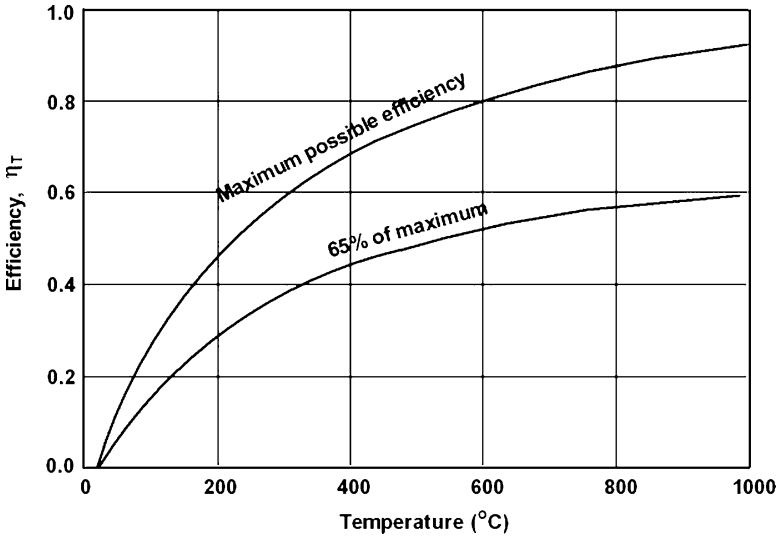

Fig. 8.12 Theoretical efficiency for high temperature hydrogen splitting (Source: O'Brien et al. [161])

8.6.3.1 Sulfur-Iodine Cycle (S-I Cycle)

The sulfur–iodine (S-I) cycle was developed by the General Atomics, USA, in the mid-1970s. The cycle involves three chemical reactions that lead to the dissociation of water and produce hydrogen [178–198]. The chemical reactions involved in the S-I cycle are shown in Fig. 8.13.

As shown in Fig. 8.13, Equations 8.1 and 8.3 are endothermic, whereas Equation 8.2 is exothermic. All reactions occur in the fluid phase and no solid phase is involved or formed during these reactions. All reagents, sulfuric acid, HI, and byproducts such as SO_2, and I_2 are recycled, resulting in no effluents from the system. Only water is added to the system, and H_2SO_4 or HI is replenished from time to time. The sulfur-iodine cycle is very advanced; each of the chemical reactions in this process was demonstrated in the laboratory by the US Department of Energy Laboratories, and General Atomics. Japan Atomic Energy Research Institute has developed a demonstration unit. The thermodynamic properties of the cycle have been determined and evaluated and are shown in Fig. 8.14 in a very basic flow diagram.

Based on the three reactions shown in Fig. 8.13, the S-I cycle may be divided into three sections:

Section I: Sulfuric Acid Concentration and Decomposition Section
Section II: Bunsen Reaction Section
Section III: Hydrogen Iodide Decomposition Section

Table 8.6 Most promising thermochemical cycles for hydrogen production from water using nuclear heat

Cycle	Name	T/E[a]	T°C	Reaction	F[b]
1	Westinghouse [183]	T	850	$2H_2SO_4(g) = 2SO_2(g) + 2H_2O(g) + O_2(g)$	1/2
		E	77	$SO_2(g) + 2H_2O(a) = H_2SO_4(a) + H_2(g)$	1
2	Ispra Mark 13 [184]	T	850	$2H_2SO_4(g) = 2SO_2(g) + 2H_2O(g) + O_2(g)$	1/2
		E	77	$2HBr(a) = Br_2(a) + H_2(g)$	1
		T	77	$Br_2(l) + SO_2(g) + 2H_2O(l) = 2HBr(g) + H_2SO_4(a)$	1
3	UT-3 Univ. of Tokyo [185]	T	600	$2Br_2(g) + 2CaO = 2CaBr_2 + O_2(g)$	1/2
		T	600	$3FeBr_2 + 4H_2O = Fe_3O_4 + 6HBr + H_2(g)$	1
		T	750	$CaBr_2 + H_2O = CaO + 2HBr$	1
		T	300	$Fe_3O_4 + 8HBr = Br_2 + 3FeBr_2 + 4H_2O$	1
4	GA Sulfur-Iodine [186]	T	850	$2H_2SO_4(g) = 2SO_2(g) + 2H_2O(g) + O_2(g)$	1/2
		T	300	$2HI = I_2(g) + H_2(g)$	1
		T	100	$I_2 + SO_2(a) + 2H_2O = 2HI(a) + H_2SO_4(a)$	1
5	Julich Center EOS [187]	T	800	$2Fe_3O_4 + 6FeSO_4 = 6Fe_2O_3 + 6SO_2 + O_2(g)$	1/2
		T	700	$3FeO + H_2O = Fe_3O_4 + H_2(g)$	1
		T	200	$Fe_2O_3 + SO_2 = FeO + FeSO_4$	6
6	Tokyo Inst. Tech. Ferrite [188]	T	1,000	$2MnFe_2O_4 + 3Na_2CO_3 + H_2O = 2Na_3MnFe_2O_6 + 3CO_2(g) + H_2(g)$	1
		T	600	$4Na_3MnFe_2O_6 + 6CO_2(g) = 4MnFe_2O_4 + 6Na_2CO_3 + O_2(g)$	1/2
7	Hallett Air Products 1965 [187]	T	800	$2Cl_2(g) + 2H_2O(g) = 4HCl(g) + O_2(g)$	1/2
		E	25	$2HCl = Cl_2(g) + H_2(g)$	1

(continued)

Table 8.6 (continued)

Cycle	Name	T/E[a]	T°C	Reaction	F[b]
8	Gaz de France [187]	T	725	$2K + 2KOH = 2K_2O + H_2(g)$	1
		T	825	$2K_2O = 2K + K_2O_2$	1
		T	125	$2K_2O_2 + 2H_2O = 4KOH + O_2(g)$	1/2
9	Nickel Ferrite [189]	T	800	$NiMnFe_4O_6 + 2H_2O = NiMnFe_4O_8 + 2H_2(g)$	1
		T	800	$NiMnFe_4O_8 = NiMnFe_4O_6 + O_2(g)$	1/2
10	Aachen Univ Julich 1972 [187]	T	850	$2Cl_2(g) + 2H_2O(g) = 4HCl(g) + O_2(g)$	1/2
		T	170	$2CrCl_2 + 2HCl = 2CrCl_3 + H_2(g)$	1
		T	800	$2CrCl3 = 2CrCl_2 + Cl_2(g)$	1
11	Ispra Mark 1C [184]	T	100	$2CuBr_2 + Ca(OH)_2 = 2CuO + 2CaBr_2 + H_2O$	1
		T	900	$4CuO(s) = 2Cu_2O(s) + O_2(g)$	1/2
		T	730	$CaBr_2 + 2H_2O = Ca(OH)_2 + 2HBr$	2
		T	100	$Cu_2O + 4HBr = 2CuBr_2 + H_2(g) + H_2O$	1
12	LASL-U [187]	T	25	$3CO_2 + U_3O_8 + H_2O = 3UO_2CO_3 + H_2(g)$	1
		T	250	$3UO_2CO_3 = 3CO_2(g) + 3UO_3$	1
		T	700	$6UO_3(s) = 2U_3O_8(s) + O_2(g)$	1/2
13	Ispra Mark 8 [184]	T	700	$3MnCl_2 + 4H_2O = Mn_3O_4 + 6HCl + H_2(g)$	1
		T	900	$3MnO_2 = Mn_3O_4 + O_2(g)$	1/2
		T	100	$4HCl + Mn_3O_4 = 2MnCl_2(a) + MnO_2 + 2H_2O$	3/2
14	Ispra Mark 6 [184]	T	850	$2Cl_2(g) + 2H_2O(g) = 4HCl(g) + O_2(g)$	1/2
		T	170	$2CrCl_2 + 2HCl = 2CrCl_3 + H_2(g)$	1
		T	700	$2CrCl_3 + 2FeCl_2 = 2CrCl_2 + 2FeCl_3$	1
		T	420	$2FeCl_3 = Cl_2(g) + 2FeCl_2$	1

Table 8.6 (continued)

Cycle	Name	T/E[a]	T°C	Reaction	F[b]
15	Ispra Mark 4 [184]	T	850	$2Cl_2(g) + 2H_2O(g) = 4HCl(g) + O_2(g)$	1/2
		T	100	$2FeCl_2 + 2HCl + S = 2FeCl_3 + H_2S$	1
		T	420	$2FeCl_3 = Cl_2(g) + 2FeCl_2$	1
		T	800	$H_2S = S + H_2(g)$	1
16	Ispra Mark 3 [184]	T	850	$2Cl_2(g) + 2H_2O(g) = 4HCl(g) + O_2(g)$	1/2
		T	170	$2VOCl_2 + 2HCl = 2VOCl_3 + H_2(g)$	1
		T	200	$2VOCl_3 = Cl_2(g) + 2VOCl_2$	1
17	Ispra Mark 2 (1972) [184]	T	100	$Na_2O.MnO_2 + H_2O = 2NaOH(a) + MnO_2$	2
		T	487	$4MnO_2(s) = 2Mn_2O_3(s) + O_2(g)$	1/2
		T	800	$Mn_2O_3 + 4NaOH = 2Na_2O.MnO_2 + H_2(g) + H_2O$	1
18	Ispra CO/Mn_3O_4 [190]	T	977	$6Mn_2O_3 = 4Mn_3O_4 + O_2(g)$	1/2
		T	700	$C(s) + H_2O(g) = CO(g) + H_2(g)$	1
		T	700	$CO(g) + 2Mn_3O_4 = C + 3Mn_2O_3$	1
19	Ispra Mark 7B [184]	T	1,000	$2Fe_2O_3 + 6Cl_2(g) = 4FeCl_3 + 3O_2(g)$	3/4
		T	420	$2FeCl_3 = Cl_2(g) + 2FeCl_2$	3/2
		T	650	$3FeCl_2 + 4H_2O = Fe_3O_4 + 6HCl + H_2(g)$	1
		T	350	$4Fe_3O_4 + O_2(g) = 6Fe_2O_3$	1/4
		T	400	$4HCl + O_2(g) = 2Cl_2(g) + 2H_2O$	3/2
20	Vanadium Chloride [191]	T	850	$2Cl_2(g) + 2H_2O(g) = 4HCl(g) + O_2(g)$	1/2
		T	25	$2HCl + 2VCl_2 = 2VCl_3 + H_2(g)$	1
		T	700	$2VCl_3 = VCl_4 + VCl_2$	2
		T	25	$2VCl_4 = Cl_2(g) + 2VCl_3$	1

(continued)

Table 8.6 (continued)

Cycle	Name	T/E[a]	T°C	Reaction	F[b]
21	Mark 7A [184]	T	420	$2FeCl_3(l) = Cl_2(g) + 2FeCl_2$	3/2
		T	650	$3FeCl_2 + 4H_2O(g) = Fe_3O_4 + 6HCl(g) + H_2(g)$	
		T	350	$4Fe_3O_4 + O_2(g) = 6Fe_2O_3$	1/4
		T	1,000	$6Cl_2(g) + 2Fe_2O_3 = 4FeCl_3(g) + 3O_2(g)$	1/4
		T	120	$Fe_2O_3 + 6HCl(a) = 2FeCl_3(a) + 3H_2O(l)$	1
22	GA Cycle 23 [192]	T	800	$H_2S(g) = S(g) + H_2(g)$	1
		T	850	$2H_2SO_4(g) = 2SO_2(g) + 2H_2O(g) + O_2(g)$	1/2
		T	700	$3S + 2H_2O(g) = 2H_2S(g) + SO_2(g)$	1/2
		T	25	$3SO_2(g) + 2H_2O(l) = 2H_2SO_4(a) + S$	1/2
		T	25	$S(g) + O_2(g) = SO_2(g)$	
23	US-Chlorine [187]	T	850	$2Cl_2(g) + 2H_2O(g) = 4HCl(g) + O_2(g)$	1/2
		T	200	$2CuCl + 2HCl = 2CuCl_2 + H_2(g)$	1
		T	500	$2CuCl_2 = 2CuCl + Cl_2(g)$	1
24	Ispra Mark 9 [184]	T	420	$2FeCl_3 = Cl_2(g) + 2FeCl_2$	3/2
		T	150	$3Cl_2(g) + 2Fe_3O_4 + 12HCl = 6FeCl_3 + 6H_2O + O_2(g)$	1/2
		T	650	$3FeCl_2 + 4H_2O = Fe_3O_4 + 6HCl + H_2(g)$	1
25	Ispra Mark 6C [184]	T	850	$2Cl_2(g) + 2H_2O(g) = 4HCl(g) + O_2(g)$	1/2
		T	170	$2CrCl_2 + 2HCl = 2CrCl_3 + H_2(g)$	1
		T	700	$2CrCl_3 + 2FeCl_2 = 2CrCl_2 + 2FeCl_3$	1
		T	500	$2CuCl_2 = 2CuCl + Cl2(g)$	1

Source: Brown et al. [167]

[a] *T* Thermochemical, *E* Electrochemical

[b] Reactions are stored in database with minimum integer coefficients. Multiplier from reaction junction table converts the results to the basis of one mole of water decomposed

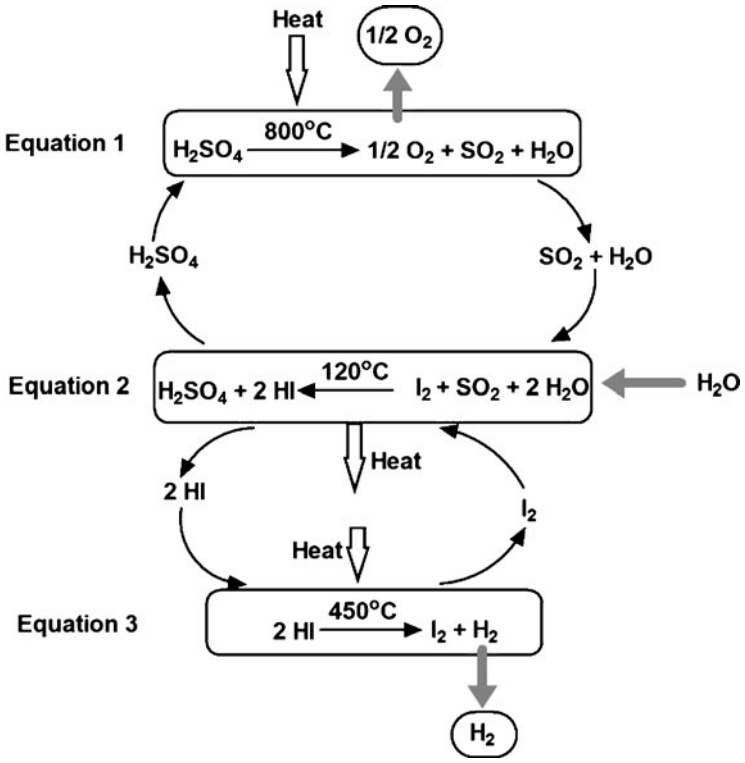

Fig. 8.13 Sulfur-iodine process (Source: Brown [199])

Section I: Sulfuric Acid Concentration and Decomposition Section

This section of the S-I cycle is the most critical and also determines the efficiency of the process. In this section, H_2SO_4 is decomposed to SO_2, O_2, and H_2O. A temperature greater than 850°C is required to decompose H_2SO_4. Sulfuric acid stream from this section that contains approximately 57% acid is concentrated to about 86% acid in the first step. The concentration of acid is generally carried out under a vacuum of 0.1 bar. The acid stream is then pressurized to about 70 bars. A schematic flow diagram of this section is shown in Fig. 8.15.

The decomposition reaction consists of the two following reactions:

$$H_2SO_4 = SO_3 + H_2O \tag{8.26}$$

$$SO_3 = SO_2 + 1/2\ O_2 \tag{8.27}$$

The first reaction (Eq. 8.26) takes place at around 350°C with or without catalysts. The second reaction (Eq. 8.27) occurs above 750°C in the presence of a catalyst. Both the reactions are endothermic and the required heat could be supplied by Generation IV-Very High Temperature Reactors (VHTR), which use helium as a

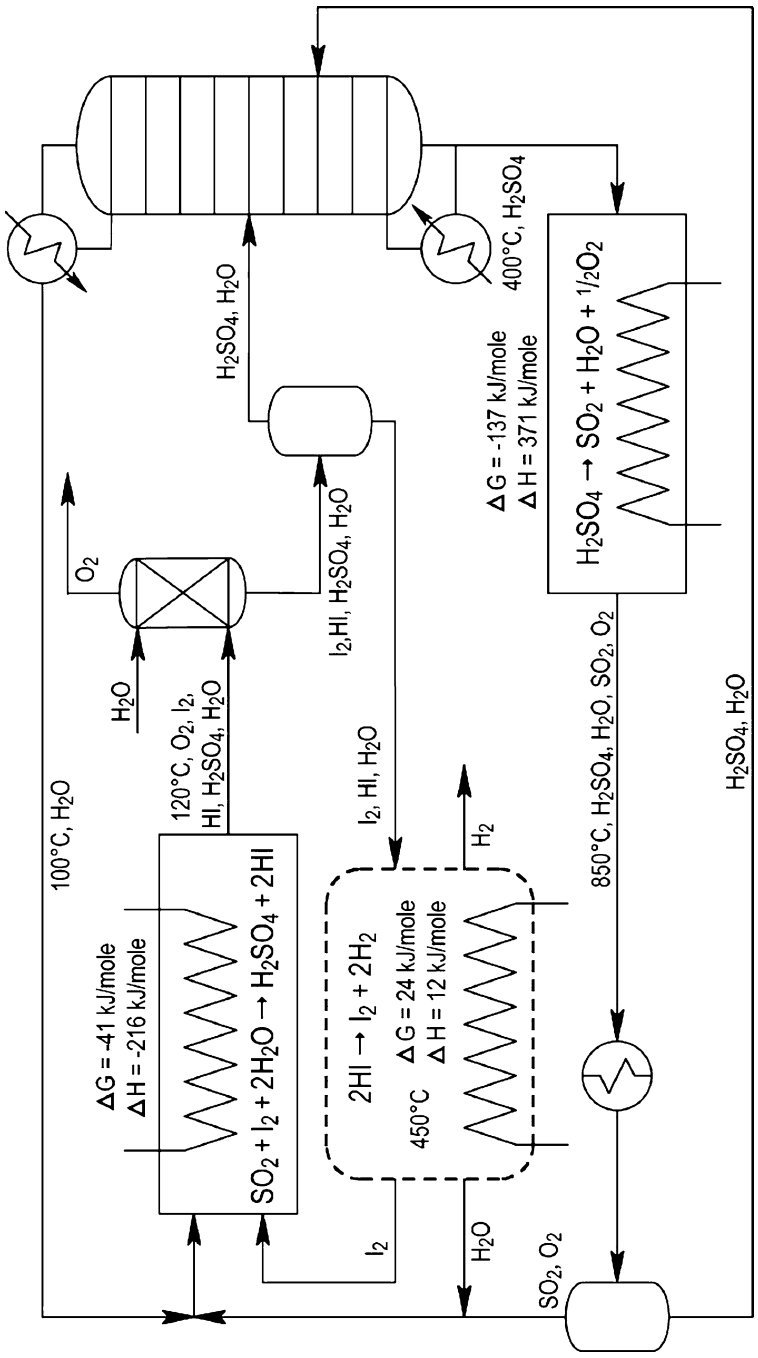

Fig. 8.14 Schematic representation of sulfur-iodine cycle (Brown et al. [200])

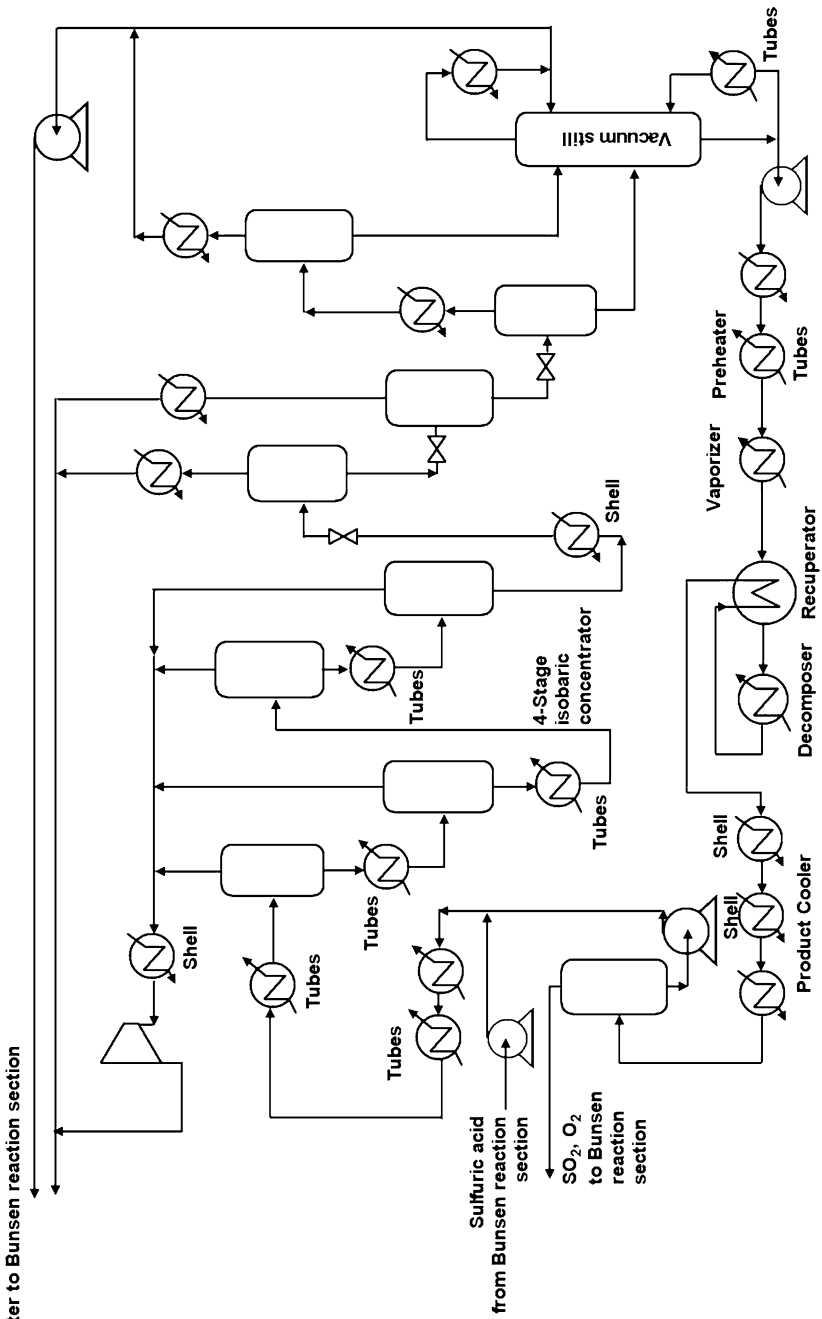

Fig. 8.15 A schematic flow diagram of the sulfuric acid concentration and decomposition section (Brown et al. [200])

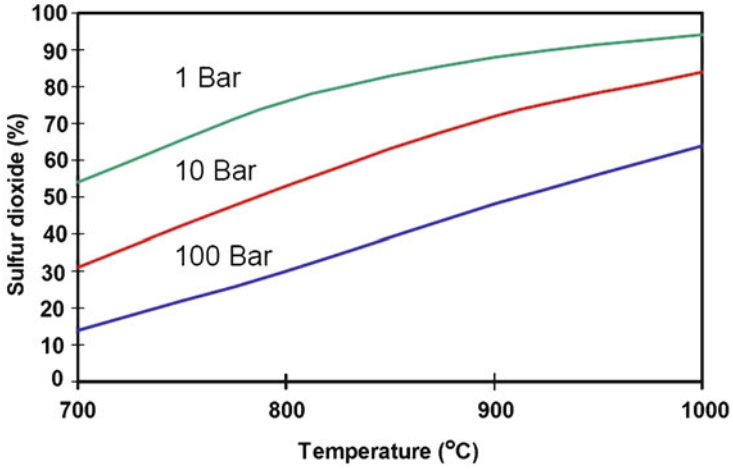

Fig. 8.16 Effect of pressure on SO_2 production during H_2SO_4 decomposition in the S-I cycle (Source: Pickard [201])

cooling gas that is pressurized over 40 bars. The VHTR systems have been described in detail in Chap. 9 of Volume I of this book series. For efficient operation of the heat exchanger, H_2SO_4 decomposition reactions should be carried out under a pressure as high as the heat exchanger wall would permit, although, the equilibrium conversion to SO_3 and H_2O, and SO_2 and O_2 are unfavorable according to the Le Chatelier's principle. As can be seen from Fig. 8.16, at higher pressures, decomposition of H_2SO_4 to SO_2 decreases.

Various types of catalysts have been explored for H_2SO_4 decomposition reaction and high SO_2 yield [202–216]. Platinum on porous metal oxides as the support material is found to be the most promising than other catalyst in terms of SO_2 yield, stability, and resistance to corrosion [217]. However, Pickard [201] noted that Pt based catalysts are not stable in the high-temperature reaction environment and deactivate due to sintering of Pt and supports. As much as 30% of Pt was lost during 10 days of testing. Both sintering and volatilization of Pt were noted. Test results using Pt catalysts with different loading are shown in Fig. 8.17. Although Pt based catalysts were found to be the most promising, their cost is a major issue in determining the overall economics of the process. A number of other catalysts were explored under the US DOE hydrogen program. The SO_2 yield by various non-Pt based catalysts is summarized in Fig. 8.18. Among these catalysts $CuCr_2O_4$, $NiCr_2O_4$, and $FeTiO_3$ had leaching problems. Activity of $FeTiO_3$ and $NiFe_2O_4$ decreased at the highest temperature, and $CuFe_2O_4$-spinel was found to be most promising at high temperatures.

Both reactants and products of these two reactions are highly corrosive, and only a few materials may be used at these severe reaction conditions of high temperature and pressure [217–220]. Sandia National Laboratory (SNL), USA, has designed a H_2SO_4 decomposer in which both reactions could take place.

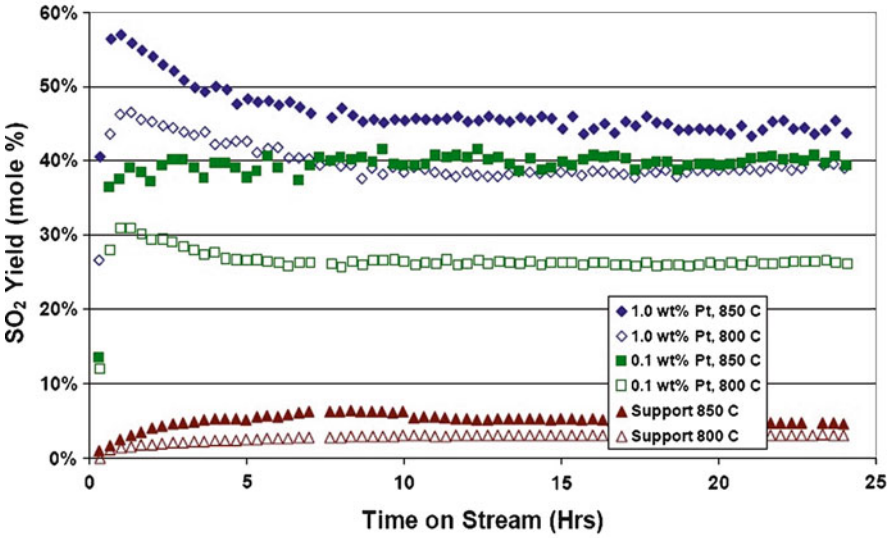

Fig. 8.17 SO_2 yield by Pt based catalysts (Source: Pickard [221])

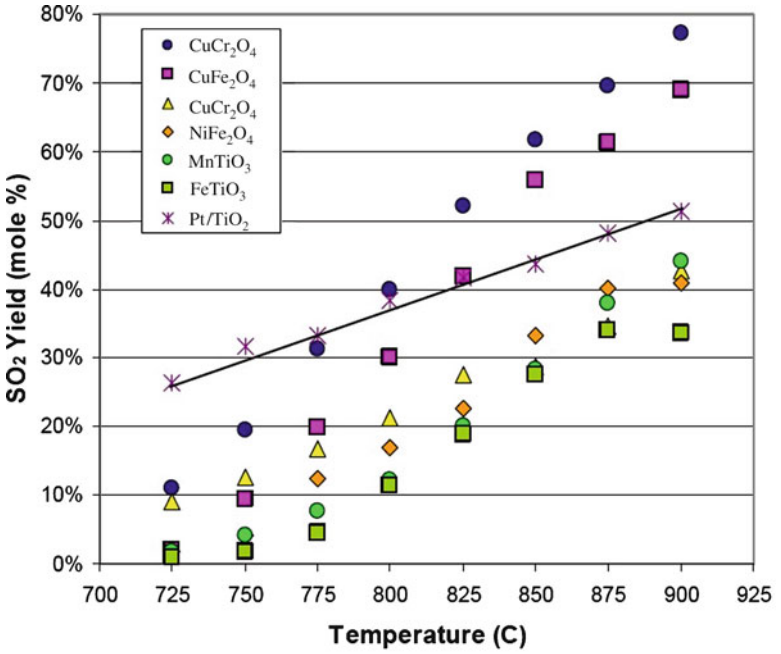

Fig. 8.18 SO_2 yield by non-Pt based catalysts (Source: Pickard [221])

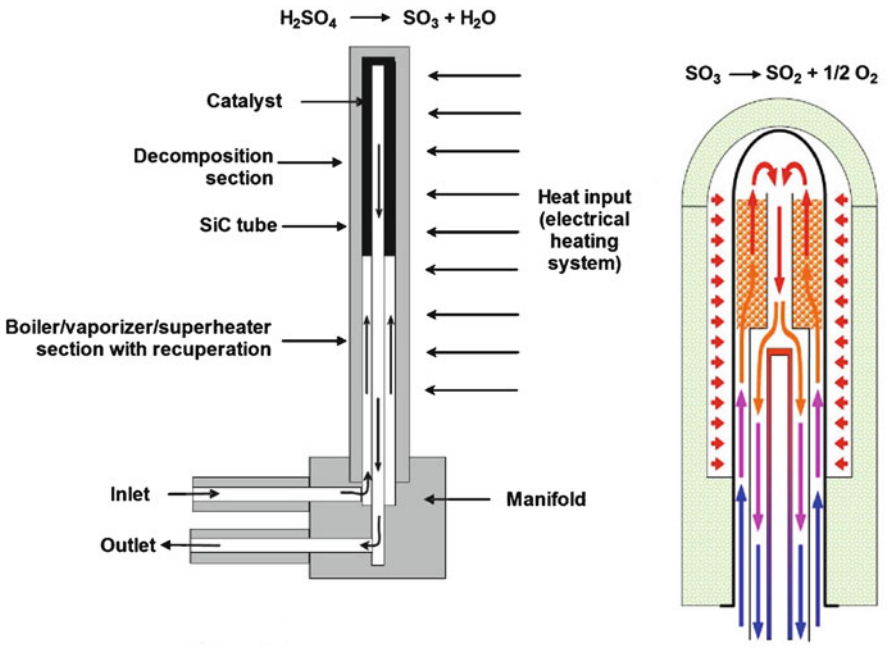

Fig. 8.19 SiC bayonet heat exchanger (Source: Evans [222])

The decomposition reaction takes place within the individual tube of a multi-tube reactor that is fed with liquid H_2SO_4 at 50–150°C. SNL proposed to use silicon carbide (SiC) for the reactor, which has excellent resistance to sulfuric acid and SO_3 at high temperatures, but it possesses ceramic-like properties. Various problems such as the lack of flexible connection between parts and high pressure sealing still need to be resolved (see Fig. 8.19).

Section II: Bunsen Reaction Section

Water reacts with iodine and SO_2 spontaneously at a temperature between 80°C and 120°C and 10 bar pressure [223–232]. The Bunsen reaction is conducted with an excess of iodine to promote the separation of the two phases. Two liquid immiscible phases, one containing a mixture of H_2SO_4 and water, and the other containing HI, I_2 and water, are formed. These two phases are separated from each other by utilizing the difference in their specific gravity. There are four steps, including the Bunsen reaction in this section. A schematic flow diagram of this Bunsen section is shown in Fig. 8.20.

Oxygen that is formed from the water decomposition reaction is removed from the stream to avoid any complex formation later in the process. Sulfur dioxide is also removed from the product stream to prevent any side reaction. Finally, water

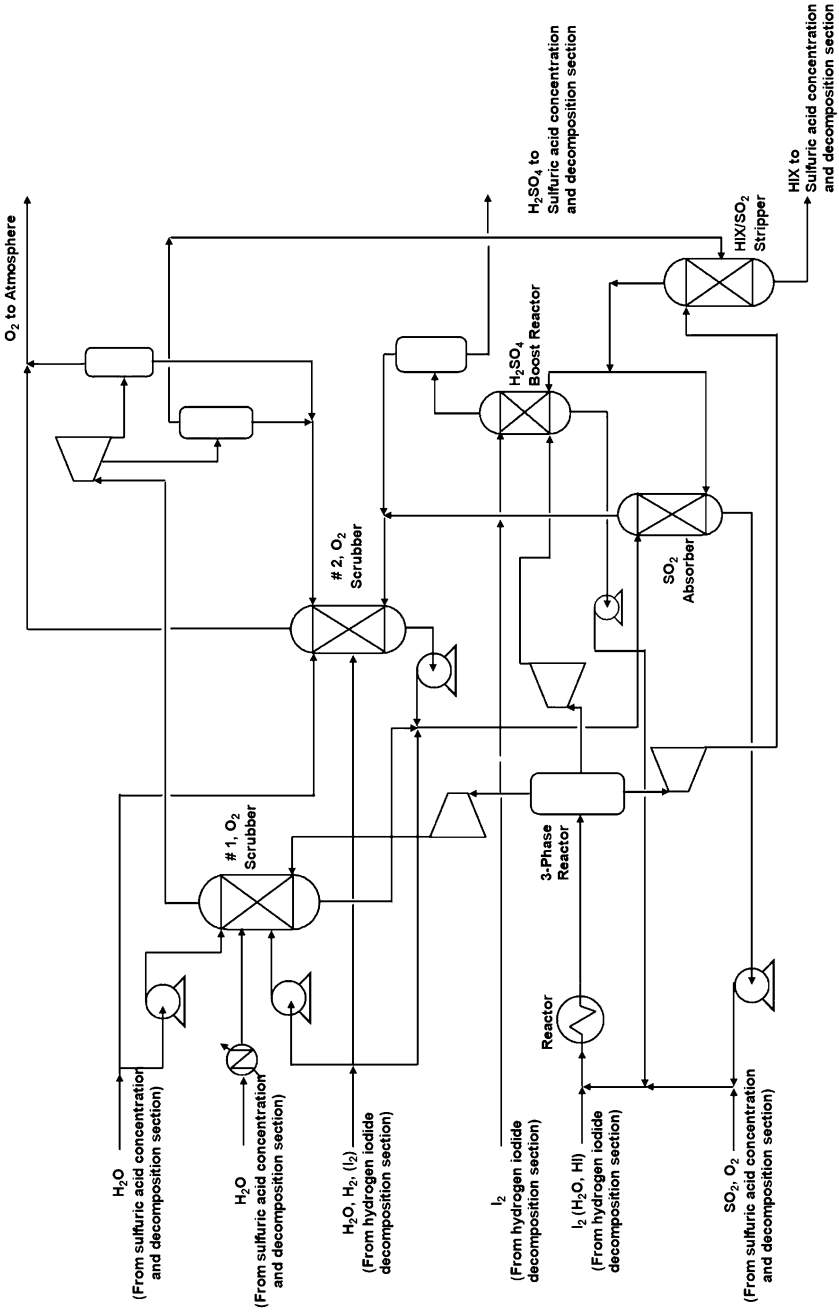

Fig. 8.20 A schematic flow diagram of a Bunsen reaction (Adapted from Brown et al. [200])

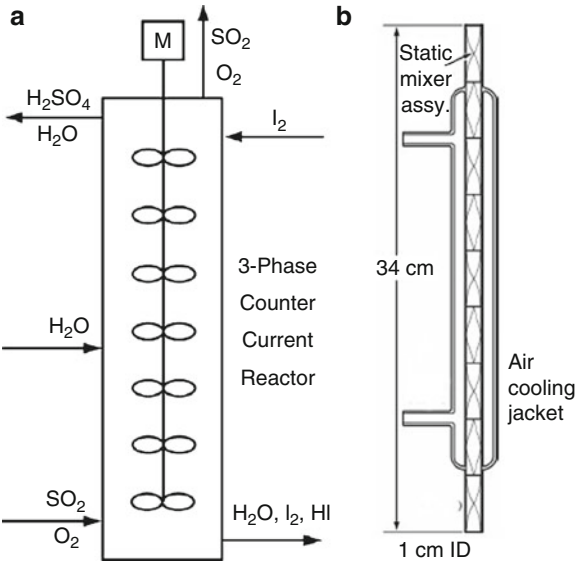

Fig. 8.21 Reactor design for a Bunsen reaction of the sulfur-iodine cycle (**a**) countercurrent reactor (**b**) co-current reactor (Source: Brown [199])

present in the HI–I_2 product stream is removed before it is sent to Section III: Hydrogen Iodide Decomposition Section. This helps in the energy balance of the system since water does not have to be evaporated again in Section III: Hydrogen Iodide Decomposition Section. The $H_2SO_4-H_2O$ phase contains about 50–57%w/w H_2SO_4 and is sent back to Section II: Bunsen Reaction Section to further concentrate H_2SO_4 to 90–98%w/w.

The reactor for the Bunsen reaction may play a critical role in the process evaluation. Both counter-current and co-current configurations have been studied. A co-current Bunsen reactor has the following characteristics:

- Short residence time
- Efficient heat exchanger
- No side reactions
- Reactor previously demonstrated

The characteristics of the counter-current reactor are as follows:

- Fewer pieces of equipment
- Fewer streams
- Less recycle
- Scale-up concerns

Both reactor designs are shown in Fig. 8.21. The co-current design features do not provide any significant advantages over the counter-current configurations. Further study is necessary before selecting a configuration.

Section III: Hydrogen Iodide Decomposition Section

This section produces H_2 by decomposing hydrogen iodide (HI) that is present in the HI_x feed stream [233–238]. Hydrogen iodide is separated from the feed stream followed by decomposition into H_2 and I_2. Two approaches have been suggested for this section: extractive and reactive distillation. Extractive distillation is more advanced than the reactive distillation, and all processing steps are well studied and demonstrated in laboratories. The reactive distillation is a fairly new concept and various processing steps and corresponding data are yet to be obtained. Although the reactive distillation needs fewer pieces of equipment with less streams, it is based on extrapolated phase equilibria data. These two distillation systems are described next.

Extractive Distillation A schematic diagram of the extractive distillation process is shown in Fig. 8.22. One of the main issues of separating HI, I_2, and H_2O from their mixture is that the mixture forms an azeotrope (i.e., the whole mixture starts boiling at a certain temperature resulting in a composition of gas phase that is the same as that of the liquid phase near the boiling point).

The extractive distillation process takes advantage of the solubility of HI and H_2O and the insolubility of I_2 in phosphoric acid (H_3PO_4). Additionally, H_3PO_4 breaks down the azeotrope mixture. About 96 wt% H_3PO_4 is added to the feed stream of HI_x from Section I: Sulfuric Acid Concentration and Decomposition Section. This results in a formation of two phases that are separated from each other by gravity. The denser phase, I_2, is returned to the Bunsen reaction section and the lighter phase containing HI and H_2O is fed to the distillation column. Hydrogen iodide is boiled off in the column and the gaseous HI stream is fed to the decomposition vessel where it breaks down to H_2 and I_2 in the presence of a carbon based catalyst. The HI decomposition reaction can be carried out either in the gas phase at 350–450°C or in the liquid phase at 150–300°C. The hydrogen and unreacted HI are separated from I_2, which is returned to the Bunsen reactor. The gaseous H_2 product is separated from HI by using a membrane. Hydrogen iodide is recycled back to the reactor, and pure hydrogen is stored in an appropriate storage medium. At 450°C, the equilibrium decomposition of HI is about 22%, therefore, the reaction products must be removed from the reaction chamber to maintain this equilibrium conversion rate. Phosphoric acid is concentrated to 96% in the distillation column and is added to the incoming stream from Section I: Sulfuric Acid Concentration and Decomposition Section.

Reactive Distillation In the reactive distillation method, no attempt is made to break the azeotrope point of the mixture. The mixture from Section I: Sulfuric Acid Concentration and Decomposition Section is distilled under pressure in the distillation column. HI is decomposed within the column by a catalyst in the gas phase. A schematic diagram of the process is shown in Fig. 8.23. HI_x feed from Section I: Sulfuric Acid Concentration and Decomposition Section is heated to about 260–265°C from 120°C before feeding it to the reactive distillation column. The temperature at the bottom of the column is maintained at about 300°C at which

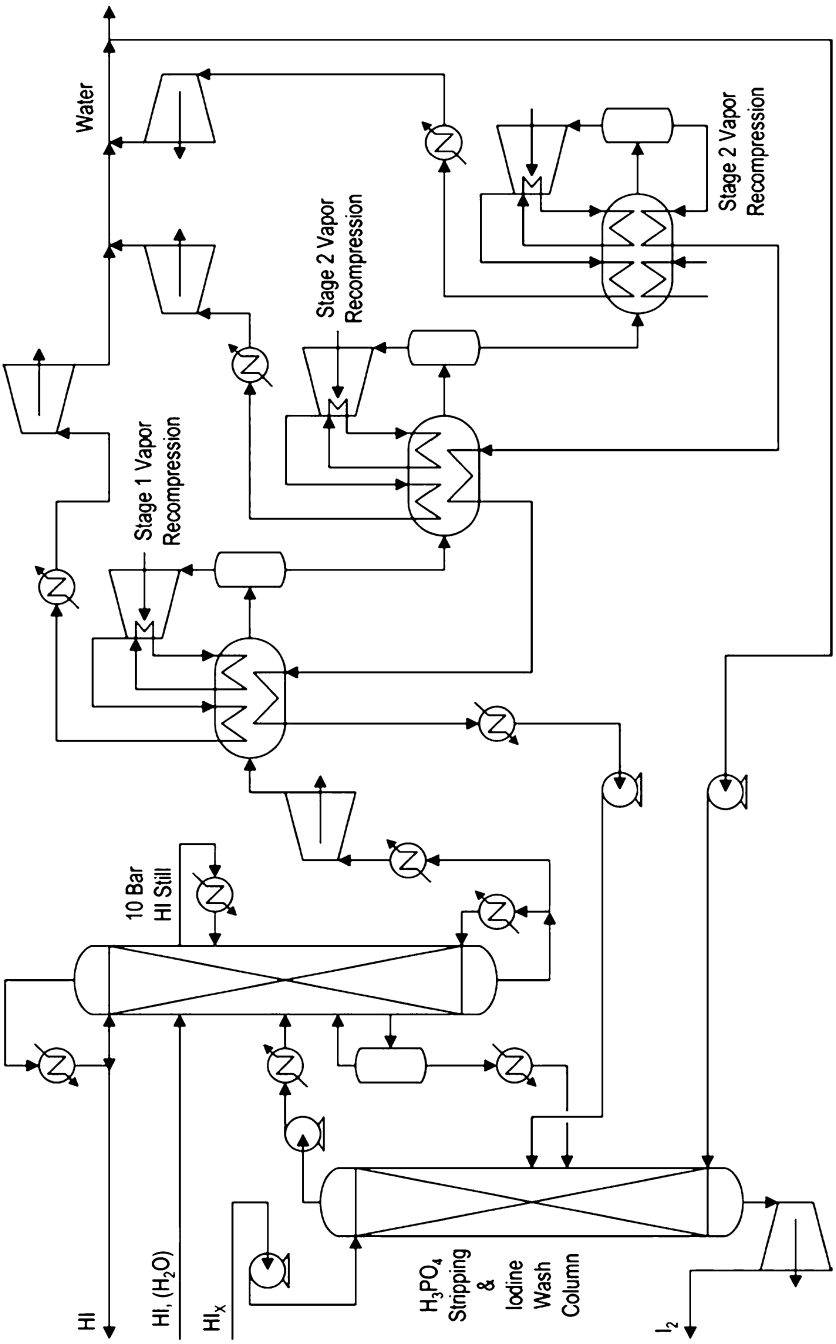

Fig. 8.22 Extractive distillation flowsheet (Source: Brown [199])

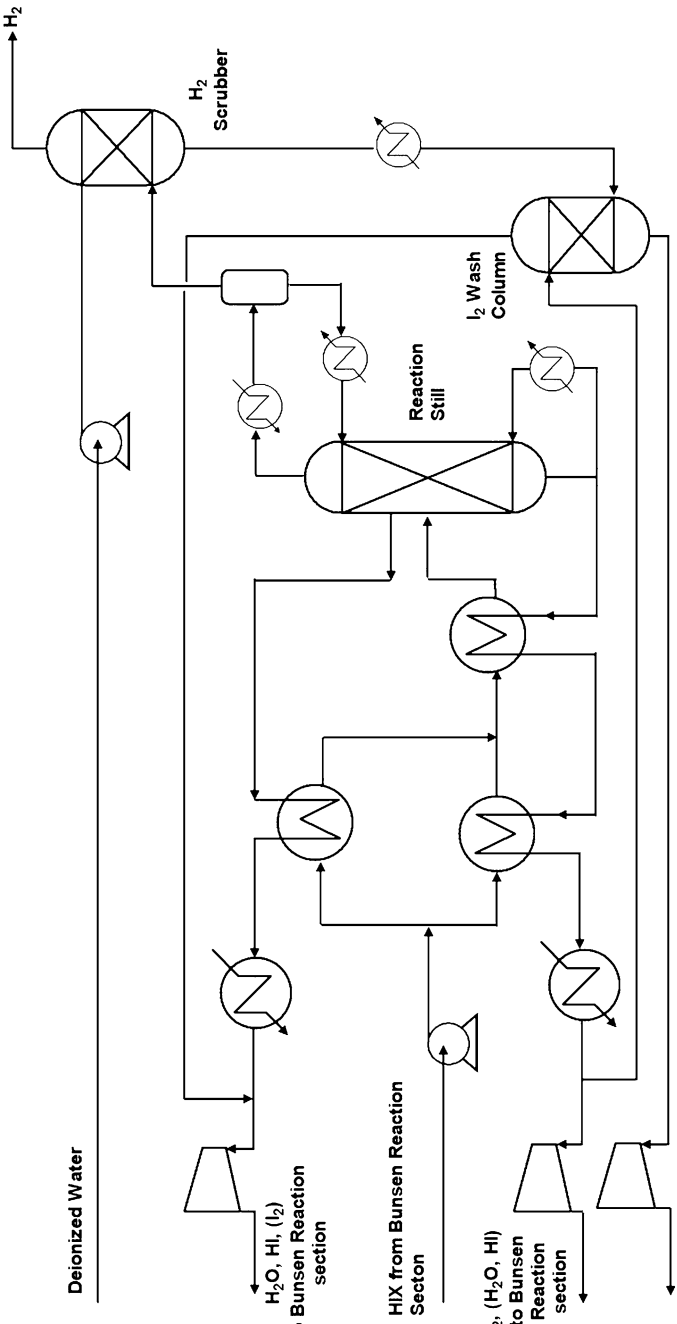

Fig. 8.23 A schematic flow diagram of reactive distillation method for a Bunsen reaction (Adapted from Brown et al. [199])

HI_x boils and maintains a vapor pressure of about 52 bar. The mixture of HI, I_2, and H_2O flows upward through a bed of activated carbon catalyst placed at the upper half of the column. HI is decomposed to H_2 and I_2 within the column in the presence of the catalyst, which is maintained at a temperature of 300°C. A condenser removes unreacted HI, I_2 and water from the stream, and the liquid stream from the condenser is recycled back to the column.

Brown et al. [200] noted that about 16% of the HI is decomposed in a single pass in the reactive distillation configuration. The recycling, together with approximately five times of excesses iodine, is required in the product flow stream from the Bunsen reaction section to the sulfuric acid concentration and decomposition section. Also, the equal amount of water is necessary, which means that for each mole of hydrogen produced, approximately 6 moles of HI, 30 moles of iodine and 30 moles of water must flow from the Bunsen Reaction Section to the Sulfuric Acid Concentration and Decomposition Section, and 5 moles of HI, 30 moles of iodine and 30 moles of water must flow back from the sulfuric acid concentration and decomposition section to the Bunsen Reaction Section.

Efficiency of the S-I Cycle

The efficiency of the S-I cycle depends on the mode of operation and the flow sheet followed for the cycle [239,240]. If high temperature helium from the reactor is split into two streams to provide the energy for Sections II: Bunsen Reaction Section and Section III: Hydrogen Iodide Decomposition Section in a parallel configuration, an efficiency of 42% may be expected. The efficiency may be increased to 48% (when both hydrogen and electricity production are considered) by heating Section III: Hydrogen Iodide Decomposition Section with the waste heat from a Brayton cycle. Even a higher efficiency could be achieved by raising the process temperature. The graph shown in Fig. 8.24 indicates that a hydrogen production efficiency of 51% could be obtained using a peak process temperature of 900°C. The efficiency of an S-I cycle may be expressed by the following expression:

$$\eta_{H,SI} = \frac{Q_{H,out}}{Q_{in,SI}} = \frac{HHV_H}{Q_{in,SI}} \tag{8.28}$$

where $Q_{H,out}$ is the High Heating Value (HHV) carried away by hydrogen per unit basis, and $Q_{in,SI}$ is the total thermal energy necessary to produce a unit amount of hydrogen. A more effective heat recuperation configuration, better heat exchanger materials that can withstand high pressure differential and materials that can perform at higher temperatures can further increase the efficiency.

Efficiencies of various processes under different operating conditions are shown in Fig. 8.25.

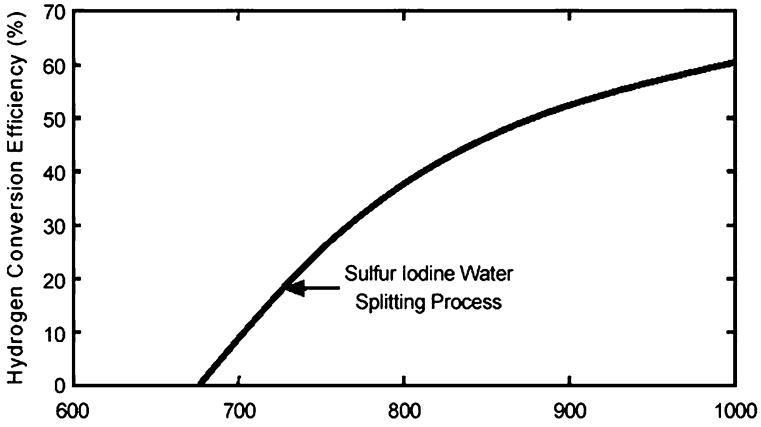

Fig. 8.24 Estimated sulfur iodine hydrogen production efficiency vs process temperature (Source: Brown et al. [199])

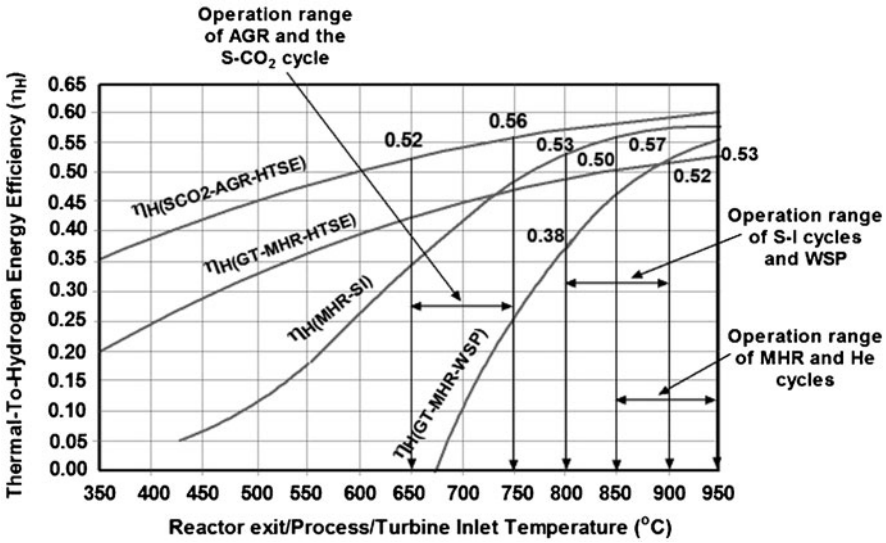

Fig. 8.25 Efficiency comparison among SI, HTSE, and WSP cycles for hydrogen production (Printed with permission from Yildiz and Kazimi [160])

8.6.3.2 Ca–Br–Fe (UT-3) Cycle

The UT-3 cycle was first proposed by the University of Tokyo, Japan. This cycle involves solid–gas interactions and requires a lower temperature compared to the S-I cycle. Various aspects of an UT-3 cycle are discussed in the following references [241–270]. The solid-gas system allows better separation of products. The UT-3

cycle involves four reactions that take place in four adiabatic fixed packed bed chemical reactors that contain the solid reactants and products.

$$\begin{aligned} CaBr_2 + H_2O &\xrightarrow{730^\circ C} CaO + 2HBr \\ CaO + Br_2 &\xrightarrow{550^\circ C} CaBr_2 + 1/2\, O_2 \\ Fe_3O_4 + 8HBr &\xrightarrow{220^\circ C} 3FeBr_2 + 4H_2O + Br_2 \\ 3FeBr_2 + 4H_2O &\xrightarrow{650^\circ C} Fe_3O_4 + 6HBr + H_2 \end{aligned} \tag{8.29}$$

A schematic diagram of the cycle is presented in Fig. 8.26. As shown in the figure, two reactors involve reactions with calcium compounds, and the other two reactors involve reactions with the iron compounds.

The thermodynamic calculations using Eq. 8.29 showed these reactions to be favorable under normal operating temperatures. Free energies of these reactions were studied at the Argonne National Laboratory (ANL), USA, which showed the viability of the process. Free energies of these reactions are given in Fig. 8.27. The cycle efficiency is found to be limited by the temperature of the first reaction, since $CaBr_2$ melts at 760°C. Because of this limitation on the temperature, the hydrogen production efficiency of the process is limited to about 40%. ANL is working on coupling a UT-3 cycle to a Secure Transportable Autonomous Reactor (STAR). However, the operation of the STAR, which is a liquid-metal reactor, requires a temperature above 600°C.

The thermal energy from a nuclear reactor can be used directly to heat the gaseous stream, which flows through the four reactors (one for each reaction) and other process equipment before being recycled back to the nuclear reactor. Solid reactants in each reactor go through a regeneration cycle. The gaseous reactant passes through the bed of solid reactant until it is all consumed. For example, the first reaction continues until all of $CaBr_2$ is converted to CaO by the reaction. At this point, the flow paths are switched and chemical reactors, in each pair, switch functions. Now the second reaction takes place in the first reactor. A similar reaction sequence occurs in Fe-reactors.

The gaseous reactants/products by themselves are not capable of carrying all the thermal energy necessary for these reactions. A large quantity of steam is used as the carrier of the thermal energy. A steam pressure of about 20 bar is used in the cycle, which also helps to remove the products from the reactors by shifting the reaction equilibrium towards completion. This is necessary since the Gibbs free energy is positive for some of the reactions.

8.6.3.3 Cu–Cl Cycle

The copper–chlorine thermochemical cycle is expected to operate at 500°C [272–292], allowing the use of a number of Generation IV reactors, such as the sodium-cooled fast reactor (SFR). Generation IV reactors are described in Chap. 9

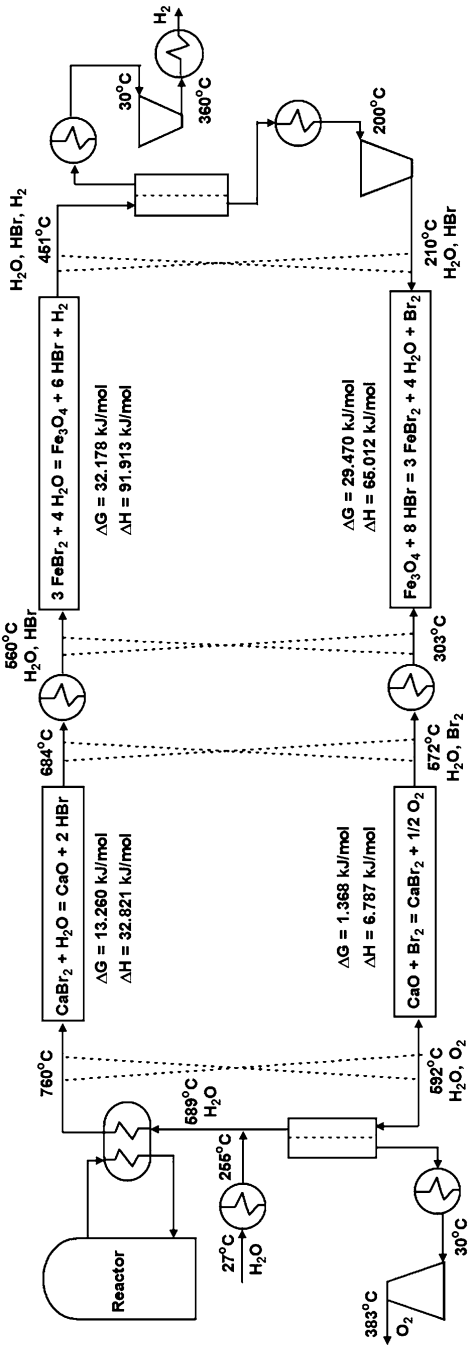

Fig. 8.26 Process flow diagram of the adiabatic UT-3 system (Source: Brown et al. [167])

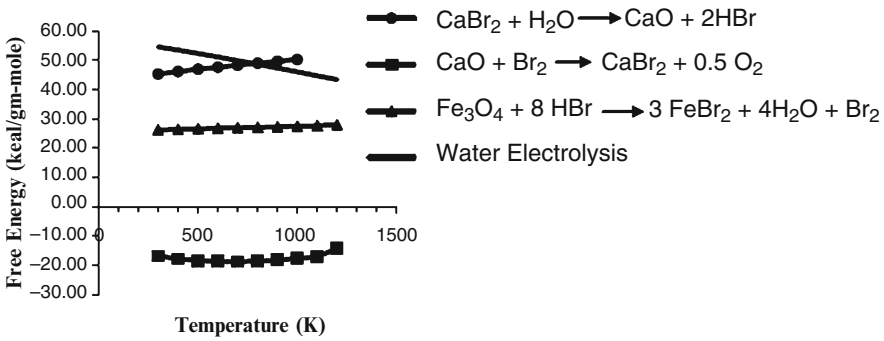

Fig. 8.27 Gibbs free energies of the reactions involved in UT-3 cycles (Adapted from Doctor et al. [271])

of Volume 1 of this book series. The materials of construction may be cheaper due to the lower temperature and less corrosion. The energy efficiency of the process is projected to be 40–45%. Both thermal and electrical energy are necessary in this cycle. The cycle involves the following reactions:

$$2Cu + 2HCl \xrightarrow{450^\circ C} 2CuCl + H_2$$

$$4CuCl + 4Cl^- \xrightarrow{30^\circ C} 4CuCl^{-2}$$

$$4CuCl^{-2} \xrightarrow{30^\circ C} 2CuCl_2 + 2Cu + 4Cl^-$$

$$2CuCl_2(aq) \xrightarrow{100^\circ C} 2CuCl_2(s)$$

$$2CuCl_2 + H_2O \xrightarrow{400^\circ C} CuO + CuCl_2 + 2HCl$$

$$CuO + CuCl_2 \xrightarrow{500^\circ C} 2CuCl + \frac{1}{2}O_2 \tag{8.30}$$

The general concept of the cycle is shown in Fig. 8.28 and a proposed schematic diagram of the cycle along with various process parameters are given in Fig. 8.29.

The first reaction of the Cu–Cl cycle occurs at 430–475°C producing H_2. The reactions of the cycle proceed as follow. Copper particles enter the reaction chamber, flow downward and react with incoming HCl vapor producing H_2 and liquid CuCl. The second reaction is carried out in an electrochemical cell where CuCl is decomposed to Cu and $CuCl_2$. The Cu particles are fed back to first reaction chamber. $CuCl_2$ goes into the aqueous phase. The aqueous $CuCl_2$ stream exiting from the electrochemical cell is preheated to 150°C before feeding into a flash dryer to produce solid $CuCl_2$(s) that reacts with water vapor to produce gaseous HCl(g) in a fluidized bed reactor. The product is HCl(g) and CuO^*CuCl_2 solid particles. The HCl(g) is recycled back for the hydrogen production, while the CuO^*CuCl_2 particles are decomposed to produce oxygen and complete the cycle.

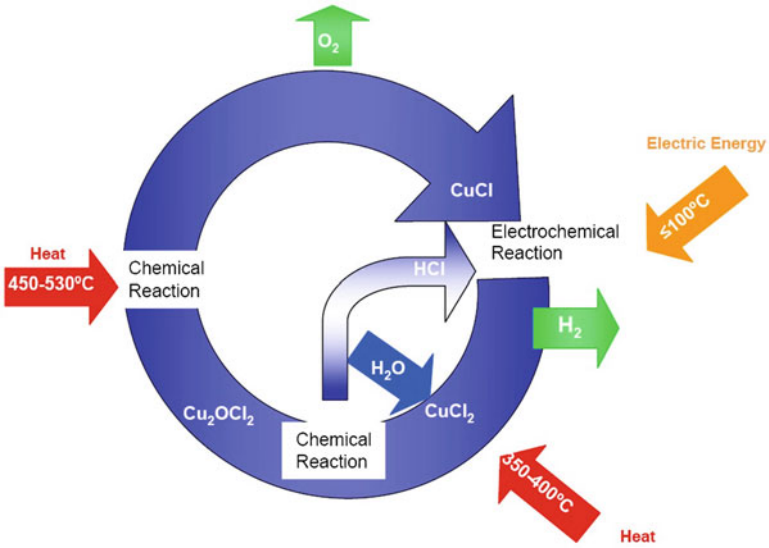

Fig. 8.28 Basic concept of Cu–Cl cycle for hydrogen production (Adapted from Lewis [292])

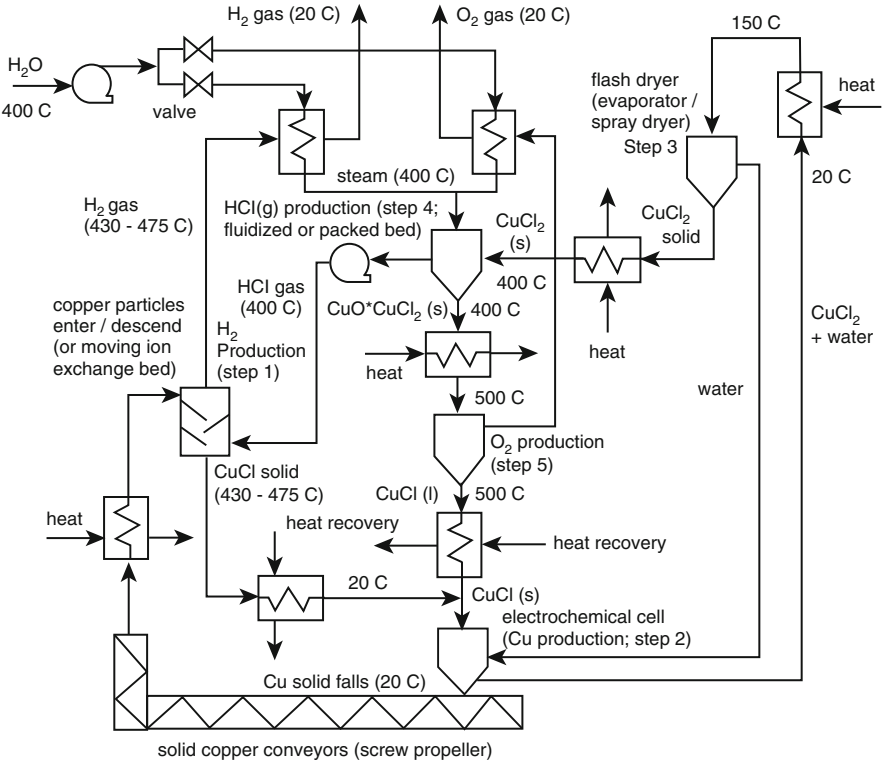

Fig. 8.29 Conceptual layout of a copper-chlorine (Cu–Cl) cycle (Adapted from Rosen et al. [293])

A detailed thermodynamic analysis of the process was carried out by ANL. The free energies of all the reaction steps were determined. It is concluded that all of these reactions are thermodynamically favorable based on the values of the free energies.

Thermal Efficiency of the Cu–Cl Cycle

The efficiency of the Cu–Cl can be calculated from the following expression:

$$\eta = \frac{-\Delta H^{o}_{25^{\circ}\mathrm{C}}(H_2O)}{Q_{hot} + \frac{W}{0.5}} \tag{8.31}$$

The thermal efficiency of the process is obtained by dividing the lower heating value (LHV) of the hydrogen products from the reaction by the sum of thermal heat and electrical energy input to the system (converted to thermal equivalent with a 50% factor). The efficiency is found to be:

$\eta = 44\%$ with thermal + electrolysis energy, or
$\eta = 41\%$ including all the energy loss + shaft work

8.6.3.4 Comparison of the Processes

Yildiz and Kazimi [167] compared various cycles that are proposed for hydrogen production using nuclear energy. Various aspects of the processes were considered in the analysis. Their analysis is given in Table 8.6. Wang et al. [285] compared the S–I and Cu–Cl cycles. They noted that the overall heat requirements of the two cycles are similar to each other, and the overall efficiencies are also in the same range; between 37% and 54%. The higher efficiencies depend on the heat recovery. However, the copper–chlorine cycle has the advantage of a lower maximum temperature of 530°C, which is 27°C lower than the maximum temperature of 850°C in the sulfur–iodine cycle.

8.6.3.5 Reactor Types for Hydrogen Production

One of the design objectives of Generation IV nuclear reactors is to facilitate hydrogen production. The plan is to use the thermal energy generated from the nuclear reactor directly to supply all the energy needs of the hydrogen production plant [294–302]. The requirements and criteria for the selection of a reactor type have been discussed by Schultz et al. [302] and are given below:

Basic requirements

1. Chemical compatibility of coolant with primary loop materials and fuel.
2. Coolant molecular stability at operating temperatures in a radiation environment.

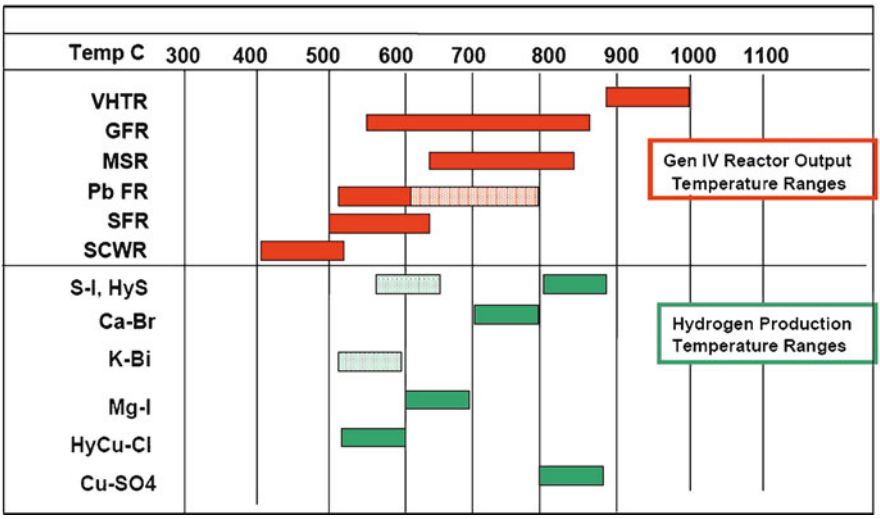

Fig. 8.30 Temperature output from various nuclear reactors and the maximum temperature requirements for thermochemical cycles (Adapted from Evans [222])

3. Pressure requirements for primary loop.
4. Nuclear requirements: parasitic neutron capture, neutron activation, fission product effects, gas buildup, etc.
5. Basic feasibility, general development requirements, and development risk.

Important Criteria

1. Safety
2. Operational issues
3. Capital costs
4. Intermediate loop compatibility
5. Other merits and issues

Based on these criteria, Schultz et al. [302] proposed several reactors that are suitable for hydrogen production which are shown in Fig. 8.30. These reactors are described in Chap. 9 of Volume 1 of this book series.

Nuclear reactors provide a number of options regarding hydrogen plant configurations [303–313]. A reactor can be dedicated for either H_2 production only or both for hydrogen production and electricity generation. The plant size can be large, modular, or distributed. These reactors also provide the operational flexibility of either electricity generation depending on the load, or hydrogen generation without changing the reactor power. Hydrogen can be produced by using either direct heat

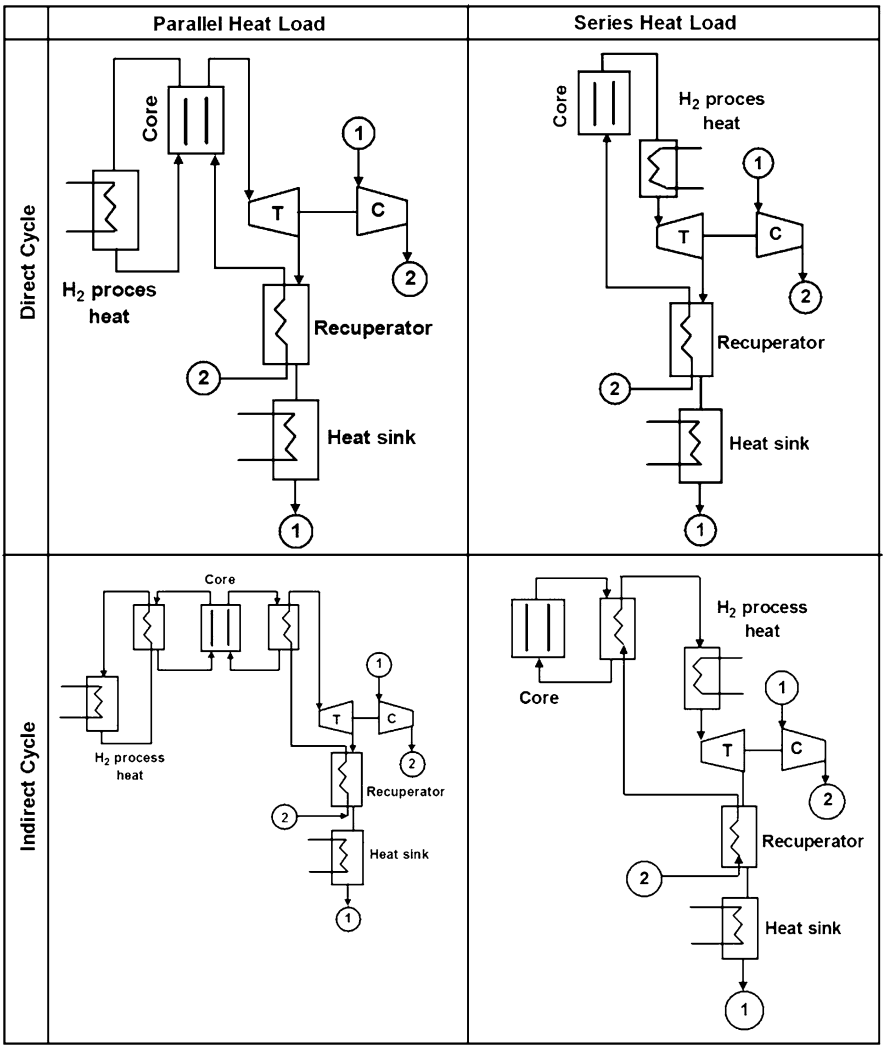

Fig. 8.31 Interface configurations for a nuclear hydrogen production plant (Adapted from Petri [314])

through thermochemical cycles or indirect heating via electricity production (only if electricity is produced by the reactor). The system configurations, as shown in Fig. 8.31, can be either in parallel or in series based on heat loads. Also, heat from a reactor can be transferred to a distant H_2 production facility (see Fig. 8.32) from the exit of the reactor or elsewhere in the plant, such as the exit stream from the turbine.

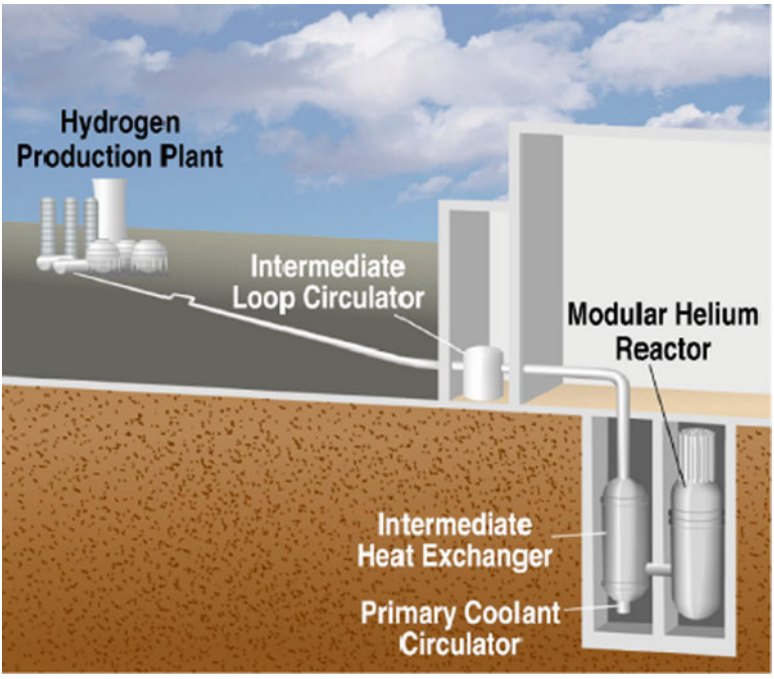

Fig. 8.32 A conceptual design of a nuclear plant-hydrogen production facility with hydrogen plant located outside the nuclear plant building (Adapted from Schultz et al. [302])

Materials of Construction

One of the biggest challenges of using thermochemical cycles is the material compatibility at high temperatures. These cycles employ corrosive chemicals. The corrosion of materials, sealing, valves, numerous fittings and their compatibility with other materials, make the material selection of construction materials extremely challenging. As noted earlier, the S-I cycle is the most advanced with significant efforts being made at identifying materials for the various section of the process.

The maximum temperature for the two acids (HIx and H_2SO_4) in Section I: Sulfuric Acid Concentration and Decomposition Section is 120°C. Iodine present in this section can also be corrosive, since it is a strong oxidizer. The material requirements for the Bunsen section are less demanding. A glass lined steel and Nb-alloys have been found to be acceptable.

Pickard [201] tested Incoloy 800 H, Saramet 23, and Hastelloy C276 materials with sulfuric acid at 850°C and ambient pressure. The results are given in Table 8.7. These materials are found to be vulnerable to acid attack under the operating conditions mentioned above.

Table 8.7 Corrosion properties of several alloys when exposed to sulfuric acid at 850°C

Species	Corrosion products (g/L)	Incoloy 800H (%)	Saramet 23 (%)	Hastelloy C276 (%)
Cr	10.0	21	18	16
Ni	8.0	32	17	57
Fe	6.6	40	55	5
Si	0.042	<5	5	<0.08
Mo	0.26	–	0.06	16
Au	0.0000046	0	0	0

Source: Adapted from Pickard [201]

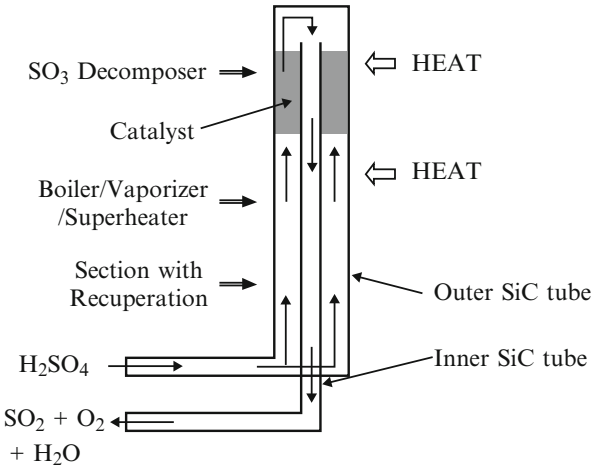

Fig. 8.33 Sulfuric acid decomposer made from SiC (Adapted from Pickard [201])

Sandia National Laboratory used a H_2SO_4 decomposer made from SiC for both SO_3 decomposer and H_2SO_4 boiler, vaporizer, and the superheating section. The design of the decomposer is shown in Fig. 8.33.

According to Pickard [201], the best materials for the HI decomposition section are found to be metals and ceramics. The performance of some selected materials is shown in Table 8.8. The University of Nevada, Las Vegas, USA and General Atomics, USA, tested 22 coupons from four classes of materials: refractory, reactive metals, superalloys and ceramics. The conclusion based on short term results are also presented in Fig. 8.8.

Wong et al. [315] noted that Hastelloy B2 and B3 have the lowest general corrosion rate after more than 1,000 h of testing. Their results are presented in Table 8.9.

Both liquid I_2 and HI acid are extremely corrosive. Wong et al. [315] noted that Ta and Ta-W alloys have the best corrosion resistance properties for use in the HI decomposition section of the S-I system. The corrosion rate of Ta and Ta-W alloys were less than 0.05 mils per year (mpy) penetration. For the high temperature operation with gaseous HI and iodine, Hastelloy compounds were found to be the most suitable as construction materials.

Table 8.8 Evaluation of various materials for construction of a HI decomposer

Excellent	Good	Fair	Poor
Ta-40Nb	Ta	Mo-47Re	Mo
Nb-1Zr	Ta-10W	Alumina	C-276
Nb-10Hf	Nb-7.5Ta		Haynes 188
SiC (CVD)	SiC (sintered)		Graphite[a]
SiC (Ceramatec sintered)	Si-SiC (3 kinds)		Zr702 Zr705
Mullite			

Source: Pickard [201]
[a]Structurally good but adsorbs HI

Table 8.9 Corrosion rates of Hastelloy B2 and B3 for exposure to HI decomposition reaction

Material	Hours of exposure	Mils per year (mpy)
Hastelloy B2	1,172	2.55
Hastelloy B3	1,022	0.14
Hastelloy C22	1,570	10.70
Hastelloy C276	1,220	13.50
Monel	970	67.8
Ta-2.5W	250	76.67
Ti grade 2	430	Disintegrated
Porous SiC	966	−24.0 (gained weight)
Hastelloy B2 (condenser)	1,172	0.82
Hastelloy B3 (condenser)	1,022	1.72
Monel	1,570	3,43

Source: Adapted from Wong et al. [315]

8.7 Solar Energy for Hydrogen Production

Solar energy can potentially be used to generate hydrogen via a number of processes. These processes include: thermolysis, thermochemical process, solar generated electricity and electrolysis, solar reforming, solar cracking, and solar gasification. Among these processes, thermochemical processes have the greatest potential for industrial scale production. The very high temperature necessary for thermochemical processes can be obtained using solar concentrators [316–326].

In the USA, the National Renewable Energy Laboratory (NREL), USA, assessed the hydrogen production capability from the solar energy driven electrolysis process. Solar irradiance received by various parts of the USA has been discussed in Chap. 2. The hydrogen generation capability via solar electrolysis assessed by NREL for various regions in the USA is presented in Fig. 8.34. The Southwest region is shown to have the highest potential. The electricity requirement of the electrolysis system was assumed to be 58.8 kWh/kg hydrogen. Counties with very

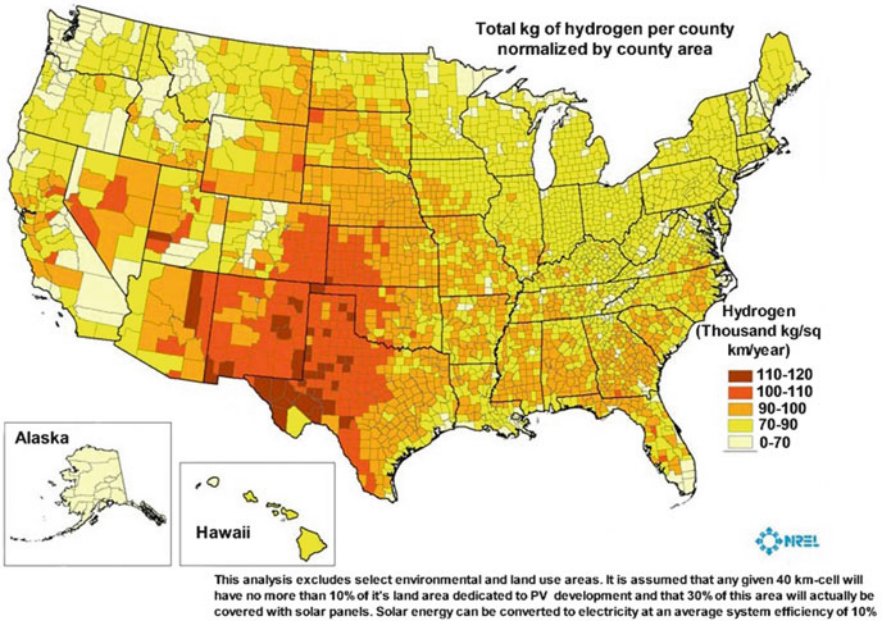

Fig. 8.34 Solar energy resource for hydrogen production (Source: Milbrandt and Mann [327])

good solar resources and low population count (such as the Rocky Mountain-Great Plains region) clearly show high potential for producing hydrogen from solar resources, per person.

8.7.1 High-Temperature Water Splitting-Solar Concentrators

Water starts to dissociate directly into hydrogen and oxygen at temperatures higher than 1,700°C [317]. A solar concentrator using mirrors and reflective or refractive lens to capture and focus sunlight can produce temperatures up to 2,000°C. This high temperature heat can be used to drive the chemical reaction for splitting water to produce hydrogen. However, as shown in Fig. 8.35, the yield at 2,000°C is just 0.01 kmol. A much higher temperature is necessary to have any appreciable amount of hydrogen production. The materials that can withstand such a high temperature are very expensive making such a process uneconomical.

Potentially, solar energy may be used, instead of nuclear energy, in most of the processes described earlier for hydrogen production. The harvesting of the solar energy is challenging, which is mainly due to the complexity in designing equipment for capturing the solar energy economically, and for providing high temperature heat, required for most of the processes. Among these processes, the solar reforming

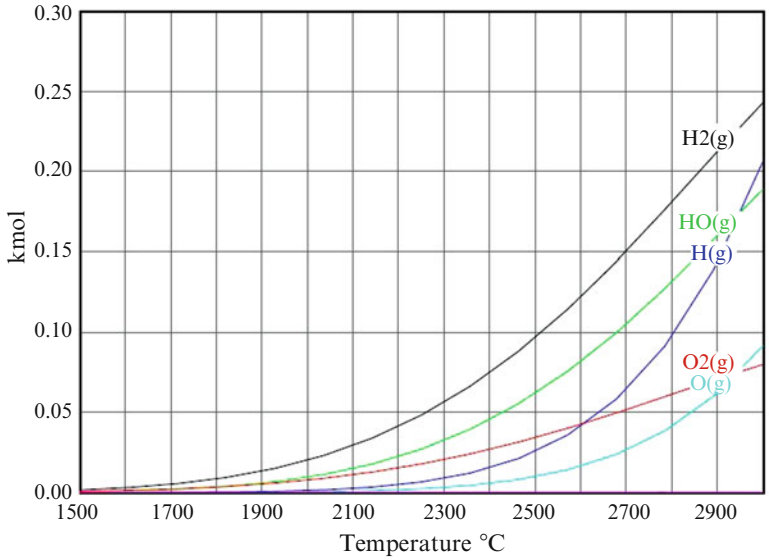

Fig. 8.35 Hydrogen production rate at different temperatures by high temperature water decomposition (Adapted from Evans [222])

of natural gas and other hydrocarbons, using either steam or CO_2 as partial oxidant, and 2-step thermochemical cycles using metal oxide redox reactions, have been extensively studied by various researchers. The processes where solar energy can be used for hydrogen production are given below and shown in Fig. 8.36.

(a) Solar oxide based redox pair cycle
(b) Sulfur-iodine cycle
(c) Hybrid-sulfur cycle
(d) Natural gas reforming
(e) Thermal splitting of methane
(f) High temperature electrolysis

8.7.2 Solar Reforming of Natural Gas

The energy necessary for reforming methane or other hydrocarbons for hydrogen or syngas production can be accomplished by using solar energy [329–336]. The decomposition of various hydrocarbons (methane, propane, gasoline) over carbon catalysts has been reported by the NERL, USA in a bench-scale fluidized bed at 850°C. A solar tubular quartz reactor was designed and tested for the decomposition of natural gas using carbon black particles as catalysts that were suspended in the feed gas stream. About 90% of the natural gas was decomposed in the reactor [337,

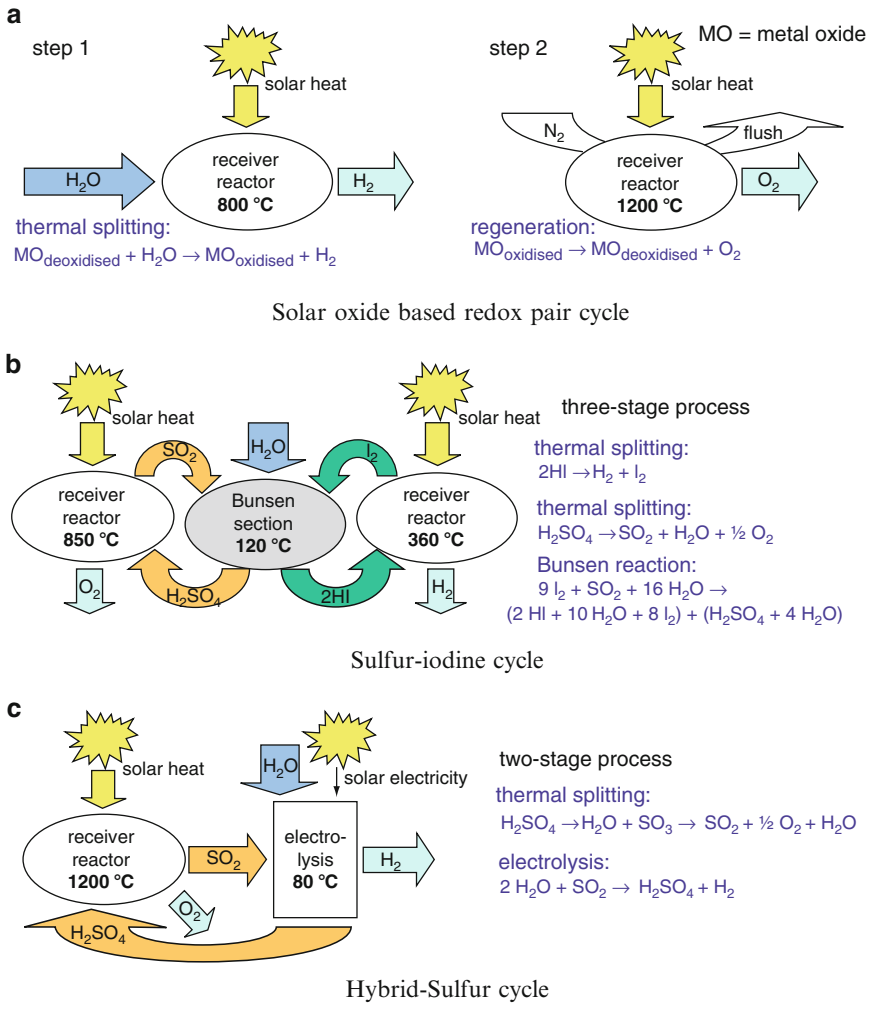

Fig. 8.36 Various processes where solar energy can be used for hydrogen production (Printed with permission from Pregger et al. [328])

338]. This reactor, called the "aerosol" solar reactor, is shown in Fig. 8.37. Two concentric graphite cylinders were used in the design. The outer tube was solid and absorbed the solar energy to provide the necessary heat, whereas the reactants flowed through the porous inner tube.

A schematic diagram of the complete system is shown in Fig. 8.38. The gaseous feed is introduced from the top along with the recycled carbon particles that are separated from the gas stream in a bag house filter, located at the outlet of the reactor. A pressure swing adsorption (PSA) system is used to separate product H_2 from the

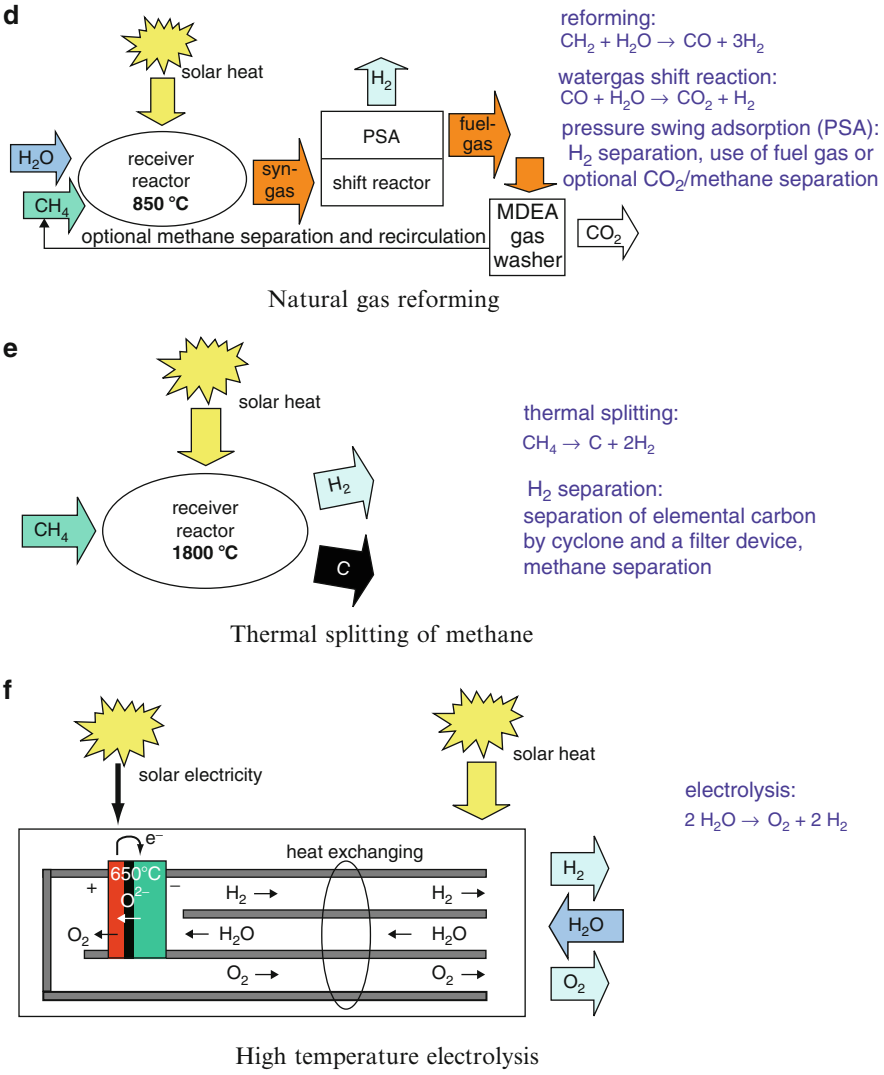

Fig. 8.36 (continued)

undecomposed feed, which is recycled to the reactor. Carbon particles escaping the baghouse can be burned and the gaseous stream can be used in a fuel cell to generate electricity for an electrolyzer to produce more H_2 from water electrolysis.

Solar reforming of the natural gas using either steam or CO_2 as a partial oxidant is accomplished in the presence of an Rh-based catalyst. The solar tower concept, using two solar reforming reactors: an indirect irradiation tubular reactor [340] and a direct-irradiation volumetric reactor [341], has been studied for generating 300–500 kW of power at 727°C and 8–10 bars pressure. The indirect-irradiated solar

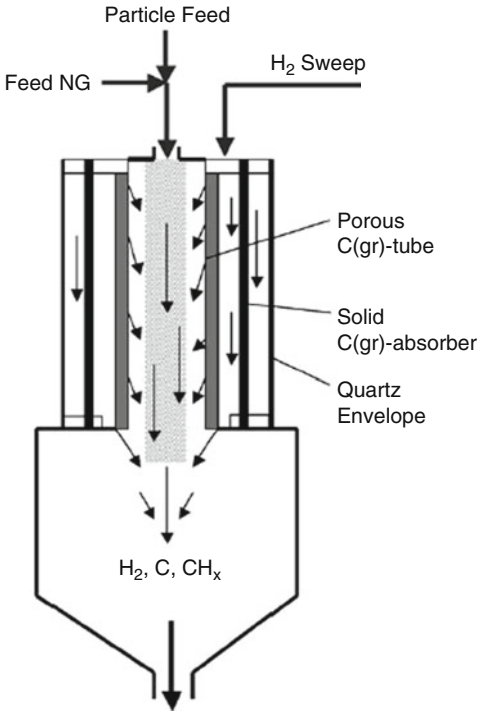

Fig. 8.37 Design concept of an aerosol flow reactor for methane decomposition using solar energy (Source: Lewandowski and Weimer [339])

reactor proposed by Epstein et al. [342] consists of a ceramic-insulated pentagonal cavity-receiver containing a set of vertical Inconel tubes filled with a packed bed of catalyst (2% Rh on Al_2O_3 support). The Compound Parabolic Concentrator (CPC) system provides uniform irradiation to all the tubes. The direct irradiated solar reactor, also referred to as the "volumetric" reactor, is shown in Fig. 8.39. A porous ceramic absorber was coated with Rh catalyst and directly exposed to the concentrated solar radiation. Methane (CH_4) and CO_2 conversions of 70% and 65%, respectively, were achieved in the absence of any added catalysts with a residence time of 10 ms at 1727°C [343].

8.7.3 Thermochemical Solar Cycle

Solar thermochemical water splitting is a two-step process [345–354]. In the first step, a metal oxide is decomposed to metal and oxygen using solar energy. In the second step, pure metal reacts with water producing hydrogen and metal oxide. These two reactions may be written as follows:

$$\text{First step:} \qquad M_xO_y = xM + 1/2\,yO_2 \tag{8.32}$$

$$\text{Second step:} \qquad xM + yH_2O = M_xO_y + yH_2 \tag{8.33}$$

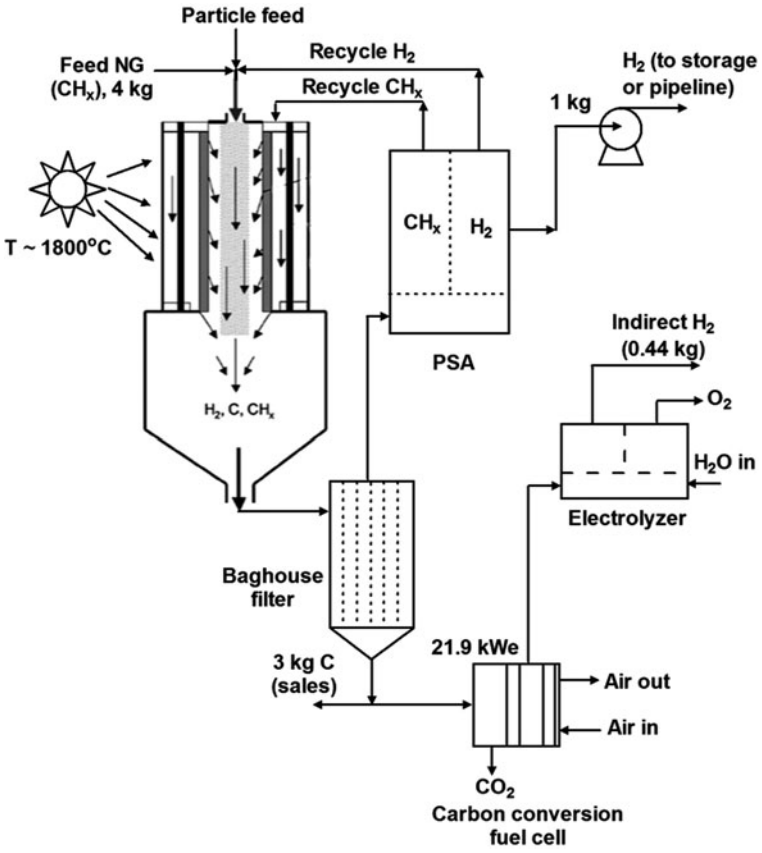

Fig. 8.38 A schematic diagram of solar natural gas reforming system (Adapted from Lewandowski and Weimer [339])

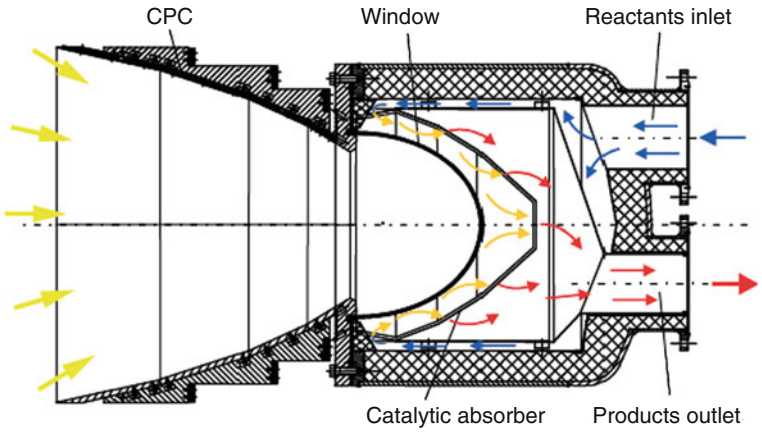

Fig. 8.39 Scheme of a "volumetric" solar reactor concept for the reforming of NG. *CPC* Compound Parabolic Concentrators (Source: Deutsches Zentrum fur Luft- und Raumfahrt e.V., Germany) (Printed with permission from Steinfeld [344])

In these reactions, M denotes metal and M_xO_y is the corresponding metal oxide. The first reaction is an endothermic reaction and for most metal oxides a temperature greater than 1727°C is required to dissociate the metal oxide to metal or the lower-valence metal oxide. The second reaction is an exothermic reaction and does not need the solar energy.

The U.S. Department of Energy's Solar ThermoChemical Hydrogen (STCH) program evaluated over 400 potential cycles. From these cycles, nine of them were selected for the detailed study. The criteria used in the selection included: the chemical reactions, suitability to various solar thermal collectors (e.g., troughs, dishes, power towers) for the reaction, use of corrosive or environmentally harmful chemicals, and the projected operating efficiency. The nine cycles given in Table 8.10 can be further divided into following two categories:

- High-temperature Cycles
  - Two-step reaction cycles
  - Multi-step reaction cycles
- Low-temperature cycles.

Although Zn/ZnO and Fe/Fe_2O_3 cycles involve two reaction steps, the oxide decomposition temperature is high, requiring expensive materials of construction, innovative designs and higher operating costs. There are several metal oxides that decompose at lower temperatures compared to ZnO and Fe_2O_3, however, these oxides, when reduced, will not directly split water. Additional steps, which require relatively high temperature, are necessary. Also, various side reactions and by-products introduce more complexity in the separation steps.

8.7.3.1 Zinc/Zinc Oxide Cycle

Zinc/zinc oxide cycle is the most studied reaction for the solar decomposition of water. Zinc oxide powder is passed through a reactor heated by a solar concentrator to about 1900°C. At this temperature, zinc oxide dissociates to zinc and oxygen. Zinc is cooled, separated, and reacted with water to form hydrogen gas and solid zinc oxide. The net result is the production of hydrogen and oxygen from water. The hydrogen is purified and stored for future use. The zinc oxide can be recycled and reused to create more hydrogen through this process. The reactions are given below:

$$\begin{aligned} 2ZnO + heat &\rightarrow 2Zn + O_2 \\ 2Zn + 2H_2O &\rightarrow 2ZnO + 2H_2 \end{aligned} \tag{8.34}$$

Several designs of the solar reactor have been proposed in the literature. However, the rotating cavity concept proposed by Haueter et al. [349] appears to be most promising. This solar reactor is shown in Fig. 8.40. In this design, ZnO particles are deposited on a rotating window and are held there by the centrifugal force. In a

Table 8.10 Various potential thermochemical cycles for hydrogen production using solar energy

Cycle	Reactions
High temperature cycles	
Zn/ZnO [347, 355–362]	$ZnO \xrightarrow{1600-1800^{\circ}C} Zn + 1/2O_2$ $Zn + H_2O \xrightarrow{400^{\circ}C} ZnO + H_2$
FeO/Fe_3O_4 [353, 363, 364]	$Fe_3O_4 \xrightarrow{2000-2300^{\circ}C} 3FeO + 1/2O_2$ $3FeO + H_2O \xrightarrow{400^{\circ}C} Fe_3O_4 + H_2$
$Cd/CdCO_3$ [349]	$CdO \xrightarrow{1450-1500^{\circ}C} Cd + 1/2O_2$ $Cd + H_2O + CO_2 \xrightarrow{350^{\circ}C} CdCO_3 + H_2$ $CdCO_3 \xrightarrow{500^{\circ}C} CO_2 + CdO$
$Cd/CdO/Cd(OH)_2$ [349]	$CdO \xrightarrow{1450-1500^{\circ}C} Cd + 1/2O_2$ $Cd + 2H_2O \xrightarrow{25^{\circ}C, Electrochemical} Cd(OH)_2 + H_2$ $Cd(OH)_2 \xrightarrow{375^{\circ}C} CdO + H_2O$
Sodium manganese [349]	$Mn_2O_3 \xrightarrow{1400-1600^{\circ}C} 2MnO + 1/2O_2$ $2MnO + 2NaOH \xrightarrow{627^{\circ}C} 2NaMnO_2 + H_2$ $2NaMnO_2 + H_2O \xrightarrow{25^{\circ}C} Mn_2O_3 + 2NaOH$
M-Ferrite (M = Co, Ni, Zn) [352, 365–387]	$Fe_{3-x}M_xO_4 \xrightarrow{1200-1400^{\circ}C} Fe_{3-x}M_xO_{4-\delta} + \frac{\delta}{2}O_2$ $Fe_{3-x}M_xO_{4-\delta} + \delta H_2O \xrightarrow{1000-1200^{\circ}C} Fe_{3-x}M_xO_4 + \delta H_2$
Mg/MgO [388]	$MgO + C \xrightarrow{1500^{\circ}-1900^{\circ}C} Mg + CO$ $or,\ MgO + CH_4 \longrightarrow Mg + CO + 2H_2$ $Mg + H_2O \longrightarrow MgO + H_2$
SnO_2/SnO [389, 390]	$SnO_2(s) \xrightarrow{1600^{\circ}C} SnO(s) + \frac{1}{2}(O_2)$ $SnO(s) + H_2O(g) \xrightarrow{550^{\circ}C} SnO_2(s) + H_2$
CeO2/Ce2O3 [391]	$2CeO_2(s) \xrightarrow{2000^{\circ}C} Ce_2O_3(s) + \frac{1}{2}O_2$ $Ce_2O_3(s) + H_2O(g) \xrightarrow{400^{\circ}-600^{\circ}C} 2CeO_2(s) + H_2(g)$
Low temperature cycles	
Sulfur-iodine [392–398]	$H_2SO_4 \xrightarrow{850^{\circ}C} SO_2 + H_2O + 1/2\ O_2$ $I_2 + SO_2 + 2H_2O \xrightarrow{100^{\circ}C} 2HI + H_2SO_4$ $2HI \xrightarrow{300^{\circ}C} I_2 + H_2$
Hybrid sulfur	$H_2SO_4 \xrightarrow{850^{\circ}C} SO_2 + H_2O + 1/2O_2$ $SO_2 + 2H_2O \xrightarrow{77^{\circ}C, Electrochemical} H_2SO_4 + H_2$
Hybrid copper chloride [399]	$Cu_2OCl_2 \xrightarrow{550^{\circ}C} 2CuCl + 1/2O_2$ $2Cu + 2HCl \xrightarrow{425^{\circ}C} H_2 + 2CuCl$ $4CuCl \xrightarrow{25^{\circ}C, Electrochemical} 2Cu + 2CuCl_2$ $2CuCl_2 + H_2O \xrightarrow{325^{\circ}C} Cu_2OCl_2 + 2HCl$

Source: Adapted from Perkins and Weimer [350]

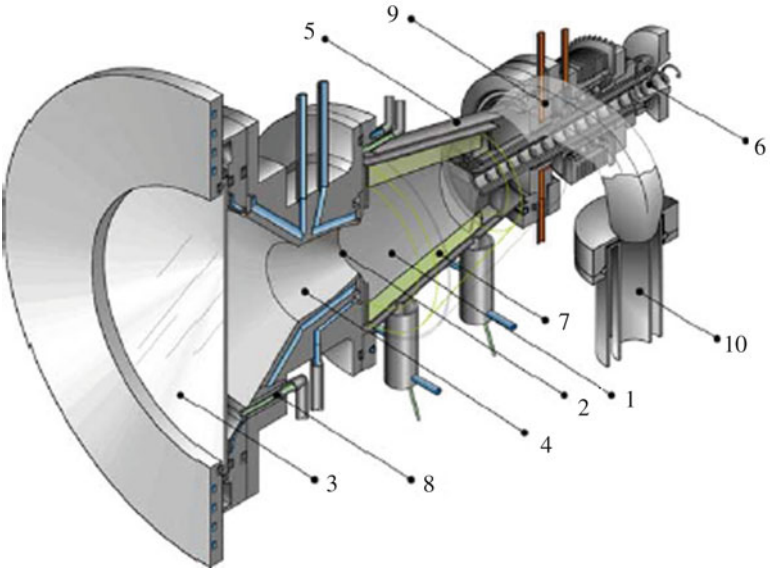

Fig. 8.40 Schematic of the "rotating-cavity" solar reactor concept for the thermal dissociation of ZnO to Zn and O_2 at 2,300 K (Printed with permission from Paul Scherrer Institute, Switzerland; Steinfeld [344])

10 kW prototype unit, ZnO was directly exposed to high-flux solar irradiation, and a temperature of 1727°C was achieved in 2 s and the ZnO coating did withstand the thermal shocks.

Steinfeld [347] studied the efficiency of the cycle by evaluating the exergy of the system and noted that an efficiency of 29% is possible without any heat recovery. The theoretical upper limit in the exergy efficiency, with complete heat recovery during the quenching and hydrolysis, was calculated to be 82%. The unique feature of the cycle is that in the absence of nucleation sites, Zn(g) and O_2 can coexist in a meta-stable state. Otherwise, these need to be quenched to avoid their recombination. Fletcher and his coworkers [400, 401] demonstrated that electrothermal separation of Zn(g) and O_2 at high temperatures is possible in situ. The sensible and latent heat of the products (e.g., 116 kJ/mol during Zn condensation) can be recovered to further enhance the system efficiency.

Stienfeld and co-workers [402] proposed a hybrid system to decompose metal oxides such as ZnO by CH_4 according to the following reactions:

$$\begin{aligned} M_x O_y + yC(gr) &= xM + yCO \\ M_x O_y + yCH_4 &= xM + y(2H_2 + CO) \end{aligned} \tag{8.35}$$

Reduction of the oxides can be achieved at a moderate temperature. The reduction of Fe_3O_4, MgO, and ZnO with C(gr) and CH_4, according to above reactions, has been demonstrated in a solar furnace using packed/fluidized beds and vortextype

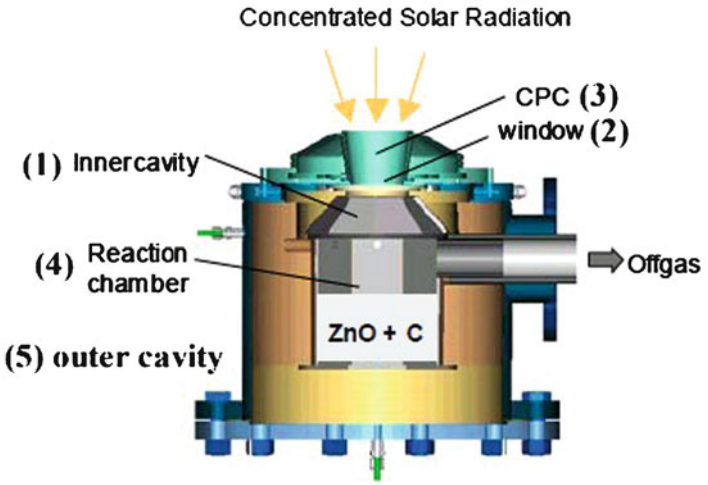

Fig. 8.41 Schematic of the "two-cavity" solar reactor concept for the carbothermal reduction of ZnO. It features two cavities in series, with the inner one functioning as the solar absorber and the outer one as the reaction chamber. The inner cavity (*#1*) is made of graphite and contains a windowed aperture (*#2*) to let in concentrated solar radiation. A CPC (*#3*) is implemented at the reactor's aperture. The outer cavity (*#4*) is well insulated and contains the ZnO/carbon mixture that is subjected to irradiation by the graphite absorber separating the two cavities. With this arrangement, the inner cavity protects the window against particles and condensable gases coming from the reaction chamber. Uniform distribution of continuously fed reactants is achieved by rotating the outer cavity (*#5*). The reactor is specifically designed for beam-down incident radiation, as obtained through a Cassegrain optical configuration that makes use of a hyperbolical reflector at the top of the tower to re-direct sunlight to a receiver located on the ground level (Source: Paul Scherrer Institute, Switzerland) (Printed with permission from Steinfeld [344])

reactors [403]. Two designs of the reactor have been investigated. The first reaction given in Eq. 8.35 is carried out in a two-cavity solar reactor that is operated based on the indirect irradiation of metal oxide and carbon. This design is shown in Fig. 8.41 when using ZnO.

As described by Steinfeld [347], "It consists of a rotating conical cavity-receiver (#1) that contains an aperture (#2) for access of concentrated solar radiation through a quartz window (#2). The solar flux concentration is further augmented by incorporating a CPC (#3) in front of the aperture. Both the window mount and the CPC are watercooled and integrated into a concentric (non-rotating) conical shell (#4). ZnO particles are continuously fed by means of a screw powder feeder located at the rear of the reactor. The centripetal acceleration forces the ZnO powder to the wall where it forms a thick layer of ZnO that insulates and reduces the thermal load on the inner cavity walls. A purge gas flow enters the cavity-receiver tangentially at the front and keeps the window cool and clear of particles or condensable gases. The gaseous products Zn and O_2 continuously exit via an outlet port to a quench device".

For the second reaction, a vortex reactor as shown in Fig. 8.42 may be used. The calculation of the equilibrium composition for various metal oxides of interest

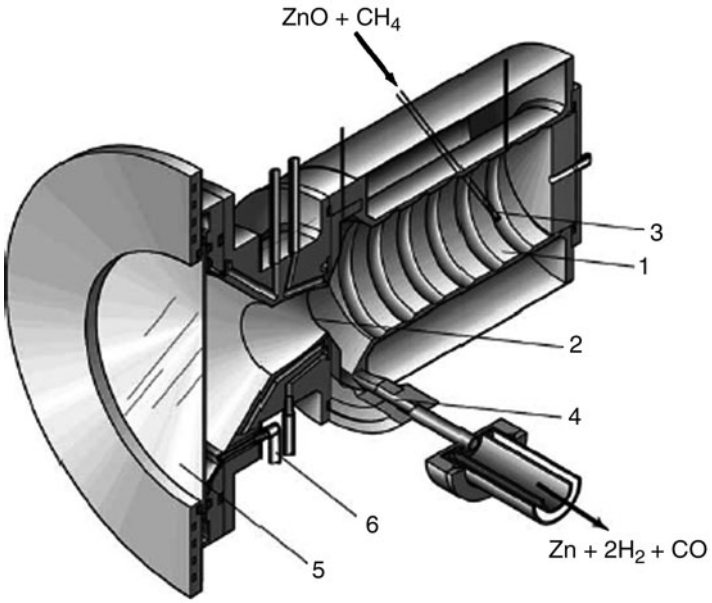

Fig. 8.42 Schematic of a "vortex" solar reactor concept for the combined ZnO reduction and CH4 reforming. It consists of a cylindrical cavity (*#1*) that contains a windowed aperture (*#2*) to let in concentrated solar energy. Particles of ZnO, conveyed in a flow of NG, are continuously injected into the reactor's cavity via a tangential inlet port (*#3*). Inside the reactor's cavity, the gas-particle stream forms a vortex flow that progresses towards the front following a helical path. The chemical products, Zn vapor and syngas, continuously exit the cavity via a tangential outlet port (*#4*) located at the front of the cavity, behind the aperture. The window (*#5*) is actively cooled and kept clear of particles by means of an auxiliary flow of gas (*#6*) that is injected tangentially and radially at the window and aperture planes, respectively. Energy absorbed by the reactants is used to raise their temperature to above about 1,300 K and to drive reaction (12) (Source: Paul Scherrer Institute, Switzerland) (Printed with permission from Steinfeld [344])

shows that only the carbothermic reduction of Fe_2O_3, MgO, and ZnO will result in a significant free metal formation [404]. However, various other carbides may also form. Stienfield [344] noted that these carbides have high value as byproducts.

8.7.3.2 Fe_3O_4/FeO Cycle

A two-step water-splitting cycle using iron oxide (or ferrite) redox pair was developed in the early 1977. This cycle is generally called "iron oxide process" or "ferrite process". In this cycle, Fe_3O_4 is reduced to FeO by thermal decomposition. FeO then reacts with H_2O to produce hydrogen. The two reactions can be written as:

$$\begin{aligned} Fe_3O_4 &\rightarrow 3FeO + 1/2\ O_2 \\ H_2O + 3FeO &\rightarrow Fe_3O_4 + H_2 \end{aligned} \tag{8.36}$$

The thermal reduction of Fe_3O_4 to FeO proceeds at temperatures above 2227°C under 1 bar. The second reaction thermodynamically proceeds at temperatures below 727°C.

8.8 Electrolytic Process

Water electrolysis takes place in an electrolyzer that contains an electrolyte, an anode, and a cathode. Several electrolytic processes have been demonstrated commercially. These processes are:

- Solid Oxide Electrolyzers
- High-Temperature Electrolysis
- Polymer Electrolyte Membrane (PEM) Electrolysis
- Alkaline Electrolyzers

The first two processes have been discussed in detail earlier in this chapter. The PEM electrolysis process will be discussed in Volume 3 of this book series. The alkaline electrolysis process is described below.

8.8.1 Alkaline Electrolysis

Alkaline electrolysis is a very mature technology and has been commercially available for many years. Alkaline electrolyzers use an aqueous KOH solution (caustic) as an electrolyte that typically circulates through the electrolytic cells. Alkaline electrolysers are suited for stationary applications and are available at operating pressures up to 25 bar. The following reactions take place inside an alkaline electrolysis cell:

Electrolyte: $$4H_2O \rightarrow 4H^+ + 4OH^- \tag{8.37}$$

Cathode: $$4H^+ + 4e^- \rightarrow 2H_2 \tag{8.38}$$

Anode: $$4OH^- \rightarrow O_2 + 2H_2O + 4e^- \tag{8.39}$$

Overall Reaction: $$2H_2O \rightarrow O_2 + 2H_2 \tag{8.40}$$

Commercial electrolyzers consist of a number of electrolytic cells arranged in a cell stack. The main components of alkaline electrolyzers are shown in Fig. 8.43.

8.9 Thermochemical Hybrid Cycles

A thermochemical hybrid process is a combined cycle in which both thermochemical and electrolytic reactions for water splitting have been incorporated. The hybrid process offers the possibility to run low-temperature reactions using electricity.

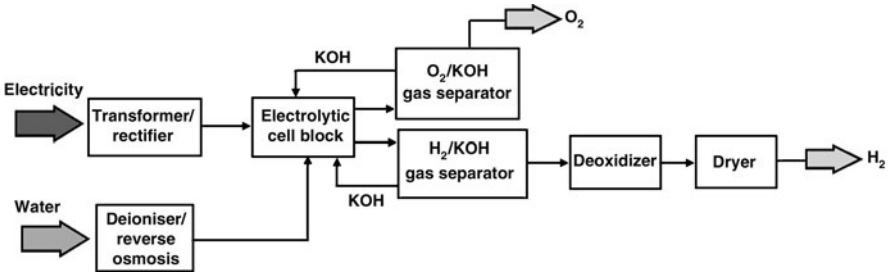

Fig. 8.43 An Alkaline electrolysis cell arrangement for hydrogen production (Adapted from International Energy Agency [405])

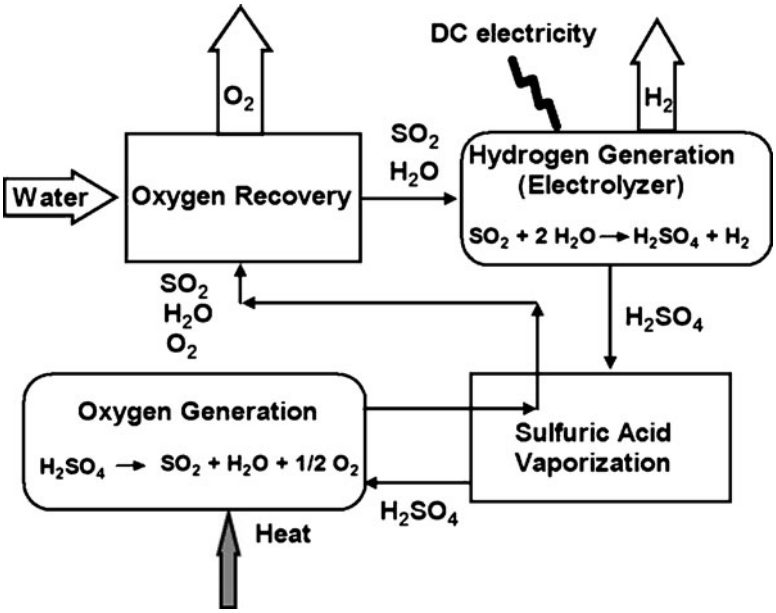

Fig. 8.44 Schematic diagram of the Westinghouse Sulfur Process (Adapted with permission from Yildiz and Kazimi [160])

One such cycle was developed by Westinghouse Electric Co., USA in 1975, called *sulfuric acid hybrid cycle* or the *Westinghouse Sulfur Process* (WSP). The reactions that take place in this cycle are given below:

$$\begin{aligned} &H_2SO_4 \rightarrow SO_2 + H_2O + \frac{1}{2}O_2 \quad (800^\circ C) \\ &2H_2O + SO_2 \rightarrow H_2SO_4 + H_2 \quad \textit{Electrolytic reaction}\ (80^\circ C) \end{aligned} \tag{8.41}$$

A schematic diagram of the WSP cycle is given in Fig. 8.44. As can be seen from this figure, the hydrogen is generated by electrolysis. The heat for the sulfuric acid

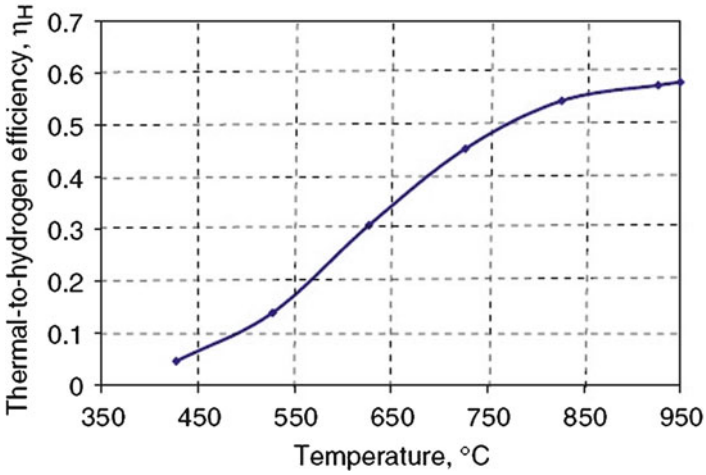

Fig. 8.45 Energy efficiency of Westinghouse Sulfur Process coupled with a GT-MHR nuclear reactor (Adapted with permission from Yildiz and Kazimi [160])

decomposition unit can be supplied from a nuclear reactor. The hydrogen generation section of the plant can be located away from the nuclear plant for safety reasons. At the same time, the part of the process that requires the high-temperature heat from the nuclear reactor can be kept close to the reactor. This type of plant configuration can also reduce the heat losses and the overall costs. The energy efficiency of the WSP cycle is shown in Fig. 8.45 as a function of process temperature. The nuclear reactor used in the analysis of the efficiency was a Gas Turbine-Modular Helium Reactor (GT-MHR). It is assumed that a helium gas turbine would be used for electricity generation. Helium gas turbines have significant advantages over steam turbines. Not only gas turbines offer higher efficiency, they are also smaller in size, as shown in Fig. 8.46. The smaller size requires a smaller footprint and is also easy to install. The use of supercritical carbon dioxide may offer even better economics, but it is still in the research stage.

8.10 Hydrogen from Wind Energy

The electricity generated by wind energy may be used to produce hydrogen via water electrolysis [406–443]. The National Renewable Energy laboratory (NREL) performed an analysis for potential hydrogen production from wind energy via electrolysis process in the USA (see Fig. 8.47). In their calculation for the hydrogen production capacity, the capacity factor for different classes of wind was taken into account. The capacity factors are given in Table 8.11. The capacity factor is discussed in detail in Chap. 1.

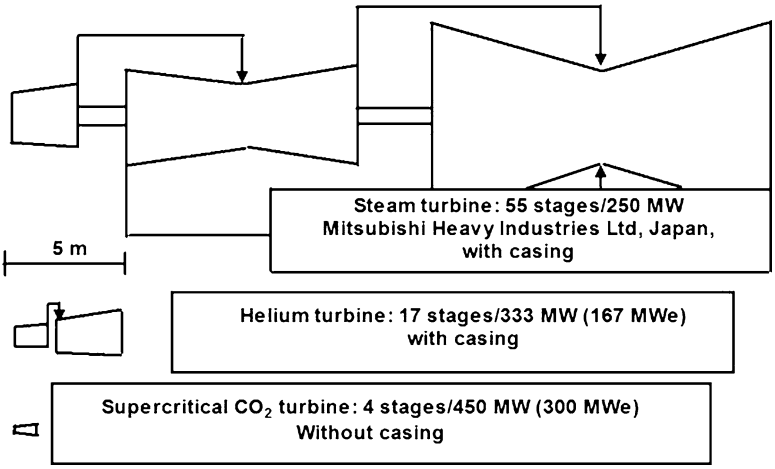

Fig. 8.46 Size comparison of various turbine systems (Adapted with permission from Yildiz and Kazimi [160])

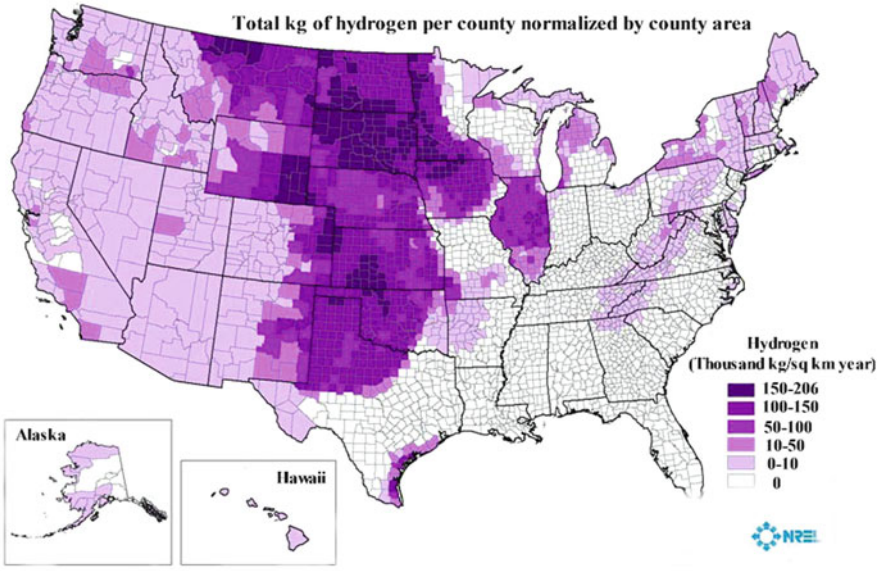

Fig. 8.47 Hydrogen production potential from wind energy in the USA (Source: Milbrandt and Mann [444])

Table 8.11 Wind class capacity factors based on year 2000 technology

Class	Capacity factor
3	0.2
4	0.251
5	0.3225
6	0.394
7	0.394

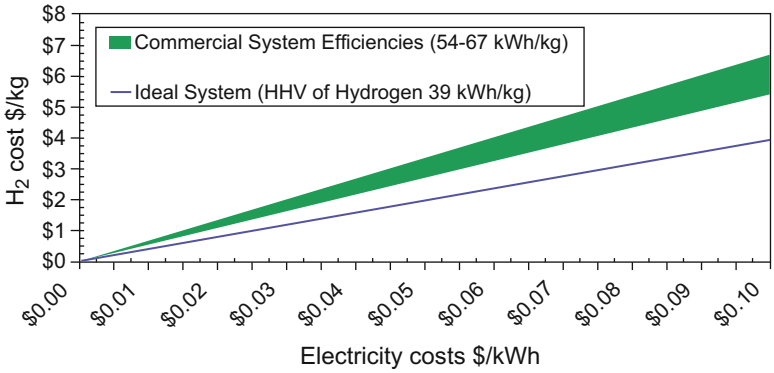

Fig. 8.48 The cost of hydrogen production via electrolysis considering only electricity contribution (no capital, operating, or maintenance costs are included). This analysis demonstrates that regardless of any additional cost elements, electricity costs will be a major price contributor to the price of hydrogen produced via electrolysis (Printed with permission from Levene et al. [430])

The other assumptions are as follows:

- 100% excluded are all national park service areas, fish and wildlife service lands, all federal lands with special designations (parks, wilderness and study areas, wildlife refuges, wildlife areas, recreational areas, battlefields, monuments, conservation areas, recreational areas, and wild and scenic rivers), conservation areas, water, wetlands, urban areas, and airports/airfields. The land areas also exclude a 3 km surrounding perimeter.
- 50% exclusions were applied to the remaining forest service lands, Department of Defense lands, and non-ridge crest forest.
- This study also excluded areas with slopes greater than 20% for the high-resolution data. These areas are considered too steep for siting wind turbines.

The main route for the hydrogen production using renewable energy sources is via electrolysis. H_2 cost is dependent on the cost of electricity that is generated by renewable energy sources. Levene et al. [430] estimated H_2 production costs as a function of the cost of electricity, and, as expected, the H_2 production cost increased with the increase of the electricity cost (see Fig. 8.48). Electricity generated from renewable energy sources, except from hydropower, costs more than from conventional sources such as coal and nuclear. Although water electrolysis

process is 80–85% efficient for H_2 production, when combined with the efficiency of electricity generation, which is around 30–40%, the overall efficiency becomes only 25–32%.

8.11 Hydrogen from Biomass

Various routes explored for hydrogen production from biomass [445,446] are shown in Fig. 8.49. These processes are described in Chap. 6. There is an inherent problem associated with hydrogen production from biomass. The yield of hydrogen is low due to the low hydrogen content in biomass, which is approximately 6% versus 25% for methane. The energy content is also low due to the 40% oxygen content of biomass. Biomass has long been considered a leading near term source for renewable hydrogen. A conservative estimate shows that the near-term economic potential of the annual hydrogen production from biomass in the USA is about 40 million tons, which would supply fuel for 150 million fuel cell vehicles. The distribution of biomass resources for H_2 production in the United States is shown in Fig. 8.50. The cost for growing, harvesting and transporting biomass is high. As a result, at the present time, the biomass route for hydrogen production is uneconomical even with reasonable energy efficiencies. Unless the by-products have high commercial value, it may not be competitive with the natural gas steam reforming process.

8.12 Photolytic Processes

Photolytic processes are defined as those processes in which the solar energy is used indirectly to split water into H_2 and O_2 [448–457]. Two photolytic processes that are currently investigated show promise for the future. These processes are:

- Photobiological Water Splitting
- Photoelectrochemical Water Splitting

8.12.1 Photobiological Water Splitting

In this process, hydrogen is produced from water using sunlight and specialized microorganisms, such as green algae and cyanobacteria. The process may be divided into two main steps: photosynthesis and biophotolysis.

During photosynthesis, plants convert solar energy to biochemical energy by a photochemical reaction that utilizes CO_2 and H_2O according to the following reaction:

$$CO_2 + H_2O + light \rightarrow 6(CH_2O) + O_2 \tag{8.42}$$

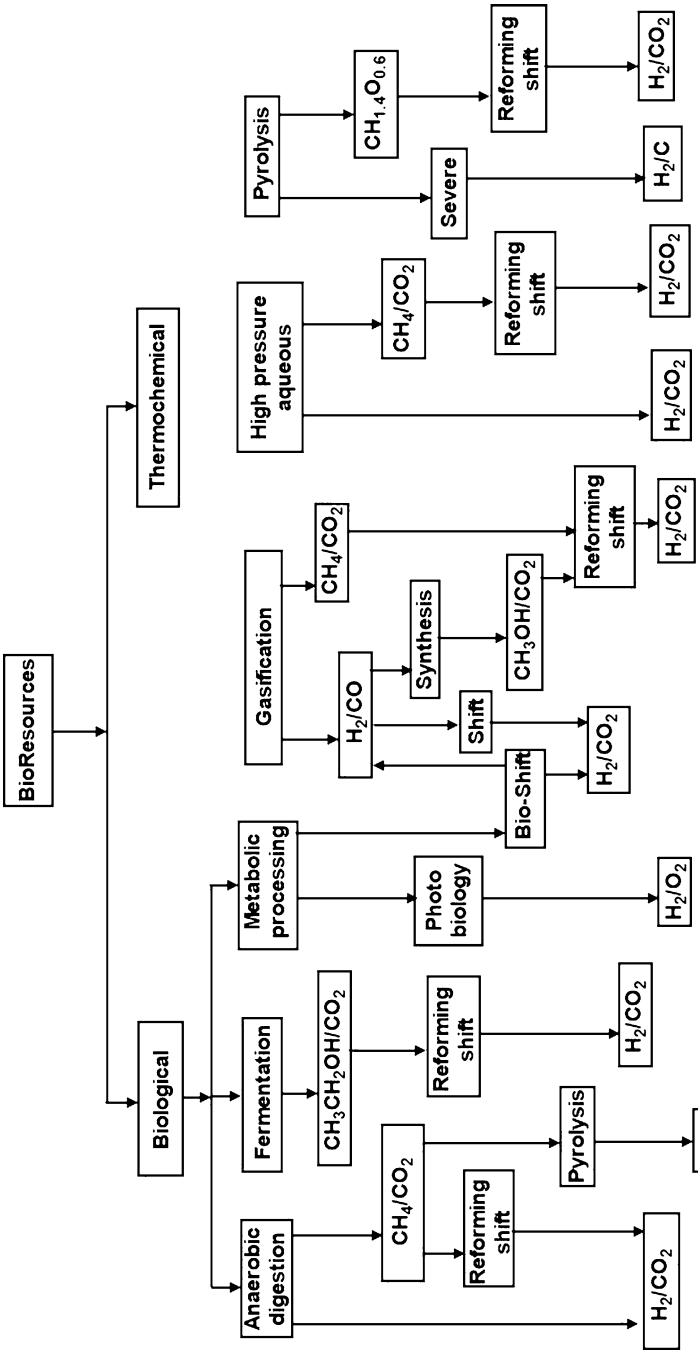

Fig. 8.49 Various methods for hydrogen production from biomass (Milne et al. [447])

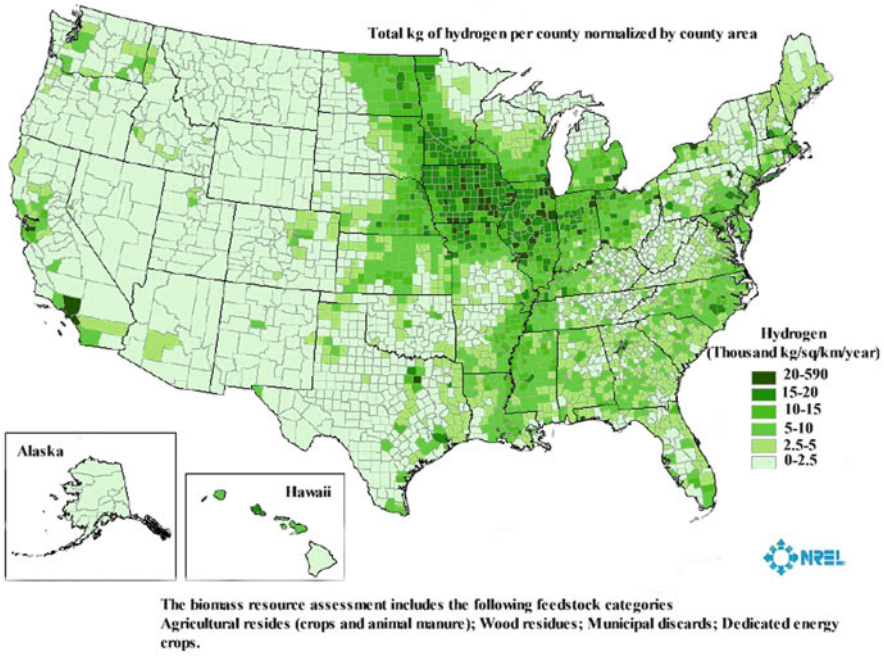

Fig. 8.50 Hydrogen production potential from biomass at different region of the USA (Source: Milbrandt and Mann [444])

The reaction may be referred to as reduction or fixation of CO_2 to organic compounds such as sugar phosphates. Approximately, 114 kcal of free energy are stored in plant biomass for every mole of CO_2 fixed during photosynthesis. Under certain conditions, some microalgae and cyanobacteria can utilize biochemical energy to produce molecular hydrogen directly. Both hydrogenase and nitrogenase enzymes are capable of hydrogen production [458–500].

8.12.1.1 Hydrogenase Enzyme-Catalyzed Hydrogen Production

Gaffron and Rubin [500] noted that Green alga, *Scenedesmus*, can produce molecular hydrogen under light conditions after being kept under anaerobic and dark conditions. The mechanism for hydrogen production via hydrogenase-pathway may be described by the scheme shown in Fig. 8.51.

The reaction involved in the H_2 production may be written as shown below. An electron carrier is necessary for the reaction to proceed.

$$2H^+ + 2X_{reduced} \rightarrow 6H_2 + 2X_{oxidized} \tag{8.43}$$

where X is the electron carrier. It is often not clear how the electron transfer occurs. The ferredoxin (fd) is considered to be the electron carrier. Since ferredoxin is

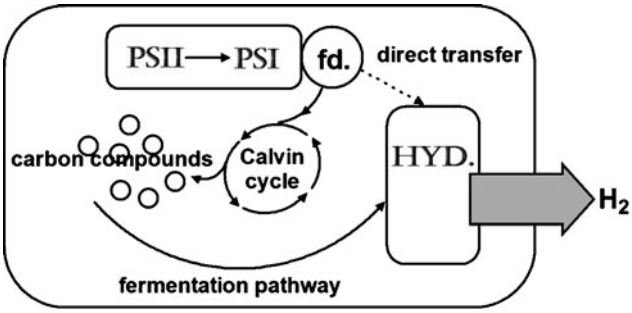

Fig. 8.51 Hydrogenase-mediated hydrogen production (Source: Miyamoto [501])

reduced with water as an electron donor by the photochemical reaction, green algae are theoretically water-splitting microorganisms.

The process is very slow, and the challenge is to increase the hydrogen yield through development of sophisticated engineering processes before commercial scale production. One of the main issues is how to reduce the reactor area. A schematic of such a process is shown in Fig. 8.52.

8.12.1.2 Nitrogenase-Enzyme Catalyzed Hydrogen Production

Nitrogen-fixing cyanobacterium, *Anabaena cylindrica*, is capable of producing hydrogen and oxygen gas simultaneously under an inert atmosphere. Hydrogen production occurs as a side reaction at a rate of one-third to one-fourth that of nitrogen-fixation, even in a 100% nitrogen gas atmosphere. The reactions can be described as follows:

$$N_2 + 6H1^+ + 6e^- \rightarrow 2HN_3 \tag{8.44}$$

$$12ATP \rightleftharpoons 12(ADP + Pi) \tag{8.45}$$

$$2H^+ + 2e^- \rightarrow H_2 \tag{8.46}$$

$$4ATP \rightleftharpoons 4(ADP + Pi) \tag{8.47}$$

A schematic diagram showing the H_2 production mechanism is given in Fig. 8.53.

8.12.2 Photocatalytical Processes

Photocatalytic splitting of water into H_2 and O_2 using sunlight was first reported by Fujishima and Honda in 1971 [502]. The mechanism for photocatalysis of water is shown in Fig. 8.54.

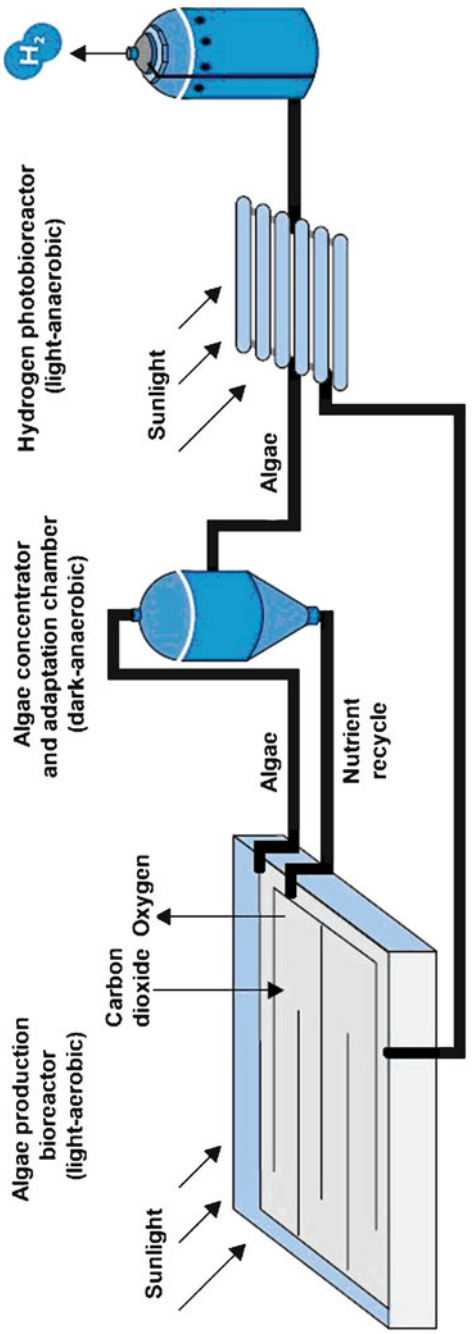

Fig. 8.52 Photobiological method for hydrogen production (International Energy Agency [405])

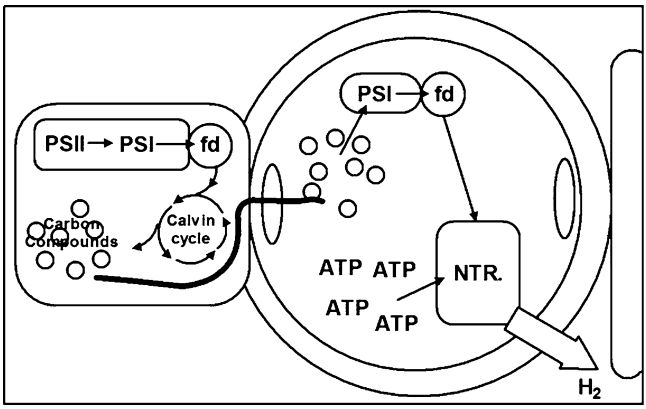

Fig. 8.53 Nitrogenase-mediated hydrogen production in heterocystous cyanobacteria (Source: Miyamoto [501])

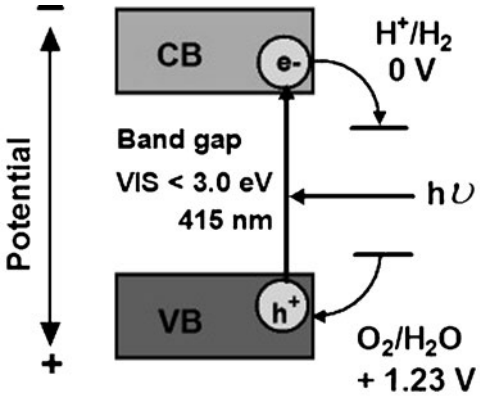

Fig. 8.54 Working principle of photocatalysis for hydrogen production from water

In this process, the catalyst, which is a semiconductor material, absorbs sunlight leading to creation of electrons and holes in the conduction band and valance band, respectively [502–552]. The process is described in Chap. 2. The photo-generated electrons and holes cause redox reactions similar to electrolysis. Water molecules are reduced by electrons to form hydrogen and are oxidized by the holes to form oxygen for the overall reaction. Almost half of the energy that reaches us from the sun arrives as visible light. Therefore, recent research focus is to develop photocatalyst capable of direct splitting of water using visible light. The quantum yield of the process is 0.66%, and a better photocatalyst is necessary for commercial viability of this process. Titanium oxide is found to exhibit high activity as a photocatalyst for the decomposition of water. Modification of TiO_2 by doping it with various compounds was investigated by a number of researchers to enhance its activity. A list of various photocatalysts has been compiled by Kudo [449] and is presented in Table 8.12.

Table 8.12 Various types of photocatalysts used by researchers for hydrogen production

UV responsive photocatalysts	Visible light responsive photocatalysts		
Overall water splitting	H_2-evolution (sacrificial)	O_2-evolution (sacrificial)	Overall water splitting
$ZnNb_2O_6$	$SrTiO_3$: Cr,Sb	TiO_2: Cr,Sb	$SrTiO_3$: Rh−$BiVO_4$
$Sr_2Nb_2O_7$	$SrTiO_3$: Cr,Ta	TiO_2: Ni,Nb	$SrTiO_3$: Rh−Bi_2MoO_6
$Cs_2Nb_4O_{11}$	$SrTiO_3$: Rh	$PbMoO_4$: Cr	$SrTiO_3$: Rh−WO_3
$Ba_5Nb_4O_{15}$	$SnNb_2O_6$	$BiVO_4$	
$ATaO_3$(A: Li, Na, K)	ZnS: Cu	Bi_2MoO_6	
		Bi_2WO_6	
$NaTaO_3$: A (A=Ln, Ca, Sr, Ba)	ZnS: Ni	$AgNbO_3$	
ATa_2O_6(A=Mg, Ca, Sr, Ba)	ZnS: Pb,Cl	Ag_3VO_4	
		$In_2O_3(ZnO)_3$	
$Sr_2Ta_2O_7$	$NaInS_2$		
$K_3Ta_3Si_2O_{13}$	$AgGaS_2$		
$K_3Ta_3B_2O_{12}$	$CuInS_2$−$AgInS_2$-ZnS		
$K_2LnTa_5O_{15}$	$In_2O_3(ZnO)_3$		
$AgTaO_3$			

Source: Kudo [449]

8.13 Cost of Hydrogen Production

Although hydrogen can be produced from a variety of sources, its production cost will determine the use of a particular source. Hydrogen produced by steam reformation costs approximately three times more than the cost of natural gas per unit of energy produced. If natural gas costs $6/million BTU, then the cost of hydrogen will be $18/million BTU. Electrolysis processes with electricity at 5 cents/kWh will cost $28/million BTU. The cost of hydrogen production from electricity is a linear function of electricity costs. The cost and performance characteristics of various hydrogen production processes are given in Table 8.13.

8.14 Hydrogen Storage

Hydrogen can be stored both is gaseous and liquid states. However, for its use in automobiles, an onboard storage system that can store hydrogen safely is necessary. Although a number of technologies have been explored for onboard storage of hydrogen for automobile applications, a number of issues that include safety, cost, storage capacity, storage volume, and mass of the storage system still need to be

Table 8.13 A listing of the cost and performance characteristics of various hydrogen production processes

Process	Energy required (kWh/Nm^3)		Status of tech.	Efficiency (%)	Costs relative to SMR
	Ideal	Practical			
Steam methane reforming (SMR)	0.78	2–2.5	Mature	70–80	1
Methane/ NG pyrolysis			R&D to mature	72–54	0.9
H_2S methane reforming	1.5	–	R&D	50	<1
Landfill gas dry reformation			R&D	47–58	∼1
Partial oxidation of heavy oil	0.94	4.9	Mature	70	1.8
Naphtha reforming			Mature		
Steam reforming of waste oil			R&D	75	<1
Coal gasification (TEXACO)	1.01	8.6	Mature	60	1.4–2.6
Partial oxidation of coal			Mature	55	
Steam-iron process			R&D	46	1.9
Grid electrolysis of water	3.54	4.9	R&D	27	3–10
Solar & PV-electrolysis of water			R&D to mature	10	>3
High-temp. electrolysis of water			R&D	48	2.2
Thermochemical water splitting			Early R&D	35–45	6
Biomass gasification			R&D	45–50	2.0–2.4
Photobiological			Early R&D	<1	
Photolysis of water			Early R&D	<10	
Photoelectrochemical decomp. of water			Early R&D		
Photocatalytic decomp. of water			Early R&D		

Source: T-Raissi and Block [553]

resolved before its commercial use. Among these concerns, safety is the main issue. Various storage systems are listed below:

- Gaseous Hydrogen Storage System
  - High pressure cylinder
  - Glass microspheres
- Liquid Hydrogen Storage System
  - Cryogenic liquid hydrogen
  - $NaBH_4$ solutions
  - Rechargeable organic liquids

- Carbon and Other High surface Area Materials
  - Activated charcoals
  - Carbon nanotubes
  - Graphite nanofibers
  - MOFs, Zeolites, etc.
  - Clathrate hydrates
- Hydrides
  - Encapsulated NaH
  - LiH and MgH_2 slurries
  - CaH_2, $LiAlH_4$, etc

The amount of hydrogen that can be stored in these materials per volume or per weight basis is critical in choosing a storage medium. The volumetric and gravimetric H_2 densities of some of the most common storage options are shown in Fig. 8.55. There are other system requirements that need to be fulfilled and they are discussed in the following section.

8.14.1 High Pressure Cylinder

The most common method for storing hydrogen in gaseous form is in high pressure cylinders, which are classified into four categories. The classification is based mainly on construction materials and is given below:

Type I: Metal tanks.
Type II: Metal tanks wrapped with filament, such as glass fiber, around the cylindrical part.
Type III: Composite material tanks with a metal liner.
Type IV: Composite tanks (mainly made of carbon fiber) with a polymer liner.

Although metal tanks are suitable for stationary storage, Type III and Type IV are more suitable for onboard storage. Lightweight composite tanks are now designed to endure higher pressures, up to 700 bar (10,000 psi). The density of compressed H_2 under cryogenic conditions is shown in Fig. 8.56.

A comparison of these four types of cylinders is provided in Fig. 8.57.

8.14.1.1 Composite Tanks

Type IV composite tanks offer several advantages over other types of tanks. These are light weight, less expensive, and exhibit longer life span. A schematic diagram of a typical high-pressure, carbon fiber-wrapped H_2 storage composite tank designed by Quantum Inc [557] is shown in Fig. 8.58. These tanks are designed for 350 bar (5000 psi) and are already commercially available. The design of tanks that can

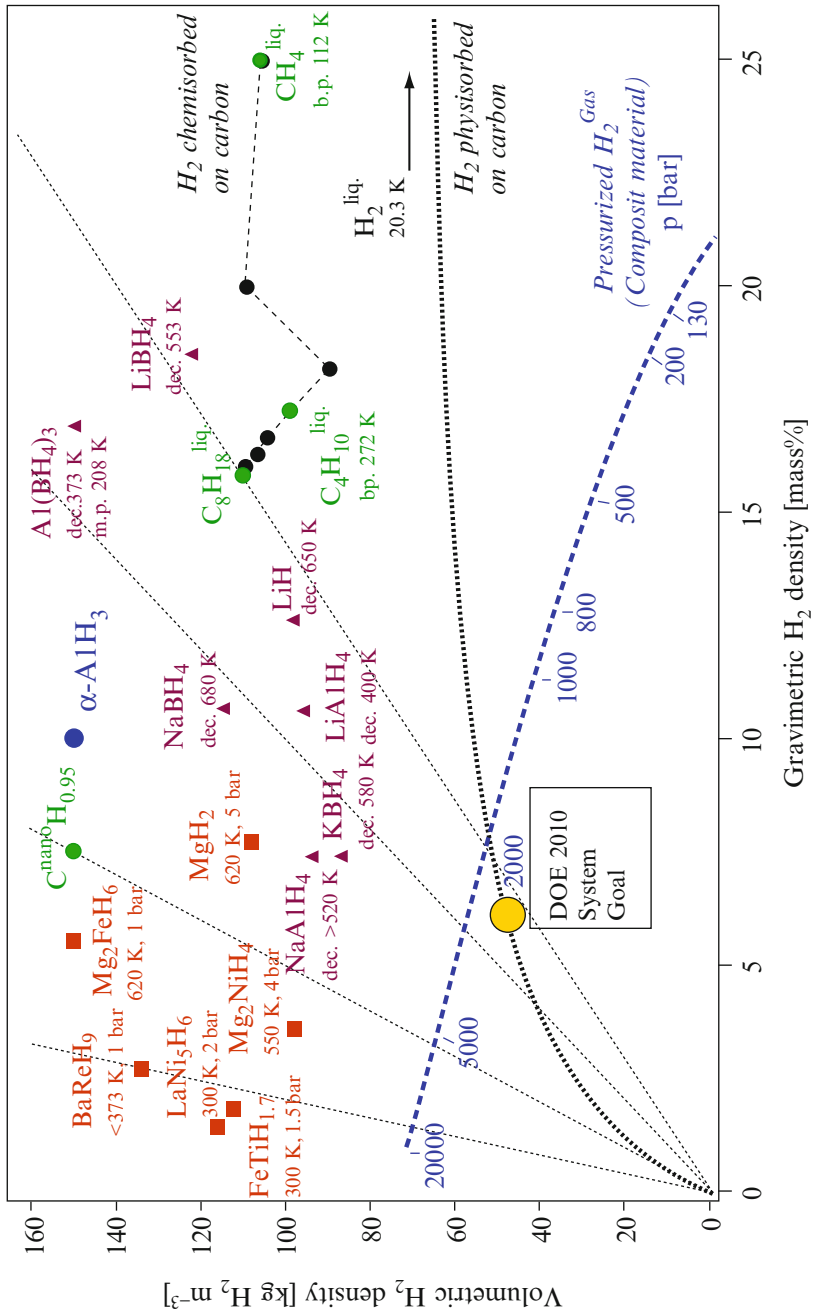

Fig. 8.55 Hydrogen storage capacity of various materials and systems (Adapted from Sandrock [554])

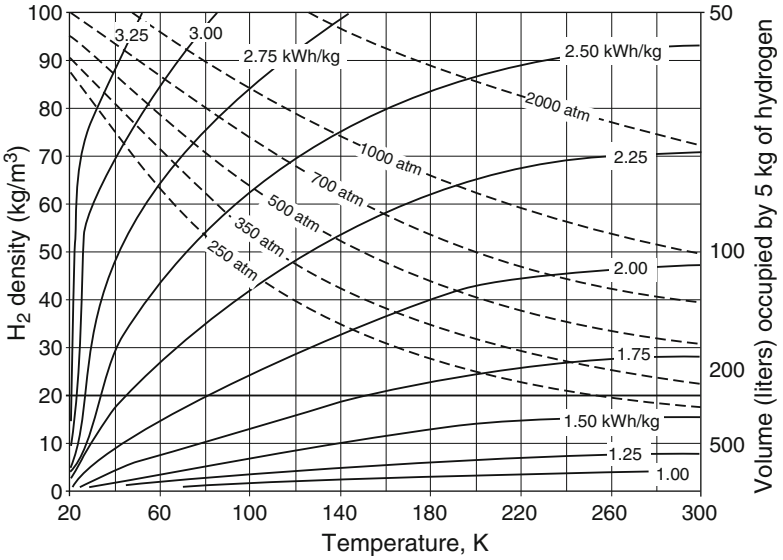

Fig. 8.56 Density of cryo-compressed hydrogen (Adapted from Aceves et al. [555])

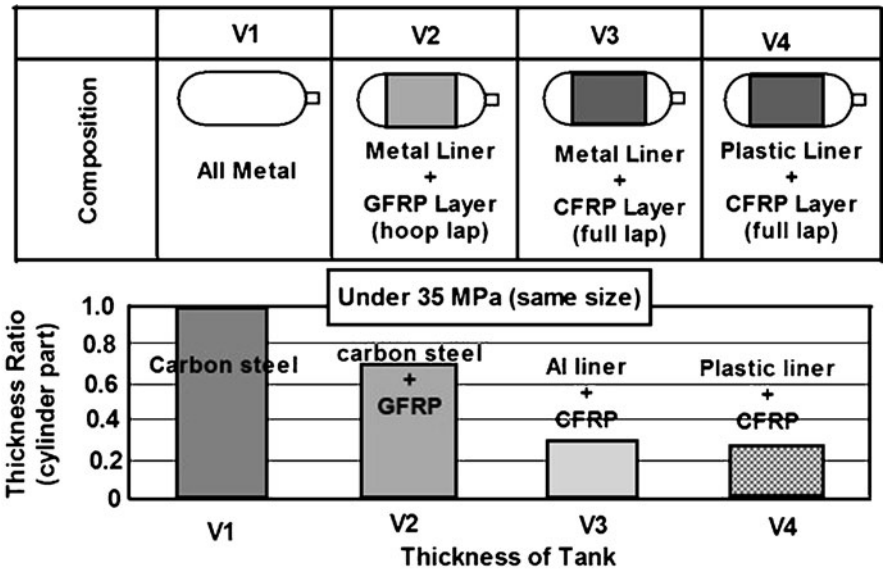

Fig. 8.57 Various types of tanks for high pressure hydrogen storage (Printed with permission from Mori and Hirose [556])

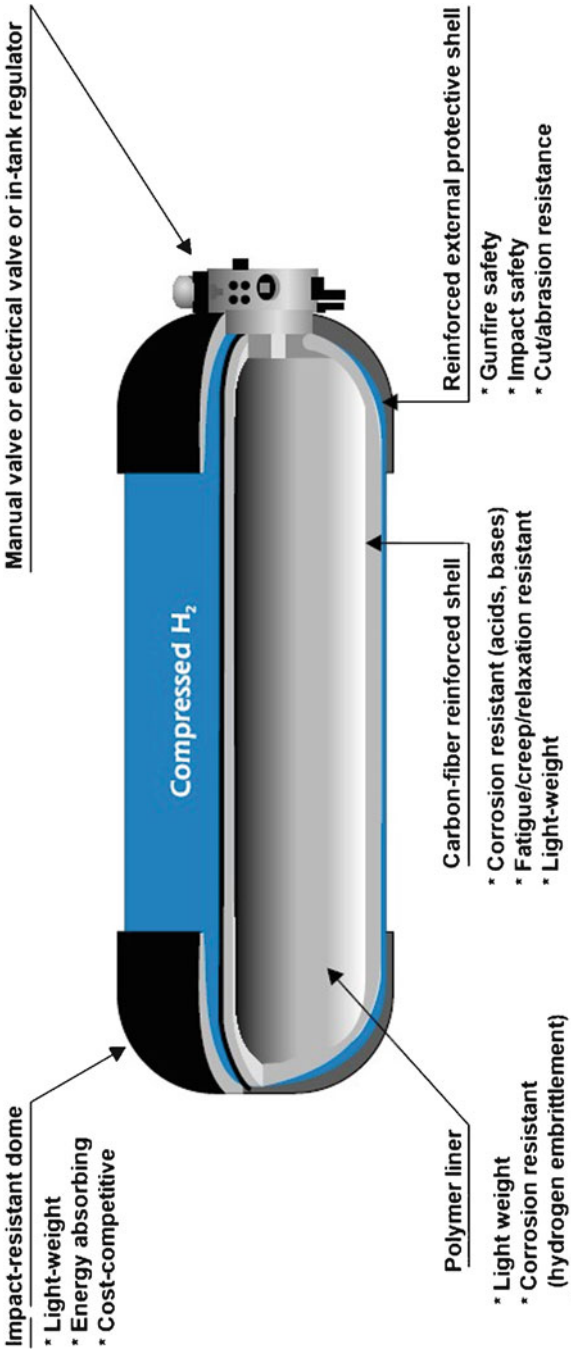

Fig. 8.58 A typical composite tank for storing compressed hydrogen (International Energy Agency [405])

be pressurized up to 700 bar (10,000 psi) is underway. These tanks must meet international codes that are accepted in several countries for pressures in the range of 350–700 bar. Composite tanks require no internal heat exchanger and may be usable for cryogas.

The compression of hydrogen is rather energy intensive. The work necessary to compress a gas depends on the thermodynamic process that is followed to compress it. The isothermal compression requires the least energy; however, it is difficult to maintain the isothermal condition. The work necessary during isothermal compression may be expressed by the following equation:

$$W = P_i V_i \, \ell n \left(\frac{P_f}{P_i} \right) \tag{8.48}$$

where,

W = Specific compression work (J/kg)
P_i = Initial pressure (Pa)
P_f = Final pressure (Pa)
V_i = Initial specific volume (m^3/kg)

Since, it is extremely difficult to maintain isothermal conditions, generally, an adiabatic compression process is followed. The work input necessary during the adiabatic compression of an ideal gas is expressed by:

$$W = \left[\frac{\gamma}{\gamma - 1} \right] P_i V_i \left(\left[\frac{P_f}{P_i} \right]^{\frac{\gamma - 1}{\gamma}} - 1 \right) \tag{8.49}$$

where, γ is the ratio of specific heats. For hydrogen, γ is 1.41.

As shown in Fig. 8.59, the energy consumed during the adiabatic compression of hydrogen is significantly higher than that during isothermal compression. In order to reduce the energy consumption, multistage compression with cooling between each compression stage is used. Various aspects of gas storage systems are discussed by several researchers [558–562].

The disadvantages of hydrogen storage in high pressure cylinders include: the requirement of large physical volume, difficult to fit the system in the available space, and high cost (500–600 USD/kg H_2). Safety issues still have not been resolved, particularly the problem of rapid loss of H_2 in an accident. The long-term effect of hydrogen on materials under cyclic or cold conditions is also not fully understood.

8.14.1.2 Glass Microspheres

Teitel [563] at the Brookhaven National Laboratory, USA, suggested that hollow glass micro spheres could be filled with hydrogen gas at high pressures [563, 564]. Following loading of H_2 at high pressure (350–700 bar) and high temperature

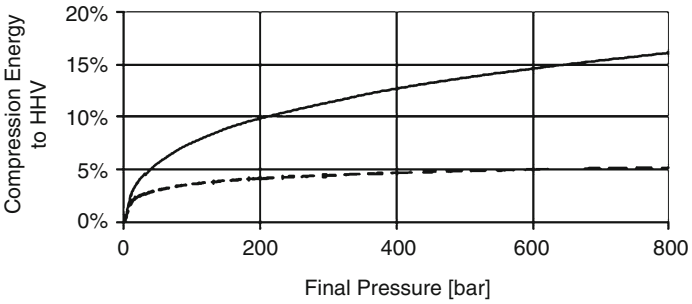

Fig. 8.59 Energy consumption during compression of hydrogen (Source: Eliasson and Bossel [562])

(300°C) by the permeation process, microspheres are next cooled to room temperature for storage. Hydrogen is released from microspheres by heating at 200–300°C. The main challenge to this process is the preparation of hollow glass spheres that can withstand high pressure. A thicker wall glass sphere may be necessary. However, this may require higher temperatures for the release of hydrogen from the glass spheres.

8.14.2 Liquid Hydrogen Storage System

8.14.2.1 Cryogenic Liquid Hydrogen (LH2)

The most common method to store hydrogen in a liquid form is to cool it down to a cryogenic temperature (−253°C) [565–574]. Other storage options include dissolving hydrogen as a constituent in other liquids, such as $NaBH_4$ solutions, rechargeable organic liquids, or anhydrous ammonia (NH_3).

Hydrogen can be liquefied at −253°C (normal boiling point of hydrogen at atmospheric pressure) and stored in specially designed cylinders. Liquid hydrogen (LH2) has a density of 70.8 kg/m^3 at normal boiling point (−253°C). Liquid hydrogen has a much better energy density than the pressurized gas. The liquefaction of hydrogen at this cryogenic temperature requires about 30–40% of its heating value. The other main disadvantage with LH2 is the boil-off loss during dormancy. The structure of a cryogenic, liquid hydrogen storage container is shown in Fig. 8.60.

Several methods are available for cryogenic compression of gaseous hydrogen to liquid hydrogen. One such compression process is shown in Fig. 8.61. In this process, liquid nitrogen is used for cooling hydrogen streams between compressors. Several compression stages are necessary to liquefy hydrogen. The process is also very energy intensive. The majority of the cost is associated with the capital investment. Although the operating and maintenance costs of a hydrogen liquefaction plant are about 12% of the total plant cost, the power costs are about 30% of the total cost.

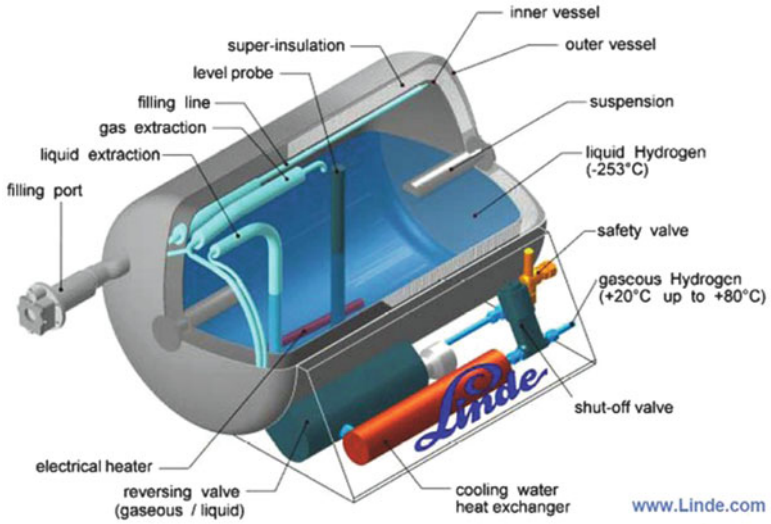

Fig. 8.60 Liquid hydrogen storage tank (Courtesy of Linde group [575])

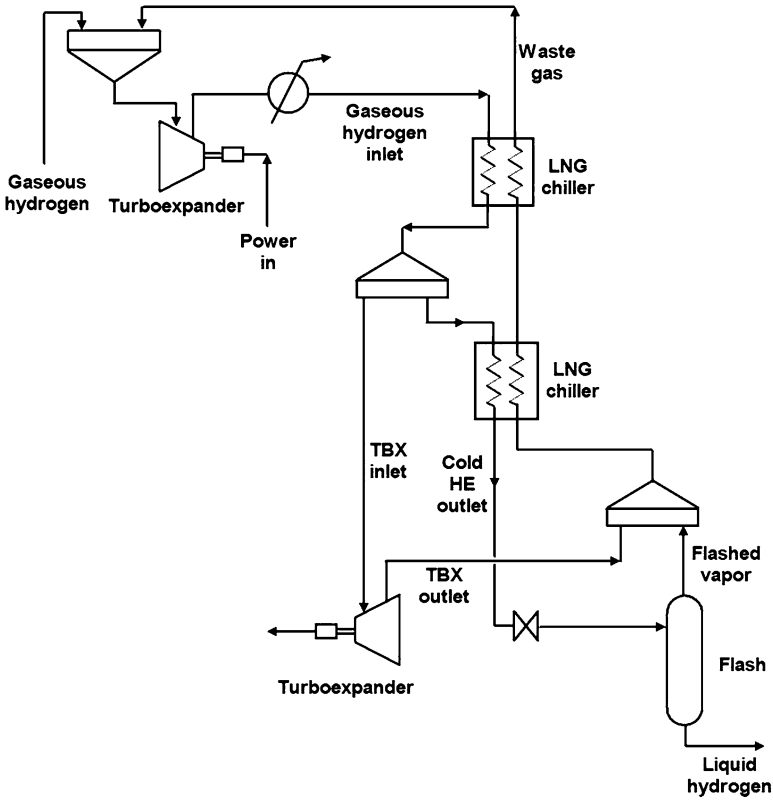

Fig. 8.61 Hydrogen liquefaction process (Source: Shimko [576])

8.14.2.2 $NaBH_4$ Solutions

Borohydride ($NaBH_4$) solutions can be used as a liquid storage medium for hydrogen. The release of hydrogen takes place by reacting it with water in the presence of a catalyst. The catalytic hydrolysis reaction is given below:

$$NaBH_4(l) + 2H_2O(l) \rightarrow 4H_2(g) + NaBO_2(s) \tag{8.50}$$

The theoretical maximum hydrogen energy storage density for $NaBH_4$ is 10.9 wt% H_2. The $NaBH_4$ solutions can be stored safely onboard and controllable onboard generation of H_2 is possible. The main disadvantage is that the reaction product $NaBO_2$ must be regenerated back to $NaBH_4$ off-board. Currently, the use of $NaBH_4$ solutions in vehicles is expensive due to the regeneration cost. Millennium Cell in the U.S. and MERIT in Japan, however, are promoting this technology, particularly for specialized applications.

8.14.2.3 Rechargeable Organic Liquids

Several organic liquids can also be used to indirectly store hydrogen in the liquid form. The basic concept is as follows. An organic liquid can be dehydrogenated by a catalytic process to produce H_2 gas onboard. The dehydrogenated organic compound will be next rehydrogenated in a central processing plant. For example, methylcyclohexane (C_7H_{14}) can be used as the carrier of hydrogen. The dehydrogenation reaction produces toluene (C_7H_8) and proceeds as follows:

$$C_7H_{14}(l) \Leftrightarrow C_7H_8(l) + 3H_2, \ (T_{\text{dehyd}} = 300 - 400^{\circ}\text{C}) \tag{8.51}$$

8.14.3 Carbon and Other High Surface Area Materials

Storage of hydrogen in porous solid materials (called adsorbents) can be a safe and efficient way of storing hydrogen, particularly for onboard storage. Among various porous solids, carbon-based adsorbents including carbon nanotubes and graphite nanofibers are considered to have the best capacity per mass basis [577–612]. A variety of carbonaceous adsorbents that include activated carbon, carbon fibers, carbon nanotubes, fullerenes, and graphite nanofibers have been investigated for their hydrogen adsorption capacity. Although some initial studies reported the adsorption capacity in the range of 30–60% on per unit mass basis, later studies, both theoretical and experimental, concluded that the adsorption capacity of carbon based adsorbents could be only in the 2–4% range. The adsorption capacity depends mainly on the surface area and temperature. Several studies indicated that a new bonding mechanism with energies between physisorption and strong covalent chemisorption may be necessary to increase adsorption capacity at room

temperature. The surface and bulk properties needed to achieve practical room temperature storage are not clearly understood, and it is far from certain that useful carbon can be economically and consistently synthesized. A number of studies focused on the modification of carbon or carbon nanotubes for enhancement of hydrogen storage [613–641]. Although it was assumed that carbon based materials might be the best adsorbents for hydrogen due to their large surface area, several studies were focused on the development of non-carbon based porous adsorbents [642–656]. However, the hydrogen storage capacity remained in the same range as that of carbon based adsorbents. In Table 8.14, the hydrogen storage capacity of carbon based materials reported by various researchers is summarized. Thomas [657] compiled data on the hydrogen storage capacity of various non-carbon adsorbents and plotted it as a function of the surface area of adsorbents (see Fig. 8.62).

8.14.4 Clathrates

Clathrates are compounds in which guest molecules are incorporated inside the cage of clathrates through a hydrogen bonded water network [706–728]. Rovetto et al. [729] noted that a binary H_2 /Tetrahydrofuran binary clathrate can store hydrogen at pressures nearly two orders of magnitude lower than that in pure hydrogen hydrates. Fundamental understanding of the structures of the clathrates and the hydrogen formation and release mechanism is underway. Lee et al. [730] reported that hydrogen storage capacities in THF-containing binary-clathrate hydrates can be increased to about 4 wt% at modest pressures by tuning their composition to allow the hydrogen guests to enter both the larger and the smaller cages, while retaining low-pressure stability.

8.14.5 Hydrides

Metal hydrides have the potential for on-board hydrogen storage. Hydrogen can be loaded to a number of metals (i.e., formation of hydride) at a relatively low temperature, and released at higher temperatures and pressures [647, 656, 731–741]. Sandrock [554] developed a hydride family tree incorporating various types of hydrides compounds that have potential for use as a hydrogen storage medium. However, hydrogen loading and release mechanisms of all the hydrides are not the same, and these may be divided into following categories based on how hydrogen is released from them.

- Rechargeable Hydrides
- Alanates
- Borohydrates
- Water Reactive Hydrides
- Thermally Activated Hydrides

Table 8.14 Summary of literature on adsorbtion of hydrogen by carbon based adsorbents

Adsorbent type	Hydrogen storage capacity (wt%)	Temperature (K)	Pressure (MPa)	Reference
SWNT	11	80	10	[658]
SWNT	2	80	10	[659]
SWNT	6.5	300	16	[660]
SWNT	5–10	300	0.04	[661]
SWNT	8	80	8	[662]
SWNT	10	300	0.04	[663]
SWNT	4	300	12	[664]
MWNT	5	300	10	[665]
MWNT	0.25	300	0.1	[666]
Li doped MWNT	20	200–400	0.1	[667]
K doped MWNT	14	300	0.1	[667]
Li doped MWNT	2.5	200–400	0.1	[668]
K doped MWNT	1.8	300	0.1	[669]
GNF	6.5	300	12	[670]
GNF	6.5	300	12	[671]
GNF	10	300	12	[672]
Purified SWNT	1.7	292	12.2	[673]
As Prepared MWNT	0.2	293	12.04	[673]
SWNT	3.5–4.5	Ambient	0.067	[674]
SWNT	1–15	77–300	8	[675]
SWNT	1.2	Ambient	4.8	[676]
MWNT	56	298	12.16	[677]
MWNT	0.68	Ambient	10	[678]
MWNT	13.8	300	1.0	[679]
MWNT	0.7–0.8	300	7	[680]
AC − K3[a]	5.63	77	20bar	[681]
AC − K5[b]	7.08	77	20bar	[681]
AX − 21(AC)[c]	4.6	77	10bar	[682]
KUA − 6(AC)[d]	5.6	77	40bar	[683]
Maxsorb-3000 (AC)[e]	5.2	77	40bar	[683]
CB850h(TC)[f]	6.9	77	20bar	[684]
TC[g]	5.3	77	20bar	[685]
Pure OMC	0.024	298	0.011	[686]
Pd-OMC (1% Pd)	0.064	298	0.011	[686]
Pd-OMC (10% Pd)	0.083	298	0.011	[686]
Pt-OMC (1% Pt)	0.069	298	0.011	[686]
Pt-OMC (10% Pt)	0.099	298	0.011	[686]

GNF Graphite nano-fiber
Surface area [a]2009 m^2/g
[b]3190 m^2/g
[c]2800 m^2/g
[d]3808 m^2/g
[e]3178 m^2/g
[f]3150 m^2/g
[g]2535 m^2/g

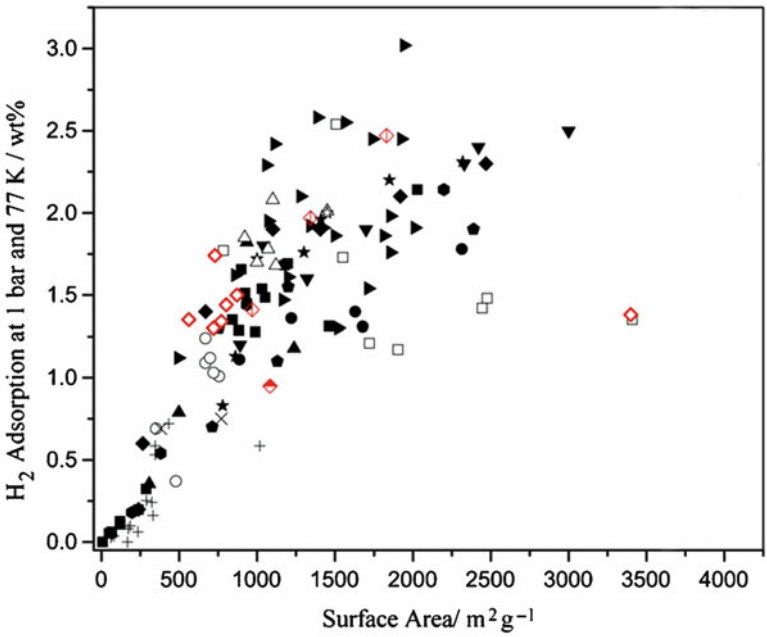

Fig. 8.62 Hydrogen storage capacity of several adsorbents. Carbon materials (*solid symbols*): (■) Nijkamp et al. [687], (●) Pang et al. [688], (◆) Parra et al. [689], (★) Takagi et al. [690,691], (▲) Zhao et al. [692,693], (⬢) Schimmel et al. [694,695], (▼) Texier-Mandoki et al. [696], (⬟) Gadiou et al. [697], (►) Gogotsi et al. [698]. Silicas, alumina, zeolites (*cross symbols*): (+) Nijkamp et al. [687], (x) Takagi et al. [691]; MOFs (*open symbols*): (□) Rowsell and Yaghi [699], (○) Chapman et al. [700], (△) Chun et al. [701], (◇) Kaye and Long [702], (☆) Dybtsev et al. [703], (⟐) Chen et al. [704], (◈) Dietzel et al. [705]. Surface areas obtained mainly from the BET method [657]

8.14.5.1 Rechargeable Hydrides

A number of metals and their alloys are capable of reversibly absorbing large amounts of hydrogen [742–791]. Charging can be done using either molecular hydrogen gas or hydrogen atoms from an electrolyte. Two methods may be used for charging/loading H_2 onto metals:

Gas phase reaction with molecular hydrogen:

$$M + 1/2\ xH_2 \Leftrightarrow MH_x + heat \tag{8.52}$$

Electrochemical reaction:

$$M + xH_2O + xe^- \Leftrightarrow MH_x + xOH^- \tag{8.53}$$

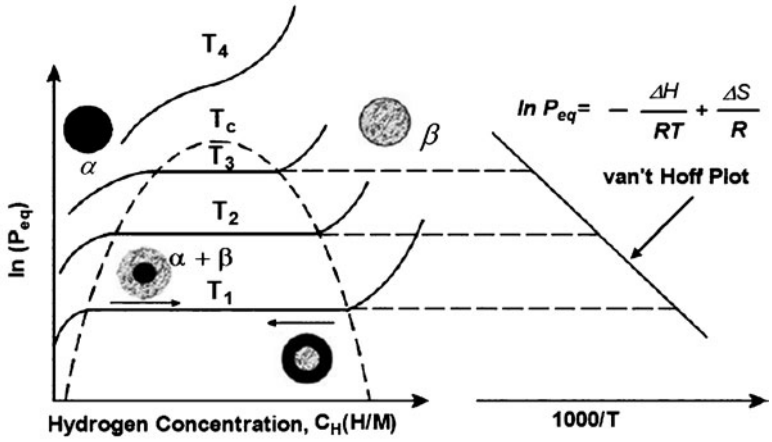

Fig. 8.63 Pressure-composition-isotherms (*left*) of a typical hydrogen absorption or desorption process and corresponding van't Hoff plot (Printed with permission from Principi et al. [792])

It is generally assumed that hydrogen is present in the form of atoms, never as molecules, on interstitial sites of the host metal lattice. Molecular hydrogen that is used as feed dissociates at the metal surface before absorption. Two hydrogen atoms recombine to H_2 during the desorption process.

The formation of hydride from gaseous hydrogen can be described by using pressure-composition isotherms of the hydride system (see Fig. 8.63). The stability of the hydrides and their decomposition temperature can be studied more accurately using this type of diagram. A flat plateau region in the isotherm is the indication of the coexistence of the solid solution and hydride phase. The amount of hydrogen that can be stored in the metal can be estimated from this plateau region. The hydrides generally exist as α and β phase. In the pure β-phase, the H_2 pressure rises steeply with the concentration. The two-phase region ends in a critical point (T_C), above which the transition from α to β-phase is continuous. The change of enthalpy that is critical in determining the energy release during charging and the heat input necessary during desorption from metal may be calculated from the von't Hoff equation and is given below:

$$\ell n\left(\frac{P_{eq}}{P_{eq}^{0}}\right) = \frac{\Delta H}{R}\frac{1}{T} - \frac{\Delta S}{R} \tag{8.54}$$

where P_{eq}^{0} and P_{eq} are equilibrium pressures at some standard state and at the system conditions, respectively, ΔH is the enthalpy, ΔS is the entropy, R is the universal gas constant, and T is the system temperature. The entropy change corresponds mostly to the change from molecular hydrogen gas to dissolved solid hydrogen and can be approximated as the entropy of H_2 at the standard state and is generally used for all metal hydride systems. The heat released during hydride

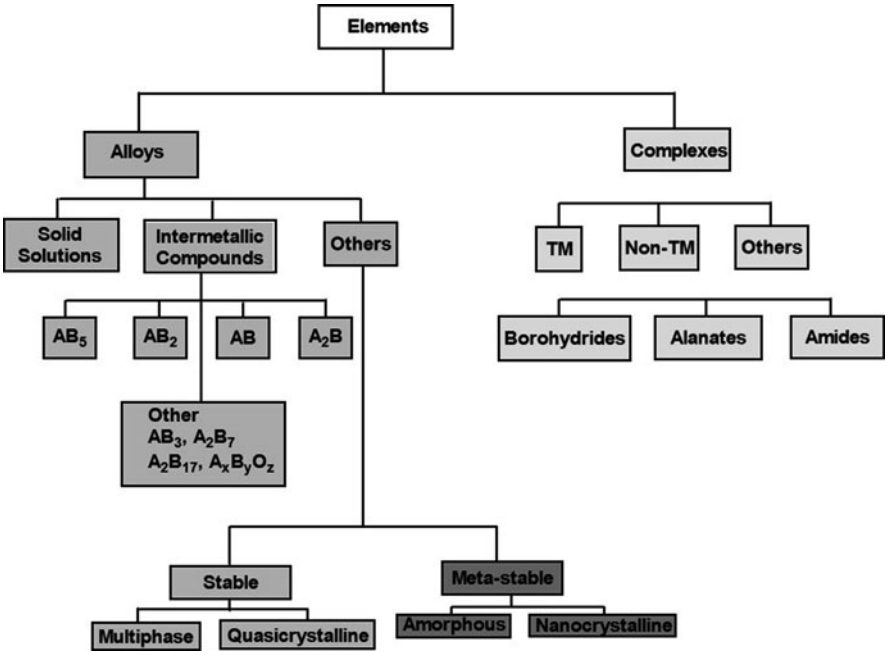

Fig. 8.64 Possible metal hydrides and their classification for hydrogen storage (Source: Sandrock [554])

formation is given by $\Delta Q = T\Delta S$. Theoretically, the same amount of heat would be necessary during decomposition of the hydride for releasing H_2. For a stable hydride like MgH_2, the heat necessary for the desorption of hydrogen at 300°C and 1 bar is approximately 25% of the higher heating value of hydrogen. A part of hydrogen is burned to provide the necessary energy during decomposition.

The Energy Information Administration-Hydrogen Implementing Agreement has developed a large database for hydrides with information about their properties (IEA HIA Annex 17; http://hydpark.ca.sandia.gov). A summary of this database (the metal hydride "family tree") is provided in Fig. 8.64.

8.14.5.2 Alanates

Alanates are hydrides containing AlH_4^- ions [793–803]. There are about 18 alanates reported in the literature that have potential for use as a H_2 storage medium. Hydrogen storage density of some of the alanates ranges from 7% to 10.5% by weight and potentially can meet the US Department of Energy's requirement for on-board hydrogen storage. The hydrogen storage capacity and desorption temperature of potential alanates are provided in Table 8.15.

Table 8.15 Storage density and desorption temperature of common alanates

Type	Storage density[a], wt% H_2	Desorption temperature, °C
$LiAlH_4$	10.6	190
$NaAlH_4$	7.5	100
$Mg(AlH_4)_2$	9.3	140
$Ca(AlH_4)_2$	7.8	>230

Source: International Energy Agency [405]
[a]Theoretical maximum

Among these alanates, $NaAlH_4$ has been studied most to get a better understanding of the properties of alanates. Alanates can be synthesized by a number of processes. The synthesis reactions for some alanates are shown below:

$$4LiH + AlCl_3 \xrightarrow{ether} LiAlH_4 + 3LiCl \tag{8.55}$$

$$NaH + Al + \frac{3}{2}H_2 \xrightarrow{140°C,5000psiH_2} NaAlH_4 \tag{8.56}$$

$$Na + Al + 2H_2 \xrightarrow{140°C,5000psiH_2} NaAlH_4 \tag{8.57}$$

$$Na + Al + 2H_2 \xrightarrow{270-280°C,2539psiH_2} NaAlH_4 \tag{8.58}$$

$$MH + AlH_3 \xrightarrow{Ball\ Milling} MAlH_4 \tag{8.59}$$

The decomposition reactions are shown below:

$$NaAlH_4 \rightarrow \frac{1}{3}Na_3AlH_6 + \frac{2}{3}Al + H_2 \tag{8.60}$$

$$Na_3AlH_6 \rightarrow 3NaH + Al + \frac{3}{2}H_2 \tag{8.61}$$

The kinetics and reversibility of the decomposition reaction are not favorable for the onboard hydrogen source. The low-temperature kinetics and reversibility of these alanates are improved by adding a catalyst, mainly metal titanium or a titanium based compound. The addition of titanium, or any other catalyst reduces the per mass basis hydrogen capacity of the material. Other issues are pyrophoricity and high cost.

8.14.5.3 Borohydrides

Borohydrides may be expressed by the general formula: $M_x(BH_4)_y$. Potentially, borohydrides have much higher hydrogen storage capacity than alanates [804–812]. However, these are not inherently reversible and have high stability. They can also

Table 8.16 Hydrogen storage capacity and desorption temperature of some borohydrides

Borohydride	Storage capacity, wt% H_2	Desorption temperature, °C
$LiBH_4$	18.5	300
$NaBH_4$	10.6	350
KBH_4	7.4	125
$Be(BH_4)_2$	20.8	125
$Al(BH_4)_3$	16.7	200
$Mg(BH_4)_2$	14.9	320
$Ca(BH_4)_2$	11.6	260

Source: Sandrock and International Energy Agency [405, 554]

produce diborane with H_2. The storage capacity and desorption temperature of several promising borohydrides are given in Table 8.16.

Hydrogen can be released from borohydrides either through thermal decomposition or via hydrolysis reaction. The thermal decomposition steps can be expressed by the following reactions:

$$\begin{aligned} 2MBH_4 &\leftrightarrow 2MH + B_2H_6 \\ 2MH &\leftrightarrow 2M + H_2 \\ B_2H_6 &\leftrightarrow 2(BH)_n + 2H_2 \end{aligned} \tag{8.62}$$

A high temperature is necessary for thermal decomposition. Some borohydrides would melt before the start of the decomposition step. This may cause significant problems in designing the storage system. Hydrogen release from borohydrides via the hydrolysis reaction may be a better route. The hydrolysis reactions may be expressed as follows:

$$\begin{aligned} MBH_4 + 2H_2O &\rightarrow MBO_2 + 4H_2 \\ MBH_4 + 4H_2O &\rightarrow MB(OH)_4 + 4H_2 \end{aligned} \tag{8.63}$$

Several alkaline borohydrides can form aqueous or alcoholic solutions that can be stored in a tank in automobiles, just like a regular gasoline storage system. Hydrogen can be released from the solution on demand by using a catalyst. One of the issues of hydrolysis reaction is that anhydrous borate is never produced. As a result, the total amount of hydrogen released in the reaction is much lower than the theoretical amount. For example, 10.8% by mass of hydrogen could be obtained from $NaBH_4$ if anhydrous borate ($NaBO_2$) is formed. This amount drops to 7.3% by mass if dihydro-borate ($NaBO_2 \cdot 2H_2O$) is formed. It drops further to 5.5% by mass if tetrahydrate is formed ($NaBO_2 \cdot 4H_2O$).

Table 8.17 Hydrogen release by hydrolysis of chemical hydrides

Hydrolysis reaction	Storage density[a], wt% H_2
$LiH + H_2O \Rightarrow H_2 + LiOH$	7.8
$NaH + H_2O \Rightarrow H_2 + NaOH$	4.8
$MgH_2 + 2H_2O \Rightarrow 2H_2 + Mg(OH)_2$	6.5
$CaH_2 + 2H_2O \Rightarrow 2H_2 + Ca(OH)_2$	5.2

Source: International Energy Agency [405]
[a]Theoretical maximum

Table 8.18 Thermal decomposition reaction of chemical hydride

Decomposition reaction	Storage density[a], wt% H_2	Decomposition temperature, °C
$NH_4BH_4 \Rightarrow NH_3BH_3 + H_2$	6.1	<25
$NH_3BH_3 \Rightarrow NH_2BH_2 + H_2$	6.5	<120
$NH_2BH_2 \Rightarrow NHBH + H_2$	6.9	>120
$NHBH \Rightarrow BN + H_2$	7.3	>500

Source: Autrey (2004) DOE EERE Program Review. International Energy Agency [405]
[a]Theoretical maximum

8.14.5.4 Chemical Hydrides (H_2O-Reactive)

A number of metal hydrides readily react with water, releasing hydrogen. For onboard storage applications, the solid hydride must be stored separately and mixed with water on demand for hydrogen production. The feeding of solid hydrides into the reaction chamber is challenging. However, attempts have been made to form a semi-liquid (i.e., slurry) by mixing the hydrides with mineral oil. In this form, hydrides can be pumped and safely handled. Controlled injection of H_2O during vehicle operation can be used to generate H_2 via hydrolysis reactions. The hydrolysis reaction is exothermic and does not require heat from the vehicle's power source. However, the reaction product is an alkaline solution that is extremely corrosive. Disposing of the alkaline solution in a refueling station would require special handling and a storage facility. An overview of the hydrolysis reactions for the most common chemical hydrides is presented in Table 8.17. The theoretical storage density of these hydrides is around 5–8 wt% H_2.

8.14.5.5 Chemical Hydrides (Thermal)

Several hydrides can be decomposed thermally to generate hydrogen. Ammonia borane is one such hydride that can be used to store hydrogen in a solid state. The decomposition takes place in four steps and at different temperatures. The hydrogen release at each step is different. These data are summarized in Table 8.18. The reactions are not reversible, and onboard regeneration is not possible.

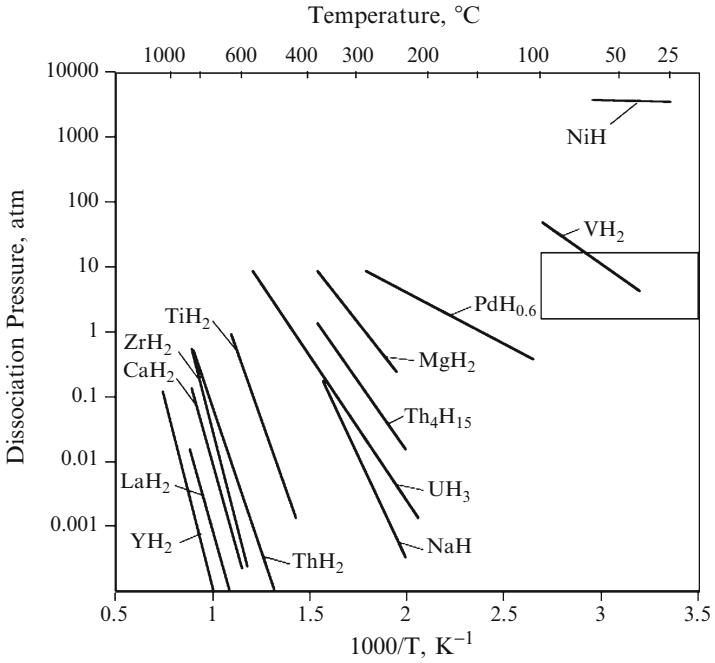

Fig. 8.65 van't Hoff lines for desorption of elemental hydride (Source: Sandrock [554])

8.14.5.6 Desorption of Hydrogen from Hydrides

Hydrogen take-up by metals and formation of metal hydrides generally occur at a low temperature and pressure, even at room temperature and at atmospheric pressure (1 bar). Some metals absorb hydrogen only at elevated pressures and temperatures. However, a much higher temperature is necessary for the desorption (release) of hydrogen. The temperature and pressure required for dissociation of hydride for the release of hydrogen can be calculated from the van't Hoff plots. Such plots for several types of metals hydrides are shown in Figs. 8.65 and 8.66.

A summary of hydrogen uptake capacity of various hydrides as a function of temperature is given in Fig. 8.67.

8.14.5.7 Borane

Boranes are chemical compounds of boron and hydrogen [813–825]. There are several borane compounds with a general formula of B_xH_y. The simplest borane, B_2H_6, is spontaneously flammable in air. Higher boranes, such as $B_{10}H_{14}$, are very stable in air, water, and heat. However, pure boranes do not have the required capacity for hydrogen on a weight basis. A number of researchers have been

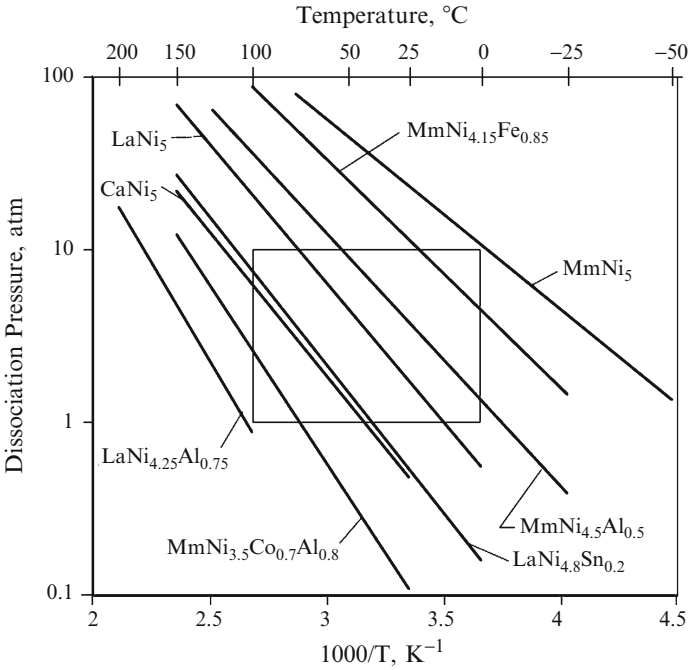

Fig. 8.66 van't Hoff lines for desorption of representative AB_5 hydrides (Source: Sandrock [554])

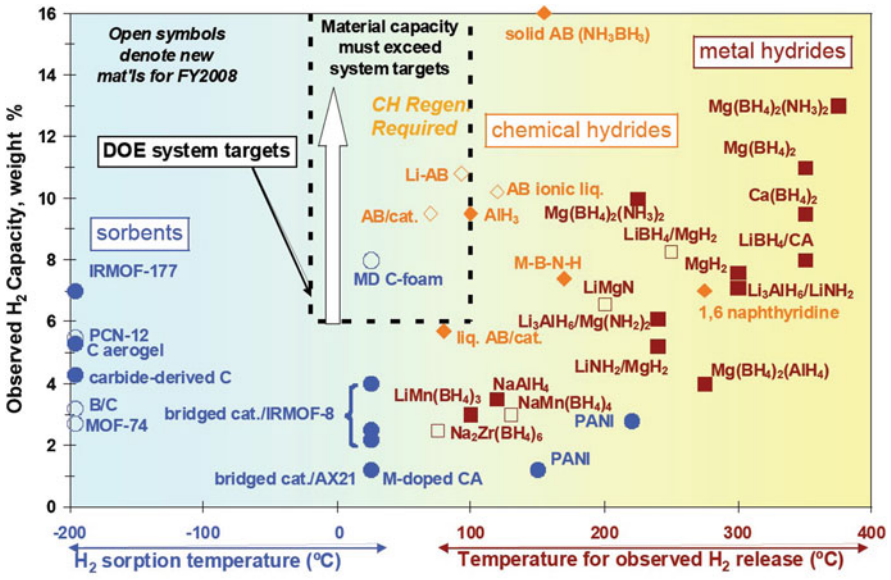

Fig. 8.67 Hydrogen storage capacity of various materials at different temperatures (Source: Sandrock [554])

Table 8.19 Comparison of 3 kg (or 215 km range) hydrogen storage by various medium

Technology	Storage system volume	Storage system weight
5,000 psi compressed H_2tanks	145 L	45 kg
10,000 psi compressed H_2tanks	100 L	50 kg
Metal hydrides	55 L	215 kg
Liquid H_2	90 L	40 kg

Source: Sirosh [827]

Table 8.20 Comparison of 7 kg (or 700 km range) hydrogen storage by various medium

Technology	Storage system volume	Storage system weight
5,000 psi compressed H_2tanks	320 L	90 kg
10,000 psi compressed H_2tanks	220 L	100 kg
Alanate hydrides	200 L	222 kg
Carbon nanotubes	∼130 L	∼120 kg

Source: Sirosh [827]

evaluating borane based compounds to increase the capacity on weight basis. Ammonia borane, which is a solid at room temperature, is composed of 19 wt% hydrogen and could be an ideal solid medium for hydrogen storage. However, ammonia borane releases hydrogen too slowly for its use as a hydrogen storage media for an automobile. A temperature higher than 170°C may be required to release hydrogen at a rate acceptable for automobile applications. Researchers are working on developing a catalyst that can increase the rate of extraction of hydrogen at a lower temperature. Blhum et al. [826] noted that both the extent and rate of hydrogen release from ammonia borane by dehydrogenation are significantly increased at 85°, 90°, and 95°C when the release reactions are carried out in 1-butyl-3-methylimidazolium chloride compared to analogous solid-state reactions.

8.15 Comparison of Hydrogen Storage Capacity

A comparison of various leading technologies for storage of 3 kg and 7 kg hydrogen is given in Tables 8.19 and 8.20, respectively.

8.16 Hydrogen Delivery Methods

The delivery and distribution of hydrogen are critical components to the cost and its wide range use as an energy source. Both a central production facility and distributed production systems are possible for hydrogen. The choice of the lowest-cost delivery mode (compressed gas trucks, cryogenic liquid trucks or gas pipelines) will depend

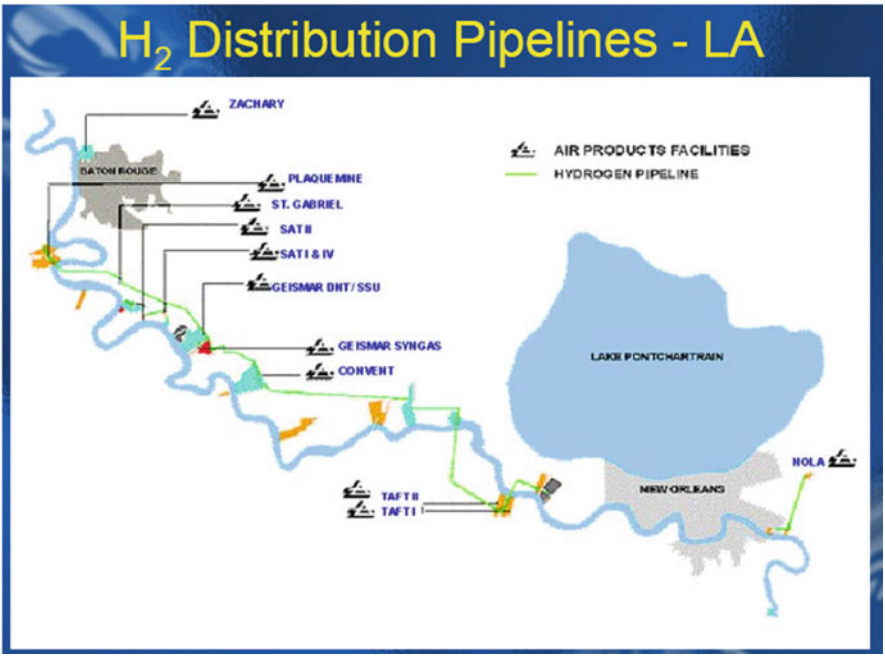

Fig. 8.68 Hydrogen distribution pipeline in Louisiana, USA (Source: Joseph [828])

upon specific geographic and market characteristics (e.g., city population and radius, population density, size and number of refueling stations and market penetration of fuel cell vehicles).

Generally, compressed gas truck delivery is ideal for small stations with very low demand. Liquid delivery is ideal for long distance delivery and moderate demand. Pipeline delivery is ideal for dense areas with large hydrogen demand. In the USA, Air Products, PA delivers H_2 through two pipelines to several facilities in Lousiana and the Gulf Coast. These two pipelines are shown in Figs. 8.68 and 8.69. Joseph [828] prepared a chart (see Fig. 8.70) showing when a distribution method is most effective.

8.17 Summary

Hydrogen is a secondary source of energy. It stores and carries energy produced from other resources (fossil fuels, water, and biomass). Hydrogen is not currently widely used, but it has potential as an energy carrier in the future. Hydrogen can be produced from a variety of resources (water, fossil fuels, or biomass) and is a byproduct of other chemical processes.

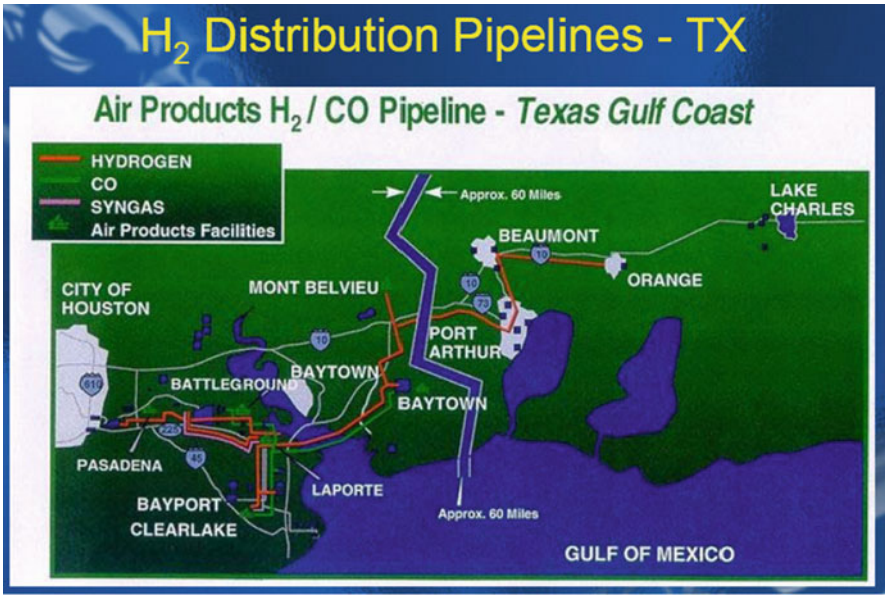

Fig. 8.69 Hydrogen distribution pipeline in Texas, USA (Source: Joseph [828])

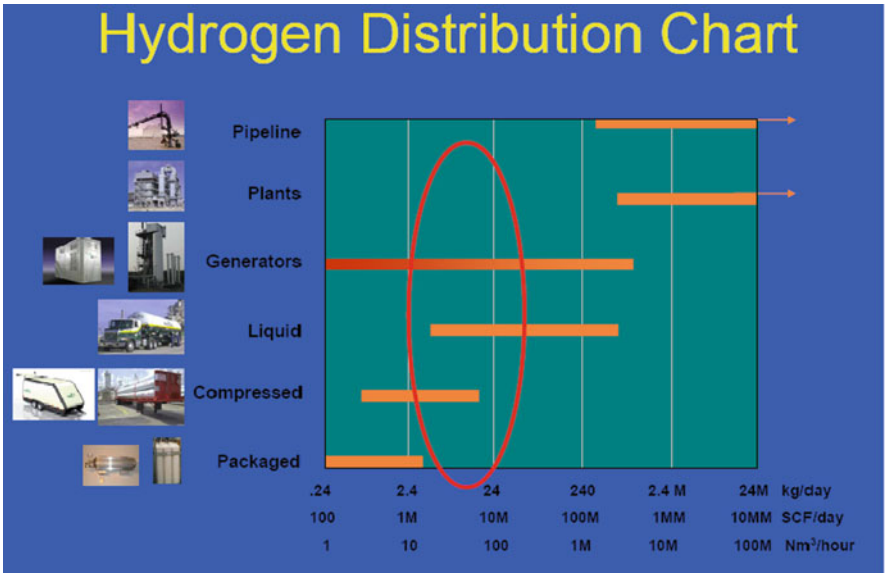

Fig. 8.70 Various hydrogen distribution method depending on demand (Source: Joseph [828])

Hydrogen has the highest energy content of any common fuel by weight (about three times more than gasoline), but the lowest energy content by volume (about four times less than gasoline).

Steam reforming is currently the least expensive method for producing hydrogen and accounts for about 95% of the hydrogen produced in the United States.

Hydrogen storage is a key enabling technology. None of the current technologies satisfy all of the hydrogen storage attributes sought by manufacturers and end users. Government, industry and academia are working together to lower costs, improve performance, and develop advanced materials for hydrogen storage. Efforts are also underway on improving existing commercial technologies, including compressed hydrogen gas and liquid hydrogen. Researchers are also exploring higher-risk storage technologies involving advanced materials (such as lightweight metal hydrides and carbon nanotubes). An energy economy based on hydrogen could resolve the growing concerns about America's energy supply, security, air pollution, and greenhouse gas emissions.

Problems

1. What is the role of hydrogen as a fuel?

2. Why use hydrogen?

3. What is a hydrogen economy?

4. What are the components of a hydrogen economy and its associated issues and challenges?

5. What are the major obstacles for implementation of hydrogen economy?

6. Is hydrogen safe to use as a fuel?

7. Assume that in the future all cars will be run on hydrogen and oxygen. The only byproduct will be water. Since oxygen from atmosphere will be used for oxygen source, will this upset the oxygen balance of air?

8. How much hydrogen is available today?

9. How do we produce hydrogen today?

10. How do you get the hydrogen to the customer?

11. What is the cost of hydrogen production by various methods?

12. Can hydrogen be put into natural gas pipelines?

13. How much will it cost to develop a hydrogen infrastructure?

14. Can diesel engines burn hydrogen instead of diesel?

15. What are the safety concerns for hydrogen use?

16. Explain how hydrogen power can help other renewable energy sources.

17. Can hydrogen energy be reliable and efficient as other conventional sources?

18. What kind of purity of water is necessary for hydrogen production?

19. Can seawater be used directly for hydrogen production?

20. Discuss the merits and demerits of various hydrogen storage systems.

21. What are the technological barriers for hydrogen production using solar energy?

22. Discuss the various potential uses of nuclear hydrogen. Can nuclear heat or electricity generated from nuclear energy be used directly in same applications? Which could be more efficient?

23. Discuss if the hydrogen generation by the hydropower system during off peak time via water electrolysis could be more efficient than a pumped storage system.

24. What kind of infrastructure is necessary for the large scale distribution of hydrogen?

25. How much hydrogen would be the lost during its storage from hydrogen refueling stations?

References

1. Bennaceur K, Clark B, Orr FM Jr, Ramakrishnan TS, Roulet C, Stout E (2005) Hydrogen: a future energy carrier? Oilfield Rev 17(1):30–41
2. Ohi J (2005) Hydrogen energy cycle: an overview. J Mater Res 20(12):3180–3187
3. Kruger P (2004) Electric power required in the world by 2050 for electric power and hydrogen fuel. World nuclear association annual symposium, 8–10 Sept 2004, London
4. Momirlan M, Veziroglu TN (2002) Current status of hydrogen energy. Renew Sustain Energy Rev 6:141–179
5. Christen K (2005) NRC finds hydrogen economy on track. Environ Sci Technol 39(19):398A
6. Penner SS (2005) Steps toward the hydrogen economy. Energy (Amsterdam, Neth) 31(1):33–43
7. Turner JA, Williams MC, Rajeshwar K (2004) Hydrogen economy based on renewable energy sources. Electrochem Soc Interface 13(3):24–30
8. Anon (2008) Event review: the potential for hydrogen as an energy source: the hydrogen economy. Chem Ind (London, UK), 21 April 2008 (8):30
9. Chapman PK, Haynes WE (2005) Power from space and the hydrogen economy. Acta Astronaut 57(2–8):372–383
10. Cooper HW (2007) Fuel cells, the hydrogen economy and you. Chem Eng Prog 103(11):34–43
11. Crabtree GW, Dresselhaus MS, Buchanan MV (2004) The hydrogen economy. Phys Today 57(12):39–44
12. Eikerling M, Kornyshev A, Kucernak A (2007) Driving the hydrogen economy. Phys World 20(7):32–36

13. Marban G, Valdes-Solis T (2008) Towards the hydrogen economy? Int J Hydrogen Energy 33(2):927
14. Suresh B, Yoneyama M, Schlag S (2007) Hydrogen. SRI Consulting, Menlo Park
15. Energy Information Administration (EIA) (2008) The impact of increased use of hydrogen on petroleum consumption and carbon dioxide emissions. Report No. SR-OIAF-CNEAF/2008-04
16. An "optimally plausible" solution based on NRC report.3 3 (2004) The NRC report. The hydrogen economy: opportunities, costs, barriers, and R&D needs. The National Academies Press, Washington, DC
17. Argonne National Laboratory (2005) Hydrogen demand, production and cost by region to 2050. Report No. ANL/ESD/05-2
18. College of the Desert (2001) Module 3 hydrogen use in internal combustion engine. Hydrogen fuel cell engines and related technologies: rev 0, December 2001
19. Van Blarigan P (1996) Development of a hydrogen fueled internal combustion engine designed for single speed/power operation. SAE Paper No. 961690
20. Van Blarigan P, Keller JO (1998) A hydrogen fuelled internal combustion engine designed for speed/power operation. Int J Hydrogen Energy 23(7):603–609
21. Verhelst S, Wallner T (2009) Hydrogen fueled internal combustion engines. Prog Energy Combust Sci 35(6):490–527
22. Sato Y, Kawamura A, Yanai T, Naganuma K, Yamane K, Takagi Y (2009) Research and development of hydrogen direct injection internal combustion engine system. In: Proceedings of the 4th IASME/WSEAS international conference on energy and environment, Cambridge, UK, pp 289–296
23. Welch AB, Mumford D, Munshi S, Holbery J, Boyer B, Younkins M, Jung H (2008) Challenges in developing hydrogen direct injection technology for internal combustion engines. SAE Paper No. 2008-01-2379
24. White CM, Steeper RR, Lutz AE (2006) The hydrogen fueled internal combustion engine: a technical review. Int J Hydrogen Energy 31(10):1292–1305
25. Berckmüller M, Rottengruber H, Eder A, Brehm N, Elsässer G, Müller-Alander G, Schwarz C (2003) Potentials of a charged SI-hydrogen engine. SAE paper no. 2003-01-3210
26. Jaura AK, Ortmann W, Stuntz R, Natkin B, Grabowski T (2004) Ford's H_2RV: an industry first HEV propelled with an H2 fueled engine – a fuel efficient and clean solution for sustainable mobility. SAE paper no. 2004-01-0058
27. Natkin RJ, Tang X, Boyer B, Oltmans B, Denlinger A, Heffel JW (2003) Hydrogen IC engine boosting performance and NOx study. SAE paper no. 2003-01-0631
28. Escher WJD (1975) The hydrogen-fueled internal combustion engine. A technical survey of contemporary U.S. projects. Technical Report, Escher Technology Associates, Inc., Report for the US Energy and Development Administration, Report No. TEC74/005
29. Department of Energy (2004) Hydrogen production overview, Fact sheet series. www.eere.energy.gov/hydrogenandfuelcells/. Accessed 20 Nov 2010
30. Singh M, Moore J, Shadis W (2005) Hydrogen demand, production, and cost by region to 2050. Argonne National Laboratory Report No. ANL/ESD/05-2
31. European Commission (2008) Hyways the European hydrogen roadmap. The sixth framework programme priority 1.6 sustainable development, global change and ecosystems, Report No. cEUR 23123
32. Mintz M, Gillette J, Elgowainy A (2007) Hydrogen production and delivery analysis in U.S. markets: cost, energy and greenhouse gas emissions. In: Proceeding of international conference on non-electric applications of nuclear power: seawater desalination, hydrogen production and other industrial applications Oarai, Japan, 16–19 Apr 2007
33. Aeatechnology Environment (2002) The feasibility, costs and markets for hydrogen production. A study for British Energy, September 2002. http://www.british-energy.com/documents/The_Feasibility,_Costs_and_Markets_for_Hydrogen_Production.pdf. Accessed 20 Nov 2010
34. Hinkle J (2007) Hydrogen supply and demand opportunities. A report to National Hydrogen Association, 22 Feb 2007. http://www.hydrogenassociation.org/policy/resources/21jun07_supplyAndDemand.pdf. Accessed 20 Nov 2010

35. Dominguez M (2006) Hydrogen generation: state of the art and future needs. European Commissions, FISA 2006 conference on EU research and training in reactor systems, 16 Mar 2006
36. Yacobucci BD, Curtright AE (2004) A hydrogen economy and fuel cells: an overview. CRS report for congress. Order Code RL32196 Congressional Research Service, The Library of Congress
37. Hydrogen production processes. National Hydrogen Association (August 2004) Hydrogen production overview. www.HydrogenAssociation.org
38. Hartstein A (2003) Hydrogen production from natural gas. In: Proceeding of the hydrogen coordination meeting. Hydrogen plants for the new millennium. Foster Wheeler, 2 June 2003 www.fwc.com/publications/tech_papers2/files/WARD1109.pdf
39. Padro CEG, Putsche V (1999) Survey of the economics of hydrogen technologies. National Renewable Energy Laboratory, Sept 1999
40. Zachariah-Wolff JL, Egyedi TM, Hemmes K (2007) From natural gas to hydrogen via the Wobbe index: the role of standardized gateways in sustainable infrastructure transitions. Int J Hydrogen Energy 32(9):1235–1245
41. New York State Energy Research and Development Authority. Hydrogen Fact Sheet Hydrogen production Steam methane reforming (SMR)
42. Simpson AP, Lutz AE (2007) Exergy analysis of hydrogen production via steam methane reforming. Int J Hydrogen Energy 32:4811–4820
43. Fulcheri L, Schwab Y (1995) From methane to hydrogen, carbon black and water. Int J Hydrogen Energy 20(3):197–202
44. Gaudernack B, Lynum S (1998) Hydrogen from natural gas without release of CO_2 to the atmosphere. Int J Hydrogen Energy 23(12):1087–1093
45. Li Y, Chen J, Qin Y, Chang L (2000) Simultaneous production of hydrogen and nanocarbon from decomposition of methane on a nickel-based catalyst. Energy Fuels 14:1188–1194
46. Muradov NZ (2001) Hydrogen via methane decomposition: an application of decarbonization of fossil fuels. Int J Hydrogen Energy 26:1165–1175
47. Otsuka K, Shigeta Y, Takenaka S (2002) (Japan) Production of hydrogen from gasoline range alkanes with reduced CO_2 emissions. Int J Hydrogen Energy 27:11–18
48. Ahmed S, Krumpelt M (2001) Hydrogen from hydrocarbon fuels for fuel cells. Int J Hydrogen Energy 26:291–301
49. Astanovsky DL, Astanovsky LZ (2001) Hydrogen production by steam catalytic natural gas conversion with using drilling gas pressure. In: Proceedings of the National Hydrogen Associations 12th Annual U.S. Hydrogen Meeting, March, Washington, D.C., USA.
50. Balthasar W, Hambleton DJ (1978) Industrial scale production of hydrogen from natural gas, naphtha and coal. In: Veziroglu TN, Seifritz W (eds) Hydrogen energy system: proceedings of the 2nd world hydrogen energy conference, Zurich, Switzerland, 21–24 August, vol 2. Pergamon Press, Oxford, pp 1007–1014
51. Bromberg L, Cohn DR, Rabinovich A (1998) Plasma reforming of methane. Energy Fuels 12:11–18
52. Pruden B (1999) Hydrogen production from natural gas. In: Proceedings 9th Canadian hydrogen conference, Vancouver, BC, Canada, 7–10 Feb, pp 494–501
53. Bhat SA, Sadhukhan J (2008) Process intensification aspects for steam methane reforming: an overview. AlChE J 55(2):408–422
54. Harale A, Hwang HT, Liu PKT, Sahimi M, Tsotsis TT (2009) Design aspects of the cyclic hybrid adsorbent-membrane reactor (HAMR) system for hydrogen production. Chem Eng Sci 65(1):427–435
55. Hopkinson BE (1975) Materials selection for steam reforming hydrogen plants. Interam Conf Mater Technol, [Proc], 4th, pp 181–185
56. Jasinski M, Dors M, Mizeraczyk J (2008) Production of hydrogen via methane reforming using atmospheric pressure microwave plasma. J Power Sources 181(1):41–45
57. Mathure PV, Patwardhan AV, Saha RK (2007) Steam reforming of methane for bulk and small scale production of hydrogen. Indian Chem Eng 49(4):480–491

58. Spath PL, Mann MK (2001) Life cycle assessment of hydrogen production via natural gas steam reforming. National Renewable Energy Laboratory. Report No. NREL/TP-570-27637
59. Elder R (2009) Thermochemical water splitting for hydrogen production. http://www.shef.ac.uk/content/1/c6/07/18/96/12%20Mar%2009%20Thermochemical%20water%20splitting%20for%20hydrogen%20production.pdf. Accessed 5 Dec 2010
60. Albrecht KO, Satrio JA, Shanks BH, Wheelock TD (2010) Application of a combined catalyst and sorbent for steam reforming of methane. Ind Eng Chem Res 49(9):4091–4098
61. Borowiecki T, Denis A, Panczyk M, Gac W, Stolecki K (2008) Steam reforming of methane on the Ni-Re catalysts. Pol J Chem 82(9):1733–1742
62. Choi SO, Moon SH (2009) Performance of La1-xCexFe0.7Ni0.3O3 perovskite catalysts for methane steam reforming. Catal Today 146(1–2):148–153
63. Graf PO, Mojet BL, Lefferts L (2009) The effect of potassium addition to Pt supported on YSZ on steam reforming of mixtures of methane and ethane. Appl Catal A Gen 362(1–2): 88–94
64. Hossain MA, Trambouze Y (1984) Steam reforming of methane to synthesis gas over cobalt catalysts. Front Chem React Eng [Proc – Int Chem React Eng Conf] 2:23–35
65. Liu H-M, Ye Q, Xu B-Q (2007) Efficient hydrogen production via stepwised steam reforming of methane using nanocomposite Ni/ZrO2 catalyst. Stud Surf Sci Catal 172:473–476 (Science and Technology in Catalysis 2006)
66. Martavaltzi CS, Pampaka EP, Korkakaki ES, Lemonidou AA (2010) Hydrogen production via steam reforming of methane with simultaneous CO2 capture over CaO-Ca12Al14O33. Energy Fuels 24(4):2589–2595
67. Moon DJ, Kim DH, Lee BG, Kim MJ, Hong SI (2008) Hydrogen production: steam reforming of light hydrocarbon over Ni-based catalysts. Prepr Symp Am Chem Soc, Div Fuel Chem 53(2):620–621
68. Mukherjee DK, Sahay BP, Bhattacharyya NB (1974) Catalytic methane-steam reformation: effect of temperature and partial pressure of methane. Technology(Sindri, India) 11(1):3–8
69. Ross JRH, Steel MCF, Zeini-Isfahani A (1975) Steam reforming of methane over nickel catalysts. Mech Hydrocarbon React, Symposium, pp 201–214
70. Ryi S-K, Park J-S, Kim D-K, Kim T-H, Kim S-H (2009) Methane steam reforming with a novel catalytic nickel membrane for effective hydrogen production. J Membr Sci 339 (1–2):189–194
71. Sabirova ZA, Danilova MM, Kuzin NA, Kirillov VA, Zaikovskii VI, Krieger TA (2009) Reinforced nickel catalysts for steam reforming of methane to synthesis gas. React Kinet Catal Lett 97(2):363–370
72. Schaedel BT, Duisberg M, Deutschmann O (2009) Steam reforming of methane, ethane, propane, butane, and natural gas over a rhodium-based catalyst. Catal Today 142(1–2):42–51
73. Shen W, Komatsubara K, Hagiyama T, Yoshida A, Naito S (2009) Steam reforming of methane over ordered mesoporous Ni-Mg-Al oxides. Chem Commun(Cambridge, UK) 42:6490–6492
74. Van Hook JP (1980) Methane-steam reforming. Catal Rev Sci Eng 21(1):1–51
75. Wu P, Li X, Ji S, Lang B, Habimana F, Li C (2009) Steam reforming of methane to hydrogen over Ni-based metal monolith catalysts. Catal Today 146(1–2):82–86
76. Abbas HF, Wan Daud WMA (2010) Hydrogen production by methane decomposition: a review. Int J Hydrogen Energy 35(3):1160–1190
77. Adachi T (1975) Uses of nuclear reactors. Gendai Kagaku 55:24–26
78. Albertazzi S, Basile F, Vaccari A (2004) Catalytic properties of hydrotalcite-type anionic clays. Interface Sci Technol 1:496–546 (Clay Surfaces)
79. Al-Ubaid AS (1987) Steam reforming of hydrocarbons catalyzed over nickel supported catalysts. Arabian J Sci Eng 12(2):189–198
80. Barelli L, Bidini G, Gallorini F, Servili S (2008) Hydrogen production through sorption-enhanced steam methane reforming and membrane technology: a review. Energy (Oxford, UK) 33(4):554–570

81. Bridger GW (1973) Coking prevention in steam reforming of methane. Redaktions-gasen Huettenw, Symposium Series 7, Published by Komm Gaserzeugung Int Gas-Union, Karlsruhe, Germany, pp 22
82. Choudhary TV, Goodman DW (2000) Methane activation on Ni and Ru model catalysts. J Mol Catal A: Chem 163(1–2):9–18
83. Graboski MS (1984) The production of synthesis gas from methane, coal and biomass. Catal Convers Synth Gas Alcohols Chem, [Proc Symp] 37–50
84. Hu YH, Ruckenstein E (2004) Catalytic conversion of methane to synthesis gas by partial oxidation and CO_2 reforming. Adv Catal 48:297–345
85. Imai N (1976) Development of HTR methane steam reforming at the Juelich Nuclear Research Center. Kagaku Kogaku 40(12):646–647
86. Inui T (1999) High speed hydrogen production technology. In: Ekuserugi Kogaku, Yoshida K (ed) Kyoritsu Shuppan, Tokyo, Japan. 195–204
87. Jackson PJ, Seddon D (1984) New Fischer-Tropsch routes for the conversion of Australian natural gas to transport fuels. Winning in the Competitive World, 12th Australian Chemical Engineering Conference, vol 2, pp 641–648
88. Kuo JCW (1992) Evaluation of direct methane conversion processes. NATO ASI Ser E: Appl Sci 225(Chemical Reactor Technology for Environmentally Safe Reactors and Products), pp 183–226
89. Ledakowicz S (1976) Possibilities of using high-temperature reactors in chemical technology. Chemik 29(3):82–86
90. S-w L, Y-d L (2005) Research advances on methane reforming for hydrogen. Wuhan Huagong Xueyuan Xuebao 27(1):20–47
91. Mayer B, Koepsel R (1978) Reaction kinetics of the methane-water vapor conversion on the GIAP 3–6 N catalyst. Freiberg Forschungsh A A591:59–114
92. Pfeifer P, Haas-Santo K, Goerke O, Bohn L, Schubert K (2005) Fuel to hydrogen – an overview over fuel conversion activities at the Institute for Micro Process Engineering. In: AIChE Spring National Meeting, Conference Proceedings, Atlanta, GA, United States, 10–14 Apr 2005: 136H/1-136H/5
93. Rostrup-Nielsen JR (1981) New uses of natural gas by steam reforming processes. Dansk Kemi 62(1):6–10
94. Scarpiello DA (1996) Catalytic conversion of methane. In: Proceedings of the international gas research conference, vol 2, pp 2707–2716
95. Sugisawa M, Teramura K, Kubonra J, Domen K (2008) Nickel oxide catalysts for methane steam reforming. Kemikaru Enjiniyaringu 53(6):423–426
96. Tada A (2008) Application of direct methane reforming for hydrogen power generation and application of nano carbon materials. Metan Kodo Kagaku Henkan Gijutsu Shusei, pp 222–233
97. Takamura H (2005) Hydrogen production from methane by using oxygen permeable ceramics. Materia 44(3):211–215
98. Tomishige K (2001) Catalytic process for synthesis gas production from natural gas. Kagaku Kogyo 52(10):767–772
99. Tomishige K (2009) Production of synthesis gas and hydrogen by oxidative steam reforming of methane: development of Ni catalysts with trace noble metals. Nenryo Denchi 8(3):57–66
100. Yasuda I, Shirasaki Y (2006) Development of highly-efficient hydrogen production system based on membrane reactor from natural gas. Shokubai 48(5):296–301
101. Zheng W, Li J, Wu H, Liu S (2008) Research progress on catalysts for stepwise steam reforming of methane for hydrogen production. Jingxi Shiyou Huagong Jinzhan 9(7):24–28
102. Berrocal GP, Da Silva ALM, Assaf JM, Albornoz A, MdC R (2010) Novel supports for nickel-based catalysts for the partial oxidation of methane. Catal Today 149(3–4):240–247
103. Beznis NV, Weckhuysen BM, Bitter JH (2010) Partial oxidation of methane over co-zsm-5: tuning the oxygenate selectivity by altering the preparation route. Catal Lett 136(1–2):52–56
104. Cheng YS, Pena MA, Yeung KL (2009) Hydrogen production from partial oxidation of methane in a membrane reactor. J Taiwan Inst Chem Eng 40(3):281–288

105. Ferreira AC, Ferraria AM, Botelho do Rego AM, Goncalves AP, Correia MR, Gasche TA, Branco JB (2009) Partial oxidation of methane over bimetallic nickel-lanthanide oxides. J Alloy Comp 489(1):316–323
106. Ferreira AC, Ferraria AM, Rego AM Botelho do, Goncalves AP, Girao AV, Correia R, Gasche TA, Branco JB (2010) Partial oxidation of methane over bimetallic copper-cerium oxide catalysts. J Mol Catal A: Chem 320(1–2):47–55
107. Ferreira AC, Goncalves AP, Gasche TA, Ferraria AM, Rego AM Botelho do, Correia MR, Bola AM, Branco JB (2010) Partial oxidation of methane over bimetallic copper- and nickel-actinide oxides (Th, U). J Alloy Comp 497(1–2):249–258
108. Fleys M, Simon Y, Marquaire P-M, Lapicque F (2009) Hydrogen production by catalytic partial oxidation of methane. Study of reaction mechanism. Récents Progrès en Génie des Procédés – Numéro 96 – 2007 ISBN 2-910239-70-5, Ed. SFGP, Paris, France
109. Gubanova EL, Schuurman Y, Sadykov VA, Mirodatos C, van Veen AC (2009) Evaluation of kinetic models for the partial oxidation of methane to synthesis gas over a Pt/PrCeZrOx catalyst coated on a triangular monolith. Chem Eng J (Amsterdam, Neth) 154(1–3):174–184
110. Habimana F, Li X, Ji S, Lang B, Sun D, Li C (2009) Effect of Cu promoter on Ni-based SBA-15 catalysts for partial oxidation of methane to syngas. J Nat Gas Chem 18(4):392–398
111. Prangsri-aroon S, Viravathana P, Worayingyong (2010) A partial oxidation of methane to syngas by LaCoO3 oxidative catalysts. In: Abstracts of Papers, 239th ACS National Meeting, San Francisco, CA, United States, 21–25 Mar 2010: PETR-12
112. Salazar-Villalpando MD, Reyes B (2009) Hydrogen production over Ni/ceria-supported catalysts by partial oxidation of methane. Int J Hydrogen Energy 34(24):9723–9729
113. Schmal M, Perez CA, Teixeira da Silva V, Padilha LF (2010) Hydrogen and ethylene production from partial oxidation of methane on CuCe, CuZr mixed oxides and ZrO2 catalysts. Appl Catal A Gen 375(2):205–212
114. Shang R, Wang Y, Jin G, Guo X-Y (2009) Partial oxidation of methane over nickel catalysts supported on nitrogen-doped SiC. Catal Commun 10(11):1502–1505
115. Kothari R, Tyagi VV, Pathak A (2010) Waste-to-energy: a way from renewable energy sources to sustainable development. Renew Sustain Energy Rev 14(9):3164–3170
116. Cai X, Cai Y, Lin W (2008) Autothermal reforming of methane over Ni catalysts supported over ZrO2-CeO2-Al2O3. J Nat Gas Chem 17(2):201–207
117. Cai X, Dong X, Lin W (2006) Autothermal reforming of methane over Ni catalysts supported on CuO-ZrO2-CeO2-Al2O3. J Nat Gas Chem 15(2):122–126
118. Cao L, Ni C, Yuan Z, Wang S (2009) Autothermal reforming of methane over CeO2-ZrO2-La2O3 supported Rh catalyst. Catal Lett 131(3–4):474–479
119. Ciambelli P, Palma V, Palo E, Iaquaniello G (2009) Natural gas autothermal reforming: an effective option for a sustainable distributed production of hydrogen. In: Barbaro P, Bianchini C (eds) Catalysis for sustainable energy production, Wiley-VCH Verlag GmbH, Weinheim, Germany, pp 287–319
120. Ciambelli P, Palma V, Palo E, Sannino D (2005) Hydrogen production via catalytic autothermal reforming of methane. World Congress of Chemical Engineering, 7th, Glasgow, United Kingdom, 10–14 July 2005: 86113/1-86113/9
121. Dias JAC, Assaf JM (2008) Autothermal reforming of methane over Ni/gamma -Al2O3 promoted with Pd. Appl Catal A Gen 334(1–2):243–250
122. Kim SH, Chung JH, Kim YT, Han J, Yoon SP, Nam S-W, Lim T-H, Lee H-I (2009) Disk-type porous Ni-Cr bulk catalyst for hydrogen production by autothermal reforming of methane. Catal Today 146(1–2):96–102
123. Lee WS, Kim TY, Woo SI (2010) High-throughput screening for the promoters of alumina supported Ni catalysts in autothermal reforming of methane. Top Catal 53(1–2):123–128
124. Meira de Souza AEA, Maciel LJL, Medeiros de Lima Filho N, Moraes de Abreu CA (2010) Catalytic activity evaluation for hydrogen production via autothermal reforming of methane. Catal Today 149(3–4):413–417
125. Nagaoka K, Eiraku T, Nishiguchi H, Takita Y (2006) Ni/(rare earth phosphate) as a new effective catalyst for autothermal reforming of methane. Chem Lett 35(6):580–581

126. Rabe S, Truong T-B, Vogel F (2007) Catalytic autothermal reforming of methane: performance of a kW scale reformer using pure oxygen as oxidant. Appl Catal A Gen 318:54–62
127. Ratnasamy C, Wagner JP, Tackett D (2004) Production of hydrogen by autothermal reforming of methane and simulated natural gas. In: AIChE Spring National Meeting, Conference Proceedings, New Orleans, LA, United States, 25–29 Apr 2004, pp 177–181
128. Souza MMVM, Schmal M (2005) Autothermal reforming of methane over Pt/ZrO2/Al2O3 catalysts. Appl Catal A Gen 281(1–2):19–24
129. Wang G, Coppens M-O (2010) Rational design of hierarchically structured porous catalysts for autothermal reforming of methane. Chem Eng Sci 65(7):2344–2351
130. Ayabe S, Omoto H, Utaka T, Kikuchi R, Sasaki K, Teraoka Y, Eguchi K (2003) Catalytic autothermal reforming of methane and propane over supported metal catalysts. Appl Catal A Gen 241(1):261–269
131. Fletcher EA, Moen RL (1977) Hydrogen and oxygen from water. Science 197:1050
132. Ihara S (1980) On the study of hydrogen production from water using solar thermal energy. Int J Hydrogen Energy 5(5):527–534
133. Ohta T (1979) Solar hydrogen energy system. Pergamon Press, Oxford, p 59
134. Kogan A (2000) Direct solar thermal splitting of water and on-site separation of the products-IV. Development of porous ceramic membranes for a solar thermal water-splitting reactor. Int J Hydrogen Energy 25:1043–1050
135. Yalcin S (1989) A review of nuclear hydrogen production. Int J Hydrogen Energy 14(8):551–561
136. Verfondern K (2007) Nuclear energy for hydrogen production. Schriften des Forschungszentrums Juelich, Reihe Energietechnik/Energy Technology 58:i-ii, 1–185
137. Ryland DK, Li H, Sadhankar RR (2007) Electrolytic hydrogen generation using CANDU nuclear reactors. Int J Energy Res 31(12):1142–1155
138. Marcus GH (2009) An international overview of nuclear hydrogen production programs. Nucl Technol 166(1):27–31
139. Verfondern K (2005) Nuclear hydrogen production. Nachrichten – Forschungszentrum Karlsruhe 37(3):124–128
140. Schulten R, Barnert H, Fedders H, Grziwa G, Schulte A (1976) The concept of ”nuclear hydrogen production” and progress of work in the Nuclear Research Center Juelich. In: Proceedings of the 1st World Hydrogen Energy Conference, vol 1, pp 1A, 19–32
141. Uhrig RE (2008) Producing hydrogen using nuclear energy. Int J Nucl Hydrogen Prod Appl 1(3):179–193
142. Kasai S, Fujiwara S, Yamada K, Ogawa T, Matsunaga K, Yoshino M, Hoashi E, Makino S (2009) Nuclear hydrogen production by high-temperature electrolysis. Nihon Genshiryoku Gakkai Wabun Ronbunshu 8(2):122–141
143. O’Brien JE, Stoots CM, Herring JS, Hartvigsen JJ (2006) Hydrogen production performance of a 10- cell planar solid-oxide electrolysis stack. J Fuel Cell Sci Technol 3:213–219
144. O’Brien JE, Stoots CM, Herring JS, Hartvigsen JJ (2007) Performance of planar high-temperature electrolysis stacks for hydrogen production from nuclear energy. Nucl Technol 158:118–131
145. Hawkes GL, O’Brien JE, Stoots CM, Herring JS (2007) CFD model of a planar solid oxide electrolysis cell for hydrogen production from nuclear energy. Nucl Technol 158:132–144
146. Herring JS, O’Brien JE, Stoots CM, Hawkes GL (2007) Progress in high-temperature electrolysis for hydrogen production using planar SOFC technology. Int J Hydrogen Energy 32(4):440–450
147. Ivy J (2004) Summary of electrolytic hydrogen production. NREL Report NREL/MP-560-36734, Sept 2004
148. Rivera-Tinoco R, Mansilla C, Bouallou C, Werkoff F (2008) Techno-economic study of hydrogen production by high temperature electrolysiscoupled with an epr, sfr or htr – water steam production and coupling possibilities. Int J Nucl Hydrogen Prod Appl 1(3):249–266

149. Anzieu P, Aujollet P, Barbier D, Bassi A, Bertrand F, Duigou AL, Leybros J, Rodriguez G (2008) Coupling a hydrogen production process to a nuclear reactor. Int J Nucl Hydrogen Prod Appl 1(3):207–218
150. Bo Y, Wenqiang Z, Jingming X, Jing C (2010) Status and research of highly efficient hydrogen production through high temperature steam electrolysis at INET. Int J Hydrogen Energy 35(7):2829–2835
151. Fujiwara S, Kasai S, Yamauchi H, Yamada K, Makino S, Matsunaga K, Yoshino M, Kameda T, Ogawa T, Momma S, Hoashi E (2008) Hydrogen production by high temperature electrolysis with nuclear reactor. Prog Nucl Energy 50(2–6):422–426
152. Harvego EA, McKellar MG, O'Brien JE, Herring JS (2009) Parametric evaluation of large-scale high-temperature electrolysis hydrogen production using different advanced nuclear reactor heat sources. Nucl Eng Des 239(9):1571–1580
153. Mansilla C, Sigurvinsson J, Bontemps A, Maréchal A, Werkoff F (2007) Heat management for hydrogen production by high temperature steam electrolysis. Energy 32(4):423–430
154. O'Brien JE, McKellar MG, Harvego EA, Stoots CM (2010) High-temperature electrolysis for large-scale hydrogen and syngas production from nuclear energy – summary of system simulation and economic analyses. Int J Hydrogen Energy 35(10):4808–4819
155. Shin Y, Park W, Chang J, Park J (2007) Evaluation of the high temperature electrolysis of steam to produce hydrogen. Int J Hydrogen Energy 32(10–11):1486–1491
156. Stoots CM, O'Brien JE, Condie KG, Hartvigsen JJ (2010) High-temperature electrolysis for large-scale hydrogen production from nuclear energy: experimental investigations. Int J Hydrogen Energy 35(10):4861–4870
157. Udagawa J, Aguiar P, Brandon NP (2007) Hydrogen production through steam electrolysis: model-based steady state performance of a cathode-supported intermediate temperature solid oxide electrolysis cell. J Power Sources 166(1):127–136
158. Utgikar V, Thiesen T (2006) Life cycle assessment of high temperature electrolysis for hydrogen production via nuclear energy. Int J Hydrogen Energy 31(7):939–944
159. Yu B, Zhang W, Chen J, Xu J, Wang S (2008) Advance in highly efficient hydrogen production by high temperature steam electrolysis. Sci China B Chem 51(4):289–304
160. Yildiz B, Kazimi MS (2006) Efficiency of hydrogen production systems using alternative nuclear energy technologies. Int J Hydrogen Energy 31:77–92
161. O'Brien JE, Stoots CM, Herring JS, Hawkees GL (2006) Hydrogen production from nuclear energy via high temperature electrolysis. 1st Energy Center Hydrogen Initiative Symposium. Paper: ECHI-I-IL-3, Purdue University, West Lafayette, 5–6 Apr 2006. Report No. INL/CON-06-01375
162. Russell JL, McCorkle KH, Norman JH, Schuster JR, Trester PW (1976) Development of thermochemical water splitting at General Atomic Company. In: Proceedings of synthetic pipeline gas symposium, vol 8, pp 335–361
163. Funk JE (1976) Thermochemical production of hydrogen via multistage water splitting processes. Int J Hydrogen Energy 1(1):33–43
164. Pangborn JB, Sharer JC (1975) Analysis of thermochemical water-splitting cycles. In: Hydrogen energy, Proceedings of the hydrogen economy Miami energy conference, Miami Beach, Fla., March 18–20, 1974. Part A. (A75-44751 22–44). Plenum Press, New York, pp 499–515
165. Russell JL, Porter JT (1975) A search for thermochemical water-splitting cycles. In: Hydrogen energy, Proceedings of the hydrogen economy Miami energy conference, Miami Beach, Fla., March 18–20, 1974, Part A. (A75-44751 22–44). Plenum Press, New York, pp 517–529
166. Funk JE (2001) Thermochemical hydrogen production: past and present. Int J Hydrogen Energy 26(3):185–190
167. Brown LC, Funk JF, Showalter SK (2000) High efficiency generation of hydrogen fuel using nuclear power. Annual report to the Department of Energy, Report No. GA-A23451
168. Brecher LE, Spewock S, Warde CJ (1977) Westinghouse sulfur cycle for the thermochemical decomposition of water. Int J Hydrogen Energy 21(1):7–15

169. Beghi GE (1986) A decade of research on thermochemical hydrogen at the joint research center, Ispra. Int J Hydrogen Energy 11(12):761–771
170. Funk JK, Reinstrom RM (1966) Energy requirements in the production of hydrogen from water. Ind Eng Chem Process Des Dev 5(3):336–342
171. Besenbruch GE (1982) General Atomic sulfur-iodine thermochemical water-splitting process. Am Chem Soc Div Pet Chem Prepr 271:48–51
172. Williams LO (1980) Hydrogen power. Pergamon Press, New York
173. Ueda R, Tagawa H, Sato S, Yasuno T, Ohno S, Maeda M (1974) Production of hydrogen from water using nuclear energy, a review. Japan Atomic Energy Research Institute, Tokyo, Japan:, pp 69
174. Tamaura Y, Steinfeld A, Kuhn P, Ehrensberger K (1995) Production of solar hydrogen by a novel, 2-step, water-splitting thermochemical cycle. Energy (Oxford, UK) 20(4):325–330
175. Bamberger CE (1978) Hydrogen production from water by thermochemical cycles; a 1977 update. Cryogenics 18:170
176. Knoche KF, Schuster P (1984) Thermochemical production of hydrogen by a vanadium/chlorine cycle. Part 1: an energy and exergy analysis of the process. Int J Hydrogen Energy 9(6):457–472
177. Russell J, Porter J (1974) Production of hydrogen from water. General Atomics Report GA–A12889
178. Schuster JR, Russell JL Jr, McCorkle KH, Mysels KJ, Norman JH, O'Keefe DR, Sharp R, Stowell SA, Trester PW, Williamson DG (1977) Development of a sulfur-iodine thermochemical water-splitting cycle for hydrogen production. In: Proceedings of the Intersociety Energy Conversion Engineering Conference, vol 1, pp 920–927
179. De Graaf JD, McCorkle KH, Norman JH, Sharp R, Webb GB, Ohno T (1978) Engineering and bench-scale studies of the sulfur-iodine cycle at General Atomic. In: Proceedings of the Intersociety Energy Conversion Engineering Conference, vol 13 No. 2, pp 1150–1157
180. De Graaf JD, McCorkle KH, Norman JH, Sharp R, Webb GB, Ohno T, (1979) Engineering and bench-scale studies on the general atomic sulfur-iodine thermochemical water-splitting cycle. Advances in Hydrogen Energy 1 (Hydrogen Energy System, vol 2): 545–567
181. Besenbruch G, Caprioglio G, McCorkle K, Mysels K, Norman J, O'Keefe D, Rode J, Sharp R, Trester P, Yoshimoto M (1979) Development of a sulfur – iodine thermochemical water-splitting cycle for hydrogen production. In: Proceedings of the 14th Intersociety Energy Conversion Engineering Conference , vol. 1, pp 737–742
182. Schuster JR, Caprioglio G, McCorkle KH, Ohno T (1979) Bench-scale investigations and process engineering on the sulfur-iodine cycle. Proceedings of the DOE Chemical/Hydrogen Energy Systems Contracts Review. Meeting Date 1978 (CONF-781142), pp 119–130
183. Hammache A, Bilgen E (1992) Nuclear hydrogen production based on sulfuric acid decomposition process. J Energy Res Technol 114(3):227–234
184. Kubo S, Nakajima H, Kasahara S, Higashi S, Masaki T, Abe H, Onuki K (2004) A demonstration study on a closed-cycle hydrogen production by the thermochemical water-splitting iodine-sulfur process. Nucl Eng Des 233(1–3):347–354
185. Sakurai M, Nakajima H, Amir R, Onuki K, Shimizu S (2000) Experimental study on side-reaction occurrence condition in the iodine-sulfur thermochemical hydrogen production process. Int J Hydrogen Energy 25(7):613–619
186. Sakurai M, Nakajima H, Onuki K, Shimizu S (2000) Investigation of 2 liquid phase separation characteristics on the iodine-sulfur thermochemical hydrogen production process. Int J Hydrogen Energy 25(7):605–611
187. Banerjee AM, Bhattacharyya K, Pai MR, Tripathi AK, Kamble VS, Bharadwaj SR, Kulshreshtha SK (2007) Studies on sulfur-iodine thermochemical cycle for hydrogen production. BARC Newsl 285:67–72
188. Cerri G, Salvini C, Corgnale C, Giovannelli A, De Lorenzo MD, Martinez AO, Le Duigou A, Borgard J-M, Mansilla C (2010) Sulfur-Iodine plant for large scale hydrogen production by nuclear power. Int J Hydrogen Energy 35(9):4002–4014

189. Leybros J, Gilardi T, Saturnin A, Mansilla C, Carles P (2010) Plant sizing and evaluation of hydrogen production costs from advanced processes coupled to a nuclear heat source. Part I: sulphur-iodine cycle. Int J Hydrogen Energy 35(3):1008–1018
190. Norman JH, Basenbruch GE, O'Keefe DR (1981) Thermochemical water-splitting for hydrogen production. General Atomic Co., San Diego
191. Norman JH, Mysels KJ, Sharp R, Williamson D (1981) Studies of the sulfur-iodine thermochemical water-splitting cycle. Advances in Hydrogen Energy 2(Hydrogen Energy Program, vol 1): 257–275
192. Norman JH, Mysels KJ, Sharp R, Williamson D (1982) Studies of the sulfur-iodine thermochemical water-splitting cycle. Int J Hydrogen Energy 7(7):545–556
193. Onuki K, Kubo S, Terada A, Sakaba N, Hino R (2009) Thermochemical water-splitting cycle using iodine and sulfur. Energy Environ Sci 2(5):491–497
194. Onuki K, Nakajima H, Kubo S, Futakawa M, Higashi S, Hwang GJ, Masaki T, Ikenoya K, Ishiyama S, Akino N, Shimizu S (2003) Thermochemical hydrogen production by iodine-sulfur cycle. Hydrogen planet, 14th world hydrogen energy conference, Montreal, QC, Canada, 9–13 June 2002, pp 1196–1204
195. Rosen MA (2010) Advances in hydrogen production by thermochemical water decomposition: a review. Energy (Oxford, UK) 35(2):1068–1076
196. Sakurai M, Nakajima H, Onuki K, Ikenoya K, Shimizu S (1999) Preliminary process analysis for the closed cycle operation of the iodine-sulfur thermochemical hydrogen production process. Int J Hydrogen Energy 24(7):603–612
197. Vitart X, Borgard JM, Goldstein S, Colette S (2004) Investigation of the I-S cycle for massive hydrogen production. Nuclear production of hydrogen, information exchange meeting, 2nd, Argonne, IL, United States, 2–3 Oct 2003, pp 99–109
198. Zhang P, Chen SZ, Wang LJ, Xu JM (2010) Overview of nuclear hydrogen production research through iodine sulfur process at INET. Int J Hydrogen Energy 35(7):2883–2887
199. Brown LC (2007) Evolution of the sulfur-iodine flowsheet. AIChE Annual Meeting, 7 Nov 2007, Salt lake City, Utah USA
200. Brown LC, Lentsch RD, Besenbruch GE, Schultz KR, Funk JE (2003) Alternative flowsheets for the sulfur-iodine thermochemical hydrogen cycle. Spring national meeting of AIChE, New Orleans, Louisiana, 30 Mar–3 Apr 2003, Report No. GA–A24266, p 33
201. Pickard P (2005) Sulfur-iodine thermochemical cycle. 2005 DOE Hydrogen Program review. PD 27
202. Banerjee AM, Pai MR, Bhattacharya K, Tripathi AK, Kamble VS, Bharadwaj SR, Kulshreshtha SK (2008) Catalytic decomposition of sulfuric acid on mixed Cr/Fe oxide samples and its application in sulfur-iodine cycle for hydrogen production. Int J Hydrogen Energy 33(1):319–326
203. Bai Y, Zhang P, Guo H, Chen S, Wang L, Xu J (2009) Purification of sulfuric and hydriodic acids phases in the iodine-sulfur process. Chin J Chem Eng 17(1):160–166
204. Barbarossa V, Brutti S, Diamanti M, Sau S, De Maria G (2006) Catalytic thermal decomposition of sulphuric acid in sulphur-iodine cycle for hydrogen production. Int J Hydrogen Energy 31(7):883–890
205. Burch KC, Ginosar DM, Petkovic LM, Houghton TP (2007) Activated carbon catalysts for the production of hydrogen via the sulfur-iodine thermochemical water splitting cycle. Abstracts, 62nd northwest regional meeting of the American Chemical Society, Boise, ID, United States, June 17–20 June, NW-012
206. Chen Y, Wang Z, Zhang Y, Zhou J, Cen K (2010) Platinum-ceria-zirconia catalysts for hydrogen production in sulfur-iodine cycle. Int J Hydrogen Energy 35(2):445–451
207. Kim J, Chang J, Park BH, Shin Y, Lee K, Lee W, Chang J (2008) A study on the dynamic behavior of a sulfur trioxide decomposer for a nuclear hydrogen production. Int J Hydrogen Energy 33(24):7361–7370
208. Lanchi M, Caputo G, Liberatore R, Marrelli L, Sau S, Spadoni A, Tarquini P (2009) Use of metallic Ni for H2 production in S-I thermochemical cycle: experimental and theoretical analysis. Int J Hydrogen Energy 34(3):1200–1207

209. Nagaraja BM, Jung KD, Ahn BS, Abimanyu H, Yoo KS (2009) Catalytic decomposition of SO3 over Pt/BaSO4 materials in sulfur-iodine cycle for hydrogen production. Ind Eng Chem Res 48(3):1451–1457
210. Nagaraja BM, Jung KD, Yoo KS (2009) Synthesis of Cu/Fe/Ti/Al2O3 composite granules for SO3 decomposition in SI cycle. Catal Lett 128(1–2):248–252
211. Onstott EI (1990) Cerium dioxide as a recycle reagent for thermochemical hydrogen production by modification of the sulfur dioxide-iodine cycle. Advances in Hydrogen Energy 8 (Hydrogen Energy Program 8, vol. 2): 531–538
212. Ozturk IT, Hammache A, Bilgen E (1995) An improved process for H2SO4 decomposition step of the sulfur-iodine cycle. Energy Convers Manage 36(1):11–21
213. Petkovic LM, Ginosar DM, Rollins HW, Burch KC, Deiana C, Silva HS, Sardella MF, Granados D (2009) Activated carbon catalysts for the production of hydrogen via the sulfur-iodine thermochemical water splitting cycle. Int J Hydrogen Energy 34(9):4057–4064
214. Rodriguez SB, Louie D, Gauntt RO, Gelbard F, Cole R, McFadden K, Drennen T, Martin B, Archuleta L, Revankar ST, Vierow K (2007) MELCOR-H2 transient analysis of sulfur-iodine cycle experiments. International topical meeting on safety and technology of nuclear hydrogen production, control, and management, Boston, MA, United States, 24–28 June 2007, pp 140–146
215. Zhang Y, Wang Z, Zhou J, Cen K (2009) Ceria as a catalyst for hydrogen iodide decomposition in sulfur-iodine cycle for hydrogen production. Int J Hydrogen Energy 34(4):1688–1695
216. Zhang Y, Wang Z, Zhou J, Liu J, Cen K (2009) Experimental study of Ni/CeO2 catalytic properties and performance for hydrogen production in sulfur-iodine cycle. Int J Hydrogen Energy 34(14):5637–5644
217. Liu H, Kantor I, Elkamel A, Fowler M (2009) Optimal synthesis of heat exchanger network for thermochemical S-I cycle. J Therm Anal Calorim 96(1):27–33
218. Peck MS, Allen JM, Mendez AE, Velez AL, Ghosh TK, Viswanath DS, Prelas MA (2007) Sulfuric acid decomposer materials study for the thermochemical hydrogen cycle. International topical meeting on safety and technology of nuclear hydrogen production, control, and management, Boston, MA, United States, 24–28 June 2007, pp 198–201
219. Wong B, Buckingham RT, Brown LC, Russ BE, Besenbruch GE, Kaiparambil A, Santhanakrishnan R, Roy A (2007) Construction materials development in sulfur-iodine thermochemical water-splitting process for hydrogen production. Int J Hydrogen Energy 32(4):497–504
220. Trester PW, Liang SS (1979) Material corrosion investigations for the General Atomic sulfur-iodine thermochemical water-splitting cycle. Advances in Hydrogen Energy 1(Hydrogen Energy System, vol 4): 2113–2159
221. Pickard P (2006) Sulfur-iodine thermochemical cycle. 2005 DOE Hydrogen Program review. PD 15
222. Evans B (2007) Thermiochemical systems overview Advanced reactor fuel cycle and energy products workshop for universities. Gaithersburg, Maryland, 20 Mar 2007
223. Giaconia A, Caputo G, Sau S, Prosini PP, Pozio A, De Francesco M, Tarquini P, Nardi L (2009) Survey of Bunsen reaction routes to improve the sulfur-iodine thermochemical water-splitting cycle. Int J Hydrogen Energy 34(9):4041–4048
224. Lee BJ, No HC, Yoon HJ, Jin HG, Kim YS, Lee JI (2009) Development of a flowsheet for iodine-sulfur thermo-chemical cycle based on optimized Bunsen reaction. Int J Hydrogen Energy 34(5):2133–2143
225. Barbarossa V, Vanga G, Diamanti M, Cali M, Doddi G (2009) Chemically enhanced separation of H2S04/HI mixtures from the Bunsen reaction in the sulfur-iodine thermochemical cycle. Ind Eng Chem Res 48(19):9040–9044
226. Elder RH, Priestman GH, Allen RWK, Orme CJ, Stewart FF (2009) The feasibility of membrane separations in the HIx processing section of the sulphur iodine thermochemical cycle. Int J Hydrogen Energy 34(16):6614–6624

227. Favuzza P, Felici C, Lanchi M, Liberatore R, Mazzocchia CV, Spadoni A, Hadj-Kali MK, Gerbaud V, Lovera P, Baudouin O, Floquet P, Joulia X, Borgard J-M, Carles P (2009) Bunsen section thermodynamic model for hydrogen production by the sulfur-iodine cycle. Int J Hydrogen Energy 34(16):6625–6635
228. Lanchi M, Laria F, Liberatore R, Marrelli L, Sau S, Spadoni A, Tarquini P (2009) HI extraction by H3PO4 in the Sulfur-Iodine thermochemical water splitting cycle: composition optimization of the HI/H2O/H3PO4/I2 biphasic quaternary system. Int J Hydrogen Energy 34(15):6120–6128
229. Larousse B, Lovera P, Borgard JM, Roehrich G, Mokrani N, Maillault C, Doizi D, Dauvois V, Roujou JL, Lorin V, Fauvet P, Carles P, Hartmann JM (2009) Experimental study of the vapor-liquid equilibria of HI-I2-H2O ternary mixtures, Part 2: experimental results at high temperature and pressure. Int J Hydrogen Energy 34(8):3258–3266
230. Liberatore R, Ceroli A, Lanchi M, Spadoni A, Tarquini P (2008) Experimental vapour-liquid equilibrium data of HI-H2O-I2 mixtures for hydrogen production by Sulphur-Iodine thermochemical cycle. Int J Hydrogen Energy 33(16):4283–4290
231. Mena SE, Cervo EG, Crosthwaite JM, Thies MC (2010) Phase equilibrium measurements for the I2-H2O and I2-HI-H2O systems of the sulfur-iodine cycle using a continuous-flow apparatus. Int J Hydrogen Energy 35(8):3347–3357
232. Tarquini P, Tito AC (2009) Decomposition of hydrogen iodide in the S-I thermochemical cycle over Ni catalyst systems. Int J Hydrogen Energy 34(9):4049–4056
233. Roth M, Knoche KF (1989) Thermochemical water splitting through direct hydrogen iodide decomposition from water/hydrogen iodide/molecular iodine solutions. Int J Hydrogen Energy 14(8):545–549
234. O'Keefe DR, Norman JH (1983) Hydrogen iodide decomposition. United States Patent 4410505
235. Russ B, Buckingham B, Brown L, Wong B, Besenbruch G (2005) HI decomposition-a comparison of reactive and extractive distillation techniques for the sulfur-iodine process. In: AIChE spring national meeting, conference proceedings, Atlanta, GA, United States, 10–14 Apr 2005, 75E/1-75E/2
236. Zhang Y, Wang Z, Zhou J, Liu J, Cen K (2009) Catalytic decomposition of hydrogen iodide over pre-treated Ni/CeO2 catalysts for hydrogen production in the sulfur-iodine cycle. Int J Hydrogen Energy 34(21):8792–8798
237. Zhang Y, Zhou J, Chen Y, Wang Z, Liu J, Cen K (2008) Hydrogen iodide decomposition over nickel-ceria catalysts for hydrogen production in the sulfur-iodine cycle. Int J Hydrogen Energy 33(20):5477–5483
238. Belaissaoui B, Thery R, Meyer XM, Meyer M, Gerbaud V, Joulia X (2005) Vapour reactive distillation process for hydrogen production by HI decomposition from H2O/HI/I2 solutions. In: 7th World congress of chemical engineering, Glasgow, United Kingdom, 10–14 July 2005, 83134/1-83134/9
239. Goldstein S, Borgard J-M, Vitart X (2005) Upper bound and best estimate of the efficiency of the iodine sulphur cycle. Int J Hydrogen Energy 30(6):619–626
240. Goldstein S, Vitart X, Borgard JM (2004) General comments about the efficiency of the iodine-sulphur cycle coupled to a high temperature gas-cooled reactor. In: Nuclear production of hydrogen, information exchange meeting, 2nd, Argonne, IL, United States, Oct 2–3, 2003. OECD, Paris, pp 85–98
241. Kameyama H, Yoshida K (1979) Bromine-calcium-iron water-decomposition cycles for hydrogen production. Advances in Hydrogen Energy 1(Hydrogen Energy System, vol 2): 829–850
242. Kameyama H, Yoshida K (1981) Reactor design for the "UT-3" thermochemical hydrogen production process. Advances in Hydrogen Energy 2(Hydrogen Energy Program, vol 4): 1939–1948
243. Yoshioka H, Nakayama T, Kameyama H, Yoshida K (1984) Operation of a bench-scale plant for hydrogen production by the UT-3 cycle. Advances in Hydrogen Energy 4(Hydrogen Energy Program 5, vol 2): 413–420

244. Aihara M, Sakurai M, Tsutsumi A, Yoshida K (1992) Reactivity improvement in the UT-3 thermochemical hydrogen production process. Int J Hydrogen Energy 17(9):719–723
245. Aihara M, Sakurai M, Yoshida K (1990) Reaction improvement in the UT-3 thermochemical hydrogen production process. Advances in Hydrogen Energy 8(Hydrogen Energy Program 8, vol 2): 493–502
246. Aihara M, Umida H, Tsutsumi A, Yoshida K (1990) Kinetic study of UT-3 thermochemical hydrogen production process. Int J Hydrogen Energy 15(1):7–11
247. Amir R, Sato T, Yamamoto KY, Kabe T, Kameyama H (1992) Design of solid reactants and reaction kinetics concerning the iron compounds in the UT-3 thermochemical cycle. Int J Hydrogen Energy 17(10):783–788
248. Aochi A, Tadokoro T, Yoshida K, Kameyama H, Nobue M, Yamaguchi T (1989) Economical and technical evaluation of UT-3 thermochemical hydrogen production process for an industrial scale plant. Int J Hydrogen Energy 14(7):421–429
249. Besenbruch GE, Brown LC, Funk JF, Showalter SK (2001) High efficiency generation of hydrogen fuels using nuclear power. In: Nuclear production of hydrogen, information exchange meeting, 1st, Paris, France, Oct 2–3, 2000. OECD, Paris, pp 205–219
250. Doctor RD, Marshall CL, Wade DC (2002) Hydrogen cycle employing calcium-bromine and electrolysis. Abstracts of papers, 224th ACS national meeting, Boston, MA, United States, 18–22 Aug 2002, FUEL-142
251. Doctor RD, Matonis DT, Wade DC (2004) Hydrogen generation using a calcium-bromine thermochemical water-splitting cycle. In: Nuclear production of hydrogen, information exchange meeting, 2nd, Argonne, IL, United States, Oct 2–3, 2003. OECD, Paris, pp 119–130
252. Kameyama H, Sato T, Amir R, Yoshida K, Aihara M, Sakurai M, Tadokoro Y, Kajiyama T, Yamaguchi T, Sakai N (1992) Cycle simulation of the UT-3 thermochemical hydrogen production process. Int J Hydrogen Energy 17(10):789–794
253. Kameyama H, Tomino Y, Orihara A, Yoshida K (1986) Process simulation of the MASCOT plant using the UT-3 thermochemical cycle for hydrogen production. Advances in Hydrogen Energy 5(Hydrogen Energy Prog. 6, vol 2): 688–695
254. Kameyama H, Tomino Y, Sato T, Amir R, Orihara A, Aihara M, Yoshida K (1989) Process simulation of "MASCOT" plant using the UT-3 thermochemical cycle for hydrogen production. Int J Hydrogen Energy 14(5):323–330
255. Lemort F, Charvin P, Lafon C, Romnicianu M (2006) Technological and chemical assessment of various thermochemical cycles: from the UT3 cycle up to the two steps iron oxide cycle. Int J Hydrogen Energy 31(14):2063–2075
256. Lemort F, Lafon C, Dedryvere R, Gonbeau D (2006) Physicochemical and thermodynamic investigation of the UT-3 hydrogen production cycle: a new technological assessment. Int J Hydrogen Energy 31(7):906–918
257. Nakayama T, Yoshioka H, Furutani H, Kameyama H, Yoshida K (1984) MASCOT – a bench-scale plant for producing hydrogen by the UT-3 thermochemical decomposition cycle. Int J Hydrogen Energy 9(3):187–190
258. Sakurai M, Akimoto K, Yokota M, Tsutsumi A, Yoshida K (1996) Reactivity improvement of Ca-reactant in the UT-3 thermochemical hydrogen production cycle. In: Hydrogen energy progress XI, Proceedings of the world hydrogen energy conference, 11th, Stuttgart, 23–28 June 1996, vol 1, pp 831–836
259. Sakurai M, Bilgen E, Tsutsumi A, Yoshida K (1996) Adiabatic UT-3 thermochemical process for hydrogen production. Int J Hydrogen Energy 21(10):865–870
260. Sakurai M, Bilgen E, Tsutsumi A, Yoshida K (1996) Solar UT-3 thermochemical cycle for hydrogen production. Sol Energy 57(1):51–58
261. Sakurai M, Bilgen E, Tsutsumi A, Yoshida K, Tadokoro Y, Yamaguchi T (1996) Nuclear hydrogen production by adiabatic UT-3 thermochemical process. In: Hydrogen energy progress XI, Proceedings of the world hydrogen energy conference, 11th, Stuttgart, 23–28 June 1996, vol 1, pp 837–842
262. Sakurai M, Miyake N, Tsutsumi A, Yoshida K (1996) Analysis of a reaction mechanism in the UT-3 thermochemical hydrogen production cycle. Int J Hydrogen Energy 21(10):871–875

263. Sakurai M, Ogiwara J, Kameyama H (2006) Reactivity improvement of Fe-compounds for the UT-3 thermochemical hydrogen production process. J Chem Eng Jpn 39(5):553–558
264. Sakurai M, Tsutsumi A, Yoshida K (1994) Analysis of a reaction mechanism in the UT-3 thermochemical hydrogen production cycle. In: Hydrogen energy progress X, Procedings of the world hydrogen energy conference, 10th, vol 2 pp 813–822
265. Sakurai M, Tsutsumi A, Yoshida K (1995) Improvement of Ca-pellet reactivity in UT-3 thermochemical hydrogen production cycle. Int J Hydrogen Energy 20(4):297–301
266. Sato T, Sakurai M, Matsumura Y, Tsutsumi A, Yoshida K (1998) Preparation, structure and reactivity of Ca pellets for the UT-3 thermochemical hydrogen production cycle. In: Hydrogen energy progress XII, Proceedings of the world hydrogen energy conference, 12th, Buenos Aires, 21–26 June 1998, vol 1 pp 581–588
267. Tadokoro Y, Kajiyama T, Yamaguchi T, Sakai N, Yoshida K, Aihara M, Sakurai M, Kameyama H, Sato T, Amir R (1990) Cycle simulation of the "UT-3" thermochemical hydrogen production process. Advances in Hydrogen Energy 8(Hydrogen Energy Prog. 8, vol 2): 513–521
268. Teo ED, Brandon NP, Vos E, Kramer GJ (2005) A critical pathway energy efficiency analysis of the thermochemical UT-3 cycle. Int J Hydrogen Energy 30(5):559–564
269. Yang J, Panchal CB, Doctor RD (2009) CaBr2 hydrolysis for HBr production using a direct sparging contactor. Int J Hydrogen Energy 34(18):7585–7591
270. Yoshida K, Kameyama H, Aochi T, Nobue M, Aihara M, Amir R, Kondo H, Sato T, Tadokoro Y et al (1990) A simulation study of the UT-3 thermochemical hydrogen production process. Int J Hydrogen Energy 15(3):171–178
271. Doctor RD, Marshall CL, Wade DC (2002) Hydrogen cycle employing calcium bromine and electrolysis. Fuel Chem Div 47(2):755–756
272. Daggupati VN, Naterer GF, Gabriel KS, Gravelsins RJ, Wang ZL (2009) Equilibrium conversion in Cu-Cl cycle multiphase processes of hydrogen production. Thermochim Acta 496(1–2):117–123
273. Ferrandon M, Lewis M, Tatterson D, Zdunek A (2008) Status of the development effort for the thermochemical Cu-Cl cycle. In: AIChE annual meeting, conference proceedings, Cincinnati, OH, United States, 30 Oct–4 Nov 2005, 87/1-87/11
274. Gong Y, Chalkova E, Akinfiev NN, Balashov VN, Fedkin MV, Lvov SN (2009) CuCl-HCl electrolyzer for hydrogen production via Cu-Cl thermochemical cycle. ECS Transactions 19(10, Hydrogen Production, Transport, and Storage 3): 21–32
275. Lewis M, Masin J (2005) An assessment of the efficiency of the hybrid copper-chloride thermochemical cycle. In: AIChE annual meeting, conference proceedings, Cincinnati, OH, United States, 30 Oct–4 Nov 2005, 348f/1-348f/3
276. Lewis MA, Ferrandon MS, Tatterson DF, Mathias P (2009) Evaluation of alternative thermochemical cycles – Part III further development of the Cu-Cl cycle. Int J Hydrogen Energy 34(9):4136–4145
277. Lewis MA, Serban M, Basco JK (2004) Hydrogen production at <550 DegC using a low temperature thermochemical cycle. Nuclear production of hydrogen, information exchange meeting, 2nd, Argonne, IL, United States, 2–3 Oct 2003, pp 145–156
278. Masin JG, Lewis MA (2006) Development of the low temperature hybrid Cu-Cl thermochemical cycle. In: AIChE annual meeting, conference proceedings, Cincinnati, OH, United States, 30 Oct–4 Nov 2005, 275b/1-275b/10
279. Naterer G, Suppiah S, Lewis M, Gabriel K, Dincer I, Rosen MA, Fowler M, Rizvi G, Easton EB, Ikeda BM, Kaye MH, Lu L, Pioro I, Spekkens P, Tremaine P, Mostaghimi J, Avsec J, Jiang J (2009) Recent Canadian advances in nuclear-based hydrogen production and the thermochemical Cu-Cl cycle. Int J Hydrogen Energy 34(7):2901–2917
280. Naterer GF, Daggupati VN, Marin G, Gabriel KS, Wang ZL (2008) Thermochemical hydrogen production with a copper-chlorine cycle, II: flashing and drying of aqueous cupric chloride. Int J Hydrogen Energy 33(20):5451–5459

281. Naterer GF, Gabriel K, Lu L, Wang Z, Zhang Y (2009) Recent advances in nuclear based hydrogen production with the thermochemical copper-chlorine cycle. J Eng Gas Turbine and Power 131(3):032905/1–032905/10
282. Orhan MF, Dincer I, Naterer GF (2008) Cost analysis of a thermochemical Cu-Cl pilot plant for nuclear-based hydrogen production. Int J Hydrogen Energy 33(21):6006–6020
283. Orhan MF, Dincer I, Rosen MA (2009) Efficiency analysis of a hybrid copper-chlorine (Cu-Cl) cycle for nuclear-based hydrogen production. Chem Eng J (Amsterdam, Neth) 155(1–2):132–137
284. Wang Z, Naterer GF, Gabriel K (2008) Multiphase reactor scale-up for Cu-Cl thermochemical hydrogen production. Int J Hydrogen Energy 33(23):6934–6946
285. Wang ZL, Naterer GF, Gabriel KS, Gravelsins R, Daggupati VN (2009) New Cu-Cl thermochemical cycle for hydrogen production with reduced excess steam requirements. Int J Green Energy 6(6):616–626
286. Zamfirescu C, Dincer I, Naterer GF (2010) Thermophysical properties of copper compounds in copper-chlorine thermochemical water splitting cycles. Int J Hydrogen Energy 35(10):4839–4852
287. Wang ZL, Naterer GF, Gabriel KS, Gravelsins R, Daggupati VN (2010) Comparison of sulfur-iodine and copper-chlorine thermochemical hydrogen production cycles. Int J Hydrogen Energy 35(10):4820–4830
288. Suppiah S, Li J, Sadhankar R, Kutchcoskie KJ, Lewis M (2006) Study of the hybrid Cu-Cl cycle for nuclear hydrogen production. Nuclear production of hydrogen: third information exchange meeting. Nuclear Energy Agency Organisation for Economic Co-operation and Development Oarai, 5–7 Japan Oct 2005
289. Ontario Institute of Technology (UIOT) (2010) Sustainable hydrogen production research at UIOT and partner institution. http://hydrogen.uoit.ca/EN/main/research/Overview_CuCl.html. Accessed 20 Nov 2010
290. Mathias P (2006) Modeling of the copper chloride thermochemical cycle. Argonne National Laboratory, Argonne
291. Wang Z, Gabriel K, Naterer GF (2008) Thermochemical process heat requirements of the copper-chlorine cycle for nuclear-based hydrogen production. 29th Conference of the Canadian Nuclear Society, Toronto, Ontario, Canada, 1–4 June 2008. http://hydrogen.uoit.ca/assets/Default/documents/Public/CNS08-Wang.pdf
292. Lewis M (2008) Part I. Summary of alternative cycle evaluation and down selection Part II. R&D status for the Cu-Cl thermochemical cycle. Argonne National Laboratory, Report PD-28
293. Rosen MA, Naterer GF, Sadhankar R, Suppiah S (2009) Nuclear based hydrogen production with a thermochemical copper-chlorine cycle and supercritical water reactor. http://hydrogen.uoit.ca/assets/Default/documents/Public/cha06.pdf. Accessed 20 Nov 2010
294. Kim YW, Kim CS, Hong SD, Lee WJ, Chang J (2009) A high temperature gas loop to simulate VHTR and nuclear hydrogen production system. VTT Symp 257:428–430
295. Onuki K (2009) Nuclear hydrogen production using HTGR. Shokubai 51(4):270–274
296. Onuki K, Inagaki Y, Hino R, Tachibana Y (2005) Research and development on nuclear hydrogen production using HTGR at JAERI. Prog Nucl Energy 47(1–4):496–503
297. Reza SMM (2007) Design modification for the modular helium reactor for higher temperature operation and reliability studies for nuclear hydrogen production processes. Ph.D. dissertation, Texas A&M University, TX, USA
298. Sato H, Kubo S, Sakaba N, Ohashi H, Tachibana Y, Kunitomi K (2009) Development of an evaluation method for the HTTR-IS nuclear hydrogen production system. Ann Nucl Energy 36(7):956–965
299. Sato H, Ohashi H, Sakaba N, Nishihara T, Kunitomi K (2008) Thermal load control methods for the HTTR-IS nuclear hydrogen production system. Nihon Genshiryoku Gakkai Wabun Ronbunshu 7(4):328–337
300. Verfondern K, Nishihara T (2005) Safety aspects of the combined HTTR/steam reforming complex for nuclear hydrogen production. Prog Nucl Energy 47(1–4):527–534

301. Vitart X, Le Duigou A, Carles P (2006) Hydrogen production using the sulfur-iodine cycle coupled to a VHTR: an overview. Energy Convers Manage 47(17):2740–2747
302. Schultz KR, Brown LC, Besenbruch GE, Hamilton CJ (2003) Large-scale production of hydrogen by nuclear energy for the hydrogen economy. Report No. GA –A24265
303. Patterson M, Park C (2008) Hydrogen production from the next generation nuclear plant. Report No. INL/CON-08-14016
304. Farbman GH (1976) The conceptual design of an integrated nuclear hydrogen production plant using the sulfur cycle water decomposition system. Westinghouse Astronucl Lab, Pittsburgh
305. Shiozawa S, Saito S, Okano K, Uotani M, Ogawa M, Hino R (2006) Infrastructure for future hydrogen economy and nuclear hydrogen production. Nihon Genshiryoku Gakkaishi 48(11):835–852
306. Brown NR, Oh S, Revankar ST, Kane C, Rodriguez S, Cole R Jr, Gauntt R (2009) Analysis model for sulfur-iodine and hybrid sulfur thermochemical cycles. Nucl Technol 166(1):43–55
307. Brown NR, Oh S, Revankar ST, Vierow K, Rodriguez S, Cole R Jr, Gauntt R (2009) Simulation of sulfur-iodine thermochemical hydrogen production plant coupled to high-temperature heat source. Nucl Technol 167(1):95–106
308. Richards MB, Shenoy AS, Schultz KR (2004) Coupling the modular helium reactor to hydrogen production processes. In: Nuclear production of hydrogen, information exchange meeting, 2nd, Argonne, IL, United States, Oct 2–3, 2003. OECD, Paris, pp 203–215
309. Southworth FH, MacDonald PE, Harrell DJ, Shaber EL, Park CV, Holbrook MR, Petti DA (2003) The next generation nuclear plant (NGNP) project. Idaho National Engineering and Environmental Laboratory. Report No. INEEL/CON-03-01150
310. Harvego EA, Reza SMM, Richards M, Shenoy A (2006) An evaluation of reactor cooling and coupled hydrogen production processes using the modular helium reactor. Nucl Eng Des 236(14–16):1481–1489
311. Elder R, Allen R (2009) Nuclear heat for hydrogen production: coupling a very high/high temperature reactor to a hydrogen production plant. Prog Nucl Energy 51(3):500–525
312. Gauthier J-C, Brinkmann G, Copsey B, Lecomte M (2006) ANTARES: the HTR/VHTR project at Framatome ANP. Nucl Eng Des 236(5–6):526–533
313. MacDonald PE, Bayless PD, Gougar HD, Moore RL, Ougouag AM, Sant RL, Sterbentz JW, Terry WK (2004) The next generation nuclear plant – insights gained from the INEEL point design studies. Idaho National Engineering and Environmental Laboratory. Report No. INEEL/CON-04-01563
314. Petri MC (2005) U.S. work on hydrogen production using light water reactor. IAEA technical meeting on advanced applications of water-cooled nuclear power plants, 11–14 Oct 2005, Vienna, Austria
315. Wong BY, Brown L, Besenbruch G, Roy A, Pal J, Koripelli RS, Hasan MH (2009) General and stress corrosion behavior of construction materials for HI gaseous decomposition. NHI-UNLV HTHX program. Report No. IFT—PB2007-102
316. Monnerie N, Mueller-Steinhagen H, Roeb M, Sattler C, Schmitz M (2005) Hydrogen production by solar thermo-chemical water splitting. World congress of chemical engineering, 7th, Glasgow, United Kingdom, 10–14 July 2005, 83387/1–83387/11
317. Bilgen E (1984) Solar hydrogen production by direct water decomposition process: a preliminary engineering assessment. Int J Hydrogen Energy 9(1–2):53–58
318. Bilgen E (1988) Solar hydrogen production by hybrid thermochemical processes. Sol Energy 41(2):199–206
319. Bilgen E, Bilgen C (1982) Solar hydrogen production using two-step thermochemical cycles. Int J Hydrogen Energy 7(8):637–644
320. Hoagland W (1979) Solar hydrogen production. Sol Energy Res Inst, Golden, pp 211–214
321. Bilgen E, Bilgen C (1981) Solar hydrogen production. Advances in Hydrogen Energy 2(Hydrogen Energy Program, vol 2): 719–734
322. Bilgen E, Bilgen C (1983) An assessment of large-scale solar hydrogen production in Canada. Int J Hydrogen Energy 8(6):441–451

323. Garcia-Conde AG, Rosa F (1993) Solar hydrogen production: a Spanish experience. Int J Hydrogen Energy 18(12):995–1000
324. Guo LJ, Zhao L, Jing DW, Lu YJ, Yang HH, Bai BF, Zhang XM, Ma LJ, Wu XM (2009) Solar hydrogen production and its development in China. Energy (Oxford, UK) 34(9):1073–1090
325. Veziroglu TN, Barbir F (1991) Solar–hydrogen energy system: the choice of the future. Environ Conserv 18:304–312
326. Wilhelm E, Fowler M (2006) A technical and economic review of solar hydrogen production technologies. Bull Sci Technol Soc 26(4):278–287
327. Milbrandt A, Mann M (2007) Potential for hydrogen production from key renewable resources in the United States. National Renewable Energy Laboratory, Golden, CO, TP-640-41134, 2007
328. Pregger T, Graf D, Krewitt W, Sattler C, Roeb M, Moller S (2009) Prospects of solar thermal hydrogen production processes. Int J Hydrogen Energy 34:4256–4267
329. Abanades S, Flamant G (2006) Solar hydrogen production from the thermal splitting of methane in a high temperature solar chemical reactor. Sol Energy 80(10):1321–1332
330. Berman A, Karn RK, Epstein M (2007) Steam reforming of methane on a Ru/Al2O3 catalyst promoted with Mn oxides for solar hydrogen production. Green Chem 9(6):626–631
331. Hirsch D, Steinfeld A (2004) Solar hydrogen production by thermal decomposition of natural gas using a vortex-flow reactor. Int J Hydrogen Energy 29(1):47–55
332. Hong H, Liu Q, Jin H (2009) Solar hydrogen production integrating low-grade solar thermal energy and methanol steam reforming. J Energy Resour Technol 131(1):012601/1–012601/10
333. Weimer AW, Dahl J, BuechlerK, Lewandowski A, Pitts R, Bingham C, Glatzmaier GC (2001) Thermal dissociation of methane using a solar coupled aerosol flow reactor. In: Proceedings of the 2001 DOE Hydrogen Program Review NREL/CP-570-30535
334. Dahl JK, Tamburini J, Weimer AW (2001) Solar-thermal processing of methane to produce hydrogen and syngas. Energy Fuels 15(5):1227–1232
335. Muir JF, Hogan Jr RE, Skocypec RD, Buck R (1990) Solar reforming of methane in a direct absorption catalytic reactor on a parabolic dish. SAND-90-2674C; CONF-910318–13
336. Huder K (1991) Investigation of methane reforming with energy supplied by direct absorption of concentrated radiation. Sol Energy Mater 24(1–2):696–706
337. Dahl JK, Barocas VH, Clough DE, Weimer AW (2002) Intrinsic kinetics for rapid decomposition of methane in an aerosol flow reactor. Int J Hydrogen Energy 27:377–386
338. Dahl J, Buechler K, Finley R, Stanislaus T, Weimer A, Lewandowski A, Bingham C, Smeets A, Schneider A (2002) Rapid solar-thermal dissociation of natural gas in an aerosol reactor. In: Proceedings of the 2002 US DOE Hydrogen Review Program. Report No. NREL/CP-610-32405
339. Lewandowski A, Weimer A (2003) High temperature solar splitting of methane to hydrogen and carbon. 2003 Hydrogen and fuel cells merit review meeting, National Renewable Energy Laboratory, 19–22 May, Berkeley, CA
340. Epstein M, Spiewak I (1996) Solar experiments with a tubular reformer. In: Proceedings of the 8th international symposium on solar thermal concentrating technologies, Cologne, Germany. Meuller Verlag, Heidelberg, pp 1209–1229
341. Moeller S, Buck R, Tamme R, Epstein M, Liebermann D, Moshe M, Fisher U, Rotstein A, Sugarmen C (2002) Solar production of syngas for electricity generation: SOLASYS project test-phase. In: Steinfeld A (ed) Proceedings of the 11th solar PACES international symposium on concentrated solar power and chemical energy technologies, Zurich, Switzerland. Paul Scherrer Institut, Villigen, pp 231–237
342. Epstein M, Ehrensberger K, Yogev A (2002) Ferro-reduction of ZnO using concentrated solar energy. In: Steinfeld A (ed) Proceedings of the 11th solar PACES symposium on concentrated solar power and chemical energy technologies, Zurich, Switzerland. Paul Scherrer Institut, Villigen, pp 261–269
343. Dahl JK, Weimer AW, Lewandowski A, Bingham C, Bruetsch F, Steinfeld A (2004) Dry reforming of methane using a solar-thermal aerosol flow reactor. Ind Eng Chem Res 43(18):5489–5495

344. Steinfeld A (2005) Solar thermochemical production of hydrogen: a review. Sol Energy 78:603–615
345. Kodama T, Gokon N (2007) Thermochemical cycles for high-temperature solar hydrogen production. Chem Rev 107:4048–4077
346. Perkins C, Weimer AW (2004) Likely near-term solar-thermal water splitting technologies. Int J Hydrogen Energy 29(15):1587–1599
347. Steinfeld A (2002) Solar hydrogen production via a 2-step water-splitting thermochemical cycle based on Zn/ZnO redox reactions. Int J Hydrogen Energy 27:611–619
348. Abanades S, Charvin P, Flamant G, Neveu P (2006) Screening of water-splitting thermo cycles potentially attractive for hydrogen production by concentrated solar energy. Energy 31(14):2805–2822
349. Haueter P, Moeller S, Palumbo R, Steinfeld A (1999) The production of zinc by thermal dissociation of zinc oxide-solar chemical reactor design. Sol Energy 67:161–167
350. Perkins C, Weimer AW (2009) Solar-thermal production of renewable hydrogen. AlChE J 55(2):286–293
351. Allendorf MD, Diver RB, Siegel NP, Miller JE (2008) Two-step water splitting using mixed-metal ferrites: thermodynamic analysis and characterization of synthesized materials. Energy Fuels 22:4115–4124
352. Kodama T, Nakamuro Y, Mizuno TJ (2006) A two-step thermochemical water splitting by iron-oxide on stabilized zirconia. J Sol Energy Eng 128(1):3–7
353. Roeb M, Sattler C, Kluser R, Monnerie N, Oliveira LD, Konstandopoulos AG, Agrafiotis C, Zaspalis V, Nalbandian L, Steele A, Stobbe PJ (2006) Sol Energy Eng 128(2):125–133
354. Abanades S, Charvin P, Lemont F, Flamant G (2008) Novel two-step SnO_2/SnO water splitting cycle for solar thermochemical production of hydrogen. Int J Hydrogen Energy 33(21):6021–6030
355. Stamatiou A, Loutzenhiser PG, Steinfeld A (2010) Solar syngas production via H_2O/CO_2-splitting thermochemical cycles with Zn/ZnO and FeO/Fe3O4 redox reactions. Chem Mater 22:851–859
356. Müller R, Steinfeld A (2008) H2O-splitting thermochemical cycle based on ZnO/Zn-redox: quenching the effluents from the ZnO dissociation. Chem Eng Sci 63(1):217–227
357. Elorza-Ricart E, Martin PY, Ferrer M, Lédé J (1999) Direct thermal splitting of ZnO followed by a quench: experimental measurements of mass balances. J Phys IV France 9:325–330
358. Fletcher EA (1999) Solar-thermal and solar quasi-electrolytic processing and separations: zinc from zinc oxide as an example. Ind Eng Chem Res 38:2275–2282
359. Kräupl S, Steinfeld A (2003) Operational performance of a 5kW solar chemical reactor for the co-production of zinc and syngas. J Sol Energy Eng 125:124–126
360. Lédé J, Elorza-Ricart E, Ferrer M (2001) Solar thermal splitting of zinc oxide: a review of some of the rate controlling factors. J Sol Energy Eng 123(2):91–97
361. Osinga T, Frommherz U, Steinfeld A, Wieckert C (2004) Experimental investigation of the solar carbothermic reduction of ZnO using a two cavity solar reactor. J Sol Energy Eng 126:633–637
362. Müller R, Haeberling P, Palumbo RD (2006) Further advances toward the development of a direct heating solar thermal chemical reactor for the thermal dissociation of ZnO(s). Sol Energy 80(5):500–511
363. Steinfeld A, Sanders S, Palumbo R (1999) Design aspects of solar thermochemical engineering- a case study: two-step water-splitting cycle using the FeO/FeO redox system. Sol Energy 65(1):43–53
364. Charvin P, Abanades S, Flamant G, Lemort F (2007) Two-step water splitting thermochemical cycle based on iron oxide redox pair for solar hydrogen production. Energy (Oxford, UK) 32(7):1124–1133
365. Alvani C, Bellusci M, La Barbera A, Padella F, Pentimalli M, Seralessandri L, Varsano F (2009) Reactive pellets for improved solar hydrogen production based on sodium manganese ferrite thermochemical cycle. J Sol Energy Eng 131(3):031015/1–031015/5

366. Alvani C, La Barbera A, Ennas G, Padella F, Varsano F (2006) Hydrogen production by using manganese ferrite: evidences and benefits of a multi-step reaction mechanism. Int J Hydrogen Energy 31(15):2217–2222
367. Hwang G-J, Park C-S, Lee S-H, Seo I-T, Kim J-W (2004) Ni-ferrite-based thermochemical cycle for solar hydrogen production. J Ind Eng Chem(Seoul, Republic of Korea) 10(6):889–893
368. Ishihara H, Kaneko H, Hasegawa N, Tamaura Y (2008) Two-step water splitting process with solid solution of YSZ and Ni-ferrite for solar hydrogen production (ISEC 2005-76151). J Sol Energy Eng 130(4):044501/1–044501/3
369. Kodama T, Gokon N, Yamamoto R (2008) Thermochemical two-step water splitting by ZrO2-supported NixFe3-xO4 for solar hydrogen production. Sol Energy 82(1):73–79
370. Tamaura Y, Ueda Y, Matsunami J, Hasegawa N, Nezuka M, Sano T, Tsuji M (1998) Solar hydrogen production by using ferrites. Sol Energy 65(1):55–57
371. Fresno F, Fernandez-Saavedra R, Belen Gomez-Mancebo M, Vidal A, Sanchez M, Isabel Rucandio M, Quejido AJ, Romero M (2009) Solar hydrogen production by two-step thermochemical cycles: evaluation of the activity of commercial ferrites. Int J Hydrogen Energy 34(7):2918–2924
372. Kodama T, Kondoh Y, Yamamoto R, Andou H, Satou N (2005) Thermochemical hydrogen production by a redox system of ZrO_2-supported Co(II)-ferrite. Sol Energy 78:623–631
373. Miller JE, Allendorf MD, Diver RB, Evans LR, Siegel NP, Stuecker JN (2008) Metal oxide composites and structures for ultra-high temperature solar thermochemical cycles. J Mater Sci 43(14):4714–4728
374. Gokon N, Murayama H, Nagasaki A, Kodama T (2009) Thermochemical two-step water splitting cycles by monoclinic ZrO_2-supported $NiFe_2O_4$ and Fe_3O_4 powders and ceramic foam devices. Sol Energy 83(4):527–537
375. Hwang GJ, Park CS, Lee SH, Seo IT, Kim JW (2004) Ni-ferrite-based thermochemical cycle for solar hydrogen production. J Ind Eng Chem 10(6):889–893
376. Kodama T, Gokon N (2010) Two-step thermochemical cycles for high temperature solar hydrogen production. Adv Sci Technol 72:119–128
377. Agrafiotis C, Roeb M, Konstandopoulos AG, Nalbandian L, Zaspalis VT, Sattler C, Stobbe P, Steele AM (2005) Solar water splitting for hydrogen production with monolithic reactors. Sol Energy 79(4):409–421
378. Roeb M, Sattler C, Kluser R, Monnerie N, de Oliveira L, Konstandopoulos AG, Agrafiotis C, Zaspalis VT, Nalbandian L (2006) Solar hydrogen production by a two-step cycle based on mixed iron oxides. J Sol Energy Eng Trans ASME 128(2):125–134
379. Aoki H, Kaneko H, Hasegawa N, Ishihara H, Suzuki A, Tamaura Y (2004) The $ZnFe_2O_4/(ZnO + Fe_3O_4)$ system for H-2 production using concentrated solar energy. Solid State Ionics 172(1–4):113–116
380. Tamaura Y, Kaneko H (2005) Oxygen-releasing step of $ZnFe_2O_4/(ZnO + Fe_3O_4)$-system in air using concentrated solar energy for solar hydrogen production. Sol Energy 78(5):616–622
381. Kaneko H, Kojima N, Hasegawa N, Inoue M, Uehara R, Gokon N, Tamaura Y, Sano T (2002) Reaction mechanism of H_2 generation for $H_2O/Zn/Fe_3O_4$ system. Int J Hydrogen Energy 27(10):1023–1028
382. Gokon N, Murayama H, Umeda J, Hatamachi T, Kodama T (2009) Monoclinic zirconia-supported Fe_3O_4 for the two-step water-splitting thermochemical cycle at high thermal reduction temperatures of 1400–1600°C. Int J Hydrogen Energy 34(3):1208–1217
383. Scheffe JR, Li J, Weimer AW (2010) A spinel ferrite/hercynite water-splitting redox cycle. Int J Hydrogen Energy 35(8):3333–3340
384. Diver RB, Miller JE, Allendorf MD, Siegel NP, Hogan RE (2008) Solar thermochemical water-splitting ferrite-cycle heat engines. J Sol Energy Eng 130(4):041001–041008
385. Kodama T, Shimizu T, Satoh T, Nakata M, Shimizu KI (2002) Stepwise production of CO-rich syngas and hydrogen via solar methane reforming by using a Ni(II)-ferrite redox system. Sol Energy 73(5):363–374

386. Lorentzou S, Agrafiotis C, Konstandopoulos A (2008) Aerosol spray pyrolysis synthesis of water-splitting ferrites for solar hydrogen production. Granular Matter 10(2):113–122
387. Han SB, Kang TB, Joo OS, Jung KD (2007) Water splitting for hydrogen production with ferrites. Sol Energy 81(5):623–628
388. Galvez ME, Frei A, Albisetti G, Lunardi G, Steinfeld A (2008) Solar hydrogen production via a two-step thermochemical process based on MgO/Mg redox reactions-Thermodynamic and kinetic analyses. Int J Hydrogen Energy 33(12):2880–2890
389. Vishnevetsky I, Epstein M (2009) Tin as a possible candidate for solar thermochemical redox process for hydrogen production. J Sol Energy Eng 131(2):021007–021008
390. Charvin P, Abanades S, Lemont F, Flamant G (2008) Experimental study on SnO2/SnO/Sn thermochemical systems for solar production of hydrogen. AlChE J 54(10):2759–2767
391. Abanades S, Flamant G (2006) Thermochemical hydrogen production from a two-step solar-driven water-splitting cycle based on cerium oxides. Sol Energy 80(12):1611–1623
392. Huang C, T-Raissi A (2005) Analysis of sulfur-iodine thermochemical cycle for solar hydrogen production. Part I: decomposition of sulfuric acid. Sol Energy 78(5):632–646
393. Leach JW, Copeland RJ (1986) Solar hydrogen production: the sulfur-iodine cycle versus water vapor electrolysis. In: Proceedings of the 21st Intersociety Energy Conversion Engineering Conference,vol 2, pp 702–707
394. Leach JW, Copeland RJ (1990) Solar hydrogen production: the sulfur-iodine cycle versus water vapor electrolysis. Int J Energy Syst 10(1):55–59
395. Norman JH, Besenbruch G, Brown L (1982) Solar production of hydrogen using the sulfur-iodine thermochemical water-splitting cycle. Gen. Atomic Co. San Diego, CA, USA, GA-A16493
396. Prosini PP, Cento C, Giaconia A, Caputo G, Sau S (2009) A modified sulphur-iodine cycle for efficient solar hydrogen production. Int J Hydrogen Energy 34(3):1218–1225
397. Bilgen C, Bilgen E (1984) Solar hydrogen production using the sulfur-iodine thermochemical process. Advances in Hydrogen Energy 4(Hydrogen Energy Progress 5, vol 2), pp 517–528
398. Graf D, Monnerie N, Roeb M, Schmitz M, Sattler C (2008) Economic comparison of solar hydrogen generation by means of thermochemical cycles and electrolysis. Int J Hydrogen Energy 33(17):4511–4519
399. Lewis MA, Basco JK (2004) Kinetic study of the hydrogen and oxygen production reactions in the copper-chloride thermochemical cycle, Serban, Manuela (Argonne National Laboratory, Chemical Engineering Division). In: 2004 AIChE Spring National Meeting, Conference Proceedings, pp 2690–2698
400. Fletcher EA (2001) Solar thermal processing: a review. J Solar Energy Eng 123:63–74
401. Fletcher EA, Macdonald F, Kunnerth D (1985) High temperature solar electrothermal processing II. Zinc from zinc oxide. Energy 10:1255–1272
402. Steinfeld A, Brack M, Meier A, Weidenkaff A, Wuillemin D (1998) A solar chemical reactor for the Co-production of zinc and synthesis gas. Energy 23:803–814
403. Kraupl S, Steinfeld A (2003) Operational performance of a 5 kW solar chemical reactor for the Co-production of zinc and syngas. ASME J Sol Energy Eng 125:124–126
404. Steinfeld A, Kuhn P, Reller A, Palumbo R, Murray JP, Tamaura Y (1998) Solar-processed metals as clean energy carriers and water-splitters. Int J Hydrogen Energy 23:767–774
405. International Energy Agency (2006) Hydrogen production and storage R&D priorities and gaps. IEA-Hydrogen Coordination Group. OECD/IEA-2006. IEA, Paris, France.
406. Agbossou K, Chahine R, Hamelin J, Laurencelle F, Anouar A, St-Arnaud JM, Bose TK (2001) Renewable energy systems based on hydrogen for remote applications. J Power Sources 96(1):168–172
407. Aguado M, Ayerbe E, Azcarate C, Blanco R, Garde R, Mallor F, Rivas DM (2009) Economical assessment of a wind-hydrogen energy system using WindHyGen software. Int J Hydrogen Energy 34(7):2845–2854
408. Altmann M, Gamallo F (1998) Design of an isolated wind-hydrogen energy supply system. In: Hydrogen energy progress XII, Proceedings of the world hydrogen energy conference, 12th, Buenos Aires, 21–26 June 1998 vol 2, pp 1699–1706

409. Bechrakis DA, Varkaraki E (2009) Chapter 5: Hydrogen production from wind energy. In: Gupta RB (ed) Hydrogen fuel production transport, and storage. CRC, Boca Raton, pp 161–183
410. Bernal-Agustin JL, Dufo-Lopez R (2008) Hourly energy management for grid-connected wind-hydrogen systems. Int J Hydrogen Energy 33(22):6401–6413
411. Calderon M, Calderon AJ, Ramiro A, Gonzalez JF (2010) Automatic management of energy flows of a stand-alone renewable energy supply with hydrogen support. Int J Hydrogen Energy 35(6):2226–2235
412. El-Osta W, Mussa M, Yagob A (1996) Harnessing the wind for hydrogen production: a possible strategic program for Libya. In: Hydrogen energy progress XI, Proceedings of the world hydrogen energy conference, 11th, Stuttgart, 23–28 June 1996, vol 1, pp 435–441
413. Fairlie M, Mazaika DM, Scott PB (2003) Wind generated hydrogen fueling station. Hydrogen planet, 14th world hydrogen energy conference, Montreal, QC, Canada, 9–13 June 2002, pp 381–389
414. Fingersh LJ (2004) Optimization of utility-scale wind-hydrogen-battery systems. World renewable energy congress VIII: linking the world with renewable energy, 8th, Denver, CO, United States, 29 Aug–3 Sept 2004, pp 909–913
415. Giatrakos GP, Tsoutsos TD, Mouchtaropoulos PG, Naxakis GD, Stavrakakis G (2009) Sustainable energy planning based on a stand-alone hybrid renewableenergy/hydrogen power system: application in Karpathos island, Greece. Renewable Energy 34(12):2562–2570
416. Glazkov VA, Solovey VV, Pishuk VK, Lotosky MV, Aliyev AM (2005) Autonomous wind-hydrogen stations. Hydrogen materials science and chemistry of carbon nanomaterials, international conference, 9th, Sevastopol, Ukraine, 5–11 Sept 2005 pp 1168–1171
417. Glockner R, Kloed C, Nyhammer F, Ulleberg O (2003) Wind/hydrogen systems for remote areas – a Norwegian case study. Hydrogen planet, World hydrogen energy conference, 14th, Montreal, QC, Canada, 9–13 June 2002, pp 398–409
418. Greiner CJ, Korpaas M, Gjengedal T (2008) Dimensioning and operating wind-hydrogen plants in power markets. In: New aspects of circuits, Proceedings of the WSEAS international conference on circuits, 12th, Heraklion, Greece, 22–24 July 2008, pp 405–414
419. Greiner CJ, Korpas M, Holen AT (2007) A Norwegian case study on the production of hydrogen from wind power. Int J Hydrogen Energy 32(10–11):1500–1507
420. Harrison KW, Martin G (2010) The wind-to-hydrogen project: results and lessons learned. Am Chem Soc Div Pet Chem Prepr 55(1):64
421. Hart D (2000) Hydrogen storage – technically viable and economically sensible? IMechE Seminar Publication (7, Renewable Energy Storage), pp 51–54
422. Hexeberg I, Hagen EF (2005) Renewable hydrogen energy systems. In: Proceedings of the world petroleum congress,18th, HEXE1-HEXE8
423. Honnery D, Moriarty P (2009) Estimating global hydrogen production from wind. Int J Hydrogen Energy 34(2):727–736
424. Infield D (2004) Hydrogen from renewable energy sources. In: Fuel cells for automotive applications, pp 75–88
425. Ipsakis D, Voutetakis S, Seferlis P, Stergiopoulos F, Elmasides C (2009) Power management strategies for a stand-alone power system using renewable energy sources and hydrogen storage. Int J Hydrogen Energy 34(16):7081–7095
426. Jensen SH, Larsen PH, Mogensen M (2007) Hydrogen and synthetic fuel production from renewable energy sources. Int J Hydrogen Energy 32(15):3253–3257
427. Khan MJ, Iqbal MT (2009) Analysis of a small wind-hydrogen stand-alone hybrid energy system. Appl Energy 86(11):2429–2442
428. Kottenstette R, Cotrell J (2004) Hydrogen storage in wind turbine towers. Int J Hydrogen Energy 29(12):1277–1288
429. Lee J-Y, An S, Cha K, Hur T (2010) Life cycle environmental and economic analyses of a hydrogen station with wind energy. Int J Hydrogen Energy 35(6):2213–2225
430. Levene JI, Mann MK, Margolis RM, Milbrandt A (2007) An analysis of hydrogen production from renewable electricity sources. Sol Energy 81(6):773–780

431. Linnemann J, Steinberger-Wilckens R (2007) Realistic costs of wind-hydrogen vehicle fuel production. Int J Hydrogen Energy 32(10–11):1492–1499
432. Mantz RJ, De Battista H (2008) Hydrogen production from idle generation capacity of wind turbines. Int J Hydrogen Energy 33(16):4291–4300
433. Matera FV, Sapienza C, Andaloro L, Dispensa G, Ferraro M, Antonucci V (2009) An integrated approach to hydrogen economy in Sicilian islands. Int J Hydrogen Energy 34(16):7009–7014
434. Menzl F, Wenske M, Lehmann J (1998) Hydrogen production by a windmill powered electrolyser. In: Hydrogen energy progress XII, Proceedings of the world hydrogen energy conference, 12th, Buenos Aires, 21–26 June 1998, vol 1, pp 757–765
435. Neill DR, Yu C, Guo Q, Huang N (1992) HNEI wind-hydrogen program. Sol World Congr Proc Bienn Congr Int Sol Energy Soc 1(Pt. 2):745–750
436. Perez-Herranz V, Perez-Page M, Beneito R (2010) Monitoring and control of a hydrogen production and storage system consisting of water electrolysis and metal hydrides. Int J Hydrogen Energy 35(3):912–919
437. Shahbazov SS, Usubov IM (1996) Hydrogen obtained by using wind energy. In: Hydrogen energy progress XI, Proceedings of the world hydrogen energy conference, 11th, Stuttgart, 23–28 June 1996 vol 1, pp 955–958
438. Sherif SA, Barbir F, Veziroglu TN (2005) Wind energy and the hydrogen economy – review of the technology. Sol Energy 78(5):647–660
439. Sopian K, Fudholi A, Ruslan MH, Sulaiman MY, Alghoul MA, Yahya M, Amin N, Haw LC, Zaharim A (2009) Hydrogen production from combined wind/PV energy hybrid system in Malaysia. In: Recent advances in energy and environment, Proceedings of the IASME/WSEAS international conference on energy & environment, 4th, Cambridge, United Kingdom, 24–26 Feb 2009, pp 431–434
440. Sopian K, Ibrahim MZ, Daud WRW, Othman MY, Yatim B, Amin N (2009) Performance of a PV-wind hybrid system for hydrogen production. Renewable Energy 34(8):1973–1978
441. Ulleberg O, Nakken T, Ete A (2010) The wind/hydrogen demonstration system at Utsira in Norway: evaluation of system performance using operational data and updated hydrogen energy system modeling tools. Int J Hydrogen Energy 35(5):1841–1852
442. Venturini NR (1996) Wind-hydrogen energy demonstration plant in Argentina: preliminary economic analysis. In: Hydrogen energy progress XI, Proceedings of the world hydrogen energy conference, 11th, Stuttgart, 23–28 June 1996, vol 1, pp 373–378
443. Yang W-J, Aydin O (2001) Wind energy-hydrogen storage hybrid power generation. Int J Energy Res 25(5):449–463
444. Milbrandt A, Mann M (2007) Potential for hydrogen production from key renewable resources in the United States. National Renewable Energy Laboratory, Golden, CO, Report No. TP-640-41134
445. Saxena RC, Seal D, Kumar S, Goyal HB (2008) Thermo-chemical routes for hydrogen rich gas from biomass: a review. Renew Sustain Energy Rev 12(7):1909–1927
446. Ni M, Leung DYC, Leung MKH, Sumathy K (2006) An overview of hydrogen production from biomass. Fuel Process Technol 87(5):461–472
447. Milne TA, Elam CC, Evans RJ (2002) Hydrogen from biomass, State of the art and research challenges. A report for the international energy agency. Agreement on the production and utilization of hydrogen task 16, hydrogen from carbon-containing materials, IEA/H2/TR-02/001
448. Esswein AJ, Nocera DG (2007) Hydrogen production by molecular photocatalysis. Chem Rev(Washington, DC, USA) 107(10):4022–4407
449. Kudo A (2007) Photocatalysis and solar hydrogen production. Pure Appl Chem 79(11):1917–1927
450. Lee M-T, Hwang DJ, Greif R, Grigoropoulos CP (2009) Nanocatalyst fabrication and the production of hydrogen by using photon energy. Int J Hydrogen Energy 34(4):1835–1843

451. Rangan K, Arachchige SM, Brown JR, Brewer KJ (2009) Solar energy conversion using photochemical molecular devices: photocatalytic hydrogen production from water using mixed-metal supramolecular complexes. Energy Environ Sci 2(4):410–419
452. Ryu SY, Choi J, Balcerski W, Lee TK, Hoffmann MR (2007) Photocatalytic production of H2 on nanocomposite catalysts. Ind Eng Chem Res 46(23):7476–7488
453. Wang X, Shih K, Li XY (2010) Photocatalytic hydrogen generation from water under visible light using core/shell nano-catalysts. Water Sci Technol 61(9):2303–2308
454. Ni M, Leung MKH, Leung DYC, Sumathy K (2007) A review and recent developments in photocatalytic water-splitting using TiO2 for hydrogen production. Renew Sustain Energy Rev 11(3):401–425
455. Wolcott A, Kuykendall T, Smith WA, Zhao Y, Zhang JZ (2008) Photoelectrochemical hydrogen production utilizing metal oxide nanomaterials. Abstracts of papers, 235th ACS national meeting, New Orleans, LA, United States, 6–10 Apr 2008, PHYS-504
456. Menth A, Stucki S (1979) Present state and outlook of the electrolytic hydrogen production route. Advances in Hydrogen Energy 1(Hydrogen Energy Syst., vol 1) pp 55–63
457. Willner I, Steinberger-Willner B (1988) Solar hydrogen production through photobiological, photochemical, and photoelectrochemical assemblies. Int J Hydrogen Energy 13(10):593–604
458. Benemann JR (1997) Feasibility analysis of photobiological hydrogen production. Int J Hydrogen Energy 22(10–11):979–987
459. Hallenbeck PC, Benemann JR (2002) Biological hydrogen production; fundamentals and limiting processes. Int J Hydrogen Energy 27(11–12):1185–1193
460. Das D, Khanna N, Veziroglu TN (2008) Recent developments in biological hydrogen production processes. Chem Ind Chem Eng Q 14(2):57–67
461. Das D, Veziroglu TN (2007) Advances in biological hydrogen production processes. Al'ternativnaya Energetika i Ekologiya 7:72–84
462. Akano T, Miura Y, Fukatsu K, Miyasaka H, Ikuta Y, Matsumoto H, Hamasaki A, Shioji N, Mizoguchi T, et al. (1996) Hydrogen production by photosynthetic microorganisms. Applied Biochemistry and Biotechnology 57/58(Seventeenth Symposium on Biotechnology for Fuels and Chemicals, 1995), pp 677–688
463. Akkerman I, Janssen M, Rocha J, Wijffels RH (2002) Photobiological hydrogen production: photochemical efficiency and bioreactor design. Int J Hydrogen Energy 27(11–12): 1195–1208
464. Anon (2009) An improved photobioreactor design for photobiological hydrogen production. Biotechnol Bioeng 104(1): fmv
465. Asada Y (1996) Photobiological hydrogen production-state of the art with special reference to IEA's hydrogen program. In: Hydrogen energy progress XI, Proceedings of the world hydrogen energy conference, 11th, Stuttgart, 23–28 June 1996, vol 1, pp 403–406
466. Asada Y, Miyake J (1999) Photobiological hydrogen production. J Biosci Bioeng 88(1):1–6
467. Benemann JR (1994) Feasibility analysis of photobiological hydrogen production. In: Hydrogen energy progress X, Proceedings of the world hydrogen energy conference, 10th, vol 2, pp 931–940
468. Benemann JR (1994) Photobiological hydrogen production. In: Proceedings of the intersociety energy conversion engineering conference 29TH(PT. 4), pp 1636–1640
469. Blake DM, Amos WA, Ghirardi ML, Seibert M (2008) Materials requirements for photobiological hydrogen production. In: Thomas GJ, Jones RH (eds) Materials for the hydrogen economy. CRC, Boca Raton, pp 123–145
470. Carlozzi P, Lambardi M (2009) Fed-batch operation for bio-H2 production by Rhodopseudomonas palustris (strain 42OL). Renewable Energy 34(12):2577–2584
471. Dawar S, Masukawa H, Mohanty P, Sakurai H (2006) Prospects of biohydrogen production using cyanobacteria – an overview. Proc Indian Natl Sci Acad 72(4):213–223
472. Dickson DJ, Page CJ, Ely RL (2009) Photobiological hydrogen production from Synechocystis sp. PCC 6803 encapsulated in silica sol-gel. Int J Hydrogen Energy 34(1):204–215

473. Gaudernack B (1998) Photoproduction of hydrogen. Annex 10 of the IEA Hydrogen Program. In: Hydrogen energy progress XII, Proceedings of the world hydrogen energy conference, 12th, Buenos Aires, 21–26 June 1998, vol 3, pp 2011–2023
474. Ghirardi ML (2007) Hydrogenases as catalysts for renewable hydrogen production. Abstracts of papers, 233rd ACS national meeting, Chicago, IL, United States, 25–29 Mar 2007, INOR-482
475. Ghirardi ML (2007) Photobiological and bio-hybrid hydrogen production based on the activity of hydrogenase enzymes. Abstracts of papers, 233rd ACS national meeting, Chicago, IL, United States, 25–29 March 2007, PHYS-114
476. Ghirardi ML, Cohen J, King P, Schulten K, Kim K, Seibert M (2006) [FeFe]-hydrogenases and photobiological hydrogen production. In: Proceedings of SPIE-The International Society for Optical Engineering 6340(Solar Hydrogen and Nanotechnology): 63400X/1-63400X/6
477. Ghirardi ML, Dubini A, Yu J, Maness P-C (2009) Photobiological hydrogen-producing systems. Chem Soc Rev 38(1):52–61
478. Ghirardi ML, Kosourov S, Seibert M (2001) Cyclic photobiological algal H2-production. In: Proceedings of the 2001 US DOE hydrogen program review, Baltimore, MD, United States, 17–19 Apr 2001, pp 67–76
479. Hemschemeier A, Melis A, Happe T (2009) Analytical approaches to photobiological hydrogen production in unicellular green algae. Photosynth Res 102(2–3):523–540
480. Ikuta Y, Akano T, Shioji N, Maeda I (1998) Hydrogen production by photosynthetic microorganisms. In: BioHydrogen, [Proceedings of an international conference on biological hydrogen production], Waikoloa, HI, 23–26 June 1997, pp 319–328
481. Juantorena AU, Sebastian PJ, Santoyo E, Gamboa SA, Lastres OD, Sanchez-Escamilla D, Bustos A, Eapen D (2007) Hydrogen production employing Spirulina maxima 2342: a chemical analysis. Int J Hydrogen Energy 32(15):3133–3136
482. Masukawa H, Nakamura K, Mochimaru M, Sakurai H (2001) Photobiological hydrogen production and nitrogenase activity in some heterocystous cyanobacteria. Biohydrogen II: an approach to environmentally acceptable technology [Workshop on Biohydrogen], 2nd, Tsukuba, Japan, June 1999, pp 63–66
483. Melandri BA, Zannoni D, Casadio R, De Santis A (1985) Photobiological hydrogen production by facultative photosynthetic bacteria. Inst. Bot Univ Bologna, Bologna
484. Melis A, Melnicki MR (2006) Integrated biological hydrogen production. Int J Hydrogen Energy 31(11):1563–1573
485. Ogbonna JC, Tanaka H (2001) Photobioreactor design for photobiological production of hydrogen. Biohydrogen II: an approach to environmentally acceptable technology, [Workshop on Biohydrogen], 2nd, Tsukuba, Japan, June 1999, pp 245–261
486. Prince R, Kheshgi H (2005) The photobiological production of hydrogen: potential efficiency and effectiveness as a renewable fuel. Crit Rev Microbiol 31(1):19–31
487. Raghavendra AS, Vallejos RH (1980) Photobiological production of hydrogen. Proc Int Symp Biol Appl Sol Energy: 193–195
488. Rai AN, Soderback E, Bergman B (2000) Tansley review no. 116: Cyanobacterium-plant symbioses. New Phytol 147(3):449–481
489. Sakurai H, Masukawa H, Dawar S, Yoshino F (2004) Photobiological hydrogen production by cyanobacteria utilizing nitrogenase systems: present status and future development. Biohydrogen III: renewable energy system by biological solar energy conversion, [International Symposium on Biohydrogen], 3rd, Kyoto, Japan, Oct 2002, pp 83–92
490. Sasikala C, Ramana CV, Rao PR, Venkataraman LV (1996) Hydrogen by bio-routes: a perspective. Proc Natl Acad Sci India B Biol Sci 66(1):1–20
491. Schutz K, Happe T, Troshina O, Lindblad P, Leitao E, Oliveira P, Tamagnini P (2004) Cyanobacterial H(2) production – a comparative analysis. Planta 218(3):350–359
492. Seibert M, Lien S, Weaver PF (1979) Photobiological hydrogen production. Sol Energy Res Inst, Golden
493. Seibert M, Lien S, Weaver PF (1980) Photobiological hydrogen production. Proc Jt US/USSR Conf Microb Enzyme React Proj US/USSR Jt Work Group Prod Subst Microbiol Means, 5th, pp 480–498

494. Seibert M, Lien S, Weaver PF, Janzen AF (1981) Photobiological production of hydrogen and electricity. Sol Energy Convers 2 [Two], Sel Lect Int Symp Sol Energy Util, pp 273–292
495. Tramm-Werner S, Hackethal M, Weng M, Hartmeier W (1996) Photobiological hydrogen production using a new plate loop reactor. In: Hydrogen energy progress XI, Proceedings of the world hydrogen energy conference, 11th, Stuttgart, 23–28 June 1996, vol 3, pp 2407–2416
496. Tramm-Werner S, Weng M, Hartmeier W, Modigell M (1996) Photobiological hydrogen production using immobilized Rhodobacteria: biofilm formation in a loop reactor. In: Biomass for energy and the environment, Proceedings of the European Bioenergy Conference, 9th, Copenhagen, 24–27 June 1996, vol 3, pp 1674–1679
497. Weaver P, Lien S, Seibert M (1979) Photobiological production of hydrogen: a solar energy conversion option. Sol Energy Res Inst Golden, CO, USA, Report No. SERI/TR-33-122
498. Weaver PF, Lien S, Seibert M (1980) Photobiological production of hydrogen. Sol Energy 24(1):3–45
499. Wuenschiers R (2003) Photobiological hydrogen metabolism and hydrogenases from green algae. In: Nalwa HS (ed) Handbook of photochemistry and photobiology, vol 4. American Scientific Publishers, North Lewis Way, pp 353–382
500. Gaffron H, Rubin J (1942) Fermentative and photochemical production of hydrogen in algae. The Journal of General Physiology 26(2):219–240
501. Miyamoto K (1997) Renewable biological systems for alternative sustainable energy production (FAO agricultural services bulletin - 128). FAO – Food and Agriculture Organization of the United Nations, Rome. ISBN 92-5-104059-1
502. Fujishima A, Honda K (1971) Verification of the photo senitized electrolytic oxidation of TiO2 electrode by pH measurement. J Chem Soc Japan 74:355–360
503. Arakawa H, Shiraishi C, Takeuchi A, Yamaguchi T (2006) Solar hydrogen production by water splitting using TiO2 based photoelectrodes. In: Proceedings of SPIE-The International Society for Optical Engineering 6340(Solar Hydrogen and Nanotechnology): 63400G/1-63400G/14
504. Augustynski J, Calzaferri G, Courvoisier JC, Gratzel M (1996) Photoelectrochemical hydrogen production: state of the art with special reference to IEA's Hydrogen Program. In: Hydrogen Energy Progress XI, Proceedings of the World Hydrogen Energy Conference, 11th, Stuttgart, 23–28 June 1996 vol 3, pp 2379–2387
505. Bandara J, Udawatta CPK, Rajapakse CSK (2005) Highly stable CuO incorporated TiO2 catalyst for photocatalytic hydrogen production from H2O. Photochem Photobiol Sci 4(11):857–861
506. Best JP, Dunstan DE (2009) Nanotechnology for photolytic hydrogen production: colloidal anodic oxidation. Int J Hydrogen Energy 34(18):7562–7578
507. Broda E (1978) Hydrogen production through solar radiation by means of water photolysis in membranes. Int J Hydrogen Energy 3(1):119–121
508. Caramori S, Cristino V, Argazzi R, Meda L, Bignozzi CA (2010) Photoelectrochemical behavior of sensitized TiO_2 photoanodes in an aqueous environment: application to hydrogen production. Inorg Chem (Washington, DC, USA) 49(7):3320–3328
509. Chiarello GL, Forni L, Selli E (2009) Photocatalytic hydrogen production by liquid- and gas-phase reforming of CH_3OH over flame-made TiO_2 and Au/TiO_2. Catal Today 144(1–2): 69–74
510. Chung K-H, Park D-C (1996) Water photolysis reaction on cerium oxide photocatalysts. Catal Today 30(1–3):157–162
511. Dholam R, Patel N, Adami M, Miotello A (2009) Hydrogen production by photocatalytic water-splitting using Cr- or Fe-doped TiO_2 composite thin films photocatalyst. Int J Hydrogen Energy 34(13):5337–5346
512. Berr M, Vaneski A, Susha A, Rodriguez-Fernandez J, Doblinger M, Jackel F, Rogach AL, Feldmann J (2010) Colloidal CdS nanorods decorated with subnanometer sized Pt clusters for photocatalyti hydrogen generation. Appl Phys Lett 97(9):093108–093111

513. Girginer B, Galli G, Chiellini E, Bicak N (2009) Preparation of stable CdS nanoparticles in aqueous medium and their hydrogen generation efficiencies in photolysis of water. Int J Hydrogen Energy 34(3):1176–1184
514. Ikuma Y, Bessho H (2007) Effect of Pt concentration on the production of hydrogen by a TiO_2 photocatalyst. Int J Hydrogen Energy 32(14):2689–2692
515. Ingler WB Jr, Naseem A (2010) Indium oxide/indium iron oxide thin films for photoelectrochemical hydrogen production with a-silicon solar cells. J Mater Res 25(1):25–31
516. Jang JS, Choi SH, Kim DH, Jang JW, Lee KS, Lee JS (2009) Enhanced photocatalytic hydrogen production from water-methanol solution by nickel intercalated into titanate nanotube. J Phys Chem C 113(20):8990–8996
517. Jang JS, Hwang DW, Lee JS (2007) CdS-AgGaS2 photocatalytic diodes for hydrogen production from aqueous Na2S/Na2SO3 electrolyte solution under visible light (l >= 420 nm). Catal Today 120(2):174–181
518. Jang JS, Ji SM, Bae SW, Son HC, Lee JS (2007) Optimization of CdS/TiO2 nano-bulk composite photocatalysts for hydrogen production from Na2S/Na2SO3 aqueous electrolyte solution under visible light (l >= 420 nm). J Photochem Photobiol, A 188(1):112–119
519. Jang JS, Kim HG, Joshi UA, Jang JW, Lee JS (2008) Fabrication of CdS nanowires decorated with TiO_2 nanoparticles for photocatalytic hydrogen production under visible light irradiation. Int J Hydrogen Energy 33(21):5975–5980
520. Jing D, Guo L (2007) WS2 sensitized mesoporous TiO_2 for efficient photocatalytic hydrogen production from water under visible light irradiation. Catal Commun 8(5):795–799
521. Kanade KG, Baeg J-O, Kong K-j, Kale BB, Lee SM, Moon S-J (2008) A novel nanostructured semiconductor photocatalyst for solar hydrogen production. In: Proceedings of SPIE 7044(Solar Hydrogen and Nanotechnology III): 70440O/1-70440O/11
522. Kanade KG, Kale BB, Baeg J-O, Lee SM, Lee CW, Moon S-J, Chang H (2007) Self-assembled aligned Cu doped ZnO nanoparticles for photocatalytic hydrogen production under visible light irradiation. Mater Chem Phys 102(1):98–104
523. Kawai T, Sakata T (1980) Photocatalytic hydrogen production from liquid methanol and water. J Chem Soc, Chem Commun 15:694–695
524. Kiwi J (1980) Hydrogen and oxygen production via redox catalysis in colloidal systems. Isr J Chem 18(3–4):369–374
525. Kiwi J, Gratzel M (1979) Hydrogen evolution from water induced by visible light mediated by redox catalysis. Nature(London, UK) 281(5733):657–658
526. Krishna Reddy J, Suresh G, Hymavathi CH, Durga Kumari V, Subrahmanyam M (2009) Ce (III) species supported zeolites as novel photocatalysts for hydrogen production from water. Catal Today 141(1–2):89–93
527. Kryukov AI, Smirnova NP, Korzhak AV, Eremenko AM, Kuchmii SY (1997) Photocatalysis of reaction of hydrogen production by cadmium and zinc sulfide nanoparticles incorporated into silicate matrixes. Theor Exp Chem(Translation of Teoreticheskaya i Eksperimental'naya Khimiya) 33(1):30–33
528. Kwak BS, Chae J, Kim J, Kang M (2009) Enhanced hydrogen production from methanol/water photo-splitting in TiO2 including Pd component. Bull Korean Chem Soc 30(5):1047–1053
529. Lee SG, Kim J-H, Lee S, Lee H-I (2001) Photochemical production of hydrogen from alkaline solution containing polysulfide dyes. Korean J Chem Eng 18(6):894–897
530. Li Y, Ma G, Peng S, Lu G, Li S (2009) Photocatalytic H_2 evolution over basic zincoxysulfide (ZnS1-x-0.5yOx(OH)y) under visible light irradiation. Appl Catal A Gen 363(1–2):180–187
531. Liu Y, Guo L, Yan W, Liu H (2006) A composite visible-light photocatalyst for hydrogen production. J Power Sources 159(2):1300–1304
532. Liu Y, Xie L, Li Y, Yang R, Qu J, Li Y, Li X (2008) Synthesis and high photocatalytic hydrogen production of SrTiO3 nanoparticles from water splitting under UV irradiation. J Power Sources 183(2):701–707
533. Nann T, Ibrahim SK, Woi P-M, Xu S, Ziegler J, Pickett CJ (2010) Water splitting by visible light: a nanophotocathode for hydrogen production. Angew Chem Int Ed 49(9):1574–1577

534. Navarro Yerga RM, Alvarez Galvan MC, del Valle F, Villoria de la Mano JA, Fierro JLG (2009) Water splitting on semiconductor catalysts under visible-light irradiation. ChemSusChem 2(6):471–485
535. Park H, Choi W, Hoffmann MR (2008) Effects of the preparation method of the ternary CdS/TiO2/Pt hybrid photocatalysts on visible light-induced hydrogen production. J Mater Chem 18(20):2379–2385
536. Paulauskas IE, Katz JE, Jellison GE, Lewis NS, Boatner LA (2008) Photoelectrochemical studies of semiconducting photoanodes for hydrogen production via water dissociation. Thin Solid Films 516(22):8175–8178
537. Rocheleau RE, Miller E, Misra A (1996) Photoelectrochemical hydrogen production. In: Proceedings of the US DOE Hydrogen Program Review, Miami, 1–2 May 1996, vol 1, pp 345–357
538. Rosseler O, Shankar MV, Du Karkmaz-Le M, Schmidlin L, Keller N, Keller V (2010) Solar light photocatalytic hydrogen production from water over Pt and Au/TiO2(anatase/rutile) photocatalysts: influence of noble metal and porogen promotion. J Catal 269(1):179–190
539. Ryu SY, Balcerski W, Lee TK, Hoffmann MR (2007) Photocatalytic production of hydrogen from water with visible light using hybrid catalysts of CdS attached to microporous and mesoporous silicas. J Phys Chem C 111(49):18195–18203
540. Sahu N, Upadhyay SN, Sinha ASK (2009) Kinetics of reduction of water to hydrogen by visible light on alumina supported Pt-CdS photocatalysts. Int J Hydrogen Energy 34(1):130–137
541. Streich D, Astuti Y, Orlandi M, Schwartz L, Lomoth R, Hammarstroem L, Ott S (2010) High-turnover photochemical hydrogen production catalyzed by a model complex of the [FeFe]-hydrogenase active site. Chem Eur J 16(1):60–63, S/1-S/9
542. Subramanian E, Baeg J-O, Lee SM, Moon S-J, K-j K (2008) Dissociation of H2S under visible light irradiation (l >= 420nm) with FeGaO3 photocatalysts for the production of hydrogen. Int J Hydrogen Energy 33(22):6586–6594
543. Tode R, Ebrahimi A, Fukumoto S, Iyatani K, Takeuchi M, Matsuoka M, Lee CH, Jiang C-S, Anpo M (2010) Photocatalytic decomposition of water on double-layered visible light-responsive TiO_2 thin films prepared by a magnetron sputtering deposition method. Catal Lett 135(1–2):10–15
544. Turner J, Sverdrup G, Mann MK, Maness P-C, Kroposki B, Ghirardi M, Evans RJ, Blake D (2008) Renewable hydrogen production. Int J Energy Res 32(5):379–407
545. Villoria JA, Navarro Yerga RM, Al-Zahrani SM, Fierro JLG (2010) Photocatalytic hydrogen production on Cd1-xZnxS solid solutions under visible light: influence of thermal treatment. Ind Eng Chem Res 49(15):6854–6861
546. Wang X, Maeda K, Thomas A, Takanabe K, Xin G, Carlsson JM, Domen K, Antonietti M (2009) A metal-free polymeric photocatalyst for hydrogen production from water under visible light. Nat Mater 8(1):76–80
547. Wang Y, Zhang Z, Zhu Y, Li Z, Vajtai R, Ci L, Ajayan PM (2008) Nanostructured VO2 photocatalysts for hydrogen production. ACS Nano 2(7):1492–1496
548. Weidenkaff A, Nuesch P, Wokaun A, Reller A (1997) Mechanistic studies of the water-splitting reaction for producing solar hydrogen. Solid State Ionics 101–103(Pt. 2):915–922
549. Werner HAF, Bauer R (1996) Hydrogen production by water photolysis using nitrilotriacetic acid as electron donor. J Photochem Photobiol, A 97(3):171–173
550. Yan H, Yang J, Ma G, Wu G, Zong X, Lei Z, Shi J, Li C (2009) Visible-light-driven hydrogen production with extremely high quantum efficiency on Pt-PdS/CdS photocatalyst. J Catal 266(2):165–168
551. Yang H, Guo L, Yan W, Liu H (2006) A novel composite photocatalyst for water splitting hydrogen production. J Power Sources 159(2):1305–1309
552. Yuan Y, Zhang X, Liu L, Jiang X, Lv J, Li Z, Zou Z (2008) Synthesis and photocatalytic characterization of a new photocatalyst BaZrO3. Int J Hydrogen Energy 33(21):5941–5946
553. T-Raissi A, Block D (2004) Hydrogen: automotive fuel of the future. IEEE Power Energy 2(6):43

554. Sandrock G (2008) Overview of hydrogen storage: gas liquid and solid. DOE EERE/NIST joint workshop on combinatorial materials science for applications in energy (MCMC-14) NIST Combinatorial Center 5 Nov 2008. Zuttel A (2004) Hydrogen storage methods. Naturwissenschaften 91:157–172
555. Aceves S, Berry G, Espinosa F, Ross T, Switzer V, Weisberg A, Ledesma-Orozco E (2008) Lawrence Livermore National Laboratory, Automotive cryogenic capable pressure vessels for compact, high dormancy (L)H2 storage, DOE Annual Hydrogen Program Merit Review, 10 June 2008
556. Mori D, Hirose K (2009) Recent challenges of hydrogen storage technologies for fuel cell vehicles. Int J Hydrogen Energy 34:4569–4574
557. QUANTUM Technologies WorldWide, Inc. Irvine, CA, USA
558. Anzulovic I (1992) Optimization of gaseous hydrogen storage system. Int J Hydrogen Energy 17(2):129–138
559. Barthelemy H, Bryselbout J, Barbe C (1983) Testing methods to select steels for gaseous hydrogen storage and transport vessels. Cent Rech Claude-Delorme, Jouy en Josas, pp 366–377
560. Itoh Y, Tamura Y, Mitsuishi H, Watanabe S (2007) Numerical study of the thermal bahavior on fast filling of compressed gaseous hydrogen tanks. Society of Automotive Engineers, [Special publication] SP SP-2098(Applications of fuel cells in vehicles), pp 19–24
561. Koroteev AS, Mironov VV, Smolyarov VA (2004) Perspectives in hydrogen use in means of transportation. Isjaee 1:5–13
562. Eliasson B, Bossel U (2010) The future of the hydrogen economy: bright or bleak? http://www.woodgas.com/hydrogen_economy.pdf. Accessed 20 Nov 2010
563. Teitel R (1981) Hydrogen storage in glass microspheres. Brookhaven National Laboratories, Report No. BNL 51439
564. Sass JP, Fesmire JE, Nagy ZF, Sojourner SJ, Morris DL, Augustynowicz SD (2008) Thermal performance comparison of glass microsphere and perlite insulation systems for liquid hydrogen storage tanks. In: AIP Conference Proceedings, vol 985(Advances in Cryogenic Engineering, vol 53B), pp 1375–1382
565. Amaseder F, Krainz G (2006) Liquid hydrogen storage systems developed and manufactured for the first time for customer cars. Society of Automotive Engineers, [Special publication] SP SP-2009(Hydrogen IC Engines), pp 23–33
566. Emans M, Mori D, Krainz G (2006) Analysis of back-gas behaviour of an automotive liquid hydrogen storage system during refilling at the filling station. In: CryoPrague 2006, Multiconference, Proceedings, Praha, Czech Republic, 17–21 July 2006: 186/1–186/5
567. Furuhama S, Sakurai T, Shindo M (1993) Study of evaporation loss of liquid hydrogen storage tank with LH2 pump. Int J Hydrogen Energy 18(1):25–30
568. Hedayat A, Hastings LJ, Bryant C, Plachta DW (2002) Large scale demonstration of liquid hydrogen storage with zero boiloff. In: AIP Conference Proceedings, vol 613(Advances in Cryogenic Engineering), pp 1276–1283
569. Khurana TK, Prasad BVSSS, Ramamurthi K, Murthy SS (2006) Thermal stratification in ribbed liquid hydrogen storage tanks. Int J Hydrogen Energy 31(15):2299–2309
570. Krainz G, Bartlok G, Bodner P, Casapicola P, Doeller C, Hofmeister F, Neubacher E, Zieger A (2004) Development of automotive liquid hydrogen storage systems. In: AIP Conference Proceedings, vol 710(Advances in Cryogenic Engineering), pp 35–40
571. Londer H, Myneni GR, Adderley P, Bartlok G, Setina J, Knapp W, Schleussner D (2006) New high capacity getter for vacuum-insulated mobile liquid hydrogen storage systems. In: AIP Conference Proceedings, vol 837(Hydrogen in Matter), pp 210–220
572. Matsuoka Y (2008) Liquid hydrogen storage and transportation technology. Enerugi no Chozo – Yuso, pp 363–376
573. Peschka W, Edeskuty FJ, Stewart WF (1983) Liquid-hydrogen storage and refueling for automotive applications. Altern Energy Sources 3(5):407–417

574. Sass JP, St. Cyr WW, Barrett TM, Baumgartner RG, Lott JW, Fesmire JE (2010) Glass bubbles insulation for liquid hydrogen storage tanks. In: AIP Conference Proceedings, vol 1218, pp 772–779
575. Linde Group. Hydrogen solution. www.linde.com. Accessed 20 Nov 2010
576. Shimko MA (2005) Combined reverse Brayton Joule Thompson Hydrogen liquefaction cycle. DOE Hydrogen Program. FY 2005 progress report. Contract Number: DE-FG36-05GO15021
577. Arai M, Utsumi S, Kanamaru M, Urita K, Fujimori T, Yoshizawa N, Noguchi D, Nishiyama K, Hattori Y, Okino F, Ohba T, Tanaka H, Kanoh H, Kaneko K (2009) Enhanced hydrogen adsorptivity of single-wall carbon nanotube bundles by one-step C60-pillaring method. Nano Lett 9(11):3694–3698
578. Avdeenkov AV, Bibikov AV, Bodrenko IV, Nikolaev AV, Taran MD, Tkalya EV (2009) Modified carbon nanostructures as materials for hydrogen storage. Russ Phys J 52(11):1235–1241
579. Balathanigaimani MS, Shim W-G, Kim T-H, Cho S-J, Lee J-W, Moon H (2009) Hydrogen storage on highly porous novel corn grain-based carbon monoliths. Catal Today 146(1–2): 234–240
580. Bianco S, Giorcelli M, Musso S, Castellino M, Agresti F, Khandelwal A, Lo Russo S, Kumar M, Ando Y, Tagliaferro A (2009) Hydrogen adsorption in several types of carbon nanotubes. J Nanosci Nanotechnol 9(12):6806–6812
581. Bianco S, Giorcelli M, Musso S, Castellino M, Agresti F, Khandelwal A, Russo SL, Kumar M, Ando Y, Tagliaferro A (2010) Hydrogen adsorption in several types of carbon nanotubes. J Nanosci Nanotechnol 10(6):3860–3866
582. Burress J, Kraus M, Beckner M, Cepel R, Suppes G, Wexler C, Pfeifer P (2009) Hydrogen storage in engineered carbon nanospaces. Nanotechnology 20(20):204026/1–204026/10
583. Fierro V, Szczurek A, Zlotea C, Mareche JF, Izquierdo MT, Albiniak A, Latroche M, Furdin G, Celzard A (2010) Experimental evidence of an upper limit for hydrogen storage at 77K on activated carbons. Carbon 48(7):1902–1911
584. Gao F, Zhao D-L, Li Y, Li X-G (2010) Preparation and hydrogen storage of activated rayon-based carbon fibers with high specific surface area. J Phys Chem Solids 71(4):444–447
585. Gayathri V, Devi NR, Geetha R (2010) Hydrogen storage in coiled carbon nanotubes. Int J Hydrogen Energy 35(3):1313–1320
586. Geng H-Z, Kim TH, Lim SC, Jeong H-K, Jin MH, Jo YW, Lee YH (2010) Hydrogen storage in microwave-treated multi-walled carbon nanotubes. Int J Hydrogen Energy 35(5): 2073–2082
587. Hirano S (2010) Fuel cell research and development at Ford Motor Company. J Fuel Cell Tech (Nenryo Denchi) 9(3):38–45
588. Huang C-C, Chen H-M, Chen C-H, Huang J-C (2010) Effect of surface oxides on hydrogen storage of activated carbon. Sep Purif Technol 70(3):291–295
589. Jimenez V, Sanchez P, Diaz JA, Valverde JL, Romero A (2010) Hydrogen storage capacity on different carbon materials. Chem Phys Lett 485(1–3):152–155
590. Jurewicz K (2009) Influence of charging parameters on the effectiveness of electrochemical hydrogen storage in activated carbon. Int J Hydrogen Energy 34(23):9431–9435
591. Kuchta B, Firlej L, Pfeifer P, Wexler C (2009) Numerical estimation of hydrogen storage limits in carbon-based nanospaces. Carbon 48(1):223–231
592. Kunowsky M, Marco-Lozar JP, Cazorla-Amoros D, Linares-Solano A (2010) Scale-up activation of carbon fibres for hydrogen storage. Int J Hydrogen Energy 35(6):2393–2402
593. Lan J, Cao D, Wang W (2009) Li12Si60H60 fullerene composite: a promising hydrogen storage medium. ACS Nano 3(10):3294–3300
594. Liu C, Chen Y, Wu C-Z, Xu S-T, Cheng H-M (2009) Hydrogen storage in carbon nanotubes revisited. Carbon 48(2):452–455
595. Martin JB, Kinloch IA, Dryfe RAW (2010) Are carbon nanotubes viable materials for the electrochemical storage of hydrogen? J Phys Chem C 114(10):4693–4703
596. Meisner GP, Hu Q (2009) High surface area microporous carbon materials for cryogenic hydrogen storage synthesized using new template-based and activation-based approaches. Nanotechnology 20(20):204023/1–204023/10

597. Muniz AR, Meyyappan M, Maroudas D (2009) On the hydrogen storage capacity of carbon nanotube bundles. Appl Phys Lett 95(16):163111/1–163111/3
598. Openov LA, Podlivaev AI (2010) Thermal desorption of hydrogen from graphane. Tech Phys Lett 36(1):31–33
599. Paggiaro R, Benard P, Polifke W (2010) Cryo-adsorptive hydrogen storage on activated carbon. I: thermodynamic analysis of adsorption vessels and comparison with liquid and compressed gas hydrogen storage. Int J Hydrogen Energy 35(2):638–647
600. Paggiaro R, Michl F, Benard P, Polifke W (2010) Cryo-adsorptive hydrogen storage on activated carbon. II: investigation of the thermal effects during filling at cryogenic temperatures. Int J Hydrogen Energy 35(2):648–659
601. Qin X, Li F (2010) Synthesis of the novel porous carbon nanotubes. Advanced Materials Research (Zuerich, Switzerland) 96(Advance in Ecological Environment, Functional Materials and Ion Industry), pp 241–243
602. Reyhani A, Golikand AN, Mortazavi SZ, Irannejad L, Moshfegh AZ (2010) The effects of multi-walled carbon nanotubes graphitization treated with different atmospheres and electrolyte temperatures on electrochemical hydrogen storage. Electrochim Acta 55(16): 4700–4705
603. Roman TA, Dino WA, Nakanishi H, Kasai H, Sugimoto T, Tange K (2007) Graphite utilization in hydrogen storage: a computational perspective. Condens Matter Theor 21:275–283
604. Saha D, Wei Z, Valluri SH, Deng S (2010) Hydrogen adsorption in ordered mesoporous carbon synthesized by a soft-template approach. J Porous Media 13(1):39–50
605. Suarez-Garcia F, Vilaplana-Ortego E, Kunowsky M, Kimura M, Oya A, Linares-Solano A (2009) Activation of polymer blend carbon nanofibres by alkaline hydroxides and their hydrogen storage performances. Int J Hydrogen Energy 34(22):9141–9150
606. Sufian S, Yusup S, Walker GS, Shariff AM (2009) Synthesis of graphitic nanofibres using iron (III) oxide catalyst for hydrogen storage application. Mater Res Innovations 13(3):221–224
607. Vasiliev LL, Kanonchik LE (2010) Activated carbon fibres and composites on its base for high performance hydrogen storage system. Chem Eng Sci 65(8):2586–2595
608. Venkataramanan NS, Mizuseki H, Kawazoe Y (2009) Hydrogen storage on nanofullerene cages. Nano 4(5):253–263
609. Wu H-C, Li Y-Y, Sakoda A (2010) Synthesis and hydrogen storage capacity of exfoliated turbostratic carbon nanofibers. Int J Hydrogen Energy 35(9):4123–4130
610. Xia Y, Walker GS, Grant DM, Mokaya R (2009) Hydrogen storage in high surface area carbons: experimental demonstration of the effects of nitrogen doping. J Am Chem Soc 131(45):16493–16499
611. Zhou Z, Zhao J (2008) Gas adsorption in carbon nanotubes and technological applications. Recent Research Activities of Micro- and Nano-Scale Carbon Related Materials INBN No 978-81-7895-350-2, pp 37–57
612. Zini G, Marazzi R, Pedrazzi S, Tartarini P (2010) A solar hydrogen hybrid system with activated carbon storage. Int J Hydrogen Energy 35(10):4909–4917
613. Reyhani A, Mortazavi SZ, Moshfegh AZ, Golikand AN (2010) A study on the effects of Fex/Niy/MgO(1-x-y) catalysts on the volumetric and electrochemical hydrogen storage of multi-walled carbon nanotubes. Int J Hydrogen Energy 35(1):231–237
614. Schaller R, Mari D, Marques dos Santos S, Tkalcec I, Carreno-Morelli E (2009) Investigation of hydrogen storage in carbon nanotube-magnesium matrix composites. Mate Sci Eng A 521–522:147–150
615. Xu F, Lu Y, Sun L, Zhi L (2010) A novel ZnO nanostructure: rhombus-shaped ZnO nanorod array. Chem Commun(Cambridge, UK) 46(18):3191–3193
616. Yamauchi M, Kobayashi H, Kitagawa H (2009) Hydrogen storage mediated by Pd and Pt nanoparticles. Chemphyschem 10(15):2566–2576
617. Lee H, Huang B, Duan W, Ihm J (2010) Ab initio study of beryllium-decorated fullerenes for hydrogen storage. J Appl Phys 107(8):084304/1–084304/4

618. Tsao C-S, Liu Y, Li M, Zhang Y, Leao JB, Chang H-W, Yu M-S, Chen S-H (2010) Neutron scattering methodology for absolute measurement of room-temperature hydrogen storage capacity and evidence for spillover effect in a Pt-doped activated carbon. J Phys Chem Lett 1(10):1569–1573
619. Tsao C-S, Tzeng Y-R, Yu M-S, Wang C-Y, Tseng H-H, Chung T-Y, Wu H-C, Yamamoto T, Kaneko K, Chen S-H (2010) Effect of catalyst size on hydrogen storage capacity of Pt-impregnated active carbon via spillover. J Phys Chem Lett 1(7):1060–1063
620. Wang L, Lee K, Sun Y-Y, Lucking M, Chen Z, Zhao JJ, Zhang SB (2009) Graphene oxide as an ideal substrate for hydrogen storage. ACS Nano 3(10):2995–3000
621. Wang L, Yang RT (2009) Hydrogen storage properties of N-doped microporous carbon. J Phys Chem C 113(52):21883–21888
622. Wang P-J, Fang Z-Z, Ma L-P, Kang X-D, Wang P (2010) Effect of carbon addition on hydrogen storage behaviors of Li-Mg-B-H system. Int J Hydrogen Energy 35(7):3072–3075
623. Wang Q, Sun Q, Jena P (2009) Hydrogen storage in AlN-based nanostructures. Prepr Symp Am Chem Soc, Div Fuel Chem 54(2):751
624. Wang Z, Yang RT (2010) Enhanced hydrogen storage on Pt-doped carbon by plasma reduction. J Phys Chem C 114(13):5956–5963
625. Wu HY, Fan XF, Kuo J-L, Deng W-Q (2010) Carbon doped boron nitride cages as competitive candidates for hydrogen storage materials. Chem Commun (Cambridge, UK) 46(6):883–885
626. Xia J, Yuan S, Wang Z, Kirklin S, Dorney B, Liu D-J, Yu L (2010) Nanoporous polyporphyrin as adsorbent for hydrogen storage. Macromolecules (Washington, DC, USA) 43(7): 3325–3330
627. Diaz E, Leon M, Ordonez S (2010) Hydrogen adsorption on Pd-modified carbon nanofibres: influence of CNF surface chemistry and impregnation procedure. Int J Hydrogen Energy 35(10):4576–4581
628. Jeong Y, Mike Chung TC (2010) The synthesis and characterization of a super-activated carbon containing substitutional boron (BCx) and its applications in hydrogen storage. Carbon 48(9):2526–2537
629. Chang J-K, Chen C-Y, Tsai W-T (2009) Decorating carbon nanotubes with nanoparticles using a facile redox displacement reaction and an evaluation of synergistic hydrogen storage performance. Nanotechnology 20(49):495603/1–495603/7
630. Lee H, Ihm J, Cohen ML, Louie SG (2010) Calcium-decorated graphene-based nanostructures for hydrogen storage. Nano Lett 10(3):793–798
631. Lee H, Ihm J, Cohen ML, Louie SG (2009) Calcium-decorated carbon nanotubes for high-capacity hydrogen storage: first-principles calculations. Phys Rev B Condensed Matter Mater Phys 80(11):115412/1–115412/5
632. Huang L, Liu Y-C, Gubbins KE, Nardelli MB (2010) Ti-decorated C60 as catalyst for hydrogen generation and storage. Appl Phys Lett 96(6):063111/1–063111/3
633. Yang C-C, Li YJ, Chen W-H (2010) Electrochemical hydrogen storage behavior of single-walled carbon nanotubes (SWCNTs) coated with Ni nanoparticles. Int J Hydrogen Energy 35(6):2336–2343
634. Yu L-M, Shi G-S, Wang Z-G, Ji G-F, Lu Z-P (2009) Adsorption mechanism of hydrogen on boron-doped fullerenes. Chin Phys Lett 26(8):086804/1–086804/4
635. Giraudet S, Zhu Z, Yao X, Lu G (2010) Ordered mesoporous carbons enriched with nitrogen: application to hydrogen storage. J Phys Chem C 114(18):8639–8645
636. Grigorova E, Mandzhukova T, Khristov M, Tzvetkov P, Tsyntsarski B (2010) Investigation of hydrogen storage properties of magnesium based composites with addition of activated carbon derived from apricot stones. Bulg Chem Commun 42(1):70–74
637. Chang J-K, Chen C-Y, Tsai W-T (2009) Preparation and hydrogen storage performance of Pd nanoparticles decorated carbon nanotubes. ECS Transactions 19(10, Hydrogen Production, Transport, and Storage 3): 33–40
638. Neiner D, Kauzlarich SM (2010) Hydrogen-capped silicon nanoparticles as a potential hydrogen storage material: synthesis, characterization, and hydrogen release. Chem Mater 22(2):487–493

639. Ni M, Huang L, Guo L, Zeng Z (2010) Hydrogen storage in Li-doped charged single-walled carbon nanotubes. Int J Hydrogen Energy 35(8):3546–3549
640. Chen C-Y, Chang J-K, Lin K-Y, Chung S-T, Tsai W-T (2010) Enhanced hydrogen storage in MWCNTs decorated by electroless nickel nanoparticles deposited in supercritical CO2 bath. Mater Sci Forum 638–642, 1148–1151, (Pt. 2, THERMEC 2009)
641. Liu Q (2010) Monodisperse polystyrene nanospheres with ultrahigh surface area: application for hydrogen storage. Macromol Chem Phys 211(9):1012–1017
642. Ahmad M, Rafi-ud D, Pan C, Zhu J (2010) Investigation of hydrogen storage capabilities of ZnO-based nanostructures. J Phys Chem C 114(6):2560–2565
643. Chu Z, He R, Zhang X, Cheng H, Li X, Wang Y (2010) Hydrogen adsorption properties of polymer-derived nanoporous SiCx fibers. Int J Hydrogen Energy 35(7):3165–3169
644. Hu T, Zhang H, Li T, Liu R, Meng C, Qiu J (2009) Zeolite supported nickel cluster and its adsorption towards hydrogen molecules. Prepr Symp Am Chem Soc, Div Fuel Chem 54(2):591–592
645. Korili SA, Gil A (2008) Recent advances in hydrogen adsorption and storage on porous materials. Recent Research Developments in Environmental Technology, pp 143–155
646. Chung K-H (2010) High-pressure hydrogen storage on microporous zeolites with varying pore properties. Energy (Oxford, UK) 35(5):2235–2241
647. Lim KL, Kazemian H, Yaakob Z, Daud WRW (2010) Solid-state materials and methods for hydrogen storage: a critical review. Chem Eng Technol 33(2):213–226
648. Hunt AJ, Gross K, Mao SS (2009) Mesoporous oxides and their applications to hydrogen storage. Mater Matters (Milwaukee, WI, USA) 4(2):47–54
649. Niemann MU, Srinivasan SS, Phani AR, Kumar A, Goswami DY, Stefanakos EK (2009) Room temperature reversible hydrogen storage in polyaniline (PANI) nanofibers. J Nanosci Nanotechnol 9(8):4561–4565
650. Kuchta B, Firlej L, Cepel R, Pfeifer P, Wexler C (2010) Structural and energetic factors in designing a nanoporous sorbent for hydrogen storage. Colloids Surf A Physicochem Eng Aspects 357(1–3):61–66
651. Park S-J, Lee S-Y (2010) A study on hydrogen-storage behaviors of nickel-loaded mesoporous MCM-41. J Colloid Interface Sci 346(1):194–198
652. Reddy ALM, Tanur AE, Walker GC (2010) Synthesis and hydrogen storage properties of different types of boron nitride nanostructures. Int J Hydrogen Energy 35(9):4138–4143
653. Sepehri S, Cao G (2010) Nanostructured materials for hydrogen storage. Annu Rev Nano Res 3:487–514
654. Sun X, Hwang J-Y, Shi S (2010) Hydrogen storage in mesoporous metal oxides with catalyst and external electric field. J Phys Chem C 114(15):7178–7184
655. Zuettel A (2009) Materials for hydrogen storage. In: Barbaro P, Bianchini C (eds) Catalysis for sustainable energy production. Wiley-VCH, Weinheim, pp 107–169
656. Bogdanovic B, Felderhoff M, Streukens G (2009) Hydrogen storage in complex metal hydrides. J Serb Chem Soc 74(2):183–196
657. Thomas KM (2007) Hydrogen adsorption and storage on porous materials. Catal Today 120:389–398
658. Darkrim F, Levesque D (2000) High adsorptive property of opened carbon nanotubes at 77 K. J Phys Chem B 104:6773–6776
659. Wang Q, Johnson JK (1999) Molecular simulation of hydrogen adsorption in single–walled carbon nanotubes and idealized carbon slit pores. J Chem Phys 110:557–567
660. Yin YF, Mays T, McEnaney B (2000) Molecular simulations of hydrogen storage in carbon nanotube arrays. Langmuir 16:10521–10527
661. Dillon AC, Jones KM, Bekkedahl TA, Kiang CH, Bethune DS, Heben MJ (1997) Storage of hydrogen in single-walled carbon nanotubes. Nature 386:377–379
662. Ye Y, Ahn CC, Witham C, Fultz B, Liu J, Rinzler G, Colbert D, Smith KA, Smalley RE (1999) Hydrogen adsorption and cohesive energy of single-walled carbon nanotubes. Appl Phys Lett 74:2307–2309

663. Dillon AC, Bekkedahl TA, Jones KM, Heben MJ (1996) Oxidative opening and filling by hydrogen of single wall carbon nanotubes. In: Kadish KM, Ruoff RS (eds) Proceedings of the symposium on recent advances in the chemistry and physics of fullerenes and related materials, 5–10 May 1996, Los Angeles, California. Electrochemical Society Proceedings Volume 96–10. Pennington, NJ. The Electrochemical Society, Inc. 3, pp 716–727 NREL Report No. 24407
664. Liu C, Fan YY, Liu M, Cong HT, Cheng HM, Dresselhaus MS (1999) Hydrogen storage in single-walled carbon nanotubes at room temperature. Science 286:1127–1129
665. Zhu HW, Ci LJ, Chen A, Mao ZQ, Xu CL, Xiao X, Wei BQ, Liang J, Wu DH (2000) Hydrogen uptake in multi-walled carbon nanotubes at room temperature. In: Mao ZQ, Veziroglu TN (eds) Proceedings of the 13th World Hydrogen Energy Conference, 11–15 June 2000, Beijing, China. International Hydrogen Association 2000, pp 560
666. Wu H-i LuJ, Li B-L (2000) A coupled oscillatory model mimicking avian circadian regulatory systems. J Biol Phys 26:261–272
667. Chen P, Wu X, Lin J, Tan KL (1999) High H_2 uptake by alkali-doped carbon nanotubes under ambient pressure and moderate temperatures. Science 285:91–93
668. Yang RT (2000) Hydrogen storage by alkali-doped carbon nanotubes-revisited. Carbon 38:623–626
669. Pinkerton F, Wickle B, Olk C, Tibbetts G, Meisner G, Meyer MS, Herbst J (2000) Thermogravimetric measurement of hydrogen storage in carbon-based materials: promise and pitfalls. In: Proceedings of the 10th Canadian Hydrogen Conference, Quebec, Canadian Hydrogen Association
670. Rodriguez N (1996) Hydrogen storage. MRS 1996 Fall Meeting, 2–6 Dec, Boston, Paper D 11.6
671. Browning DJ, Gerrard ML, Laakeman JB, Mellor IM, Mortimer RJ, Turpin MC (2000) Investigation of the hydrogen storage capacities of carbon nanofibres prepared from an Ethylene precursor. In: Mao ZQ, Veziroglu TN (eds) Proceedings of the 13th World Hydrogen Energy Conference, Beijing, China. International Hydrogen Association, 2000, p 580
672. Gupta BK, Awasthi K, Srivastava ON (2000) New carbon variants: graphitic nanofibres and nanotubules as hydrogen storage materials. In: Mao ZQ, Veziroglu TN (eds) Proceedings of the 13th World Hydrogen Energy Conference, Beijing, China.International Hydrogen Association, 2000, p 487
673. Liu C, Chen Y, Wu C-Z, Xu S-T, Cheng H-M (2010) Hydrogen storage in carbon nanotubes revisited. Carbon 48:452–455
674. Dillon AC, Gennett T, Jones KM, Alleman JL, Parilla PA, Heben MJ (1999) Carbon nanotubes materials for hydrogen storage. In: Proceedings of the 1999 DOE/NREL Hydrogen Program Review, U.S. DOE, Washington DC 1999
675. Chen X (2002) Hydrogen storage. In: Proceedings of the 3rd Materials Research Society Symposiu. Materials Research Society Press, Boston
676. Smith MR Jr, Bittner EW, Shi W, Johnson JK, Bockrath BC (2003) Chemical activation of single-walled carbon nanotubes for hydrogen adsorption. J Phys Chem B 107(16):3752–3760
677. Chambers A, Park C, Baker RTK, Rodriguez NM (1998) Hydrogen storage in graphite nanofibers. J Phys Chem B 102(22):4253–4256
678. Zhu H, Cao A, Li X, Xu C, Mao Z, Ruan D, Liang J (2001) Hydrogen adsorption in bundles of well aligned carbon nanotubes at room temperature. Appl Surf Sci 178(1–4):50–55
679. Chen Y, Shaw DT, Bai XD, Wang EG, Lund C, Lu WM, Chung DDL (2001) Hydrogen storage in aligned carbon annotubes. Appl Phys Lett 78(15):2128–2130
680. Badzian A, Badzian T, Breval E, Piotrowski A (2001) Nanostructured, nitrogen doped carbon materials for hydrogen storage. Thin Solid Films 398–399:170–174
681. Wang H, Gao Q, Hu J (2009) High hydrogen storage capacity of porous carbons prepared by using activated carbon. J Am Chem Soc 131:7016–7022
682. Cheng F, Liang J, Zhao J, Tao Z, Chen J (2008) Biomass waste-derived microporous carbons with controlled texture and enhanced hydrogen uptake. Chem Mater 20:1889–1895

683. Jordá-Beneyto M, Suárez-Garcá F, Lozano-Castelló D, Cazorla-Amorós D, Linares-Solano A (2007) Hydrogen storage on chemically activated carbons and carbon nanomaterials at high pressures. Carbon 45:293–303
684. Yang Z, Xia Y, Mokaya R (2007) Enhanced hydrogen storage capacity of high surface area zeolite-like carbon materials. J Am Chem Soc 129:1673–1679
685. Pacula A, Mokaya R (2008) Synthesis and high hydrogen storage capacity of zeolite-like carbons nanocast using as-synthesized zeolite templates. J Phys Chem C 112:2764–2769
686. Saha D, Deng S (2009) Hydrogen adsorption in ordered mesoporous carbon Doped with Pt, Pd, Ru and Ni. Langmuir 25(21):12550–12560
687. Nijkamp MG, Raaymakers JEMJ, Van Dillen AJ, De Jong KP (2001) Hydrogen storage using physisorption-materials demands. Appl Phys A: Mater Sci Process 72:619–623
688. Pang J, Hampsey JE, Wu Z, Hu Q, Lu Y (2004) Hydrogen adsorption in mesoporous carbons. Appl Phys Lett 85:4887–4889
689. Parra JB, Ania CO, Arenillas A, Rubiera F, Palacios JM, Pis JJ (2004) Textural development and hydrogen adsorption of carbon materials from PET waste. J Alloy Comp 379:280–289
690. Takagi H, Hatori H, Soneda Y, Yoshizawa N, Yamada Y (2004) Adsorptive hydrogen storage in carbon and porous materials. Mater Sci Eng B Solid State Mater Advan Technol 108: 143–147
691. Takagi H, Hatori H, Yamada Y, Matsuo S, Shiraishi M (2004) Hydrogen adsorption properties of activated carbons with modified surfaces. J Alloy Comp 385:257–263
692. Zhao X, Villar-Rodil S, Fletcher AJ, Thomas KM (2006) Kinetic isotope effect for H2 and D2 quantum molecular sieving in adsorption/desorption on porous carbon materials. J Phys Chem B 110:9947–9955
693. Zhao XB, Xiao B, Fletcher AJ, Thomas KM (2005) Hydrogen adsorption on functionalized nanoporous activated carbons. J Phys Chem B 109:8880–8888
694. Schimmel HG, Kearley GJ, Nijkamp MG, Visser CT, de Jong KP, Mulder FM (2003) Hydrogen adsorption in carbon nanostructures: comparison of nanotubes, fibers, and coals. Chem Eur J 9:4764–4770
695. Schimmel HG, Nijkamp G, Kearley GJ, Rivera A, De Jong KP, Mulder FM (2004) Hydrogen adsorption in carbon nanostructures compared. Mater Sci Eng B Solid State Mater Advan Technol 108:124–129
696. Texier-Mandoki N, Dentzer J, Piquero T, Saadallah S, David P, Vix-Guterl C (2004) Hydrogen storage in activated carbon materials: role of the nanoporous texture. Carbon 42:2744–2747
697. Gadiou R, Saadallah SE, Piquero T, David P, Parmentier J, Vix-Guterl C (2005) The influence of textural properties on the adsorption of hydrogen on ordered nanostructured carbons. Microporous Mesoporous Mater 79:121–128
698. Gogotsi Y, Dash RK, Yushin G, Yildirim T, Laudisio G, Fischer JE (2005) Tailoring of nanoscale porosity in carbide-derived carbons for hydrogen storage. J Am Chem Soc 127:16006–16007
699. Rowsell JLC, Yaghi OM (2006) Effects of functionalization, catenation, and variation of the metal oxide and organic linking units on the low-pressure hydrogen adsorption properties of metal-organic frameworks. J Am Chem Soc 128:1304–1315
700. Chapman KW, Southon PD, Weeks CL, Kepert CJ (2005) Reversible hydrogen gas uptake in nanoporous Prussian blue analogues. Chem Commun 26:3322–3324
701. Chun H, Dybtsev DN, Kim H, Kim K (2005) Synthesis, x-ray crystal structures, and gas sorption properties of pillared square grid nets based on paddle-wheel motifs: implications for hydrogen storage in porous materials. Chem Eur J 11:3521–3529
702. Kaye SS, Long JR (2005) Hydrogen storage in the dehydrated prussian blue analogues M3[Co(CN)6]2 (M = Mn, Fe, Co, Ni, Cu, Zn). J Am Chem Soc 127:6506–6507
703. Dybtsev DN, Chun H, Kim K (2004) Rigid and flexible: a highly porous metal–organic framework with unusual guest-dependent dynamic behavior. Angew Chem Int Ed 43:5033–5036
704. Chen B, Ockwig NW, Millward AR, Contreras DS, Yaghi OM (2005) High H_2 adsorption in a microporous metal-organic framework with open metal sites. Angew Chem Int Ed 44: 4745–4749

705. Dietzel PDC, Panella B, Hirscher M, Blom R, Fjellvag H (2006) Hydrogen adsorption in a nickel based coordination polymer with open metal sites in the cylindrical cavities of the desolvated framework. Chem Commun 9:959–961
706. Belosludov VR, Subbotin OS, Belosludov RV, Mizuseki H, Kawazoe Y, Kudoh J (2009) Thermodynamics and hydrogen storage ability of binary hydrogen + help gas clathrate hydrate. Int J Nanosci 8(1 & 2):57–63
707. Di Profio P, Arca S, Rossi F, Filipponi M (2009) Comparison of hydrogen hydrates with existing hydrogen storage technologies: energetic and economic evaluations. Int J Hydrogen Energy 34(22):9173–9180
708. Gutowski M, Abramov AV (2009) Hierarchical storage of hydrogen in clathrates of ammonia borane. Prepr Symp Am Chem Soc, Div Fuel Chem 54(2):849–852
709. Lee H, J-W L, Kim DY, Park J, Seo Y-T, Zeng H, Moudrakovski IL, Ratcliffe CI, Ripmeester JA (2005) Tuning clathrate hydrates for hydrogen storage. Nature (London, UK) 434(7034):743–746
710. Martin A, Peters CJ (2009) Hydrogen storage in sH clathrate hydrates: thermodynamic model. J Phys Chem B 113(21):7558–7563
711. Mulder FM, Wagemaker M, van Eijck L, Kearley GJ (2008) Hydrogen in porous tetrahydrofuran clathrate hydrate. Chemphyschem 9(9):1331–1337
712. Nakayama T, Tomura S, Ozaki M, Ohmura R, Mori YH (2010) Engineering investigation of hydrogen storage in the form of clathrate hydrates: conceptual design of hydrate production plants. Energy Fuels 24(4):2576–2588
713. Ogata K, Tsuda T, Amano S, Hashimoto S, Sugahara T, Ohgaki K (2010) Hydrogen storage in trimethylamine hydrate: thermodynamic stability and hydrogen storage capacity of hydrogen+trimethylamine mixed semi-clathrate hydrate. Chem Eng Sci 65(5):1616–1620
714. Papadimitriou NI, Tsimpanogiannis IN, Stubos AK (2010) Computational approach to study hydrogen storage in clathrate hydrates. Colloids Surf A Physicochem Eng Aspects 357(1–3): 67–73
715. Prasad PR, Sum AK, Sloan ED, Koh CA (2009) Hydrogen storage in clathrate materials. Abstracts of Papers, 237th ACS National Meeting, Salt Lake City, UT, United States, 22–26 March 2009, FUEL-154
716. Prasad PSR, Sugahara T, Kim Y, Sum AK, Sloan ED, Koh CA (2009) Hydrogen storage in clathrate materials. Prepr Symp Am Chem Soc, Div Fuel Chem 54(2):855
717. Prasad PSR, Sugahara T, Sum AK, Sloan ED, Koh CA (2009) Hydrogen storage in double clathrates with tert-butylamine. J Phys Chem A 113(24):6540–6543
718. Saha D, Deng S (2009) Enhanced hydrogen adsorption in ordered mesoporous carbon through clathrate formation. Int J Hydrogen Energy 34(20):8583–8588
719. Shin K, Kim Y, Strobel TA, Prasad PSR, Sugahara T, Lee H, Sloan ED, Sum AK, Koh CA (2009) Tetra-n-butylammonium borohydride semiclathrate: a hybrid material for hydrogen storage. J Phys Chem A 113(23):6415–6418
720. Sluiter MHF, Adachi H, Belosludov RV, Belosludov VR, Kawazoe Y (2004) Ab initio study of hydrogen storage in hydrogen hydrate clathrates. Mater Trans 45(5):1452–1454
721. Strobel TA, Hester KC, Koh CA, Sum AK, Sloan ED Jr (2009) Properties of the clathrates of hydrogen and developments in their applicability for hydrogen storage. Chem Phys Lett 478(4–6):97–109
722. Strobel TA, Kim Y, Andrews GS, Ferrell JR III, Koh CA, Herring AM, Sloan ED (2008) Chemical-clathrate hybrid hydrogen storage: storage in both guest and host. J Am Chem Soc 130(45):14975–14977
723. Strobel TA, Kim Y, Andrews GS, Ferrell JR III, Koh CA, Herring AM, Sloan ED (2009) Chemical-clathrate hybrid hydrogen storage. Prepr Symp Am Chem Soc, Div Fuel Chem 54(1):314–316
724. Strobel TA, Koh CA, Sloan ED (2009) Thermodynamic predictions of various tetrahydrofuran and hydrogen clathrate hydrates. Fluid Phase Equilib 280(1–2):61–67

725. Su F, Bray CL, Carter BO, Overend G, Cropper C, Iggo JA, Khimyak YZ, Fogg AM, Cooper AI (2009) Reversible hydrogen storage in hydrogel clathrate hydrates. Advan Mater 21(23):2382–2386
726. Sugahara T, Haag JC, Prasad PSR, Warntjes AA, Sloan ED, Sum AK, Koh CA (2009) Increasing hydrogen storage capacity using tetrahydrofuran. J Am Chem Soc 131(41): 14616–14617
727. Tsuda T, Ogata K, Hashimoto S, Sugahara T, Moritoki M, Ohgaki K (2009) Storage capacity of hydrogen in tetrahydrothiophene and furan clathrate hydrates. Chem Eng Sci 64(19): 4150–4154
728. Van den Berg AWC, Bromley ST, Jansen JC, Maschmeyer T (2004) Clathrates as potential hydrogen storage materials. Advances in Science and Technology (Faenza, Italy) 42(Computational Modeling and Simulation of Materials III, Part A), pp 549–556
729. Rovetto LJ, Strobel TA, Hester KC, Dec SF, Koh CA, Miller KT, Solan ED (2006) Molecular hydrogen storage in novel binary clathrate hydrates at near-ambient temperatures and pressures. DOE Hydrogen Program. FY 2006 Program review. http://www.hydrogen.energy.gov/pdfs/progress06/iv_i_11_sloan.pdf. Accessed 22 Nov 2010
730. Lee H, Lee J-W, Kim DY, Park J, SeoY-T ZH, Moudrakovski IL, Ratcliffe CL, Ripmeester JA (2005) Tuning clathrate hydrates for hydrogen storage. Nature 434(7034):743–746
731. Hirose K (2010) Handbook of hydrogen storage: new materials for future energy storage. Wiley-VCH, Weinheim
732. Zuttel A, Schlapbach L (2009) Science and technology of hydrogen: book series on complex metallic alloys 2(Properties and Applications of Complex Intermetallics) pp 331–363
733. Biniwale RB, Rayalu S, Devotta S, Ichikawa M (2008) Chemical hydrides: a solution to high capacity hydrogen storage and supply. Int J Hydrogen Energy 33(1):360–365
734. Dornheim M, Eigen N, Barkhordarian G, Klassen T, Bormann R (2006) Tailoring hydrogen storage materials towards application. Adv Eng Mater 8(5):377–385
735. John V, Pinkerton F, Stetson N (2009) Nanoscale phenomena in hydrogen storage. Nanotechnology 20(20):200201–200202
736. Nico E, Claude K, Martin D, Thomas K, Rudiger B (2007) Industrial production of light metal hydrides for hydrogen storage. Scr Mater 56(10):847–851
737. Orimo S-I, Nakamori Y, Eliseo JR, Zuttel A, Jensen CM (2007) Complex hydrides for hydrogen storage. Chem Rev 107(10):4111–4132
738. Sakintuna B, Lamari-Darkrim F, Hirscher M (2007) Metal hydride materials for solid hydrogen storage: a review. Int J Hydrogen Energy 32(9):1121–1140
739. Satyapal S, Petrovic J, Read C, Thomas G, Ordaz G (2007) The U.S. Department of Energy's National Hydrogen Storage Project: progress towards meeting hydrogen-powered vehicle requirements. Catal Today 120(3–4):246–256
740. Vincent B, Gregg R, Mildred D, Gang C (2007) Size effects on the hydrogen storage properties of nanostructured metal hydrides: a review. Int J Energy Res 31(6–7):637–663
741. Yamamoto H, Miyaoka H, Hino S, Nakanishi H, Ichikawa T, Kojima Y (2009) Recyclable hydrogen storage system composed of ammonia and alkali metal hydride. Int J Hydrogen Energy 34(24):9760–9764
742. Sabitu ST, Gallo G, Goudy AJ (2010) Effect of TiH2 and Mg2Ni additives on the hydrogen storage properties of magnesium hydride. J Alloy Comp 499(1):35–38
743. Kalisvaart WP, Harrower CT, Haagsma J, Zahiri B, Luber EJ, Ophus C, Poirier E, Fritzsche H, Mitlin D (2010) Hydrogen storage in binary and ternary Mg-based alloys: a comprehensive experimental study. Int J Hydrogen Energy 35(5):2091–2103
744. Weidenthaler C, Pommerin A, Felderhoff M, Sun W, Wolverton C, Bogdanovic B, Schuth F (2009) Complex rare-earth aluminum hydrides: mechanochemical preparation, crystal structure and potential for hydrogen storage. J Am Chem Soc 131(46):16735–16743
745. Dornheim M, Doppiu S, Barkhordarian G, Boesenberg U, Klassen T, Gutfleisch O, Bormann R (2007) Hydrogen storage in magnesium-based hydrides and hydride composites. Scr Materialia 56(10):841–846

746. Zidan R, Garcia-Diaz BL, Fewox CS, Harter A, Stowe AC, Gray JR (2009) Aluminum hydride: a reversible material for hydrogen storage. US Department of energy. http://sti.srs.gov/fulltext/SRNL-STI-2009-00015.pdf. Accessed 20 Nov 2010
747. Khandelwal A, Agresti F, Capurso G, Lo Russo S, Maddalena A, Gialanella S, Principi G (2010) Pellets of MgH2-based composites as practical material for solid state hydrogen storage. Int J Hydrogen Energy 35(8):3565–3571
748. Molinas B, Ghilarducci AA, Melnichuk M, Corso HL, Peretti HA, Agresti F, Bianchin A, Lo Russo S, Maddalena A, Principi G (2009) Scaled-up production of a promising Mg-based hydride for hydrogen storage. Int J Hydrogen Energy 34(10):4597–4601
749. Tsubota M, Hino S, Fujii H, Oomatsu C, Yamana M, Ichikawa T, Kojima Y (2010) Reaction between magnesium ammine complex compound and lithium hydride. Int J Hydrogen Energy 35(5):2058–2062
750. Zhao X, Ma L (2009) Recent progress in hydrogen storage alloys for nickel/metal hydride secondary batteries. Int J Hydrogen Energy 34(11):4788–4796
751. Liu Y, Liang C, Wei Z, Jiang Y, Gao M, Pan H, Wang Q (2010) Hydrogen storage reaction over a ternary imide Li2Mg2N3H3. Phys Chem Chem Phys 12(13):3108–3111
752. Lu D-S, Li W-S (2009) Electrochemical codeposition of magnesium and nickel alloy for hydrogen storage. Mater Chem Phys 117(2–3):395–398
753. Ma L-P, Wang P, Cheng H-M (2010) Hydrogen sorption kinetics of MgH2 catalyzed with titanium compounds. Int J Hydrogen Energy 35(7):3046–3050
754. Mao J, Guo Z, Yu X, Liu H, Wu Z, Ni J (2010) Enhanced hydrogen sorption properties of Ni and Co-catalyzed MgH2. Int J Hydrogen Energy 35(10):4569–4575
755. Kwon SN, Mumm DR, Park HR, Song MY (2010) Effects of transition metal oxide and Ni addition on the hydrogen-storage properties of Mg. J Mater Sci 45(19):5164–5170
756. Langmi HW, Culligan SD, McGrady GS (2009) Mixed-metal Li3N-based systems for hydrogen storage: Li3AlN2 and Li3FeN2. Int J Hydrogen Energy 34(19):8108–8114
757. Li SL, Wang P, Chen W, Luo G, Chen DM, Yang K (2009) Hydrogen storage properties of LaNi3.8Al1.0M0.2 (M═Ni, Cu, Fe, Al, Cr, Mn) alloys. J Alloy Comp 485(1–2):867–871
758. Li W, Vajo JJ, Cumberland RW, Liu P, Hwang S-J, Kim C, Bowman RC (2010) Hydrogenation of magnesium nickel boride for reversible hydrogen storage. J Phys Chem Lett 1(1):69–72
759. Chaise A, de Rango P, Marty P, Fruchart D, Miraglia S, Olives R, Garrier S (2009) Enhancement of hydrogen sorption in magnesium hydride using expanded natural graphite. Int J Hydrogen Energy 34(20):8589–8596
760. Cho Y, Dahle AK (2010) Characterization of hydrogen sorption properties and microstructure of cast Mg-10wt%Ni alloys. Mater Sci Forum 638–642:1085–1090 (Pt. 2, THERMEC 2009)
761. Fang W, H-f S, W-b F, Wang B (2009) Effect of Al and Zn additives on grain size of Mg-3Ni-2MnO2 alloy. Trans Nonferrous Met Soc China 19(Spec. 2):s355–s358
762. Giusepponi S, Celino M, Cleri F, Montone A (2009) Hydrogen storage in MgH2 matrices: a study of Mg-MgH2 interface using CPMD code on ENEA-GRID. Il Nuovo Cimento C 32C(2):139–142
763. Hong TW, Kim IH, Ur SC, Lee YG, Kim YJ (2005) Hydriding/dehydriding behavior of Mg-Ni systems. Mater Sci Forum 486–487:582–585 (Eco-Materials Processing & Design VI)
764. Imamura H, Tanaka K, Kitazawa I, Sumi T, Sakata Y, Nakayama N, Ooshima S (2009) Hydrogen storage properties of nanocrystalline MgH2 and MgH2/Sn nanocomposite synthesized by ball milling. J Alloy Comp 484(1–2):939–942
765. Jain IP, Lal C, Jain A (2010) Hydrogen storage in Mg: a most promising material. Int J Hydrogen Energy 35(10):5133–5144
766. Jaron T, Grochala W (2010) Y(BH4)3 – an old-new ternary hydrogen store aka learning from a multitude of failures. Dalton Trans 39(1):160–166
767. Johnson SR, Anderson PA, Edwards PP, Gameson I, Prendergast JW, Al-Mamouri M, Book D, Harris IR, Speight JD, Walton A (2005) Chemical activation of MgH2; a new route to superior hydrogen storage materials. Chem Commun (22): 2823–2825

768. Liu DM, Fang CH, Zhang QA (2009) Hydrogen storage properties of MgH2-(Sr, Ca)2AlH7 composite. J Alloy Comp 485(1–2):391–395
769. Milanese C, Girella A, Bruni G, Cofrancesco P, Berbenni V, Matteazzi P, Marini A (2009) Mg-Ni-Cu mixtures for hydrogen storage: a kinetic study. Intermetallics 18(2):203–211
770. Rousselot S, Guay D, Roue L (2010) Synthesis of fcc Mg-Ti-H alloys by high energy ball milling: structure and electrochemical hydrogen storage properties. J Power Sources 195(13):4370–4374
771. Niemann MU, Srinivasan SS, Kumar A, Stefanakos EK, Goswami DY, McGrath K (2009) Processing analysis of the ternary LiNH2-MgH2-LiBH4 system for hydrogen storage. Int J Hydrogen Energy 34(19):8086–8093
772. Spassov T, Delchev P, Madjarov P, Spassova M, Himitliiska T (2010) Hydrogen storage in Mg-10at.% LaNi5 nanocomposites, synthesized by ball milling at different conditions. J Alloy Comp 495(1):149–153
773. Nogita K, Ockert S, Duguid A, Pierce J, Greaves M (2009) Mechanism of improved hydrogen absorption kinetics in cast Mg-Ni alloys. Mater Sci Forum 618–619:391–394 (Light Metals Technology 2009)
774. Orban RL, Lucaci M, Salomie D, Orban M (2008) Nanocrystalline Fe-Ti-AI-Ni alloys for hydrogen storage processing by reactive mechanical alloying. Adv Powder Metall Partic Mater 9/251–9/263
775. Osborn W, Markmaitree T, Shaw LL (2007) Evaluation of the hydrogen storage behavior of a LiNH2 + MgH2 system with 1:1 ratio. J Power Sources 172(1):376–378
776. Varin RA, Jang M, Polanski M (2009) The effects of ball milling and molar ratio of LiH on the hydrogen storage properties of nanocrystalline lithium amide and lithium hydride (LiNH2 + LiH) system. J Alloy Comp 491(1–2):658–667
777. Vella C, Renouard J, Goudon JP, Yvart P (2009) Solid hydrogen storage: hydride based composition for gaseous hydrogen generation. In: International Annual Conference of ICT 40th(Energetic Materials), pp 25/1–25/11
778. Visaria M, Mudawar I, Pourpoint T, Kumar S (2010) Study of heat transfer and kinetics parameters influencing the design of heat exchangers for hydrogen storage in high-pressure metal hydrides. Int J Heat Mass Transfer 53(9–10):2229–2239
779. Vojtech D, Guhlova P, Mortanikova M, Janik P (2010) Hydrogen storage by direct electrochemical hydriding of Mg-based alloys. J Alloy Comp 494(1–2):456–462
780. Wang J, Liu T, Wu G, Li W, Liu Y, Araujo CM, Scheicher RH, Blomqvist A, Ahuja R, Xiong Z, Yang P, Gao M, Pan H, Chen P (2009) Potassium-modified Mg(NH2)2/2 LiH system for hydrogen storage. Angew Chem Int Ed 48(32):5828–5832, S/1–S/2
781. Wang Y, Adroher XC, Chen J, Yang XG, Miller T (2009) Three-dimensional modeling of hydrogen sorption in metal hydride hydrogen storage beds. J Power Sources 194(2):997–1006
782. Osborn W, Markmaitree T, Shaw LL (2009) The long-term hydriding and dehydriding stability of the nanoscale LiNH2 + LiH hydrogen storage system. Nanotechnology 20(20):204028/1–204028/9
783. Shaw LL, Wan X, Hu JZ, Kwak JH, Yang Z (2010) Solid-state hydriding mechanism in the LiBH4 + MgH2 system. J Phys Chem C 114(17):8089–8098
784. Pentimalli M, Padella F, La Barbera A, Pilloni L, Imperi E (2009) A metal hydride-polymer composite for hydrogen storage applications. Energy Convers Manage 50(12):3140–3146
785. Pourpoint TL, Velagapudi V, Mudawar I, Zheng Y, Fisher TS (2010) Active cooling of a metal hydride system for hydrogen storage. Int J Heat Mass Transfer 53(7–8):1326–1332
786. Ranjbar A, Guo ZP, Yu XB, Calka A, Liu HK (2009) Hydrogen storage properties of Mg-BCC composite. Int J Green Energy 6(6):607–615
787. Xiao X, Liu G, Peng S, Yu K, Li S, Chen C, Chen L (2010) Microstructure and hydrogen storage characteristics of nanocrystalline Mg+ x wt% LaMg2Ni (x = 0–30) composites. Int J Hydrogen Energy 35(7):2786–2790
788. Xiong Z, Hu J, Wu G, Chen P (2005) Hydrogen absorption and desorption in Mg-Na-N-H system. J Alloy Comp 395(1–2):209–212

789. Zhang J, Yan W, Bai C, Pan F (2009) Mechanochemical synthesis of a Mg-Li-Al-H complex hydride. J Mater Res 24(9):2880–2885
790. Zlotea C, Sahlberg M, Moretto P, Andersson Y (2009) Hydrogen sorption properties of a Mg-Y-Ti alloy. J Alloy Comp 489(2):375–378
791. Ismail M, Zhao Y, Yu XB, Dou SX (2010) Effects of NbF5 addition on the hydrogen storage properties of LiAlH4. Int J Hydrogen Energy 35(6):2361–2367
792. Principi G, Agresti F, Maddalena A, Lo Russo S (2009) The problem of solid state hydrogen storage. Energy 34:2087–2091
793. Ahluwalia RK, Hua TQ, Peng JK (2009) Automotive storage of hydrogen in alane. Int J Hydrogen Energy 34(18):7731–7740
794. Luo K, Liu Y, Wang F, Gao M, Pan H (2009) Hydrogen storage in a Li-Al-N ternary system. Int J Hydrogen Energy 34(19):8101–8107
795. Xiao X, Fan X, Yu K, Li S, Chen C, Wang Q, Chen L (2009) Catalytic Mechanism of New TiC-Doped Sodium Alanate for Hydrogen Storage. J Phys Chem C 113(48):20745–20751
796. M-u-d N, S-u R, So CS, Hwang SW, Kim AR, Nahm KS (2009) Thermal decomposition of LiAlH4 chemically mixed with Lithium amide and transition metal chlorides. Int J Hydrogen Energy 34(21):8937–8943
797. Luo W, Cowgill D, Stewart K, Stavila V (2010) High capacity hydrogen generation on-demand from (NH3 + LiAlH4). J Alloy Comp 497(1–2):L17–L20
798. Beattie SD, McGrady GS (2009) Hydrogen desorption studies of NaAlH4 and LiAlH4 by in situ heating in an ESEM. Int J Hydrogen Energy 34(22):9151–9156
799. Mao JF, Guo ZP, Liu HK, Yu XB (2009) Reversible hydrogen storage in titanium-catalyzed LiAlH4-LiBH4 system. J Alloy Comp 487(1–2):434–438
800. Schmidt T, Roentzsch L (2010) Reversible hydrogen storage in Ti-Zr-codoped NaAlH4 under realistic operation conditions. J Alloy Comp 496(1–2):L38–L40
801. Dathar GKP, Mainardi DS (2010) Kinetics of hydrogen desorption in NaAlH4 and Ti-containing NaAlH4. J Phys Chem C 114(17):8026–8031
802. Zheng X, Liu S (2009) Effect of LaCl3 and Ti on hydrogen storage properties of NaAlH4 and LiAlH4. Xiyou Jinshu Cailiao Yu Gongcheng 38(8):1328–1332
803. Yang J, Wang X, Mao J, Chen L, Pan H, Li S, Ge H, Chen C (2010) Investigation on reversible hydrogen storage properties of Li3AlH6/2LiNH2 composite. J Alloy Comp 494(1–2):58–61
804. Liu J, Ge Q (2009) Hydrogen interaction in Ti-doped LiBH4 for hydrogen storage: a density functional analysis. J Chem Theory Comput 5(11):3079–3087
805. Frankcombe TJ (2010) Calcium borohydride for hydrogen storage: a computational study of Ca(BH4)2 crystal structures and the CaB2Hx intermediate. J Phys Chem C 114(20):9503–9509
806. Gao L, Guo YH, Xia GL, Yu XB (2009) Low temperature hydrogen generation from ammonia combined with lithium borohydride. J Mater Chem 19(42):7826–7829
807. Karkamkar A, Heldebrant D, Linehan J, Autrey T (2009) Ammonium borohydride: solid hydrogen storage material with highest gravimetric hydrogen content. Prepr Symp Am Chem Soc, Div Fuel Chem 54(2):889–890
808. Liu C-H, Kuo Y-C, Chen B-H, Hsueh C-L, Hwang K-J, Ku J-R, Tsau F, Jeng M-S (2010) Synthesis of solid-state NaBH4/Co-based catalyst composite for hydrogen storage through a high-energy ball-milling process. Int J Hydrogen Energy 35(9):4027–4040
809. Yu XB, Guo YH, Sun DL, Yang ZX, Ranjbar A, Guo ZP, Liu HK, Dou SX (2010) A combined hydrogen storage system of Mg(BH4)2-LiNH2 with favorable dehydrogenation. J Phys Chem C 114(10):4733–4737
810. Vajo JJ, Skeith SL, Mertens F (2005) Reversible storage of hydrogen in destabilized LiBH4. J Phys Chem B 109(9):3719–3722
811. Matsunaga T, Buchter F, Mauron P, Bielman M, Nakamori Y, Orimo S, Ohba N, Miwa K, Towata S, Züttel A (2008) Hydrogen storage properties of Mg[BH4]2. J Alloy Comp 459(1–2):583–588

812. Chater PA, Anderson PA, Prendergast JW, Walton A, Mann VSJ, Book D, David WIF, Johnson SR, Edwards PP (2007) Synthesis and characterization of amide-borohydrides: new complex light hydrides for potential hydrogen storage. J Alloy Comp 446–447:350–354
813. Basu S, Diwan M, Abiad MG, Zheng Y, Campanella OH, Varma A (2010) Transport characteristics of dehydrogenated ammonia borane and sodium borohydride spent fuels. Int J Hydrogen Energy 35(5):2063–2072
814. Burrell AK, Diyabalanage HVK, Shrestha RL, Ryan K, Jones MO, David WIF (2009) Hydrogen from ammonia borane and derivatives. Prepr Symp Am Chem Soc, Div Fuel Chem 54(2):858–859
815. Xiong Z, Yong CK, Wu G, Chen P, Shaw W, Karkamkar A, Autrey T, Jones MO, Johnson SR, Edwards PP, David WIF (2008) High-capacity hydrogen storage in lithium and sodium amidoboranes. Nat Mater 7(2):138–141
816. Chua YS, Wu G, Xiong Z, He T, Chen P (2009) Calcium amidoborane ammoniate – synthesis, structure, and hydrogen storage properties. Chem Mater 21(20):4899–4904
817. Demirci UB, Miele P (2010) Hydrolysis of solid ammonia borane. J Power Sources 195(13):4030–4035
818. Sundberg MR, Sanchez-Gonzalez A (2007) Hydrogen storage in ammonia triborane: properties and behavior of the chemical bonds. Inorg Chem Commun 10(10):1229–1232
819. Swinnen S, Nguyen V-S, Nguyen M-T (2010) Potential hydrogen storage of lithium amidoboranes and derivatives. Chem Phys Lett 489(4–6):148–153
820. Wu C, Wu G, Xiong Z, Han X, Chu H, He T, Chen P (2010) LiNH2BH3. NH3BH3: structure and hydrogen storage properties. Chem Mater 22(1):3–5
821. Demirci UB, Miele P (2009) Sodium borohydride versus ammonia borane, in hydrogen storage and direct fuel cell applications. Energy Environ Sci 2(6):627–637
822. Diwan M, Hanna D, Varma A (2010) Method to release hydrogen from ammonia borane for portable fuel cell applications. Int J Hydrogen Energy 35(2):577–584
823. Graham KR, Kemmitt T, Bowden ME (2009) High capacity hydrogen storage in a hybrid ammonia borane-lithium amide material. Energy Environ Sci 2(6):706–710
824. Himmelberger DW, Yoon CW, Bluhm ME, Carroll PJ, Sneddon LG (2009) Base-promoted ammonia borane hydrogen-release. J Am Chem Soc 131(39):14101–14110
825. Rassat SD, Aardahl CL, Autrey T, Smith RS (2010) Thermal Stability of Ammonia Borane: A Case Study for Exothermic Hydrogen Storage Materials. Energy Fuels 24(4):2596–2606
826. Me B, Bradley MG, Butterick I, Kusari U, Sneddon LG (2006) Amineborane-based chemical hydrogen storage: enhanced ammonia borane dehydrogenation in ionic liquids. J Am Chem Soc 128(24):7748–7749
827. Sirosh N (2002) Hydrogen composite tank program. In: Proceedings of the 2002 US DOE Hydrogen Program Review. Report No. NREL/CP-610-32405
828. Joseph T (2006) Fuel solutions for industrial applications. Air Products Ltd, Allentown